

Amir Farughian

**Novel methods
for earth fault
passage indication
in non-effectively
grounded
electricity
distribution
networks**



ACTA WASAENSIA 500



Vaasan yliopisto
UNIVERSITY OF VAASA

Copyright © Vaasan yliopisto and the copyright holders.

ISBN 978-952-395-054-2 (print)
978-952-395-055-9 (online)

ISSN 0355-2667 (Acta Wasaensia 500, print)
2323-9123 (Acta Wasaensia 500, online)

URN <https://urn.fi/URN:ISBN:978-952-395-055-9>

Hansaprint Oy, Turenki, 2022.

ACADEMIC DISSERTATION

*To be presented, with the permission of the Board of the School of Technology
and Innovations of the University of Vaasa, for public examination on
the 15th of December, 2022, at noon.*

Article based dissertation, School of Technology and Innovations, Electrical Engineering

Author Amir Farughian  <https://orcid.org/0000-0001-9448-4541>

Supervisor(s) Professor Kimmo Kauhaniemi
University of Vaasa. School of Technology and Innovations,
Electrical Engineering.

Professor Timo Vekara
University of Vaasa. School of Technology and Innovations,
Electrical Engineering.

Custos Professor Kimmo Kauhaniemi
University of Vaasa. School of Technology and Innovations,
Electrical Engineering.

Reviewers Professor Matti Lehtonen
Aalto University. Department of Electrical Engineering and
Automation.

Professor Hans Kristian Høidalen
Norwegian University of Science and Technology (NTNU).
Department of Electric Power Engineering.

Opponent Professor Petr Toman
Brno University of Technology, Faculty of Electrical Engineering
and Communication.

Tiivistelmä

Sähkönjakeluverkoissa esiintyy vikoja, jotka aiheuttavat sähkönjakelun keskeytyksiä eli sähkökatkoja. Tämä väitöskirja käsittelee keskijänniteverkkoja, jotka koostuvat sähköasemista ja niiltä lähtevistä johtolähdöistä. Johtolähtöjen varrella sijaitsevat pienjänniteverkkoa syöttävät muuntamot. Kun jollain johto-osuudella (tässä ns. muuntamovälillä, joka yhdistää kaksi peräkkäistä muuntamoaa) ilmenee pysyvä vika, viallinen johto-osuus on tunnistettava ja erotettava. Viallisen johto-osuuden tunnistaminen tapahtuu vianilmaisimien avulla. Viallisen johto-osuuden tunnistaminen on yksinkertaista, kun vikatyyppejä on oikosulku, sillä oikosuluille ominaista ovat yleensä suuret vikavirrat. Haasteena on kuitenkin edelleen viallisten johto-osuuksien tunnistaminen maasulkutilanteissa ei-tehokkaasti maadoitetuissa keskijänniteverkoissa, joissa maasulkuvirta on tyypillisesti hyvin pieni. Tämän väitöskirjana tavoitteena on ollut kehittää uusia menetelmiä maasulkuvikojen paikantamiseen keskijänniteverkossa ja varmentaa niiden toimivuus simuloinnein ja todellisesta verkosta saatujen mittausten avulla.

Kattavan kirjallisuuskatsauksen jälkeen tässä väitöskirjassa esitellään innovatiivisia menetelmiä vikavirran reitin ilmaisuun jakeluverkkojen maasuluissa. Ehdotetut menetelmät tukeutuvat teoreettiseen analyysiin, jossa johtolähdön virrat maasulkutilanteessa on kuvattu symmetristen komponenttien avulla. Menetelmät perustuvat verkon eri pisteissä mitattuihin virran symmetristen komponenttien vertailuun. Käytännön toteutuksessa nämä mittaukset tulee siirtää keskitettyyn järjestelmään prosessointia ja päätöksentekoa varten, mutta tämä voidaan tehdä ilman tarkkaa aikasyntekronointia. Ehdotettujen menetelmien kehittämisessä ja testaamisessa hyödynnettiin simulointeja ja kokeellista mittaustietoa. Yhteistyö teollisuuden kanssa mahdollisti menetelmien toiminnan todentamisen hyödyntäen todellisista verkoista mitattua dataa, jota saatiin sekä verkkoyhtiöiltä että laitevalmistajilta. Simulointien tulokset ja mittaukset todellisessa verkossa tehdyistä testeistä osoittavat, että virran symmetriset komponentit toimivat hyvin vian paikannuksessa kun vikaresistanssi on nollan ja muutaman tuhannen ohmin välillä. Käytännössä menetelmien luotettavuus riippuu virran mittauksen tarkkuudesta.

Asiasanat: Maasulku, vianilmaisin, keskijännite, sähkönjakeluverkot

Abstract

Electricity distribution networks are commonly subject to supply interruptions and outages caused by faults. This dissertation focuses on medium voltage distribution networks, which typically consist of primary substations having multiple feeders along which secondary substations are located. When a permanent fault occurs on a segment (the part linking two consecutive secondary substations) of a distribution feeder, the faulted segment needs to be identified and isolated. Identifying the faulted segment can be realized through fault passage indicators. This is a straightforward task when the fault type is a short circuit, as these types of faults involve large currents. However, faulted segment identification for earth faults in non-effectively grounded medium voltage distribution networks has remained a challenge as the earth fault current in those networks is typically relatively small. Therefore, the main objective of this dissertation was to develop novel methods for locating single-phase earth faults in medium voltage distribution networks and validating them through simulations and real system measurements.

After comprehensive review of state-of-the-art approaches presented in the literature, the dissertation proposes innovative methods for earth fault passage indication aimed at non-effectively grounded urban or rural distribution networks with radial feeders. The proposed methods are underpinned by a theoretical analysis based on the symmetrical components of the currents on a distribution feeder under an earth fault condition. The comparison of the sequence currents collected from various measuring points on the network forms the backbone of the methods. For practical implementation, current measurements need to be transferred to a central location for processing and decision making, but this can be done without accurate time synchronization. The proposed methods were developed and verified through simulations and empirical data. This work is a product of close collaboration between academia and industry that enabled the validation of the proposed methods with the help of empirical data that was provided by system operators and relay manufacturers. The results obtained from simulations and field tests show the efficacy of utilizing sequence current quantities, in the manner proposed in this work, for identifying the passage of earth faults with fault resistances ranging from zero to several kilo-ohms. In practice, the methods are reliable as long as the current measurements are accurate enough.

Keywords: Earth fault, fault passage indication, medium voltage, electricity distribution networks

ACKNOWLEDGEMENT

This doctoral dissertation has been developed mainly from several research projects conducted at the University of Vaasa during the years 2015 – 2022. In addition to the support that I received from academic people, this thesis benefited from the advice and knowledge of several people involved in industry. I want to express my gratitude to all those who made this dissertation possible.

I would like to thank my supervisor Prof. Kimmo Kauhaniemi for his unwavering support and encouragement throughout my doctoral studies. I am very grateful to Lauri Kumpulainen for the pleasant cooperation we had and for providing the initial idea at the early stage of my studies. I also express my gratitude to Prof. Timo Vekara for his encouragement during my studies.

I wish to acknowledge the comments, information and real-life fault recordings I received from Mika Loukkalahti from Helen Sähköverkko Oy. I am grateful to Seppo Pettissalo from Vaspec Oy, Ville Sallinen from Emtele Oy, and Petri Hovila from ABB Oy for providing a number of field test recordings.

Special thanks is extended to Safegrid Oy personnel, especially Jussi Hakunti (CEO) and Tapio Mäntysalo (VP, Products and Engineering), for providing a great deal of data and field test recordings. This enriched my doctoral dissertation, helped with developing the methods proposed in the dissertation, and enabled the experimental verification of them.

Contents

| | |
|---|-----|
| TIIVISTELMÄ..... | V |
| ABSTRACT | VI |
| ACKNOWLEDGEMENT | VII |
| 1 INTRODUCTION..... | 1 |
| 1.1 Background | 1 |
| 1.2 Smart distribution networks..... | 1 |
| 1.3 Fault management..... | 2 |
| 1.4 Fault location..... | 3 |
| 1.5 Network types | 3 |
| 1.6 Earth fault location | 5 |
| 1.7 Objectives of the work..... | 6 |
| 1.8 Thesis outline..... | 6 |
| 1.9 Scientific contribution..... | 7 |
| 1.10 Summary of publications | 8 |
| 1.11 Other publications..... | 8 |
| 2 EARTH FAULT LOCATION – OVERVIEW..... | 10 |
| 2.1 Introduction | 10 |
| 2.2 Centralized methods | 11 |
| 2.2.1 Impedance-based..... | 11 |
| 2.2.2 Traveling waves | 12 |
| 2.2.3 Artificial intelligence | 14 |
| 2.3 Decentralized methods..... | 14 |
| 2.3.1 Signal injection | 14 |
| 2.3.2 Fault-passage-indication based methods | 16 |
| 2.3.3 Smart meters | 17 |
| 2.4 Discussion..... | 18 |
| 3 THEORETICAL BACKGROUND..... | 20 |
| 3.1 Background | 20 |
| 3.2 Sequence currents in neutral-isolated networks and compensated networks..... | 22 |
| 3.2.1 Sequence currents in neutral-isolated networks..... | 23 |
| 3.2.2 Sequence currents in compensated networks | 26 |
| 3.3 Negative sequence current | 28 |
| 3.4 Conclusion and summary | 32 |
| 4 PROPOSED METHODS..... | 33 |
| 4.1 Fault passage indication using zero and negative sequence currents..... | 33 |
| 4.1.1 Correct installation of current sensors..... | 33 |
| 4.1.2 Method 1 | 34 |
| 4.1.3 Method 2 | 35 |
| 4.2 Simulations..... | 36 |

| | | |
|-------|--|----|
| 4.2.1 | Simulation model | 36 |
| 4.2.2 | Simulation results | 37 |
| 4.2.3 | Impact of fault resistance | 44 |
| 4.3 | Method 2 vs conventional methods | 46 |
| 4.3.1 | Neutral-isolated network | 47 |
| 4.3.2 | Compensated network | 49 |
| 4.4 | Discussion..... | 51 |
| 5 | INTERMITTENT EARTH FAULT | 54 |
| 5.1 | Introduction | 54 |
| 5.2 | Phenomenon | 55 |
| 5.3 | Problem formulation..... | 58 |
| 5.4 | Literature review..... | 58 |
| 5.5 | Method 2 modification | 60 |
| 5.6 | Simulation and experimental results | 60 |
| 5.7 | Discussion..... | 62 |
| 6 | TECHNICAL REQUIREMENTS AND EXPERIMENTAL VERIFICATION | 64 |
| 6.1 | Technical aspects | 64 |
| 6.1.1 | Measurements | 64 |
| 6.1.2 | Data acquisition..... | 67 |
| 6.1.3 | Triggering and sensitivity..... | 67 |
| 6.1.4 | Recording structure | 67 |
| 6.1.5 | Sampling rate | 68 |
| 6.1.6 | Communication | 68 |
| 6.2 | Field tests..... | 69 |
| 6.2.1 | Network 1 specifications | 69 |
| 6.2.2 | Scenario 1 | 70 |
| 6.2.3 | Scenario 2..... | 74 |
| 6.2.4 | Scenario 3..... | 78 |
| 6.2.5 | Network 2..... | 81 |
| 7 | CONCLUSION | 83 |
| 7.1 | Main conclusions and findings..... | 83 |
| 7.2 | Contributions | 84 |
| 7.3 | Future research work..... | 87 |
| 7.3.1 | Fault passage indication using direction of transient part of residual current..... | 87 |
| 7.3.2 | Universal method..... | 87 |
| | REFERENCES | 89 |
| | PUBLICATIONS | 97 |

Figures

| | | |
|------------------|---|----|
| Figure 1. | Classification of earth fault location methods (modified figure, from Publication I)..... | 11 |
|------------------|---|----|

| | | |
|-------------------|---|----|
| Figure 2. | Lattice diagram illustrating reflections and refractions of traveling waves caused by a fault on a power line (IEEE Guide Fault Location, 2015)..... | 13 |
| Figure 3. | Earth fault location by injecting a signal to the neutral during an earth fault occurrence (Druml et al., 2013). | 15 |
| Figure 4. | Simplified isolated distribution line under earth fault condition..... | 24 |
| Figure 5. | Earth fault current i_F in the simplified isolated network shown in Figure 4..... | 24 |
| Figure 6. | Zero sequence currents calculated for measuring points of network shown in Figure 4. | 25 |
| Figure 7. | Negative sequence currents calculated for measuring points of network shown in Figure 4. | 25 |
| Figure 8. | Simplified compensated distribution line under earth fault condition..... | 27 |
| Figure 9. | Earth fault current i_F in simplified compensated network shown in Figure 8..... | 27 |
| Figure 10. | Single line diagram of a distribution network. (a) Two arbitrary secondary substations are shown, (b) <i>B</i> and <i>A</i> are not electrically the same location..... | 29 |
| Figure 11. | Single line diagram of a distribution network. | 31 |
| Figure 12. | Simplified circuit of Figure 11..... | 32 |
| Figure 13. | Installation of current sensors on a radial feeder of a typical distribution network..... | 34 |
| Figure 14. | Medium voltage network with various measuring points under earth fault condition..... | 37 |
| Figure 15. | Phase currents measured at five measuring points at network shown in Figure 14 when it operates in its neutral-isolated mode. | 39 |
| Figure 16. | Fault current at fault point in network of Figure 14 when it operates in its neutral-isolated mode. | 40 |
| Figure 17. | Magnitudes of ZSC and NSC phasors. | 40 |
| Figure 18. | Magnitudes of ZSC and NSC phasors (at steady state during the fault) along the faulted feeder of network shown in Figure 14 when it operates in its neutral-isolated mode. | 40 |
| Figure 19. | Phase currents measured at five measuring points at network shown in Figure 14 when it operates in its compensated mode..... | 42 |
| Figure 20. | Fault current at fault point in network shown in Figure 14 when it operates in its compensated mode..... | 43 |
| Figure 21. | Magnitudes of ZSC and NSC phasors. | 43 |
| Figure 22. | Magnitudes of ZSC and NSC phasors (steady state) along the faulted feeder of network shown in Figure 14 when it operates in its compensated mode..... | 43 |
| Figure 23. | Conventional fault passage indication using zero sequence admittance, (Altonen & Wahlroos, 2016) (simplified)..... | 47 |

| | | |
|-------------------|---|----|
| Figure 24. | Line-to-ground voltages at Point 3 (on the fault passage) and Point 4 (off the fault passage) when network of Figure 14 operates in its neutral-isolated mode..... | 48 |
| Figure 25. | Residual currents flowing in same directions in transient state and in steady states in a neutral-isolated distribution network..... | 48 |
| Figure 26. | Phasor diagram of zero sequence voltages, currents and admittances during an earth fault period in the network of Figure 14 when it operates in its neutral-isolated mode. | 49 |
| Figure 27. | Line-to-ground voltages at Point 3 (on the fault passage) and Point 4 (off the fault passage) when network of Figure 14 operates in its compensated mode. | 50 |
| Figure 28. | Residual currents flowing in opposite directions in transient state and almost same direction in steady state in a compensated network. | 50 |
| Figure 29. | Phasor diagram of zero sequence voltages, currents and admittances during an earth fault period in the network shown in Figure 14 when operating in its compensated mode. | 51 |
| Figure 30. | Faulty phase current and voltage obtained from a field test recording (Publication IV). | 55 |
| Figure 31. | Zero sequence voltage and current of the intermittent earth fault of Figure 30 (Publication IV). | 56 |
| Figure 32. | Real-life recordings of an intermittent earth fault on an MV distribution network, courtesy of Safegrid Oy. | 57 |
| Figure 33. | Residual currents at points before and after the fault point in the event of an intermittent earth fault on the network shown in Figure 14. | 61 |
| Figure 34. | NSC (magnitudes) at points before and after the fault point in the event of an intermittent earth fault on the network shown in Figure 14. | 61 |
| Figure 35. | NSC (magnitudes) of the real-life recordings of the intermittent earth fault shown in Figure 32. | 62 |
| Figure 36. | Rogowski-coil-based current sensor, showing a) operational principles, and b) actual sensor (Publication V)..... | 66 |
| Figure 37. | Correct installation of a Rogowski coil set at a given measuring point (Publication V, modified). | 66 |
| Figure 38. | FPI devices installed at pad-mounted secondary substations (Publication V). | 69 |
| Figure 39. | Earth fault field testing on an MV distribution feeder with seven secondary substations and six measurement points, courtesy of Safegrid Oy. | 70 |
| Figure 40. | Current measurements at five points during earth fault testing, Scenario 1, courtesy of Safegrid Oy..... | 72 |
| Figure 41. | Amplitudes of zero and negative sequence current phasors of recordings shown in Figure 40..... | 73 |

| | | |
|-------------------|---|----|
| Figure 42. | Residual currents at Point 1 (on fault passage) and Point 2 (off fault passage) for network of Figure 39 when operating in compensated mode. | 74 |
| Figure 43. | Current measurements at six points during earth fault testing, Scenario 2, courtesy of Safegrid Oy..... | 75 |
| Figure 44. | Increase in amplitudes of ZSC and NSC phasors as a result of an earth fault occurrence for recordings of Figure 39, when the network type is compensated. | 76 |
| Figure 45. | Current measurements at six points during earth fault testing, Scenario 3, courtesy of Safegrid Oy..... | 79 |
| Figure 46. | Increase in amplitudes of ZSC and NSC phasors as a result of an earth fault occurrence for recordings of Figure 39, when the network type is neutral-isolated. | 80 |
| Figure 47. | Earth fault field testing on a real compensated MV distribution network, with FPI units installed at eight measuring points, courtesy of Safegrid Oy. | 82 |

Tables

| | | |
|------------------|--|----|
| Table 1. | Summary of the main characteristics of the main methods (Publication I, modified)..... | 18 |
| Table 2. | Sequence currents along the faulted feeder of the unearthed network of Figure 4..... | 25 |
| Table 3. | Sequence currents along the faulted feeder the compensated network of Figure 8..... | 28 |
| Table 4. | ZSC and NSC phasors along with each method's output (on or off the fault path) for the network of Figure 14 when it operates in its neutral-isolated mode..... | 41 |
| Table 5. | ZSC and NSC phasors along with each method's output for the network of Figure 14 when it operates in its compensated mode. | 44 |
| Table 6. | Magnitudes of ZSC and NSC phasors at steady state for various fault resistances along with each method's output. | 44 |
| Table 7. | Summary of main principles of methods proposed for intermittent faults (Publication IV)..... | 59 |
| Table 8. | Sequence currents for pre- and during-fault periods..... | 73 |
| Table 9. | Sequence currents for pre- and during-fault periods for various fault resistances, when the network type is compensated. | 76 |
| Table 10. | Sequence currents for pre- and during-fault periods, when the network type is neutral-isolated. | 80 |
| Table 11. | Sequence currents computed for pre and during-fault periods for the eight measuring points of the network of Figure 47..... | 82 |

Abbreviations

| | |
|-------|---|
| AI | Artificial Intelligence |
| CT | Current Transformer |
| CWT | Continuous Wavelet Transform |
| DMS | Distribution Management System |
| DSO | Distribution System Operator |
| FCI | Fault Circuit Indicator |
| FPI | Fault Passage Indication |
| FDIR | Fault Detection, Isolation and Restoration |
| FLIR | Fault Location, Isolation and Restoration |
| FLISR | Fault Location, Isolation and Service Restoration |
| HV | High Voltage |
| IED | Intelligent Electronic Device |
| IEEE | Institute of Electrical and Electronics Engineering |
| MV | Medium Voltage |
| LV | Low Voltage |
| NSC | Negative Sequence Current |
| SAIDI | System Average Interruption Duration Index |
| SCADA | Supervisory Control and Data Acquisition |
| ZSC | Zero Sequence Current |
| ZSV | Zero Sequence Voltage |

Publications

- I. Farughian, A., Kumpulainen, L., & Kauhaniemi, K. (2018). Review of methodologies for earth fault indication and location in compensated and unearthed MV distribution networks. *Electric Power Systems Research*, 154, 373–380.
<https://doi.org/10.1016/j.epsr.2017.09.006>. © 2017 Elsevier B.V.
- II. Farughian, A., Kumpulainen, L., & Kauhaniemi, K. (2019). Earth Fault Location Using Negative Sequence Currents. *Energies*, 12(19), 3759.
<https://doi.org/10.3390/en12193759>. Under a Creative Commons License.
- III. Farughian, A., Kumpulainen, L., & Kauhaniemi, K. (2020). Non-Directional Earth Fault Passage Indication in Isolated Neutral Distribution Networks. *Energies*, 13(18), 4732.
<https://doi.org/10.3390/en13184732>. Under a Creative Commons License.
- IV. Farughian, A., Kumpulainen, L., Kauhaniemi, K., & Hovila, P. (2021). Intermittent Earth Fault Passage Indication in Compensated Distribution Networks. *IEEE Access*, 9, 45356–45366.
<https://doi.org/10.1109/ACCESS.2021.3067497>. Under a Creative Commons License.
- V. Farughian, A., Kumpulainen, L., Kauhaniemi, K., Pettissalo, S., & Sallinen, V. (2021). Technical requirements for practical implementation of fault passage indication. 2021 IEEE PES Innovative Smart Grid Technologies Europe (ISGT Europe), 01–06.
<https://doi.org/10.1109/ISGTEurope52324.2021.9640016>.
© 2021 IEEE. Reprinted with permission.

1 INTRODUCTION

1.1 Background

Uninterruptable supply of power is essential in today's electricity networks. Electricity networks are commonly subject to disturbances and interruptions originating from different types of faults. Some faults are temporary in nature. Wildlife, vegetation, wind, lightning, etc. can be sources of temporary faults (IEEE Guide Interruption Events, 2014), (IEEE Guide Distribution Relays, 2021), (Borghetti et al., 2021), (Napolitano et al., 2018). Some faults are permanent in nature, such as those caused by equipment failures, underground dig-ins, etc. (IEEE Guide Distribution Relays, 2021). Permanent faults may lead to electricity outage. Continuity of supply is measured by means of reliability indices. For instance, "*the System Average Interruption Duration Index (SAIDI) indicates the total duration of interruption for the average customer during a predefined period of time. It is commonly measured in minutes or hours of interruption*" (IEEE Guide Indices, 2012). Other indexes include MAIFI, SAIFI, CAIDI, ASAI, etc. Statistics show that the majority of electricity interruptions in Europe have originated from faults in medium-voltage, typically in the range of 1–70 kilovolts, networks (Siirto, 2016), (*CEER Benchmarking Report 5.2 on the Continuity of Electricity Supply*, 2015). Different types of faults can occur on distribution systems. Statistics show that countries that have a high percentage of underground cables (especially on medium voltage) generally have fewer interruptions (*CEER Benchmarking Report 6.1 on the Continuity of Electricity and Gas Supply*, 2018).

1.2 Smart distribution networks

Distribution networks are the link between transmission systems and customers. Many utilities are transitioning to the direction of smart distribution networks. The goal of smart distribution is to lower the number and duration of electricity interruptions and increase the efficiency of power delivery. Distribution automation pursues that goal through the integration of power measurements, bi-directional communications, analytical decision making, and supervision (IEEE Guide Smart Grid, 2019), (Das, 2016). Advanced automation, supervisory control, outage management systems, fault location, and fault management are important aspects of smart distribution.

Distribution automation is a foundational feature of smart distribution networks. It is “*a technique used to limit the outage duration and/or customers interrupted and restore service to customers through fault location identification and automatic switching*” (IEEE Guide Smart Grid, 2019).

1.3 Fault management

The majority of faults occurring in medium voltage (MV) distribution networks are temporary (IEEE Guide Distribution Relays, 2021), (Couto et al., 2017). These faults may originate from lightning-induced insulator flashovers, animal or tree contact to an energized line, or wind causing conductors to move together and flashover. These faults have a high chance of disappearing if the faulted segment is de-energized and isolated. The de-energizing is realized by opening a circuit breaker. After a delay, the isolated segment is restored. It is common in distribution networks to perform this type of tripping (de-energizing) and reclosing (re-energizing) sequence to increase the chance of clearing the fault (IEEE Guide Reclosing, 2021), (IEEE Guide Transmission, 2016). After the first reclosing, if the fault is still persistent, another sequence of tripping and reclosing switching may be carried out. These attempts may be continued until the fault has been cleared. After a certain number of attempts, if the fault still persists, then it is identified as a permanent fault.

When a permanent fault occurs on a section of a feeder, the faulted section needs to be identified and isolated (sectionalizing, segmentation). This functionality (sectionalizing) must be performed in such a manner that as few customers as possible are affected. Most distribution feeders operate in a radial configuration where load and fault currents flow in one direction (IEEE Guide Smart Grid, 2019), (Rios Penaloza et al., 2021). Therefore, the part of the feeder beyond the faulted section is left without supply. Reconfiguration thus needs to restore supply to the healthy sections. While reconfiguring the network, it is important to ensure that the operational constraints such as capacity constraints and voltage constraints are still satisfied. Distribution automation applications that perform these functions are called FDIR (fault detection, isolation, and restoration) or FLISR (fault location, isolation, and service restoration) and are most often used by utilities to improve their reliability across their distribution systems as it facilitates managing outages and recovering from them quickly (IEEE Guide Smart Grid, 2019), (Siirto, 2016).

The first step towards the FLISR functionality, i.e. identifying the faulted segment, is realized through fault passage indicators. “*Fault passage indicator or faulted*

circuit indicator (FCI) is a single or multi-phased device designed to sense fault current and provide an indication that the fault current has passed through the power conductor(s) at the point where the FCI sensor is installed” (IEEE Guide FPI, 2017). In this dissertation, the term fault passage indication (FPI) is used. By installing multiple FPI devices throughout the network, faulted segment identification can be achieved.

1.4 Fault location

Electrical power networks are subject to various types of faults. The most common type of fault in distribution networks is the single-phase-to-ground fault (Poethier et al., 2019), (Chollot et al., 2017). A single-phase earth fault is a failure occurring when one of the conductors is connected to ground. A falling tree, lightning strikes, birds, etc. can cause an earth fault. A reliable fault location method can help system operators to locate the actual fault in the network as soon as possible.

From an accuracy perspective, fault detection and location in distribution networks can be performed at three general levels. The following classification is based on the author’s observations during the research conducted for this dissertation.

1. Faulty feeder identification. It is determined on which feeder a fault has occurred. This is usually an integral part of feeder relay protection.
2. Fault passage indication (FPI). The faulted segment, e.g., lines or cables connecting two consecutive measuring points, is identified. FPI is realized through FPI devices. An FPI device aims at detecting the passage of a fault current through the measuring point at which the device is installed. By distributing multiple FPI devices at various locations throughout the network, faulted segment identification can be realized.
3. Distance estimation. The fault distance from the measurement point (usually the beginning of the faulted feeder) is estimated.

1.5 Network types

There are different factors affecting the amount of fault current in a network. One of them is the network’s type from the viewpoint of neutral treatment or neutral earthing arrangements. There are different practices regarding earthing the neutral point of a power system. The neutral of an MV distribution network is the

star point of the secondary windings of the HV/MV transformer located at the primary substation. The earthing arrangement impacts the earth fault current levels and permanent over voltages. In general, a low earthing impedance results in high earth fault currents but low over voltages during a fault condition. From the neutral treatment viewpoint, power distribution networks can be classified into four categories (Lakervi & Holmes, 1995):

1. **Directly earthed (or solidly grounded).** The neutral point of the system is directly connected to ground. High-voltage systems are often solidly grounded. Phase-to-ground voltages are the lowest but fault currents are high.
2. **Impedance earthed.** In this type of arrangement, the neutral is connected to ground through a resistor. Earth fault currents are lower in these types of networks than in networks with direct earthing.
3. **Isolated neutral (or unearthed or ungrounded).** In this type of network, the neutral is not grounded. Operating a system when its neutral point is not connected to ground leads to low earth fault currents. Earth fault currents are lower in these types of networks than in networks with direct earthing.
4. **Compensated (arc-suppression-coil earthing or resonant-grounded).** This involves connecting an adjustable inductance, known as Petersen's coil, between ground and the neutral. Petersen's coil is a tunable reactor used for impedance grounding a distribution or transmission system, and is usually tuned to be in resonance with the capacitance to ground of all system components (IEEE Guide Fault Location, 2015). In other words, it is adjusted so that it matches phase-to-ground capacitances of the network. The purpose of the Petersen coil is to reduce earth fault current by canceling out the capacitive component of the fault current. If adjusted correctly, earth fault currents are the lowest in this type of network. Resonant-grounded systems are widely used in European countries (IEEE Guide Distribution Relays, 2021), (Druml et al., 2014), (Schmidt et al. 2016). Benefits of this type of network include
 - Self-healing of the system without any intervention by protection systems, as the fault arc distinguishes.
 - Continuing the network operation during a sustained single line earth fault is possible. As a consequence, this reduces the number of interruptions of the customers power supply.

- Improved power quality and reliability for the customer.
 - Reduction of the current via the fault location to two to three percent of the whole capacitive current (Druml et al., 2014).
5. **Multi-grounded systems.** These types of networks are uncommon in European countries. They are often used in US and some developing countries. They *“have a neutral wire that is grounded at multiple locations along the length of the feeder. This is commonly referred to as a four-wire system supplied by a wye-grounded source. It provides power for single-phase and three-phase loads and is cost-effective for rural areas where single-phase loads are widely scattered. Phase-to-ground faults do not excessively affect voltage magnitudes on the other two healthy phases because the neutral is solidly grounded”* (IEEE Guide Distribution Relays, 2021).

1.6 Earth fault location

Different types of faults can occur in electricity networks. In general, there are two types of faults that are widely common in transmission lines and distribution networks; namely, short circuits and earth faults. A short circuit is an unwanted condition where there is an electrical path between two or more dissimilar energized phase conductors (IEEE Guide FPI, 2017). An earth fault is an unwanted condition where there is an electrical path between an energized phase conductor and ground. Statistics show that the majority of grid faults are earth faults (Druml et al., 2009). In the Nordic countries, about 50-80% of the faults are of the type earth fault (Hänninen, 2001).

Fault passage indication in case of short circuits is a straightforward task as in these types of faults, huge currents are involved. There are established methods for short circuit fault passage indication. However, there is not a globally accepted method for passage indication of earth faults. Accurate earth fault location and faulted segment identification in compensated and isolated networks are especially a more challenging task as the fault current in those types of networks is often small compared to load currents.

The magnitude of the fault current depends on several factors including the fault impedance, the location of the fault, the capacitance of the upstream network, and the length of the feeder.

In contrast to the typical earth fault, there is a special type of earth fault that is common in networks with underground cables. As opposed to typical sustained faults, this type of fault causes short but large current spikes that occur at irregular intervals. This type of fault is referred to as the intermittent earth fault. These faults require special attention as they are problematic for conventional relays and FPIs. As many DSOs are moving towards replacing their overhead lines with cables, the importance of reliably detecting and locating this type of fault is increasing. Therefore, there is a need for methods capable of locating these types of faults in addition to sustained earth faults.

1.7 Objectives of the work

The main objective of this work is to develop novel methods for locating single-phase earth faults in medium voltage distribution networks and validating them with simulations and real system measurements. Especially the goal is to develop the types of methods that can be implemented with the current technology or with technology that will become available in the near future. In addition, the aim is to answer the following research questions.

- What are the-state-of-the-art methodologies that are proposed or already in use and what are the current trends? What are the pros and cons of the existing methods?
- How do symmetrical sequence currents behave when the electricity network is under an earth fault condition?
- How can symmetrical sequence currents be utilized to locate the faulted segment of the network? How do the developed methods perform on different types of networks?
- How can the proposed methods be implemented in practice, and what are the technical requirements and apparatus? What is the efficacy of the proposed methods in practice in real distribution networks?

1.8 Thesis outline

The findings of this doctoral thesis are based on five publications. The remainder of the thesis is organized as follows.

Chapter 2 reviews the literature on the state-of-the-art methods for locating earth faults in distribution networks. It outlines the fundamental principles of existing

methods, classifies them, and highlights their limitations. This chapter is based on Publication I.

Chapter 3 serves as a basis for Chapter 4 and Chapter 5. The purpose of this chapter is to provide the theory behind the proposed methods that are introduced in Chapter 4 and Chapter 5.

Chapter 4 discusses two proposed methods for locating permanent earth faults in medium voltage distribution networks. The proposed methods are based on the theory presented in Chapter 3 and validated by means of simulation using a verified simulation model of a Finnish distribution network. The corresponding publications are Publication II and Publication III.

Chapter 5 deals with a special type of earth fault known as an intermittent earth fault. The corresponding publication is Publication IV.

Chapter 6 is devoted to technical aspects and requirements for implementing the proposed methods. Field tests verification is presented. The raw data used in this chapter is in the form of recordings obtained from an extensive series of field tests carried out by industrial partners. The corresponding publication is Publication V.

Chapter 7 concludes the dissertation by summarizing the findings and contributions of the research.

1.9 Scientific contribution

This research work attempts to advance the topic of earth fault location in medium voltage distribution networks. This work can be considered as theoretically oriented as well as practically oriented. The main contribution consists of the proposed new fault location methods. They were developed during the doctoral research which was mostly carried out in collaboration with industrial partners. In this way, it was ensured that the findings would meet the needs and requirements of industry as much as possible. In addition, industrial partners provided, to some extent, practical data in the form of recordings that helped with better understanding and studying the subject. In addition, they facilitated the experimental verification of the proposed methods and validation of the simulation results. The scientific contributions of this doctoral dissertation can be summarized as follows:

- Providing an in-depth understanding of the subject through assessing the literature and recognition of the possible future direction of earth fault location techniques.
- Developing novel FPI-based fault locating methods by further developing existing solutions along with the development of a solid theoretical foundation.
- Taking the first steps towards implementing the proposed methods in practice.

1.10 Summary of publications

Publication I reviews state-of-the-art techniques that are proposed in the literature up until the year 2018. It outlines the operational principles of each method. In addition, it carries out a comparative analysis highlighting pros and cons of each method.

Publication II puts forward a fault-passage-indication technique with which faulted segment identification can be realized. The theory behind the method is discussed. The method is applicable to both isolated networks and compensated networks.

Publication III proposes a method applicable only to a specific type of network i.e. the neutral isolated network. The simulation model used in the study is a verified model of a Finnish distribution network.

Publication IV builds upon the proposed method presented in Publication II. It adapts the method for a special type of earth fault known as intermittent earth-faults.

Publication V discusses the apparatus and technical aspects of the proposed methods. In addition, it presents, to some extent, experimental verification.

1.11 Other publications

Farughian, A., Poluektov, A., Pinomaa, A., Ahola, J., Kosonen, A., Kumpulainen, L., & Kauhaniemi, K. (2018). Power line signalling based earth fault location. *The Journal of Engineering*, 2018(15), 1155–1159.
<https://doi.org/10.1049/joe.2018.0190>

Raipala, O., Hovila, P., Leminen, J., Farughian, A., Memon, A., & Kauhaniemi, K. (2019, June 3). Utilization of a mixture of CTs and current sensors in line differential protection applications. <https://doi.org/10.34890/1026>

2 EARTH FAULT LOCATION – OVERVIEW

This chapter is based on Publication I. It reviews state-of-the-art methods for determining the location of faults in medium-voltage distribution lines. It outlines the operational principles of each method. This chapter intends to answer the following questions that were raised earlier.

What are the-state-of-the-art methodologies that are proposed or already in use and what is the current trend? What are the pros and cons of the existing methods?

2.1 Introduction

Distribution automation is a distinguished application of smart distribution networks. It aims at a self-healing system that locates the fault, isolates the faulted segment, and performs supply restoration (FLIR functionality). A reliable fault location method is a pre-requisite to this functionality and also helps with faster restoration of a power system following an outage caused by a fault. Various techniques have been put forward in the literature to determine the location of faults in transmission and distribution networks. In this chapter, the focus is on methods intended for locating earth faults in distribution networks even though some of the methods that will be discussed are capable of locating short-circuit faults as well. In general, earth fault location methods can be classified into two main categories: centralized methods and decentralized methods, as shown in Figure 1. This classification in this dissertation is based on the distribution of measuring points and their locations. The measurements required by centralized methods are mainly made at one location, which is normally the primary substation. In decentralized methods, measuring points are distributed along the feeders and communicate with a control center.

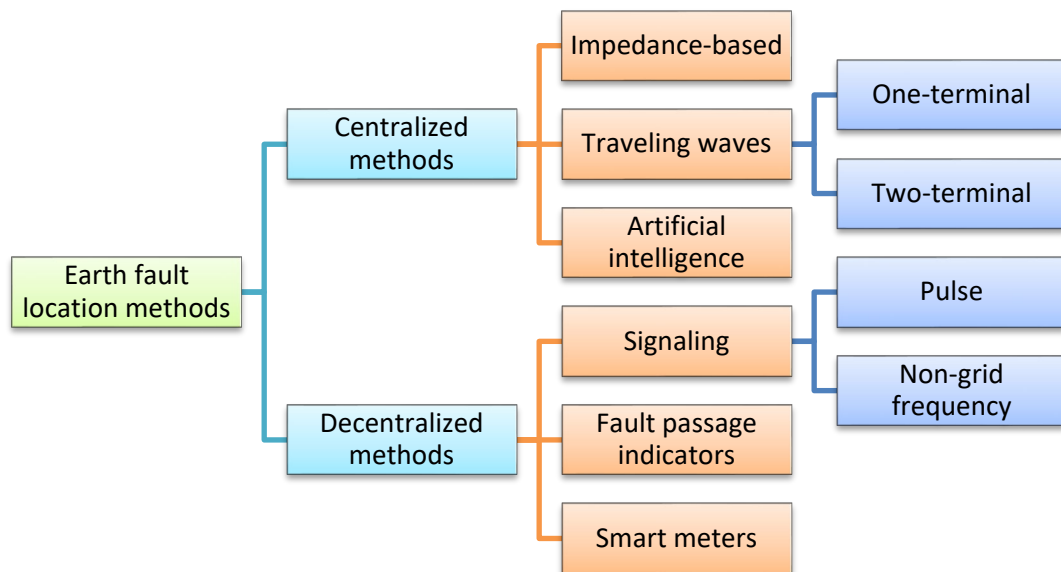


Figure 1. Classification of earth fault location methods (modified figure, from Publication I).

2.2 Centralized methods

2.2.1 Impedance-based

Impedance-based fault location is based on calculating the apparent impedance seen when looking into the line from one end during the faulted period (IEEE Guide Fault Location, 2015). The line length between the measuring point and the fault point is proportional to the calculated apparent impedance. Therefore, the fault distance from the measuring point can be estimated if the line impedance per unit is known. If the fault resistance is assumed to be zero, estimating the fault distance will be straightforward. Unfortunately, in practice, the fault resistance is unknown and usually not zero, especially in overhead lines. In impedance-based methods, making false assumptions regarding the fault impedance and line parameters may result in a substantial error in the estimated fault distance. To overcome the challenges of unknown fault resistance and uncertain line parameters, Ref. (Iurinic et al., 2016) attempts to estimate the line parameters and fault resistance by proposing a diode-based model for the fault. The paper claims that using this model, the fault distance and line parameters estimation can be performed as a minimization problem. However, the proposed method has not been verified through field tests. A more practically-oriented approach is presented in (Altonen & Wahlroos, 2007). The method is specifically devised for

isolated networks. It is based on symmetrical sequence circuit analysis. The whole load is modelled as on equivalent tap load. The method considers two scenarios regarding the locations of the load and the earth fault and analyzes the resulting sequence circuits to give an estimation of the distance. Ref. (Altonen et al., 2011) utilizes the concept presented in (Altonen & Wahlroos, 2007) and adapts the proposed method for compensated networks. The paper claims that the proposed method's dependability on line parameters accuracy is low, however, the method may perform poorly in case of high impedance earth faults. Ref. (Altonen & Wahlroos, 2013) further advances the method presented in (Altonen et al., 2011) for compensated MV networks and puts forward a method which requires a fewer number of settings. The authors of references (Altonen & Wahlroos, 2007), (Wahlroos & Altonen, 2009), (Altonen et al., 2011) and (Altonen & Wahlroos, 2013) some years later shifted their attention from impedance-based methods towards developing fault passage indicators (FPI). FPI-based methods are discussed in Section 2.3.2. Another method is presented in Ref. (Kulkarni et al., 2014) that deploys data provided by power quality monitoring devices and relays. It estimates the fault distance in terms of the line impedance.

2.2.2 Traveling waves

When a fault takes place on a power system, high-frequency voltage and current transients are generated at the fault location. They propagate away from that point in both directions towards the line ends. The propagation velocity at which these transients travel along the line is close to the speed of light. The exact propagation velocity depends on the medium. The fault distance from a specified measuring point can be estimated by capturing the exact arrival times of these waves (voltage or current transients) at the measuring point(s) and knowing the propagation velocity. These methods are also referred to as transient-based methods in some research papers. The operational principle of the traveling-wave methodology is illustrated in Figure 2. From the number of measuring points' viewpoint, there are two types of implementation namely: one-terminal, and two-terminal. In the one-terminal method, there is one measuring point from which the fault distance can be obtained as follows (IEEE Guide Fault Location, 2015):

$$d = v \times \frac{\Delta t}{2} \quad (2.1)$$

where v is the propagation velocity of the traveling wave in the line, and Δt is the time difference in the arrivals of the first traveling wave and its reflection.

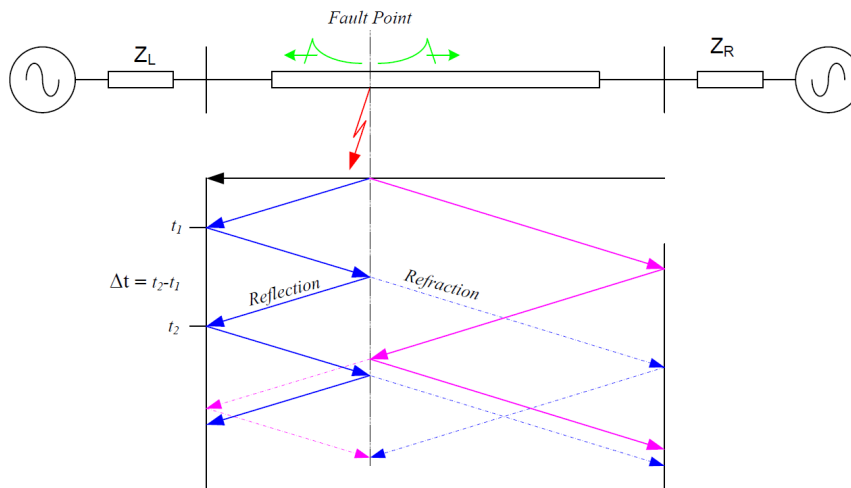


Figure 2. Lattice diagram illustrating reflections and refractions of traveling waves caused by a fault on a power line (IEEE Guide Fault Location, 2015).

In theory, if the lines are homogenous and the accurate propagation velocity is known, the exact fault distance can be obtained. However, in practice, feeders may partly consist of overhead lines and partly of cables. For instance, it is common in Finland for feeders in rural distribution networks to be cables near primary and secondary substations and to be overhead lines elsewhere. As the propagation velocity in overhead lines differs from the propagation velocity in cables, using the basic traveling-wave methodology may lead to an inaccurate or even wrong fault location estimation. In addition, distribution networks consist of many laterals and branches. This means that the reflection captured at the measuring point may have come from various sources and not necessarily from the actual fault. There have been attempts to address the latter problem. Ref. (Elkalashy et al., 2015) and Ref. (Sadeh et al., 2013) claim to have overcome the problem by utilizing the aerial mode 1 reflected pulse which is caused only by the fault. There have been other attempts to apply traveling-wave methodology on distribution networks (Liang et al., 2015). Ref. (Borghetti et al., 2008) proposes an approach using continuous wavelet transform (CWT). The method is based on analyzing the voltage transients caused by the fault. The paper claims that a correlation exists between some characteristic frequencies of the transformed signals and the paths the transients come from. Therefore, using the correlations, the faulted paths can be distinguished from unfaulted paths. However, there is no experimental verification of the method provided. A similar method presented in (Borghetti et al., 2010) is lab tested. There have been other studies on application of transients and CWT on fault localization on distribution power networks (Paolone et al., 2011) and (Rios Penaloza et al., 2021). Ref. (Druml et al., 2019) reports that fault location methods based on traveling-wave methodology have been implemented

in practice and are already in use in some countries for locating faults on transmission lines. However, these methods have not yet been implemented in distribution networks. The paper presents the results of a study on an experimental implementation of a traveling-wave-based method in a 20-kV distribution network.

2.2.3 Artificial intelligence

Methods employing Artificial Intelligence (AI) involve training an artificial intelligent system to determine the faulted area. AI-based methods have been successful in research areas such as image processing area, face recognition, etc. This has inspired researchers to attempt to apply these methods in power networks as well. The results of using such approaches are reported in (Mora et al., 2006), (Martins et al., 2003), (Mora-Florez et al., 2007), (Chunju et al., 2007), (Pourahmadi-Nakhli & Safavi, 2011), (Rafinia & Moshtagh, 2014). A more realistic effort to apply AI for fault localization purposes is presented in (Balouji et al., 2020). It proposes a machine learning based framework not for fault location but for faulty feeder identification. The framework is also applied for determining the type of fault i.e. earth fault, short circuit, etc. The data used for this study is obtained from protection relays recordings from a set of field tests carried out earlier on an MV Finnish distribution network. A total of 174 recordings from three feeders are used for training the system. The recordings include fault tests with the fault resistance ranging from 0 to 20 k Ω . The dataset with which the performance of the proposed framework is assessed is taken from another grid. The authors claim that the results show the efficacy of the framework. However, the presented framework is limited to faulted feeder identification and not intended for faulted segment identification. Overall, it can be observed that despite the research studies on the application of AI in fault localization in distribution networks, the number of research papers on these methods appears to be declining and it is hard to find references reporting on the practical implementation of these types of methods.

2.3 Decentralized methods

2.3.1 Signal injection

Injection-based methods involve injecting a pulsating signal or a non-grid-frequency current into the neutral of the system during a fault occurrence. The injected signal is detectable only on the faulted line from the injection point up to the fault point. Faulted-segment-identification can be realized by tracing the

injected signal. Ref. (Druml et al., 2012) outlines a method that is based on injecting current pulses of length 1 s. According to (Druml et al., 2012), such a signal can be generated by switching on and off a capacitor bank installed in parallel with the Petersen coil. The effectiveness of the method is limited to low-ohmic faults. One of the major drawbacks, in addition to its failure in case of high-impedance faults, is that the fault condition must persist for a minimum of 25 s, which is much too long. To overcome the restrictions of the method, a fast-pulse method utilizing high power current injection with a non-grid-frequency, has been presented in (Druml et al., 2013). The main principle of the method is illustrated in Figure 3. Ref. (Tengg et al., 2013) reports on the results of field testing the method.

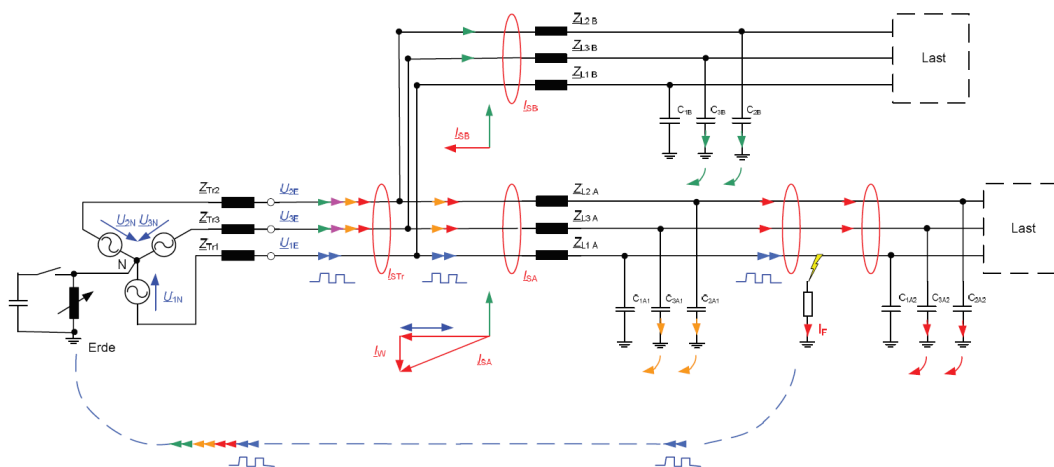


Figure 3. Earth fault location by injecting a signal to the neutral during an earth fault occurrence (Druml et al., 2013).

Ref. (Buigues et al., 2012) reviews a number of research studies conducted on signal injection methodologies among which (Raunig et al., 2010) is noteworthy. The algorithm presented in (Raunig et al., 2010) is devised for compensated networks. A non-grid-frequency current with the amplitude of 1 A and frequency of 183 Hz is injected to the neutral through the Petersen coil. Tracking the injected signal is realized through magnetic field detection sensors that are tuned to the frequency of 183 Hz and installed along the faulted feeder.

In general, signal-injection methodology is primarily intended for compensated networks. However, Ref. (Stipetić et al., 2021) claims to have applied a signal-injection method on an isolated neutral network with inaccessible neutral. The study, however, has been carried out using only simulations with no empirical verification.

2.3.2 Fault-passage-indication based methods

The purpose of Fault Passage Indication (FPI) in distribution networks is to find, on the faulty feeder, the faulted section. As stated in Publication V, FPI aims at indicating if any fault current has passed through the measuring point at which the FPI device is installed. By installing multiple FPI devices at various locations (typically secondary substations) throughout the network, the faulted section identification can be achieved and visualized for the system operator. In general, the more FPI devices installed throughout the network, the more accurate fault location can be achieved. Some of the FPI applications utilize feeder protection relay principles.

In (Wahlroos & Altonen, 2009), a neutral-admittance-based method is proposed for identifying the faulted feeder. It is based on calculating an admittance for each feeder based on the centralized residual voltage (measured across the Petersen coil) and zero sequence currents of feeders. The determination regarding the on/off-fault-passage is made based on the sign of the real part of the calculated zero sequence admittance so that a negative admittance signifies a faulted feeder (on the fault passage). A positive value is indicative of an unfaulted feeder (off the fault passage). The method is a fundamental-frequency-based method. Ref. (Altonen & Wahlroos, 2016) introduces a concept referred to as “cumulative phasor summing”. The concept was originally developed for feeder protection relays. The purpose of the concept is to utilize other frequencies components i.e. harmonics in addition to the fundamental frequency component. Ref. (Wahlroos & Altonen, 2014) utilizes this concept to advance the method presented in (Wahlroos & Altonen, 2009). It introduces a patented concept referred to as “multi-frequency admittance”. According to (Wahlroos et al., 2013) and (Wahlroos & Altonen, 2014), the fundamental frequency component guarantees protection sensitivity, while the harmonics are used to improve the security of the fault directional determination. Ref. (Altonen et al., 2017) reports on the results of experimenting with this method as FPI in a compensated distribution network. The results show the effectiveness of the method for low-impedance earth faults. As the fault resistance increases, the performance of the method decreases. In addition, the results highlight the adverse effect of local over-compensation caused by distributed compensators. Another method that is based on the residual current and voltage phasors is a patented method proposed in (Drouere & Mecreant, 2016). The method calculates “active current” I_{active} using the following formula:

$$I_{active} = \frac{Real\{I \times U^*\}}{\|U\|} \quad (2.2)$$

in which I and U are the phasors of the residual current and voltage, respectively and denotes the module of U . For a given point, the determination regarding its on/off-fault-passage status is made based on the sign of I_{active} .

In (Lehtonen et al., 2014) and (Pettissalo, 2017), two methods for earth fault FPI are devised which appear to be similar in essence. They both employ symmetrical sequence currents and are based on comparing the zero sequence current with the negative sequence current. They assume that for a given point located on the fault path, the change in the negative sequence current as a result of the earth fault occurrence is greater than a certain fraction of the change in the zero sequence current.

2.3.3 Smart meters

In neutral compensated networks, the fault current is low. For reliable earth fault detection and protection, protective relays need the magnitude of the resistive component of the fault current to be large enough. To ensure selective tripping, it is common practice for some DSOs to momentarily insert an auxiliary resistor in parallel with the centralized Petersen coil. The auxiliary resistor is used to temporarily increase the resistive component of the fault current (IEEE Guide Neutral Grounding, 2015). Ref. (Topolanek et al., 2015) proposes a method for locating earth faults in these types of compensated networks that are equipped with the auxiliary resistor. The method requires devices monitoring the low voltage at the LV network. In addition, the recorded data from these devices must be properly time-synchronized. According to (Topolanek et al., 2015), the connection of the auxiliary resistor in order to increase the fault current causes voltage sag on LV sides of distribution transformers. The highest voltage sag occurs at MV/LV substations located behind the fault point and the smallest voltage sag takes place in MV/LV substations that are closest to the HV/MV substation or at substations located on healthy feeders. The fault point is determined to be between the substation(s) with the highest recorded voltage sag and the substation(s) with the second highest voltage sag. The performance of the proposed method is evaluated using simulations. The results show the limitations of the method for earth fault with resistances higher than 800 Ω .

There have been some other similar attempts. For instance, fault location schemes proposed in (Pereira et al., 2009), (Estebansari et al., 2016), (Jia et al., 2015) and (Trindade et al., 2014) employ smart meters for monitoring asymmetry in phase voltages at different measuring points distributed along the feeder. Despite the availability of smart meters at LV side today, these methods seem to lack empirical verification.

2.4 Discussion

Earth fault location has been a challenge for distribution system operators. In the literature, various methods have been proposed. In theory, the most accurate fault location method is the traveling-waves-based method. In practice, since distribution feeders may consist of many branches, the reflection arriving at the measuring terminal might have come from sources other than the actual fault. In addition, applying these methods in distribution feeders with several branches means that an estimated fault distance could result in several fault location candidates whose distances from the measuring point are the same. On the other hand, faulted segment identification using fault passage indicators has shown promising results. By commissioning more FPI devices throughout the network, more accurate fault location can be achieved. Therefore, the combination of FPI and traveling-waves methods could overcome the drawbacks of each method so that FPI would identify the faulted segment and rule out the fault locations candidates obtained from the fault distance estimated by a traveling-waves method. A hybrid method that combines FPI and the injection method is presented in (Hand & Donagh, 2010). Once FPIs along the network have identified the faulted segment, a signal is injected to the neutral. The signal is tracked with the help of a portable fault passage indicator.

To facilitate a comparison between the presented methods, the characteristics of the more important methods, along with their pros and cons, are summarized in Table 1. AI methods are not included in the table.

Table 1. Summary of the main characteristics of the main methods (Publication I, modified).

| | Impedance based | Traveling wave | Injection | FPI | Smart meters |
|------------------------|---|--|--|---|--|
| Main advantages | <ul style="list-style-type: none"> • Simple implementation • Cost effective | <ul style="list-style-type: none"> • Most accurate in theory | <ul style="list-style-type: none"> • To some extent, verified in practice • Only current measurements required along the feeders | <ul style="list-style-type: none"> • Verified functionality • High sensitivity • Supported by smart grid development | <ul style="list-style-type: none"> • Devices already available |
| Main drawbacks | <ul style="list-style-type: none"> • Dependent on line parameters estimation | <ul style="list-style-type: none"> • Reflections and refractions coming from branches | <ul style="list-style-type: none"> • Requires an additional injection device | <ul style="list-style-type: none"> • Only faulted segment is identified and | <ul style="list-style-type: none"> • Effectiveness unknown as not many imple- |

| | Impedance based | Traveling wave | Injection | FPI | Smart meters |
|--|--|---|---|--|---------------------------------------|
| | | <ul style="list-style-type: none"> Limited experience in distribution networks | <ul style="list-style-type: none"> Applicable only to compensated networks | not the exact location | mentations reported in the literature |
| Applicable in compensated networks | No | Yes | Yes | Yes | Yes |
| Applicable in isolated neutral networks | Yes | Yes | Mostly no | Yes | Yes |
| Verified by field tests | Yes | <ul style="list-style-type: none"> High sampling rate Costly detection device | <ul style="list-style-type: none"> Injection device at the primary substation, Current sensors Communication | <ul style="list-style-type: none"> IEDs along the feeder At least current sensors Communication | Not extensively |
| Highlighted requirements | <ul style="list-style-type: none"> Requires measurement accuracy Network data | <ul style="list-style-type: none"> High sampling rate Extremely accurate timing | <ul style="list-style-type: none"> Injection device at the primary substation, Current sensors Communication | <ul style="list-style-type: none"> Current sensors Communication | Time-synchronization |
| Outlook | <ul style="list-style-type: none"> Less common in future Shift towards more accurate methods | <ul style="list-style-type: none"> Promising Worth further investigations | Worth further investigations | Along with development of smart grids, they will be increasingly common | Unclear |

3 THEORETICAL BACKGROUND

This chapter is dedicated to the theory behind the two methods proposed for locating earth faults. These two methods are discussed in depth in Chapter 4. The theoretical analysis presented in this chapter is conducted based on “symmetrical components and sequence networks” theory. The concept of symmetrical components was introduced by Charles LeGeyt Fortescue in 1918 and published in (Fortescue, 1918). The newly introduced concept considerably facilitated the analysis of unbalanced polyphase systems by converting problems into equivalent symmetrical systems. The concept was originally developed through investigating the operation of induction motors under unbalanced conditions (Brittain, 1998). After that, the applications of symmetrical components started to expand to other disciplines as well. A review of the history and evolution of symmetrical components is published in (Chicco & Mazza, 2019).

In this chapter, the “symmetrical components and sequence networks” theory is deployed for analyzing the sequence currents of a network under single-phase earth fault conditions. The objective is to gain insight into the behaviors of symmetrical sequence currents along a faulted feeder in two types of networks, namely the neutral-isolated network and the compensated network. The chapter answers the question: *How do symmetrical sequence currents behave when the electricity network is under an earth fault condition?* The findings of this chapter will form the basis for the proposed fault location methods.

Throughout chapters 3 to 6, capital letters in bold denote phasors and the three phases are designated by indices a , b , and c . It is assumed that the positive sequence is abc . Phasors representing currents will be designated by I with indices. Phasors representing voltages will be designated by U with indices.

3.1 Background

According to “symmetrical components and sequence networks” theory, the phasors of a - b - c quantities can be converted into their symmetrical sequence components and vice versa using A and A^{-1} matrixes as follows:

$$A = \begin{bmatrix} 1 & 1 & 1 \\ 1 & \alpha^2 & \alpha \\ 1 & \alpha & \alpha^2 \end{bmatrix} \quad A^{-1} = \frac{1}{3} \begin{bmatrix} 1 & 1 & 1 \\ 1 & \alpha & \alpha^2 \\ 1 & \alpha^2 & \alpha \end{bmatrix} \quad (3.1)$$

In A and A^{-1} , the operator α causes a rotation of 120° in the counterclockwise direction i.e. $\alpha = 1 \angle 120^\circ$. For example, a - b - c phase currents can be expressed in terms of the symmetrical components of current I_a and vice versa as:

$$\begin{bmatrix} I_a^{(0)} \\ I_a^{(1)} \\ I_a^{(2)} \end{bmatrix} = A^{-1} \begin{bmatrix} I_a \\ I_b \\ I_c \end{bmatrix} \quad \begin{bmatrix} I_a \\ I_b \\ I_c \end{bmatrix} = A \begin{bmatrix} I_a^{(0)} \\ I_a^{(1)} \\ I_a^{(2)} \end{bmatrix} \quad (3.2)$$

In equation (3.2), $I_a^{(0)}$, $I_a^{(1)}$, $I_a^{(2)}$ are the zero, positive, and negative sequence components of I_a , respectively and I_a , I_b and I_c are the current phasors of phases a , b , and c . By definition, the zero sequence components calculated for each phase are identical and the negative sequence components calculated for each phase are equal in magnitudes. The methods proposed in this thesis are based on the magnitudes of zero and negative sequence currents and not their phase angles. Therefore, it does not matter for which phase the sequence components are calculated. For simplicity, in this thesis, the sequence components are calculated for phase 'a' as follows (phasor representation):

$$I_a^{(0)} = \frac{1}{3} (I_a + I_b + I_c) \quad (3.3)$$

$$I_a^{(2)} = \frac{1}{3} (I_a + \alpha^2 I_b + \alpha I_c) \quad (3.4)$$

Throughout the dissertation, sequence components are calculated as a function of time. For each cycle, the phasors of phase currents are calculated using the fast Fourier transform. Then, for each cycle, the sequence components are calculated from the resulting phasors using equations (3.3) and (3.4). To calculate sequence currents, the Three-Phase Sequence Analyzer block available in MATLAB/SIMULINK® is employed. It outputs the magnitudes and phase-angles of the symmetrical components of a set of input signals. The signals can contain harmonics or not. The three sequence components of a set of three signals are computed as follows: first, the block computes the phasors of the three phase currents by applying a discrete Fourier analysis over a sliding window of one cycle of the specified frequency (i.e. 50 Hz in the simulations of this dissertation). Then the transformation is applied to the resulting phasors to compute the sequence components (Matlab Help, 2022).

3.2 Sequence currents in neutral-isolated networks and compensated networks

Distribution networks can be classified into different types from the viewpoint of their grounding principles (neutral point treatment). In the following, the behaviors of sequence currents are examined in two types of networks using numerical examples. The networks under study are of the types neutral-isolated (unearthed) and compensated. Throughout this chapter and this thesis, the following notations are used.

List of notations

$I_{pre}^{(0)}$ ZSC phasor computed for pre-fault period at the measuring point in question

$|I_{pre}^{(0)}|$ Magnitude of $I_{pre}^{(0)}$

$I_{dur}^{(0)}$ ZSC phasor computed for during-fault period at the measuring point in question

$|I_{dur}^{(0)}|$ Magnitude of $I_{dur}^{(0)}$

$\Delta I^{(0)}$ $|I_{dur}^{(0)}| - |I_{pre}^{(0)}|$

$\Delta I_N^{(0)}$ $\Delta I^{(0)}$ calculated for the measuring point in question / $\Delta I^{(0)}$ calculated for point at the beginning of the feeder

$I_{pre}^{(2)}$ NSC phasor computed at the measuring point in question

$|I_{pre}^{(2)}|$ Magnitude of $I_{pre}^{(2)}$

$I_{dur}^{(2)}$ NSC phasor computed for during-fault period at the measuring point in question

$|I_{dur}^{(2)}|$ Magnitude of $I_{dur}^{(2)}$

$\Delta I^{(2)}$ $|I_{dur}^{(2)}| - |I_{pre}^{(2)}|$

$\Delta I_N^{(2)}$ $\Delta I^{(2)}$ calculated for the measuring point in question / $\Delta I^{(2)}$ calculated for the point at the beginning of the feeder

3.2.1 Sequence currents in neutral-isolated networks

Figure 4 shows a simplified distribution line to which no load is connected. It consists of series resistances R and shunt line-to-ground capacitances C . In order to facilitate the understanding of sequence currents behaviors, the line section under study is a simplified one. Detailed line models with parameters based on actual overhead lines and underground cables in a verified PSCAD model of an MV distribution network will be used in the simulations reported in Chapter 4. The line-to-line voltage of the network of Figure 4 is 21 kV (rms). The neutral point N is unearthed which resembles a neutral-isolated (unearthed) network. For simplicity, the series impedances of the lines are represented only by resistances R . The values for resistances R , capacitances of the line-to-ground C , and system frequency f are given by:

$$R = 1 \Omega \quad C = 1 \mu F \quad f = 50 \text{ Hz} \quad (3.5)$$

A single line-to-ground fault occurs between Point 4 and Point 5 on the conductor of phase 'a'. The fault resistance $R_F = 100 \Omega$ causes the fault current i_F to be 107 A (rms) at steady state. The fault current is shown in Figure 5. Using equations (3.3) and (3.4), the zero and negative sequence currents can be calculated. The calculated zero and negative sequence magnitudes as a function of time for the measuring points are shown in Figure 6 and Figure 7, respectively. The figures show the pre-fault periods i.e. from $t = 0 \text{ s}$ to $t = 0.1 \text{ s}$ and the during-fault periods from $t = 0.1 \text{ s}$ to $t = 0.2 \text{ s}$. The magnitudes of the calculated sequence phasors are given in Table 2 (refer to the list of notations provided in Section 3.2). The values are calculated for the pre-fault period ($|I_{pre}^{(0)}|$ and $|I_{pre}^{(2)}|$) and for the steady state of the during-fault period ($|I_{dur}^{(0)}|$ and $|I_{dur}^{(2)}|$). As the system under study is perfectly symmetrical, the zero and negative sequence currents are 0 A in the pre-fault period. In addition, for each point, the increase in the magnitude of the sequence currents ($\Delta I^{(0)}$ and $\Delta I^{(2)}$) along with the division of values by the value at Point 1 ($\Delta I_N^{(0)}$ and $\Delta I_N^{(2)}$) are presented.

On-the-fault-passage

At measurement Point 1, the zero sequence current (ZSC) is 0 A as the neutral (Point N) of the network is unearthed and therefore, there is no path for the ZSC to flow. The ZSC increases as we move from Point 2 to Point 4 so that just before the fault point, it reaches its maximum value of 24.18 A. As can be seen, the ZSC increases in such a manner that the ZSC level at a given point is proportionate to the summation of all the line to ground capacitances of the line section from the beginning of the line up to the given point. On the contrary, the negative sequence

current (NSC) remains almost constant at around 48 A from Point 1 to Point 4 so that $\Delta I_N^{(2)}$ is 1.00.

Off-the-fault-passage

The ZSC starts to decrease from Point 5 to Point 6. The ZSC level at a given point is proportionate to the summation of all the line-to-ground capacitances of the line section from the given point to the end of the line. The NSC level is low at Point 5 and Point 6 but not completely zero.

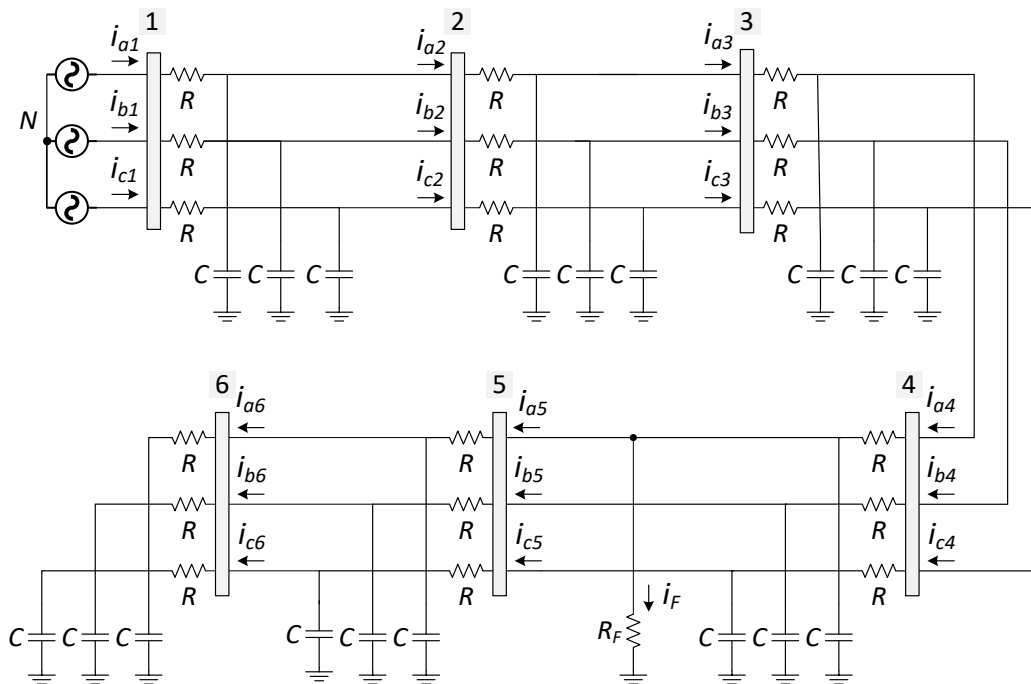


Figure 4. Simplified isolated distribution line under earth fault condition.

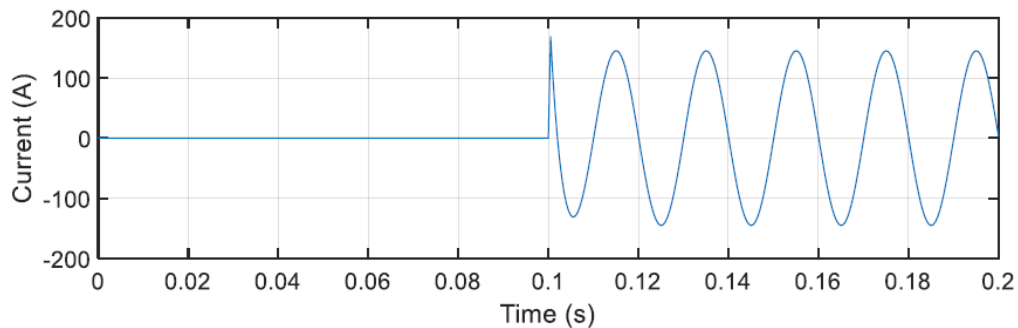


Figure 5. Earth fault current i_F in the simplified isolated network shown in Figure 4.

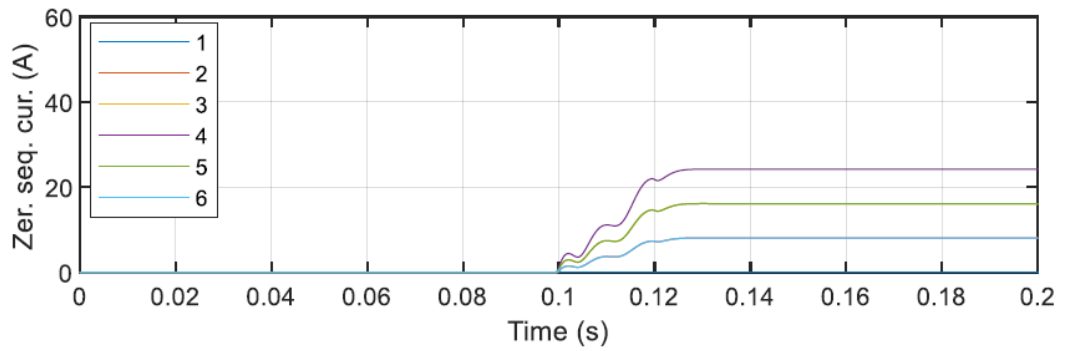


Figure 6. Zero sequence currents calculated for measuring points of network shown in Figure 4.

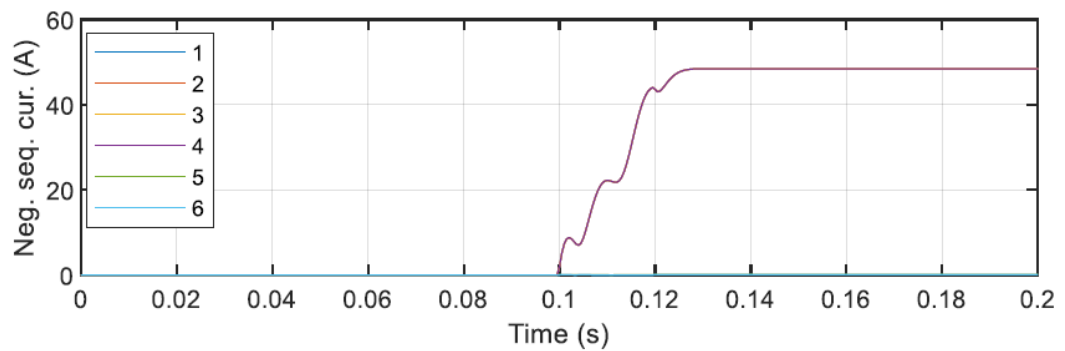


Figure 7. Negative sequence currents calculated for measuring points of network shown in Figure 4.

Table 2. Sequence currents along the faulted feeder of the unearthed network of Figure 4.

| Point | 1 | 2 | 3 | 4 | 5 | 6 |
|----------------------|-------|-------|-------|-------|-------|------|
| On/off fault passage | On | On | On | On | Off | Off |
| $ I_{pre}^{(0)} $ | 0.00 | 0.00 | 0.00 | 0.00 | 0.00 | 0.00 |
| $ I_{dur}^{(0)} $ | 0.00 | 8.06 | 16.12 | 24.18 | 16.12 | 8.06 |
| $\Delta I^{(0)}$ | 0.00 | 8.06 | 16.12 | 24.18 | 16.12 | 8.06 |
| $ I_{pre}^{(2)} $ | 0.00 | 0.00 | 0.00 | 0.00 | 0.00 | 0.00 |
| $ I_{dur}^{(2)} $ | 48.38 | 48.38 | 48.36 | 48.36 | 0.12 | 0.06 |
| $\Delta I^{(2)}$ | 48.38 | 48.38 | 48.36 | 48.36 | 0.12 | 0.06 |
| $\Delta I_N^{(2)}$ | 1.00 | 1.00 | 1.00 | 1.00 | 0.00 | 0.00 |

3.2.2 Sequence currents in compensated networks

Now consider the simplified compensated network shown in Figure 8. It has a single feeder to which no load is connected. Similarly, it consists of the same series resistances and shunt line-to-ground capacitances. The neutral point N is grounded through the Petersen coil. The purpose of the Petersen coil is to reduce the fault current by compensating the capacitive component of the fault current. In compensated networks with the compensation degree of 100 %, the Petersen coil is tuned so that all the capacitive components of the fault current is canceled out. Therefore, the value of the Petersen coil L_p for a 100% compensation can be obtained as follows:

$$j2\pi f L_p = -\frac{1}{18 j2\pi f C} \quad (3.6)$$

$$L_p = \frac{1}{18(2\pi)^2 f^2 C} \quad (3.7)$$

$$L_p = \frac{1}{18 \times (2\pi)^2 \times 50^2 \times 1 \times 10^{-6}} H \quad (3.8)$$

$$L_p = 0.5629 H \quad (3.9)$$

The same earth fault occurs on the conductor of phase 'a'. The fault current is shown in Figure 9. In this case, the fault current i_f in the steady state drops to around 2 A rms thanks to the Petersen coil. Zero and negative sequence currents can be calculated for the steady state using equations (3.3) and (3.4). The magnitudes of the calculated sequence phasors are given in Table 3.

On-the-fault-passage

Unlike in the isolated feeder, the ZSC level now decreases as we move from Point 1 to Point 4 so that at Point 4, it drops to 2 A (rms). Unlike in the isolated feeder, the ZSC level at a given point is not proportionate to the summation of all the line-to-ground capacitances of the line section from the beginning of the line up to the given point. However, the NSC behaves in a similar way as in the isolated feeder. It remains almost unchanged from Point 1 to Point 4 so that $\Delta I_N^{(2)}$ is 1.00.

Off-the-fault-passage

The ZSC starts to decrease from Point 5 to Point 6. The ZSC level at a given point is proportionate to the summation of all the line-to-ground capacitances of the line

section from the given point to the end of the line. The NSC level is low at Point 5 and Point 6 so that $\Delta I_N^{(2)} < 1$.

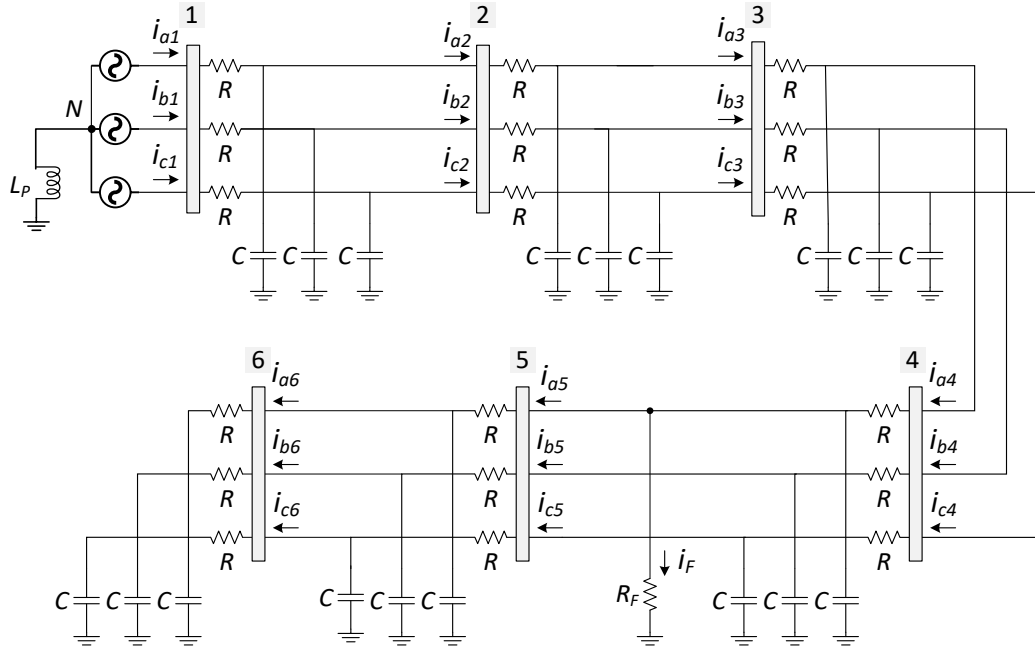


Figure 8. Simplified compensated distribution line under earth fault condition.

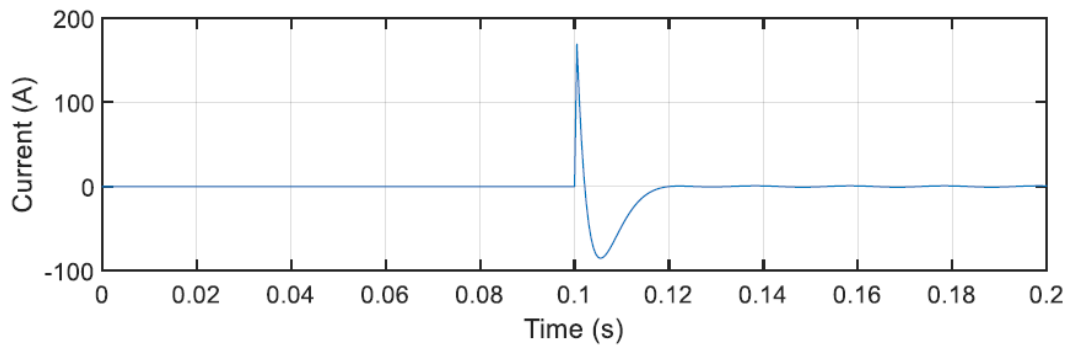


Figure 9. Earth fault current i_F in simplified compensated network shown in Figure 8.

Table 3. Sequence currents along the faulted feeder the compensated network of Figure 8.

| Point | 1 | 2 | 3 | 4 | 5 | 6 |
|-----------------------------|-----------|-----------|-----------|-----------|------------|------------|
| On/off fault passage | On | On | On | On | Off | Off |
| $ I_{pre}^{(0)} $ | 0.00 | 0.00 | 0.00 | 0.00 | 0.00 | 0.00 |
| $ I_{dur}^{(0)} $ | 55.81 | 46.49 | 37.19 | 27.90 | 18.60 | 9.30 |
| $\Delta I^{(0)}$ | 55.81 | 46.49 | 37.19 | 27.90 | 18.60 | 9.30 |
| $\Delta I_N^{(0)}$ | 1.00 | 0.83 | 0.66 | 0.49 | 0.33 | 0.16 |
| | | | | | | |
| $ I_{pre}^{(2)} $ | 0.00 | 0.00 | 0.00 | 0.00 | 0.00 | 0.00 |
| $ I_{dur}^{(2)} $ | 0.27 | 0.27 | 0.27 | 0.27 | 0.00 | 0.00 |
| $\Delta I^{(2)}$ | 0.27 | 0.27 | 0.27 | 0.27 | 0.00 | 0.00 |
| $\Delta I_N^{(2)}$ | 1.00 | 1.00 | 1.00 | 1.00 | 0.00 | 0.00 |

3.3 Negative sequence current

Figure 10.a shows an MV distribution network which is fed by a power supply through an HV/MV transformer. The MV network consists of a faulty feeder and a background network. All the unfaulted feeders are denoted by the one block named "Background network". A single-phase earth fault takes place on the segment connecting two arbitrary secondary substations H and J at point F with the fault resistance R_F . The feeder under study can be of any length and can include any number of secondary substations. This is shown by the dashed lines. The goal here is to analyze the NSC at point B , which is located before the fault point and at point A , which is after the fault location. Note that points B and A are not electrically the same location. This is clarified in Figure 10.b. The following analysis is valid for both isolated and compensated networks.

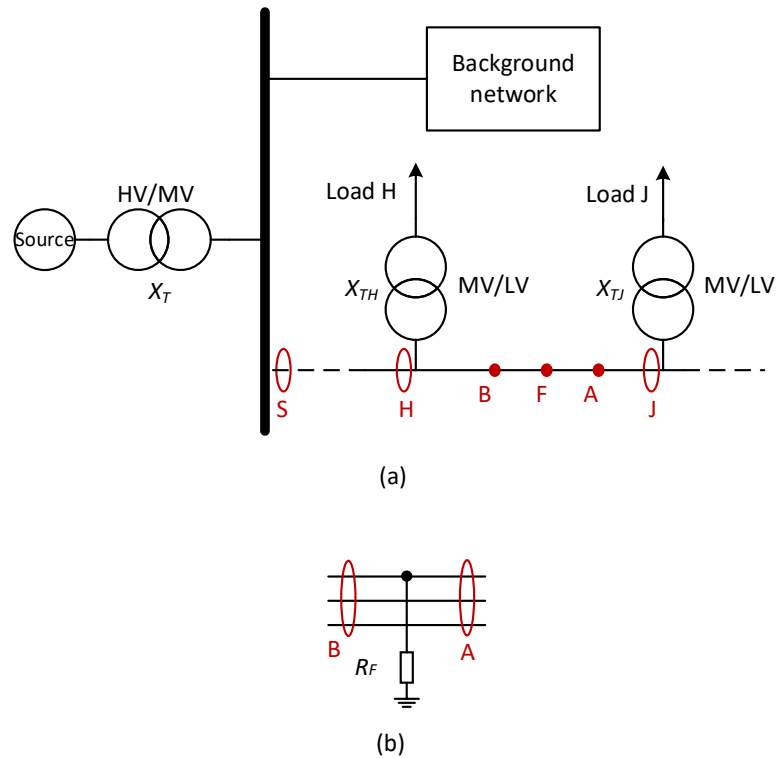


Figure 10. Single line diagram of a distribution network. (a) Two arbitrary secondary substations are shown, (b) *B* and *A* are not electrically the same location.

The sequence equivalent networks of the MV distribution system is shown in Figure 11. It is a simplified model in which the negative sequence network is shown in detail, and the positive and zero sequence networks are represented only with equivalent impedances. The notations used in the following analysis are listed below.

List of notations

- Z_1 Equivalent impedance of the positive sequence circuit of the network
- Z_{2S} Negative sequence of source impedance
- X_{2T} Negative sequence reactance of the HV/MV transformer
- Z_{2BN} Equivalent negative sequence impedance of the background network
- Z_{2SH} Negative sequence impedance of the faulted feeder between S and H
- Z_{2LH} Negative sequence impedance of load H

- X_{2TH} Negative sequence reactance of MV/LV transformer H
- Z_{2HF} Negative sequence impedance of the feeder between H and the fault location
- Z_{2FJ} Negative sequence impedance of the feeder between the fault location and J
- Z_{2LJ} Negative sequence impedance of load J
- X_{2TJ} Negative sequence reactance of MV/LV transformer J

The zero sequence network is represented by its equivalent impedances Z_1 and Z_0 . The currents I_B and I_A are the fundamental frequency components of the negative sequence currents at points B (before the fault) and A (after the fault), respectively. The shunt branches between Point S and the end of the feeder consist of the reactances of the MV/LV transformers (X_{2TH} , X_{2TJ} , etc.) in series with load impedances (Z_{2LH} , Z_{2LJ} , etc.).

First, let us assume that there is no load connected to the network. With this assumption, the shunt branches Z_{2LH} , Z_{2LJ} , etc. in the negative sequence network become open circuits and no current flows through them. As a result, the NSC measured at all points along the feeder from S to B remains constant and is zero from Point A to the end. This was seen earlier in both numerical examples discussed in Section 3.2.1 and Section 3.2.2.

With the assumption of having load connected, the NSC along the feeder from S to B will not be constant anymore as currents start to flow in the shunt branches between S and B . Similarly, the NSC will not be zero anymore at points from A to the end of the line.

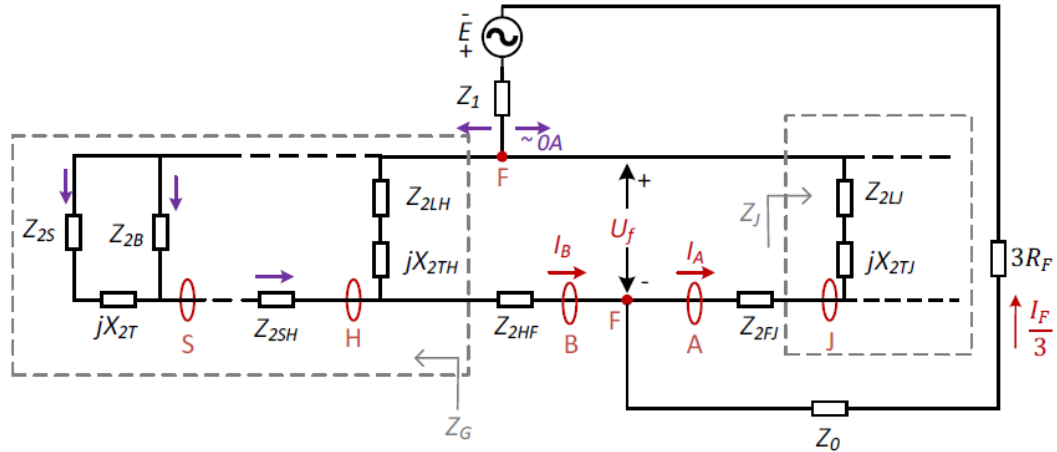


Figure 11. Single line diagram of a distribution network.

Now, consider Figure 12 which shows the simplified version of the circuit shown in Figure 11. The impedances Z_G and Z_J are the total negative sequence impedances before and after the fault point, respectively. In Figure 12, the following is valid:

$$I_B = I_A + \frac{I_F}{3} \quad (3.10)$$

$$I_B = \frac{U_f}{Z_G + Z_{2HF}} \quad (3.11)$$

$$I_A = -\frac{U_f}{Z_{2FJ} + Z_J} \quad (3.12)$$

Using (3.11) and (3.12), the ratio of I_A to I_B can be expressed by equation (3.13). It highlights an important fact i.e. this ratio is independent of the earth fault impedance.

$$\frac{I_A}{I_B} = -\frac{Z_G + Z_{2HF}}{Z_{2FJ} + Z_J} \quad (3.13)$$

In practice, $(Z_G + Z_{2HF})$ represents the equivalent negative sequence impedance of the network after the fault point and $(Z_{2FJ} + Z_J)$ is the equivalent negative sequence impedance of the network before the fault point.

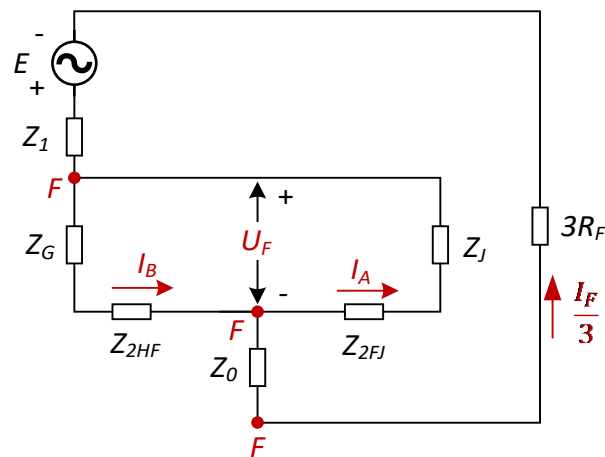


Figure 12. Simplified circuit of Figure 11.

3.4 Conclusion and summary

In the neutral-isolated network and the compensated network, the behavior of the ZSC was investigated through numerical examples. The NSC behavior was examined using numerical examples and theoretical analysis. The findings of this chapter are summarized below. These findings lay a foundation for the proposed methods introduced in Chapter 4.

The zero sequence current in a neutral-isolated (unearthed) network increases as we move from the beginning of the faulty feeder towards the fault point (Section 3.2.1, Publication II, and Publication III).

The zero sequence current in a compensated network, unlike in an isolated neutral network, decreases as we go from the beginning of the feeder towards the fault point (Section 3.2.2, Publication II, and Publication III).

In both compensated network and isolated network, the NSC on the faulty feeder from its beginning up to the fault point remains almost unchanged so that $\Delta I_N^{(2)}$ is 1 or very close to 1. After the fault point, the NSC is insignificant and $\Delta I_N^{(2)} < 1$ (Section 3.2.1 and Section 3.2.2).

4 PROPOSED METHODS

This chapter details the two proposed methods developed for radial distribution networks. The proposed methods have been developed based on the theory presented in Chapter 3. In this chapter, the following research question raised earlier in Chapter 1 will be answered. A comparative analysis is carried out between the proposed methods and conventional directional methods. This chapter is based on publications II and III.

How can symmetrical sequence currents be utilized to locate the faulted segment of the network? In what type of networks specifically?"

4.1 Fault passage indication using zero and negative sequence currents

The purpose of fault passage indication is to locate the faulted segment. An FPI device aims at detecting the passage of a fault current through the measuring point at which the device is installed. By distributing multiple FPI devices at various locations throughout the network, faulted segment identification can be realized. The faulted segment can be visualized on a map for the system operator.

In this section, two methods are proposed. The notations used throughout this chapter and the rest of the chapters are the same ones presented in Chapter 3. The proposed methods are current-based, not requiring voltage measurement. They deploy the magnitudes of ZSC and NSC phasors. In order to calculate ZSC and NSC phasors correctly, it is essential to carry out the phase current measurements properly. This is discussed in detail in Section 4.1.1.

4.1.1 Correct installation of current sensors

Figure 13 shows a single-line diagram of a three-phase distribution network with a radial feeder equipped with FPI devices installed at n measuring points. A set of current sensors (one sensor for each phase) at a given measuring point can be installed in either way in terms of polarity. This is illustrated in the figure at measuring Point 1. Two possible configurations for installing the set of current sensors are shown as Sensor 1 and Sensor 2. The blue arrows above the sensors indicate polarities. Note that only one of the two sets of sensors needs to be installed at measuring Point 1. The proposed methods are based on the magnitudes of ZSC and NSC fundamental-frequency phasors only and not their phase-angles. Therefore, the polarity of the set of the current sensors does not matter and the

sensor set can be installed in either way. In the figure, the measuring points are located at secondary substations; however, it is important to emphasize that they do not have to be installed only at secondary substations.

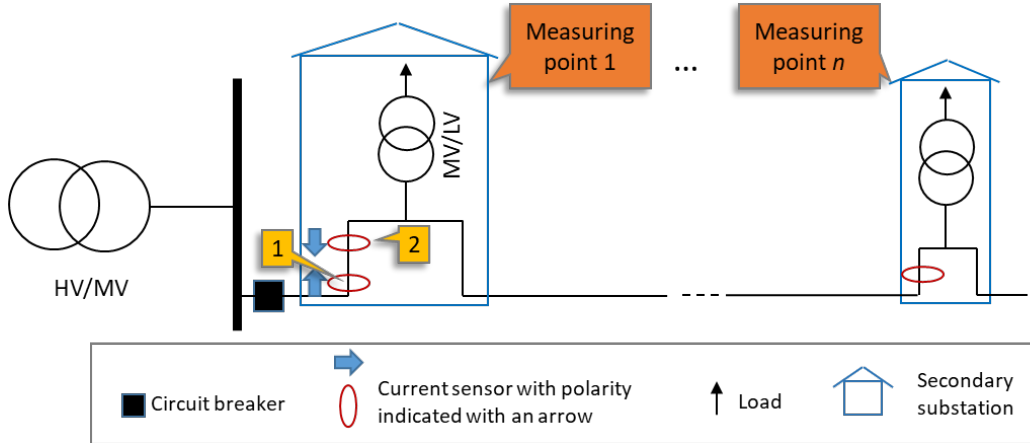


Figure 13. Installation of current sensors on a radial feeder of a typical distribution network.

4.1.2 Method 1

The findings of Chapter 3 regarding the behavior of the ZSC provides the foundation for Method 1. The method is applicable to neutral-isolated networks where ZSC increases as we move from the beginning of the faulty feeder towards the fault point. The proposed fault passage indication procedure as well as the on/off-fault-passage determination for a given measuring point are structured as follows:

1. For a given measuring point at which the FPI device is installed, the device gets triggered once the increase in the summation of all the three phase currents exceeds a pre-set threshold. Recordings are sent to a control center where for each recording, the phasors of zero sequence currents are computed for pre- and during-fault periods i.e. $I_{pre}^{(0)}$ and $I_{dur}^{(0)}$. Using these calculated phasors, the increase in the magnitude of the ZSC i.e. $\Delta I^{(0)}$ is calculated.
2. For each measuring point from which a recording has arrived at the control center, the normalized increase in the magnitude of the ZSC phasor i.e. $\Delta I_N^{(0)}$ is computed by dividing the ZSC increase of the given measuring point by the ZSC increase of the first measuring point located at the beginning of the faulted feeder. In practice, the location of the first measuring point would be near the location of the protection relay of the feeder in question.

3. The point in question is determined to be located on the fault passage if $\Delta I_N^{(0)} \geq 1$, or otherwise, off the fault passage. In addition, the measuring points from which no recording was sent to the control center are determined to be located off the fault passage.
4. The fault passage is identified using the resulting determinations regarding the measuring points. The faulted segment is identified to be the one between the last on-the-fault-passage point and the first off-the-fault-passage point.

4.1.3 Method 2

The findings of Chapter 3 about the behavior of NSC is the base of Method 2. The proposed method is applicable to both neutral-isolated networks and compensated networks. In compensated networks, the compensation coil compensates the capacitive component of the earth fault current so that the fault current at the fault point is minimized. As established in Section 3.2.2, the zero sequence current in a compensated network, unlike in a neutral-isolated network, decreases as we go from the beginning of the faulted feeder towards the end of the feeder. Therefore, utilizing only the ZSC will not provide any indication of whether the point in question is located on the fault passage or it is located off the fault passage. This makes Method 1 inapplicable to compensated networks. To remedy the shortcoming of the ZSC in fault passage indication, Method 2 employs the NSC. The following was established in Section 3.4.

- The negative sequence current is significant and remains almost the same on the faulty feeder from its beginning up to the fault point. After the fault point, it decreases and it could be even negligible, depending on the fault resistance. This will provide the base for the second proposed method.

The proposed fault passage indication procedure as well as the on/off-fault-passage determination for a given measuring point on the faulted feeder are structured as follows:

1. For a measuring point in question at which the FPI device is installed, the device starts recording once the increase in the summation of all the three phase currents exceeds a pre-set threshold. Recordings are sent to a control center where for each recording, the phasors of negative sequence currents are computed for pre- and during-fault periods i.e. $I_{pre}^{(2)}$, $I_{dur}^{(2)}$. In addition, the increase in the magnitude of the NSC i.e. $\Delta I^{(2)}$ is calculated.

2. For each measuring point from which a recording has arrived at the control center, the normalized increase in the magnitude of the NSC phasor $\Delta I_N^{(2)}$ is computed by dividing the NSC increase of the given measuring point by the NSC increase of the first measuring point located at the beginning of the faulted feeder.
3. The point in question is determined to be located on the fault passage if $\Delta I_N^{(2)} \cong 1$, or otherwise, off the fault passage. In addition, the measuring points from which no recording was sent to the control center are determined to be located off the fault passage.
4. The fault passage on the faulted feeder is identified using the resulting determinations regarding the measuring points. The faulted segment is identified to be the one between the last on-the-fault-passage point and the first off-the-fault-passage point.

4.2 Simulations

In the following, the effectiveness of the proposed methods are evaluated through simulations. In addition, the impact of the earth fault resistance is studied.

4.2.1 Simulation model

The simulations were carried out with PSCADTM using a verified model of a Finnish MV distribution network. A simplified schematic diagram of a part of the network is shown in Figure 14. The parameters and further details of the network are presented in Publication IV. This network is a local smart grid pilot in Vaasa referred to as Sundom Smart Grid and has been used in several earlier studies, e.g., in (Sirviö et al., 2020) and (Laaksonen & Hovila, 2016). It is a rural distribution network consisting of multiple feeders. The feeders are mixed i.e., they leave the primary substation as cables and after that they become overhead lines. The secondary side of the main transformer is delta and the system neutral point is connected to ground through a zig-zag transformer and a compensation coil. The compensation coil is in series with a switch so that the network can be operated as a neutral-isolated network when the switch is open. Perfect symmetry between the phases is assumed in the network. An earth fault with the resistance of 50Ω takes place at around 2 km from the primary substation. The measurements are taken from multiple points on feeder J07. Point 1 is the first measuring point located at the beginning of the feeder under study. Points 3 and 4 are located right before and

after the fault location, respectively. Points, 1, 2 and 3 are located on the fault passage and other points (4 and 5) are located off the fault passage.

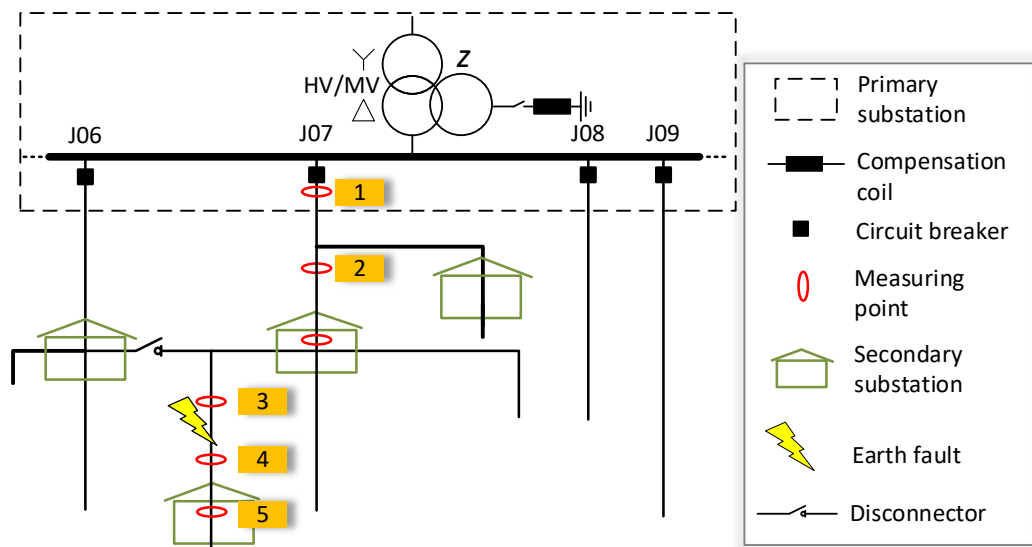


Figure 14. Medium voltage network with various measuring points under earth fault condition.

4.2.2 Simulation results

In this section, the effectiveness of the proposed methods are investigated under two scenarios i.e. once when the compensation coil is disconnected and the network under study operates in its isolated mode and once when the network operates in its compensated mode.

Isolated mode

The earth fault resistance $R_F = 1 \text{ k}\Omega$ and the fault occurs at $t = 0.5 \text{ s}$. Phase currents at each measuring point are shown in Figure 15. Figure 16 shows the fault current at the fault point. Figure 17 shows the magnitudes of ZSC and NSC phasors with respect to time. Figure 18 shows the magnitudes of ZSC and NSC phasors at the steady state of the during-fault period. As expected, the ZSC increases from Point 1 up to Point 3 and after that, it starts to decrease. Furthermore, the NSC remains almost the same at around 6 A from Point 1 to Point 3 and is insignificant at points 4 and 5. Table 4 shows the calculated quantities that the proposed methods require. It also shows the outputs of the proposed methods. Using either of the proposed methods, all the points can be correctly determined if they are on or off the fault passage. Note that since the simulated network is perfectly

symmetrical, both the ZSC and NSC in the pre-fault period i.e. $|I_{pre}^{(0)}|$ and $|I_{pre}^{(2)}|$ are 0 A.

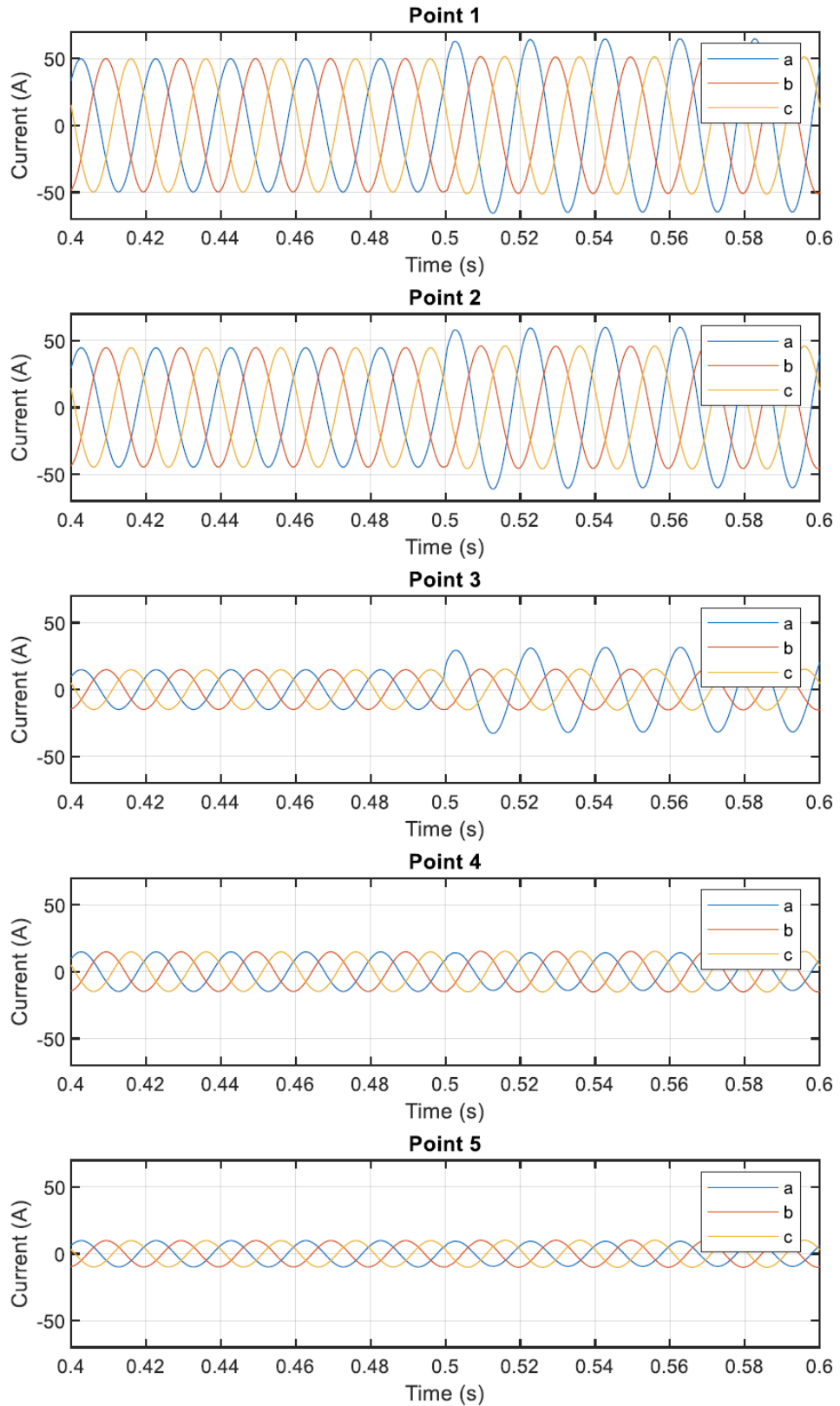


Figure 15. Phase currents measured at five measuring points at network shown in Figure 14 when it operates in its neutral-isolated mode.

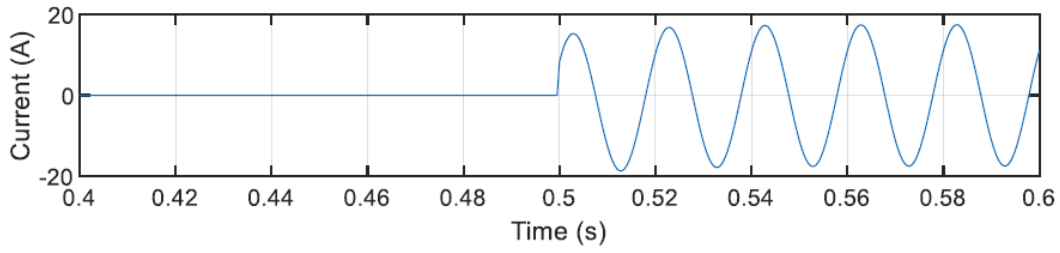


Figure 16. Fault current at fault point in network of Figure 14 when it operates in its neutral-isolated mode.

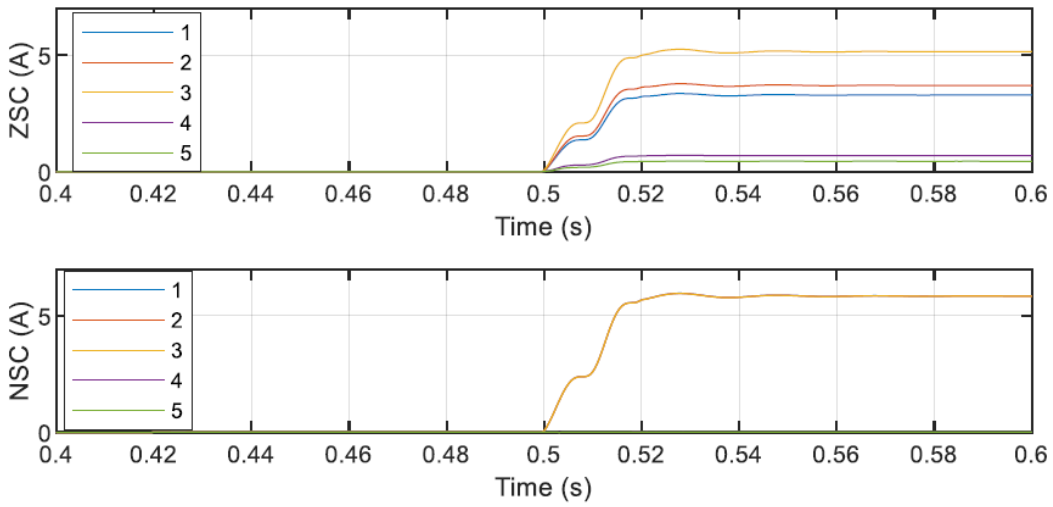


Figure 17. Magnitudes of ZSC and NSC phasors.

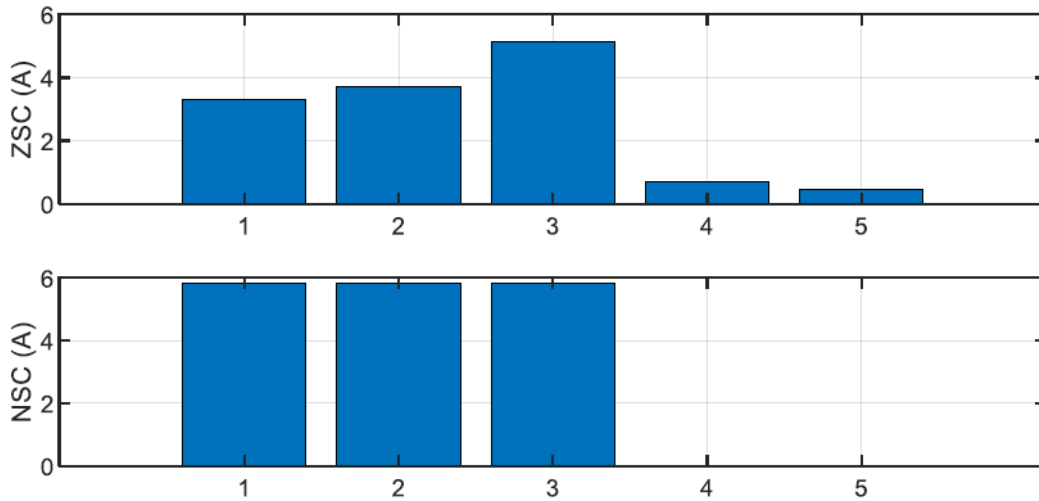


Figure 18. Magnitudes of ZSC and NSC phasors (at steady state during the fault) along the faulted feeder of network shown in Figure 14 when it operates in its neutral-isolated mode.

Table 4. ZSC and NSC phasors along with each method's output (on or off the fault path) for the network of Figure 14 when it operates in its neutral-isolated mode.

| | Point 1 | Point 2 | Point 3 | Point 4 | Point 5 |
|-----------------------|---------|---------|---------|---------|---------|
| $ I_{pre}^{(0)} $ (A) | 0.00 | 0.00 | 0.00 | 0.00 | 0.00 |
| $ I_{dur}^{(0)} $ (A) | 3.29 | 3.70 | 5.15 | 0.69 | 0.45 |
| $\Delta I^{(0)}$ | 3.29 | 3.70 | 5.15 | 0.69 | 0.45 |
| $\Delta I_N^{(0)}$ | 1.00 | 1.12 | 1.57 | 0.21 | 0.14 |
| Method 1 | On | On | On | Off | Off |
| $ I_{pre}^{(2)} $ (A) | 0.00 | 0.00 | 0.00 | 0.00 | 0.00 |
| $ I_{dur}^{(2)} $ (A) | 5.85 | 5.85 | 5.84 | 0.01 | 0.01 |
| $\Delta I^{(2)}$ | 5.85 | 5.85 | 5.84 | 0.01 | 0.01 |
| $\Delta I_N^{(2)}$ | 1.00 | 1.00 | 1.00 | 0.00 | 0.00 |
| Method 2 | On | On | On | Off | Off |

Compensated mode

In this scenario, the Petersen coil is connected and the network operates in its compensated mode. Phase currents at each measuring point are shown in Figure 19. Figure 20 shows the fault current at the fault point. Owing to the compensation coil, the fault current in this scenario is smaller compared to the previous scenario. Figure 21 shows the magnitudes of ZSC and NSC phasors with respect to time. Figure 22 shows the magnitudes of ZSC and NSC phasors during the earth fault occurrence. Table 5 shows the calculated quantities that the proposed methods require along with the outputs of Method 2. Since the type of the network in this scenario is compensated, Method 1 is inapplicable and if used, it will lead to incorrect results. Using Method 2, the points can be correctly determined to be located on or off the fault passage.

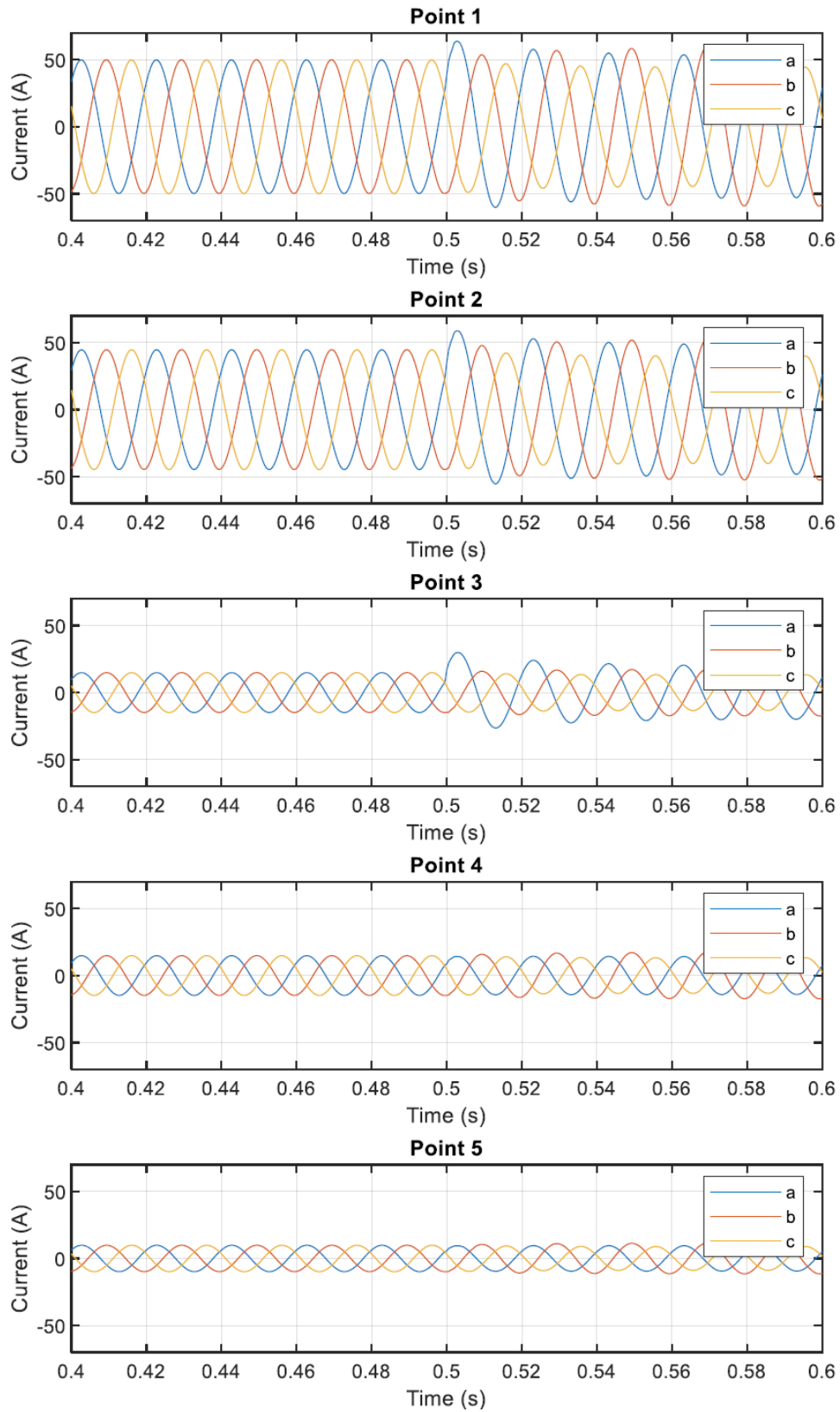


Figure 19. Phase currents measured at five measuring points at network shown in Figure 14 when it operates in its compensated mode.

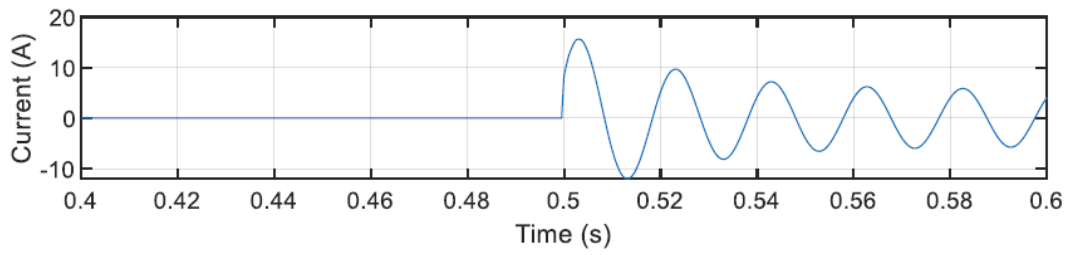


Figure 20. Fault current at fault point in network shown in Figure 14 when it operates in its compensated mode.

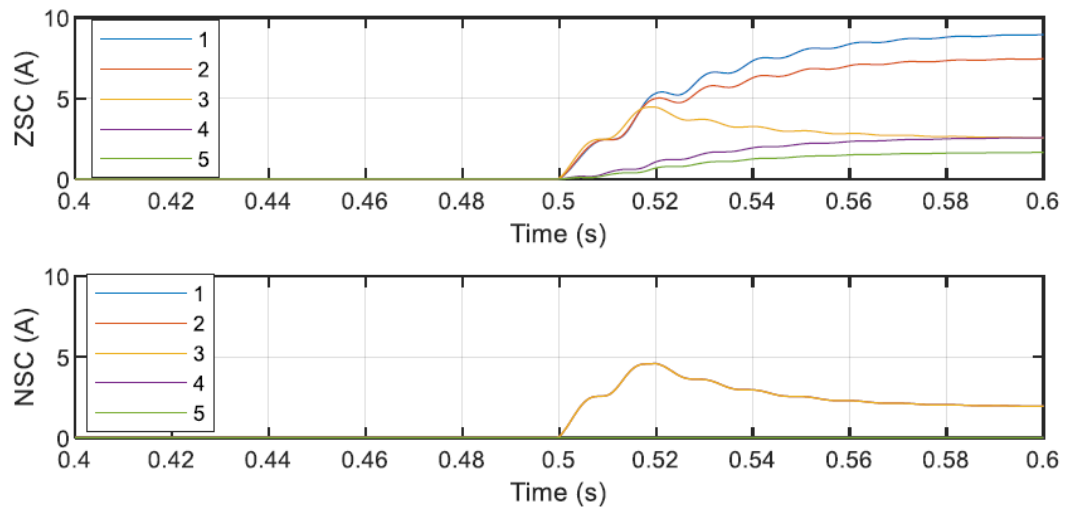


Figure 21. Magnitudes of ZSC and NSC phasors.

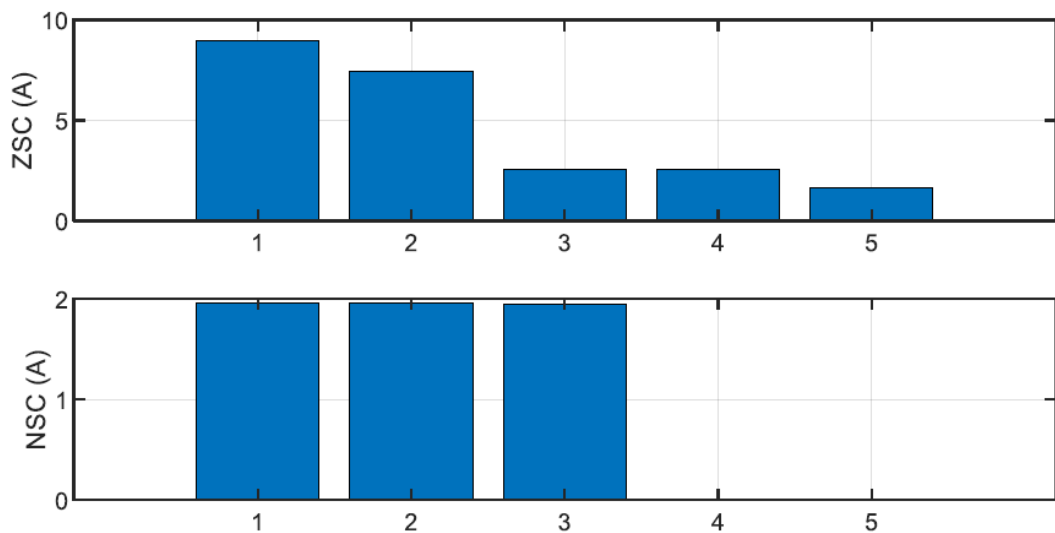


Figure 22. Magnitudes of ZSC and NSC phasors (steady state) along the faulted feeder of network shown in Figure 14 when it operates in its compensated mode.

Table 5. ZSC and NSC phasors along with each method's output for the network of Figure 14 when it operates in its compensated mode.

| | Point 1 | Point 2 | Point 3 | Point 4 | Point 5 |
|-----------------------|---------|---------|---------|---------|---------|
| $ I_{pre}^{(0)} $ (A) | 0.00 | 0.00 | 0.00 | 0.00 | 0.00 |
| $ I_{dur}^{(0)} $ (A) | 8.94 | 7.44 | 2.55 | 2.57 | 1.66 |
| $\Delta I^{(0)}$ (A) | 8.94 | 7.44 | 2.55 | 2.57 | 1.66 |
| $\Delta I_N^{(0)}$ | 1.00 | 0.83 | 0.29 | 0.29 | 0.19 |
| Method 1 | On | Off | Off | Off | Off |
| $ I_{pre}^{(2)} $ (A) | 0.00 | 0.00 | 0.00 | 0.00 | 0.00 |
| $ I_{dur}^{(2)} $ (A) | 1.96 | 1.96 | 1.95 | 0.01 | 0.00 |
| $\Delta I^{(2)}$ (A) | 1.96 | 1.96 | 1.95 | 0.01 | 0.00 |
| $\Delta I_N^{(2)}$ | 1.00 | 1.00 | 0.99 | 0.01 | 0.00 |
| Method 2 | On | On | On | Off | Off |

4.2.3 Impact of fault resistance

To investigate the effectiveness of the proposed methods, various earth fault resistances have been simulated ranging from 0 Ω to 5 k Ω . Table 6 presents ZSC and NSC phasors for various fault resistances along with each method's output. The values are calculated for both operating modes of the network. As the fault resistance increases, the ZSC and the NSC decrease, however, $\Delta I_N^{(0)}$ and $\Delta I_N^{(2)}$ are not affected by the fault resistance. This highlights an advantage that the methods offer i.e. their outputs are independent of the fault resistance. In theory, there is no limit for the proposed methods regarding how high the fault resistance can be as they are based on $\Delta I_N^{(0)}$ and $\Delta I_N^{(2)}$ as opposed to $\Delta I^{(0)}$ and $\Delta I^{(2)}$. However, when it comes to practical implementation, the limiting factor would be measurement accuracy. The proposed methods would be valid as long as the changes in sequence currents caused by an earth fault are measurable through current sensors.

Table 6. Magnitudes of ZSC and NSC phasors at steady state for various fault resistances along with each method's output.

| | Compensated | | | | | Isolated | | | | |
|--------------------|-------------|-------|------|------|------|----------|------|-------|------|------|
| $R_F = 10 \Omega$ | | | | | | | | | | |
| | 1 | 2 | 3 | 4 | 5 | 1 | 2 | 3 | 4 | 5 |
| $\Delta I^{(0)}$ | 13.17 | 11.01 | 4.08 | 3.71 | 2.40 | 17.95 | 20.2 | 28.11 | 3.76 | 2.43 |
| $\Delta I_N^{(0)}$ | 1.00 | 0.84 | 0.31 | 0.28 | 0.18 | 1.00 | 1.13 | 1.57 | 0.21 | 0.14 |

| | | | | | | | | | | |
|---------------------|----------|----------|----------|----------|----------|----------|----------|----------|----------|----------|
| M1 | On | Off | Off | Off | Off | On | On | On | Off | Off |
| $\Delta I^{(2)}$ | 3.14 | 3.14 | 3.13 | 0.01 | 0.01 | 31.9 | 31.89 | 31.88 | 0.08 | 0.06 |
| $\Delta I_N^{(2)}$ | 1.00 | 1.00 | 1.00 | 0.00 | 0.00 | 1.00 | 1.00 | 1.00 | 0.00 | 0.00 |
| M2 | On | On | On | Off | Off | On | On | On | Off | Off |
| $R_F = 100 \Omega$ | | | | | | | | | | |
| | 1 | 2 | 3 | 4 | 5 | 1 | 2 | 3 | 4 | 5 |
| $\Delta I^{(0)}$ | 12.34 | 10.24 | 3.38 | 3.58 | 2.31 | 15.81 | 17.79 | 24.76 | 3.32 | 2.14 |
| $\Delta I_N^{(0)}$ | 1.00 | 0.83 | 0.27 | 0.29 | 0.19 | 1.00 | 1.13 | 1.57 | 0.21 | 0.14 |
| M1 | On | Off | Off | Off | Off | On | On | On | Off | Off |
| $\Delta I^{(2)}$ | 2.62 | 2.62 | 2.61 | 0.01 | 0.00 | 28.09 | 28.09 | 28.08 | 0.07 | 0.05 |
| $\Delta I_N^{(2)}$ | 1.00 | 1.00 | 1.00 | 0.00 | 0.00 | 1.00 | 1.00 | 1.00 | 0.00 | 0.00 |
| M2 | On | On | On | Off | Off | On | On | On | Off | Off |
| $R_F = 1000 \Omega$ | | | | | | | | | | |
| | 1 | 2 | 3 | 4 | 5 | 1 | 2 | 3 | 4 | 5 |
| $\Delta I^{(0)}$ | 8.94 | 7.44 | 2.55 | 2.57 | 1.66 | 3.29 | 3.70 | 5.15 | 0.69 | 0.45 |
| $\Delta I_N^{(0)}$ | 1.00 | 0.83 | 0.29 | 0.29 | 0.19 | 1.00 | 1.13 | 1.57 | 0.21 | 0.14 |
| M1 | On | Off | Off | Off | Off | On | On | On | Off | Off |
| $\Delta I^{(2)}$ | 1.96 | 1.96 | 1.95 | 0.01 | 0.00 | 5.85 | 5.85 | 5.84 | 0.01 | 0.01 |
| $\Delta I_N^{(2)}$ | 1.00 | 1.00 | 1.00 | 0.00 | 0.00 | 1.00 | 1.00 | 1.00 | 0.00 | 0.00 |
| M2 | On | On | On | Off | Off | On | On | On | Off | Off |
| $R_F = 2000 \Omega$ | | | | | | | | | | |
| | 1 | 2 | 3 | 4 | 5 | 1 | 2 | 3 | 4 | 5 |
| $\Delta I^{(0)}$ | 6.54 | 5.46 | 1.99 | 1.86 | 1.2 | 1.66 | 1.87 | 2.6 | 0.35 | 0.23 |
| $\Delta I_N^{(0)}$ | 1.00 | 0.84 | 0.30 | 0.28 | 0.18 | 1.00 | 1.13 | 1.57 | 0.21 | 0.14 |
| M1 | On | Off | Off | Off | Off | On | On | On | Off | Off |
| $\Delta I^{(2)}$ | 1.54 | 1.54 | 1.53 | 0.00 | 0.00 | 2.96 | 2.96 | 2.96 | 0.01 | 0.00 |
| $\Delta I_N^{(2)}$ | 1.00 | 1.00 | 0.99 | 0.00 | 0.00 | 1.00 | 1.00 | 1.00 | 0.00 | 0.00 |
| M2 | On | On | On | Off | Off | On | On | On | Off | Off |
| $R_F = 3000 \Omega$ | | | | | | | | | | |
| | 1 | 2 | 3 | 4 | 5 | 1 | 2 | 3 | 4 | 5 |
| $\Delta I^{(0)}$ | 5.08 | 4.25 | 1.59 | 1.43 | 0.92 | 1.11 | 1.25 | 1.74 | 0.23 | 0.15 |
| $\Delta I_N^{(0)}$ | 1.00 | 0.84 | 0.31 | 0.28 | 0.18 | 1.00 | 1.13 | 1.57 | 0.21 | 0.14 |
| M1 | On | Off | Off | Off | Off | On | On | On | Off | Off |
| $\Delta I^{(2)}$ | 1.25 | 1.25 | 1.24 | 0.00 | 0.00 | 1.98 | 1.98 | 1.97 | 0.00 | 0.00 |
| $\Delta I_N^{(2)}$ | 1.00 | 1.00 | 0.99 | 0.00 | 0.00 | 1.00 | 1.00 | 1.00 | 0.00 | 0.00 |
| M2 | On | On | On | Off | Off | On | On | On | Off | Off |
| $R_F = 4000 \Omega$ | | | | | | | | | | |
| | 1 | 2 | 3 | 4 | 5 | 1 | 2 | 3 | 4 | 5 |
| $\Delta I^{(0)}$ | 4.13 | 3.46 | 1.32 | 1.16 | 0.75 | 0.83 | 0.94 | 1.3 | 0.17 | 0.11 |

| | | | | | | | | | | | |
|---------------------|----------|----------|----------|----------|----------|--|----------|----------|----------|----------|----------|
| $\Delta I_N^{(0)}$ | 1.00 | 0.84 | 0.32 | 0.28 | 0.18 | | 1.00 | 1.13 | 1.57 | 0.21 | 0.14 |
| M1 | On | Off | Off | Off | Off | | On | On | On | Off | Off |
| $\Delta I_N^{(2)}$ | 1.04 | 1.04 | 1.04 | 0.00 | 0.00 | | 1.49 | 1.49 | 1.48 | 0.00 | 0.00 |
| $\Delta I_N^{(2)}$ | 1.00 | 1.00 | 0.99 | 0.00 | 0.00 | | 1.00 | 1.00 | 1.00 | 0.00 | 0.00 |
| M2 | On | On | On | Off | Off | | On | On | On | Off | Off |
| $R_F = 5000 \Omega$ | | | | | | | | | | | |
| | 1 | 2 | 3 | 4 | 5 | | 1 | 2 | 3 | 4 | 5 |
| $\Delta I_N^{(0)}$ | 3.48 | 2.91 | 1.13 | 0.97 | 0.63 | | 0.67 | 0.75 | 1.04 | 0.14 | 0.09 |
| $\Delta I_N^{(0)}$ | 1.00 | 0.84 | 0.32 | 0.28 | 0.18 | | 1.00 | 1.13 | 1.57 | 0.21 | 0.14 |
| M1 | On | Off | Off | Off | Off | | On | On | On | Off | Off |
| $\Delta I_N^{(2)}$ | 0.89 | 0.89 | 0.89 | 0.00 | 0.00 | | 1.19 | 1.19 | 1.19 | 0.00 | 0.00 |
| $\Delta I_N^{(2)}$ | 1.00 | 1.00 | 0.99 | 0.00 | 0.00 | | 1.00 | 1.00 | 0.99 | 0.00 | 0.00 |
| M2 | On | On | On | Off | Off | | On | On | On | Off | Off |

4.3 Method 2 vs conventional methods

In conventional methods, voltage measurement is required in addition to current measurement. For instance, in (Altonen & Wahlroos, 2016), on/off-fault-passage indication is realized through calculating an admittance for each measuring point at which the FPI device is installed. The zero sequence admittance $Y^{(0)}$ can be obtained through division of the zero sequence current $I^{(0)}$ by the zero sequence voltage $U^{(0)}$ (see equations (4.1) and (4.2)). The zero sequence voltage can be calculated based on the measured line-to-ground voltages. Since line-to-ground voltages are almost the same for every measuring point, they can be used as a reference. On the other hand, in conventional methods, the assumption regarding zero sequence currents at points on and off the fault passage is that their phasors are 180 degrees apart. Therefore, the on/off-fault-passage determination can be determined based on the sign of the real part of the calculated zero sequence admittance. For instance, in (Altonen & Wahlroos, 2016), the positive sign essentially indicates on-the-fault-passage and negative sign is the off-the-fault-passage indication. This is illustrated in Figure 23 which is a simplified version of the original figure presented in (Altonen & Wahlroos, 2016). In order to provide tolerance against phase displacement errors in the measurements, the parameter “Tilt angle” is introduced. In (Altonen & Wahlroos, 2016), this parameter is set at 10 degrees.

$$U^{(0)} = (U_a + U_b + U_c)/3 \quad (4.1)$$

$$Y^{(0)} = \frac{I^{(0)}}{-U^{(0)}} \quad (4.2)$$

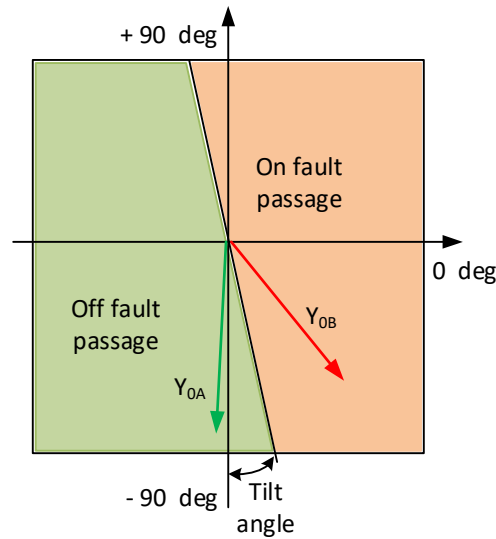


Figure 23. Conventional fault passage indication using zero sequence admittance, (Altonen & Wahlroos, 2016) (simplified).

In the two following subsections, the aforementioned assumption regarding the phase-angle difference is investigated. It is revealed that this assumption is valid in neutral-isolated networks. However, for compensated networks, care must be taken when selecting the value for the “Tilt angle” parameter. This is further explained in the following analysis by way of example.

4.3.1 Neutral-isolated network

The earth fault occurs at $t = 0.5$ s with resistance of $1 \text{ k}\Omega$. Figure 24 shows line-to-ground voltages at Point 3 and Point 4 and Figure 25 shows the residual currents (summation of all three phase currents) at those points when the network operates in its neutral-isolated mode. The figures show a 0.1-second pre-fault period and a 0.1-second during-fault period. In the during-fault period in Figure 25, the residual currents flow in opposite directions in both transient and steady-state periods. The phasor diagram of the calculated zero sequence voltage (ZSV) phasors at the two measuring points and the phasors of the zero sequence currents are shown in Figure 26. The calculated zero admittances calculated using equations (4.1) and (4.2) are depicted in the same figure. Note that since the ZSV is the same for both points, their phasors have overlapped each other. For better readability, the ZSC and the admittance phasors of Point 4 are scaled up by 6. Using the conventional method and Figure 26, one can successfully differentiate these two points and make a correct determination on the on/off-fault-passage detection.

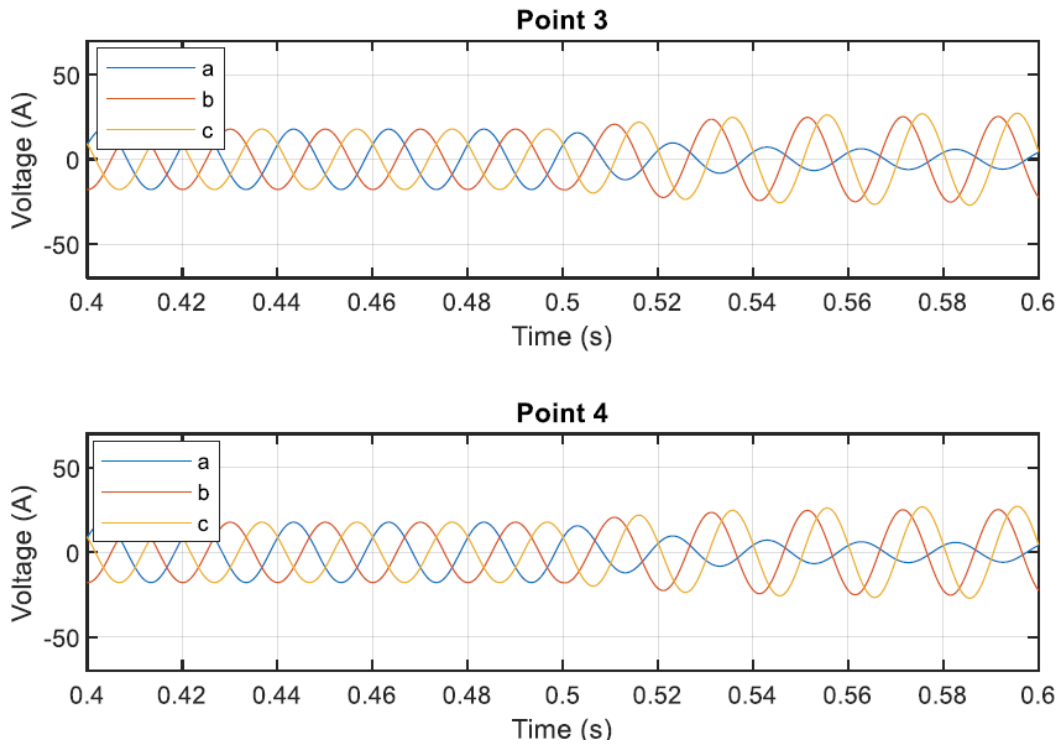


Figure 24. Line-to-ground voltages at Point 3 (on the fault passage) and Point 4 (off the fault passage) when network of Figure 14 operates in its neutral-isolated mode.

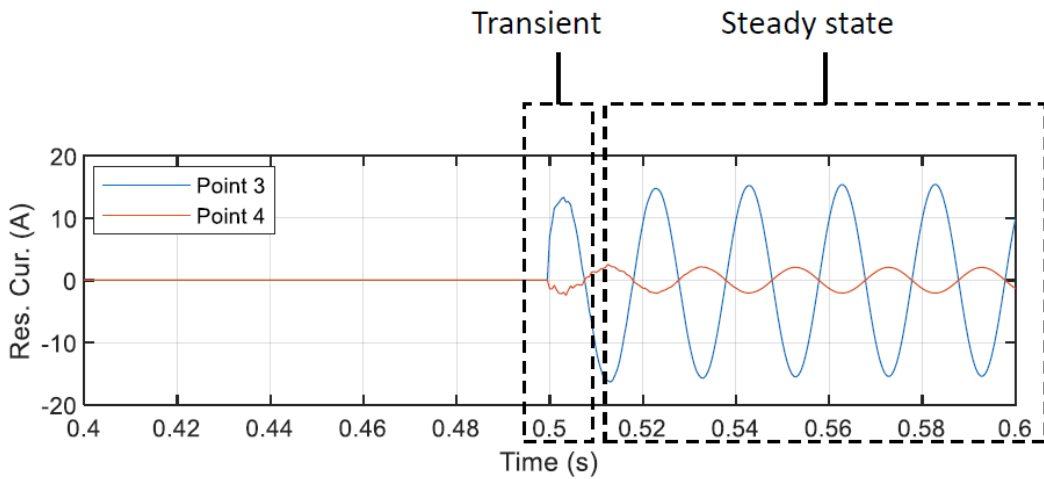


Figure 25. Residual currents flowing in same directions in transient state and in steady states in a neutral-isolated distribution network.

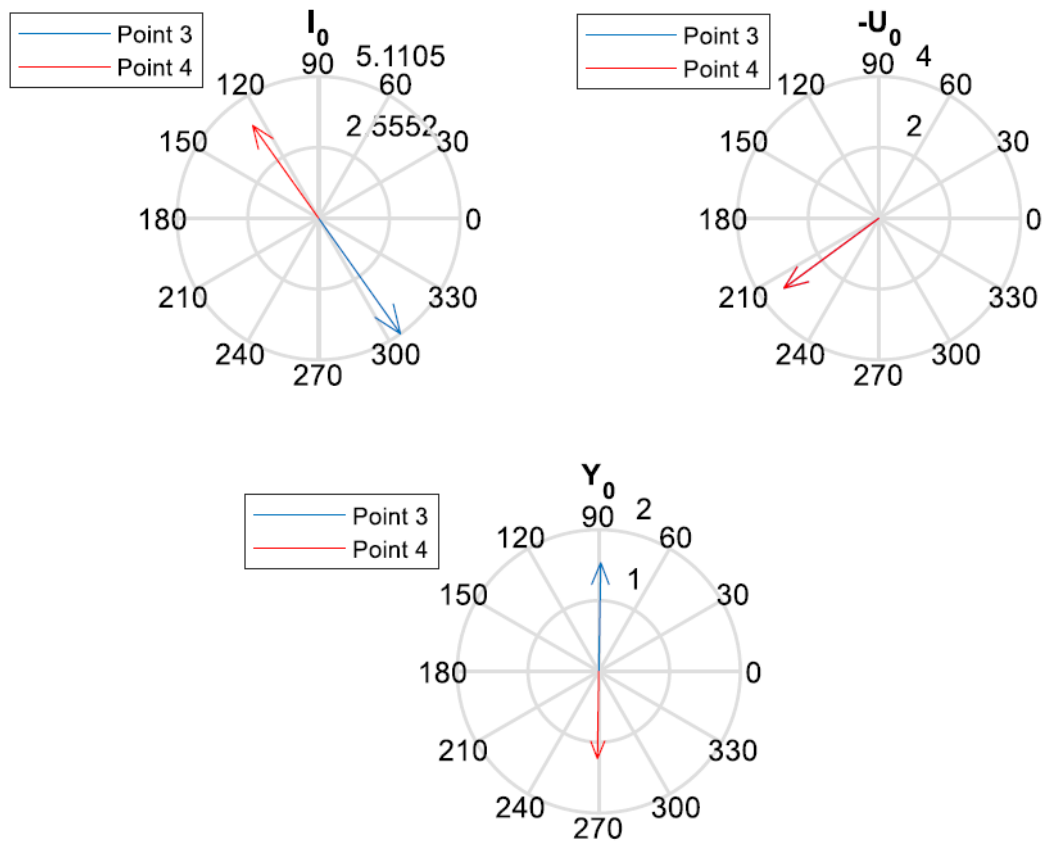


Figure 26. Phasor diagram of zero sequence voltages, currents and admittances during an earth fault period in the network of Figure 14 when it operates in its neutral-isolated mode.

4.3.2 Compensated network

Similarly, the earth fault occurs at $t = 0.5$ s and its resistance is 1 k Ω . Figure 27 shows line-to-ground voltages at Point 3 and Point 4 and Figure 28 shows the residual currents (summation of all three phase currents) at those points when the network operates in its neutral-isolated mode. The figure shows pre and during fault periods. In the transient period, the residual currents flow in opposite directions as in the previous case where the network operated in neutral-isolated mode. However, in the steady state period, they almost flow in the same direction with a small phase-angle difference. The phasor diagram of the calculated ZSV phasors at the two measuring points and the phasors of the zero sequence currents are depicted in Figure 29. The zero sequence admittances phasors are plotted in the same figure. In this case, the conventional method would again succeed to differentiate these two points with the pre-set “Tilt angle” i.e. 10 deg. However, it highlights the importance of selecting a correct value for the parameter “Tilt angle”. If this value is not selected with enough care, it could lead to an incorrect

result as both zero admittance phasors are in the same area (their real parts are positive). In conclusion, making a determination based on admittance phasors that are based on steady state period involves a risk. This challenge in fault passage indication in compensated networks using conventional methods will be also seen in Chapter 6 when experimental results are discussed.

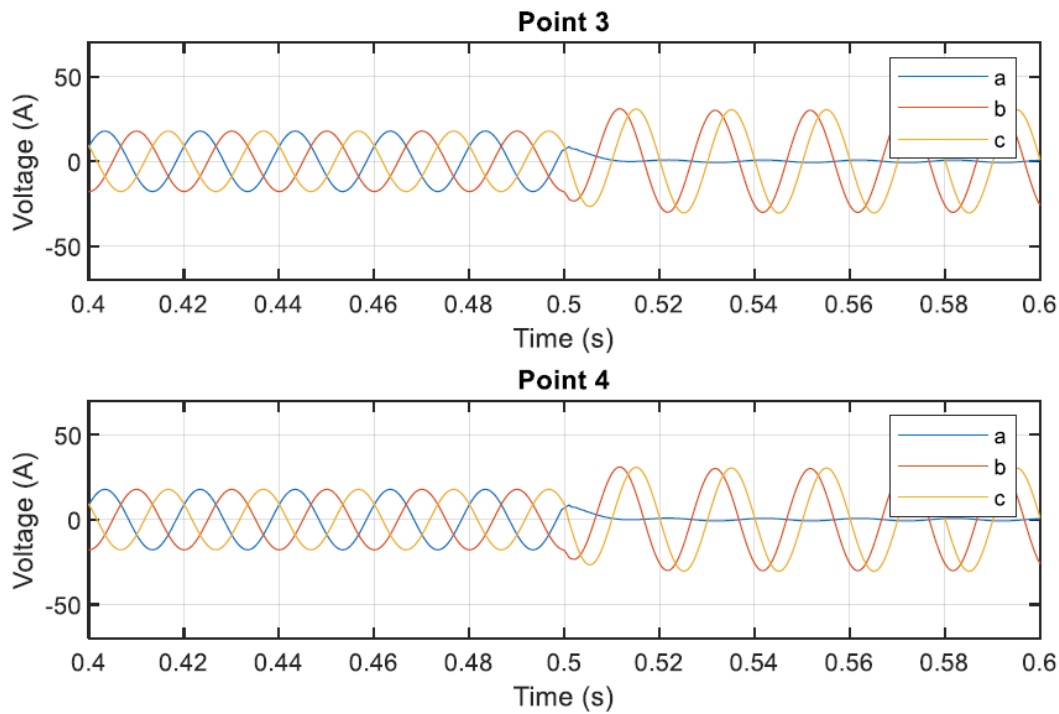


Figure 27. Line-to-ground voltages at Point 3 (on the fault passage) and Point 4 (off the fault passage) when network of Figure 14 operates in its compensated mode.

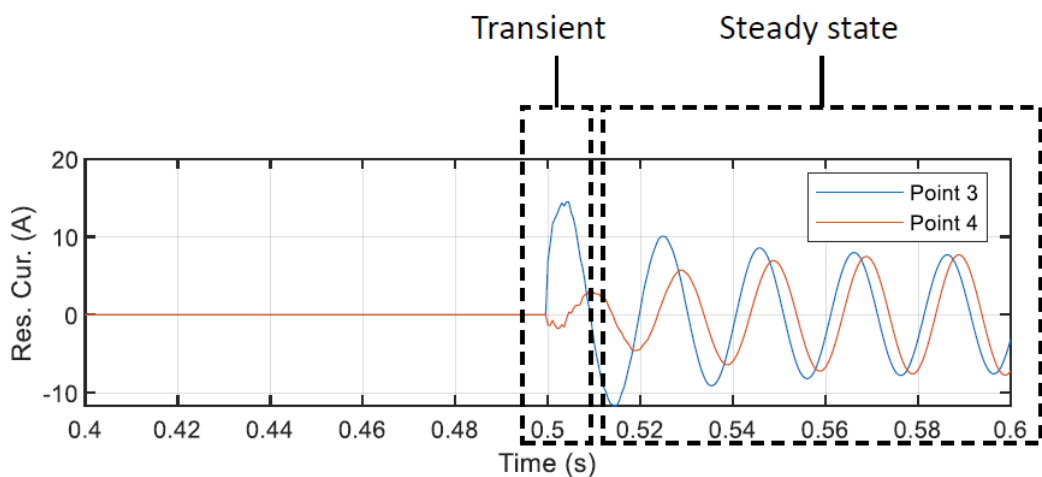


Figure 28. Residual currents flowing in opposite directions in transient state and almost same direction in steady state in a compensated network.

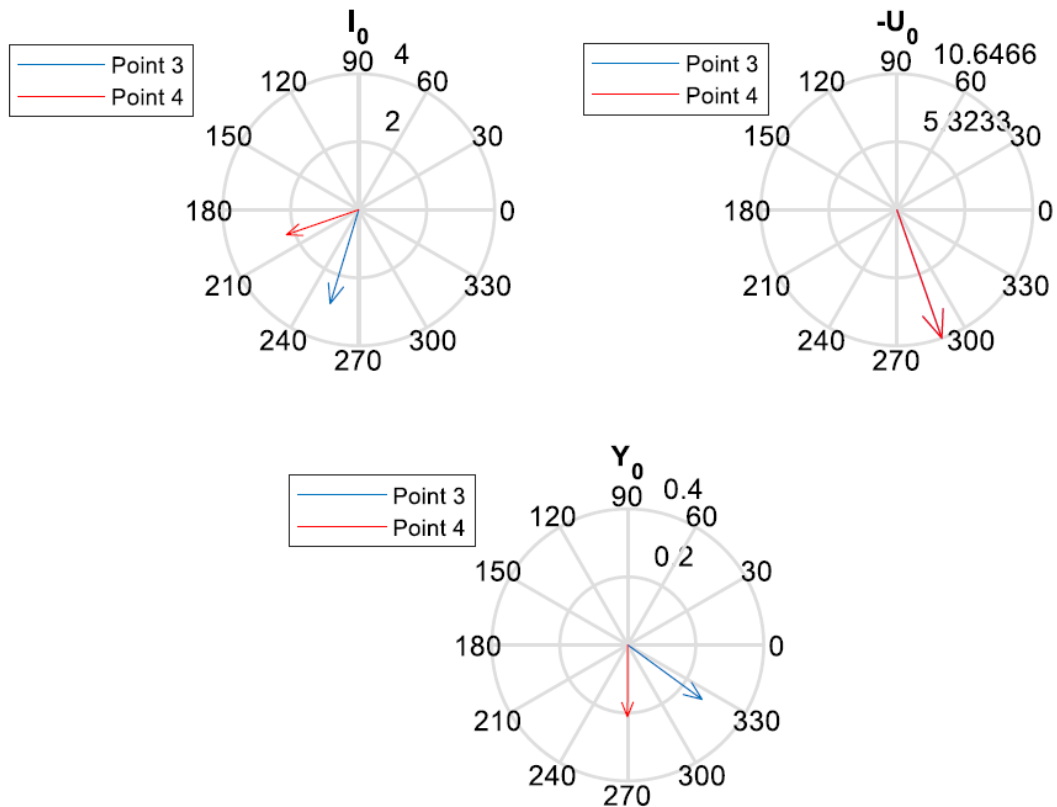


Figure 29. Phasor diagram of zero sequence voltages, currents and admittances during an earth fault period in the network shown in Figure 14 when operating in its compensated mode.

4.4 Discussion

The strength of both methods lies in the comparison of the calculated symmetrical sequence components of the currents at each measuring point with that of the first device. Since the methods are based on the magnitudes of ZSC and NSC phasors at the steady state of the during-fault period and not transient currents, accurate time synchronization is not required.

Both proposed methods are devised for radial distribution networks and not ring distribution networks. However, this is not a big concern as most medium voltage distribution networks operate in radial configuration. In fact, ring distribution networks are rather rare.

Method 1 is based on the comparing the ZSC levels of the measuring points of the faulted feeder. It is based on the assumption that the ZSC level increases from the beginning of the faulted feeder up to the fault point and after that it drops. However, the ZSC level at points on the fault passage is proportionate to the line-

to-ground capacitances of the healthy feeders and line-to-ground capacitances of the faulted feeder from its beginning up to the fault point. The ZSC level at points off the fault passage is proportionate to the line-to-ground capacitances of the line section from the fault point to the end of the feeder. If the line-to-ground capacitances of this section are greater than that of the points on the fault passage, Method 1 will fail. In theory, this could be the case in a network with a long single feeder (with no background network) when the earth fault is so close to the beginning of the feeder.

Method 2 requires a device assigned as the first device. In practice, the topology of the network and the direction of the power flow could change. Therefore, every time this type of change occurs, the method requires to know what device is currently the first device. In Section 6.2.2 and Section 6.2.3 where field tests are discussed, we will encounter such a case where the direction of the power reverses and therefore, the first device is not a fixed device. It changes whenever power flow changes its direction.

In Section 4.3, it was seen that the transient part of the residual current at the start of the earth fault can provide a clue regarding the on/off-fault-passage status of the measuring point in question. This raises a question that why not to solely utilize the transient part of the residual current to determine the on/off-fault-passage status of a measuring point. The reason is that implementing this idea in practice requires that all the current sensor sets are installed uniformly in terms of polarity. Fulfilling this requirement is technically difficult. This will become even more complicated when the topology of the network changes.

Section 4.1.2 and Section 4.1.3 propose that the FPI device sends the recording containing measured phase currents to the control center for further processing and computing the sequence current phasors. An alternative to this would be that phasors calculations were carried out by the FPI device and the device would send only the calculated phasors to the control center. This would reduce the amount of data transferred over the communication channel. However, the downside would be that some additional computing resources would be required at the sensor device.

The error sources affecting the accuracy and reliability of the proposed methods include inaccuracies in current measurements. As can be seen from Table 6, as the fault resistance increases, the computed sequence currents decrease. The proposed methods are reliable as long as the changes in sequence currents caused by an earth fault are reliably measurable. To put this into perspective, in the recordings obtained from field testing and presented in Chapter 6, the smallest measurable

current level is 0.1 A. The Rogowski coils used in the tests have the accuracy of 0,5 % and the angle accuracy is about one degree.

5 INTERMITTENT EARTH FAULT

This chapter intends to shed lights on a special type of earth fault referred to as the “intermittent earth fault”. An intermittent or re-striking earth fault is a special type of earth fault that is most common in compensated networks with underground cables. In this chapter, the phenomenon is explained using data obtained from real-life recordings and field test recordings. The efficacy of Method 2 in locating this type of fault is investigated. The method is modified so that it will be able to cope with this type of fault to some extent. This chapter is mainly based on Publication IV.

5.1 Introduction

Overhead lines are prone to faults and disruptions caused by falling trees, flying birds, thunder storms, lightning, etc. (Poethier et al., 2019). Therefore, in many countries, DSOs are replacing their overhead lines with underground cables. Refs. (Loukkalahti et al., 2017), (Siirto et al., 2017), and (Siirto et al., 2015) report on how and to what extent transition from overhead lines to cables improves the electricity supply reliability. In spite of the benefits this transition provides, a new challenge to fault management systems arises i.e., a special type of earth fault referred to as the intermittent or re-striking earth fault. It can be described as a series of cable insulation breakdowns in which a rapid electric discharge to ground occurs, which results in current spikes (Altonen et al., 2003). The fault ignites and self-extinguishes repeatedly at irregular time intervals (Altonen et al., 2003). These types of faults are problematic for conventional relays. Conventional relays operate based on phasors calculated for the steady state and these irregular current waveforms may lead to incorrect operation of conventional relays and FPIs that operate based on steady-state phasors.

The cause of intermittent earth faults on cables is mostly the deterioration of the cable insulation layer. Insulation deteriorations could be caused by moisture penetrated to an aging insulation layer, impurities originating from the cable manufacturing process, etc. (Altonen et al., 2003).

If left to ignite long enough, intermittent earth faults will eventually evolve into continuous permanent faults. According to (Loukkalahti et al., 2017), almost all earth faults occurring on compensated MV distribution networks with underground cables are intermittent ones and majority of permanent faults in these types of networks first start as intermittent ones and then evolve into short circuits or earth faults.

5.2 Phenomenon

Compensated networks with underground cables are subject to intermittent earth faults. What causes an intermittent earth fault is usually damage to the cable insulation. The damaged spot has a lower insulation level so that when the faulted phase voltage reaches a high enough level, a rapid discharge of current to ground takes place through the damaged spot. This is due to the discharge current of faulty phase capacitances and the charge current of the capacitances of healthy phases. These sudden charges and discharges cause current spikes on the faulty feeder as well as healthy feeders (Druml et al., 2014). If the faulted phase is not in direct contact with ground, the fault is likely to self-extinguish in compensated networks thanks to the low level of earth fault currents in these types of networks. However, as the damaged spot has a reduced insulation level, discharges happen again every time the voltage rises enough. This pattern keeps repeating and the result is known as the intermittent earth fault. The duration of a current spike caused by an intermittent earth fault is typically only a few ohms and the amplitude up to several hundred amperes (Kumpulainen et al., 2008).

Figure 30 shows a recording obtained from a field test mimicking an intermittent earth fault. The feeder protection relay has recorded the measured voltages and currents. The measurements are carried out at a 10 kHz sampling rate. The voltage and current of the faulty phase are plotted in the same figure to facilitate comparison. The fault occurs and causes the first current spike once the phase-to-ground voltage rises up to a certain value at the damaged spot. The fault self-extinguishes in one of the first zero crossings of the transient fault current. After the fault has been cleared, the faulty phase's phase-to-ground voltage starts to recover gradually. The corresponding residual current and voltage are shown in Figure 31. The spikes are visible in the residual current. The residual voltage recovers gradually after each current spike.

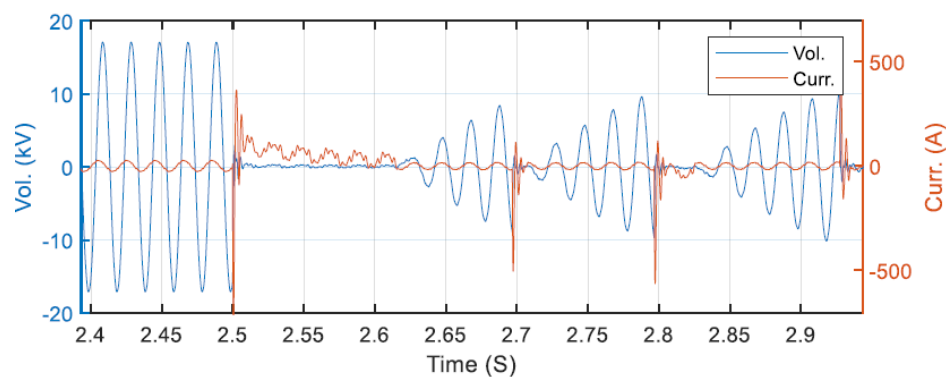


Figure 30. Faulty phase current and voltage obtained from a field test recording (Publication IV).

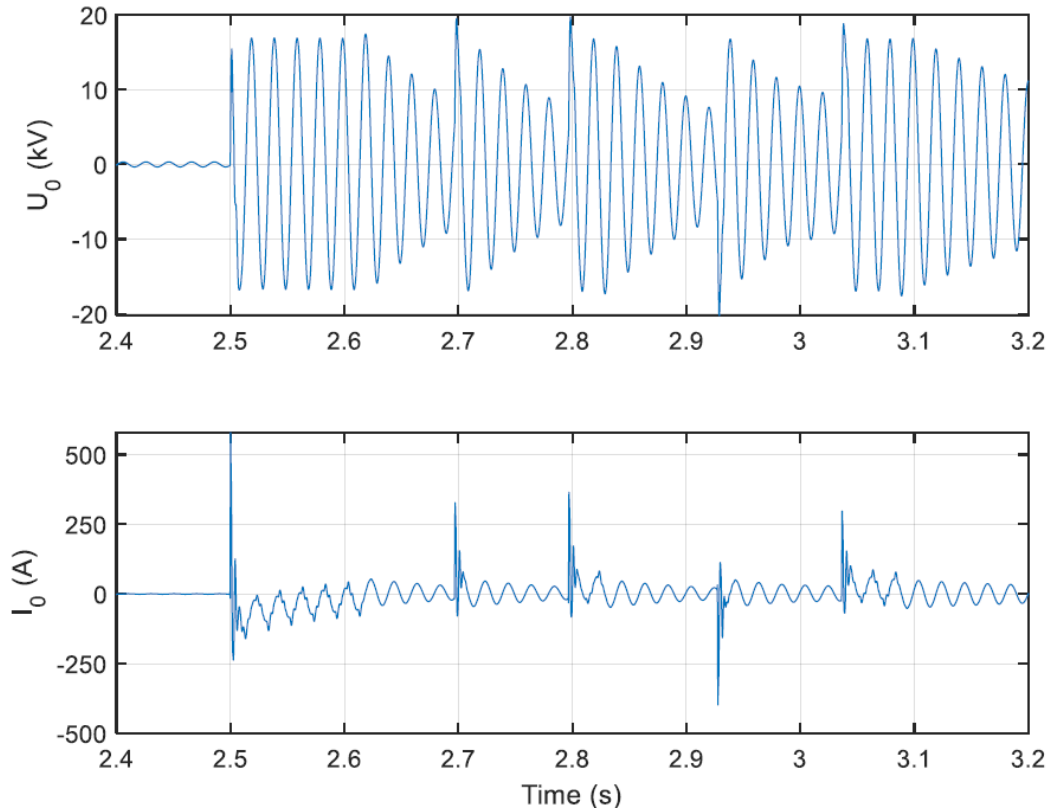


Figure 31. Zero sequence voltage and current of the intermittent earth fault of Figure 30 (Publication IV).

Figure 32 shows real-life recordings from what is believed to be an intermittent earth fault in an MV distribution network in Finland. The recordings are of the length 1.2 s and obtained from two measuring points; one from the faulted feeder and one from an adjacent healthy feeder. For each recording, the residual current (summation of all three phase currents) is also plotted in the figure. In both recordings, current spikes caused by the intermittent earth fault are noticeable.

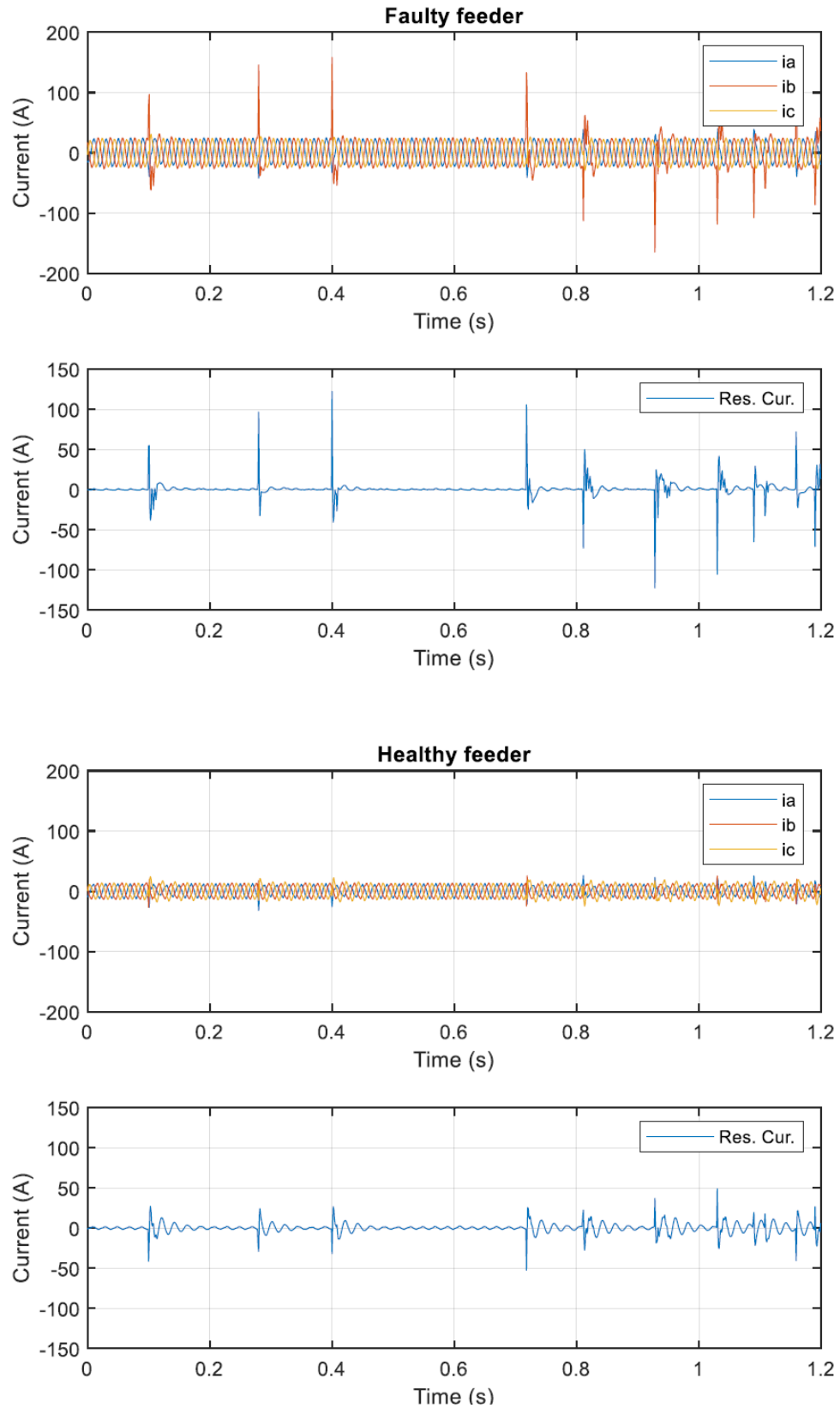


Figure 32. Real-life recordings of an intermittent earth fault on an MV distribution network, courtesy of Safegrid Oy.

5.3 Problem formulation

According to (Druml et al., 2011), conventional earth fault detection relays are designed for low-impedance faults with stationary behavior. They are not designed for intermittent earth faults, which especially occur in compensated cable networks. Conventional protection algorithms mostly compute current and voltage phasors and, consequently, have limited efficiency in the case of transient intermittent faults (Banjanin & Savic, 2021). “Since it is difficult to obtain accurate phasor results in fast transient situations, most of the feeder relays fail to correctly respond to transient/intermittent earth faults, which are, however, frequent fault cases in distribution systems” (Cui et al., 2011). The problem is that the transient behavior is also seen in the phasors so that the conventional thresholds set in the feeder relays might fail.

5.4 Literature review

To address the shortcoming of conventional relays in case of intermittent faults, a number solutions have been put forward in (Akke, 2011; Cui et al., 2011; Dong et al., 2012; Pettissalo, 2017; Virtala, 2016; Wahlroos et al., 2013; Wahlroos & Altonen, 2014). The patented solution presented in (Akke, 2011), takes a centralized residual voltage i.e. the neutral-to-ground voltage U_0 and ZSC of each feeder as inputs. The first order derivative of U_0 is calculated. The calculated value is correlated with the ZSC of each feeder. The faulty feeder is identified as the one that has the highest correlation. In (Dong et al., 2012) and (Cui et al., 2011), another patented method is presented that aims at identifying the faulted feeder in case of intermittent earth faults. The method requires the residual current and voltage as inputs. It calculates the instantaneous active and reactive powers using Hilbert transform. The method also counts the number of spikes and uses this to determine the type of the disturbance that could be intermittent faults or transient disturbances and noises.

In (Pettissalo, 2017), two separate methods are presented for faulted feeder identification; one devised for permanent earth faults and one specifically for intermittent earth faults. The methods require two phase currents and the ZSC as inputs. For permanent earth faults, the method assumes that the ratio of the magnitude of the NSC phasor to the magnitude of the ZSC phasor is high on the faulty feeder and low on healthy feeders. The other method devised specifically for intermittent earth faults is based on analyzing the transient part of the phase currents and residual currents.

A patented method intended for transient earth faults is proposed in (Virtala, 2016). The method was first proposed in 2014 but published in 2016. The method is based on calculating the zero sequence admittance for each feeder using the neutral-to-ground (measured across the Petersen coil) and zero sequence currents. The on/off-the-fault-passage determination on a specific feeder is made based on the sign of the real part of the calculated zero sequence admittance so that a negative admittance means on-the-fault passage and a positive value indicates off-the-fault passage. Ref. (Wahlroos & Altonen, 2014) proposes a method that appears to have advanced the method in (Virtala, 2016) by utilizing a new concept introduced (Wahlroos et al., 2013). The concept is referred to as “cumulative phasor summing”. The purpose of this concept is to address the random nature of intermittent earth faults. Ref. (Wahlroos & Altonen, 2014) employs the “cumulative phasor summing” concept to advance and remedy the shortcoming of the “zero sequence admittance” method. Ref. (Altonen et al., 2017) reports on the results of the field testing of the method utilized as FPI.

The presented methods, except for the method in (Wahlroos & Altonen, 2014), appear to be intended specifically for faulted feeder identification in the event of intermittent earth faults and not fault passage indication. At least, to the best of the knowledge of the author, there have not been FPI applications of the methods reported in the literature. On the other hand, these methods (except for (Pettissalo, 2017)) require voltage measurement. Therefore, even if these methods are to be used for FPI purposes, voltage measurement will be required at every point where an FPI device is installed and that leads to extra cost. The method put forward in (Topolanek et al., 2020) attempts to provide a solution for the extra costs by utilizing the voltage measurements that are typically available on the low-voltage side of distribution transformers. In order to facilitate a comparison between the reviewed methods, their main characteristics are summarized in Table 7.

Table 7. Summary of main principles of methods proposed for intermittent faults (Publication IV).

| Method | Requirements | Principles |
|--------------------------|---|--|
| Ref. (Akke, 2011) | Neutral voltage measurement and zero sequence current | Correlation between $\frac{du_0}{dt}$ and I_0 |
| Ref. (Dong et al., 2012) | Voltage measurement and zero sequence current | Instantaneous powers P and Q and counting current spikes |

| | | |
|--|---|--|
| Ref. (Pettissalo, 2017) | Two phase currents and zero sequence current | Comparison of phase current magnitudes and directions |
| Ref. (Virtala, 2016) | Zero sequence voltage and currents | $\frac{\Delta I_0}{\Delta U_0}$ |
| Ref. (Wahlroos & Altonen, 2014) | Zero sequence voltage and currents | $\frac{\sum I_0}{\sum U_0}$ |

5.5 Method 2 modification

To adapt Method 2 for intermittent earth faults as much as possible, a slightly different approach is proposed in this section in order to incorporate their specific characteristics. The modification required is to keep count of NSC spikes over a window of a certain length. In this version of Method 2, a point is determined to be on the fault passage if the number of NSC spikes over a certain timeframe exceeds a pre-set value. In this version, no comparison is made between the first and other measuring points. Proper values for the magnitude threshold, the number of required spikes, and the window length must be obtained based on studying a series of real-life recordings of intermittent earth fault. In addition, when implementing the method in practice, these parameters must be configurable by the network operator. This chapter does not intend to propose definite values for these parameters.

In short, this version of Method 2 is spike-detection-based. Needless to say, if an intermittent earth fault strikes in a manner so random that the resulting spikes are too far apart from each other so that the condition regarding the required number of spikes in the window is not met, the fault passage indication and fault detection will fail.

5.6 Simulation and experimental results

Consider the MV distribution network presented in Figure 14 (in Chapter 4). An intermittent earth fault occurs at the same fault location shown in the figure. As in earlier simulations, measurements are obtained by a sampling rate of 10 kHz from

five points. The residual currents (summation of all three phase currents) measured at Point 3 (on the fault passage) and Point 4 (off the fault passage) are shown in Figure 33. The fault causes three spikes over a 0.6 s time frame. The spikes at Point 3 and Point 4 are in opposite directions which is in line with the findings presented earlier in Chapter 4, Section 4.3.2. The residual currents overlap each other in the time periods between spikes. The magnitudes of the computed NSC phasors are plotted in Figure 34. For better readability, they are plotted in separate subplots with different scales. Due to the intermittent nature of the fault, the NSC magnitudes are in the form of spikes. It is worth noting that the width of the spikes in Figure 34 is 20 ms, which equals one cycle of the fundamental frequency.

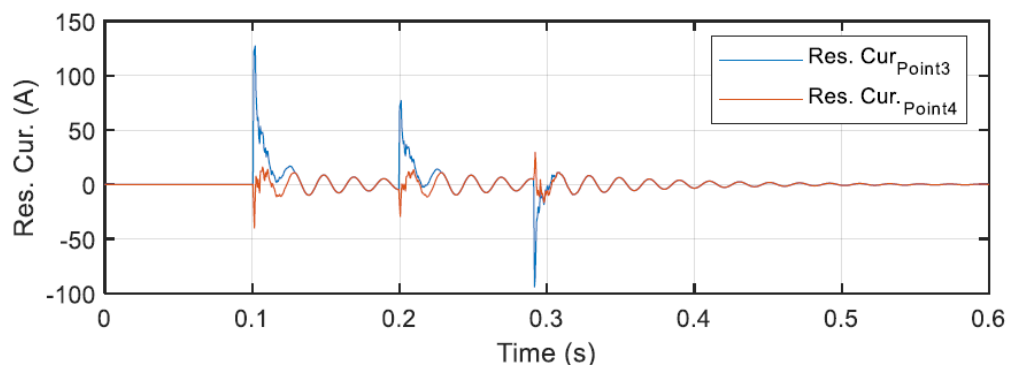


Figure 33. Residual currents at points before and after the fault point in the event of an intermittent earth fault on the network shown in Figure 14.

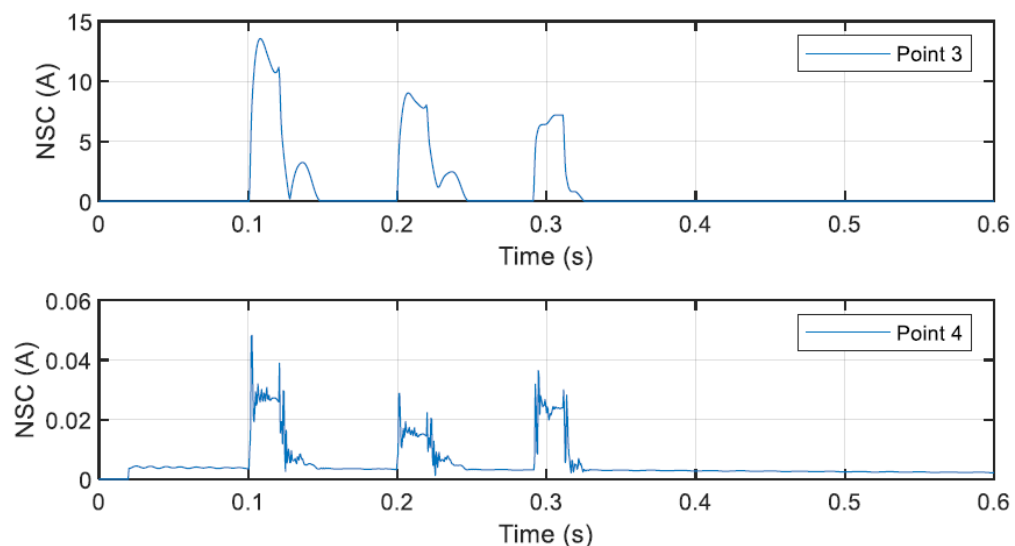


Figure 34. NSC (magnitudes) at points before and after the fault point in the event of an intermittent earth fault on the network shown in Figure 14.

Although, as mentioned earlier, no specific values are proposed for the parameters the method requires (the magnitude threshold, the number of required spikes, and the window length), one can distinguish the faulty feeder from the point off the fault path from the point on it. There are three significant spikes (greater than 5 A) in the NSC during a 0.6-second timeframe at Point 3 and therefore, it is identified to be located on the fault path. In contrast, Point 4 is determined to be off the fault path as there are no significant spikes in the NSC.

Now consider the real-life recordings presented in Figure 32. The calculated negative sequence currents of the recordings are shown in Figure 35. On the faulty feeder, there are nine spikes of the magnitude larger than 5 A during a 1.2-second timeframe. Therefore, using the proposed method, intermittent earth fault passage indication is possible.

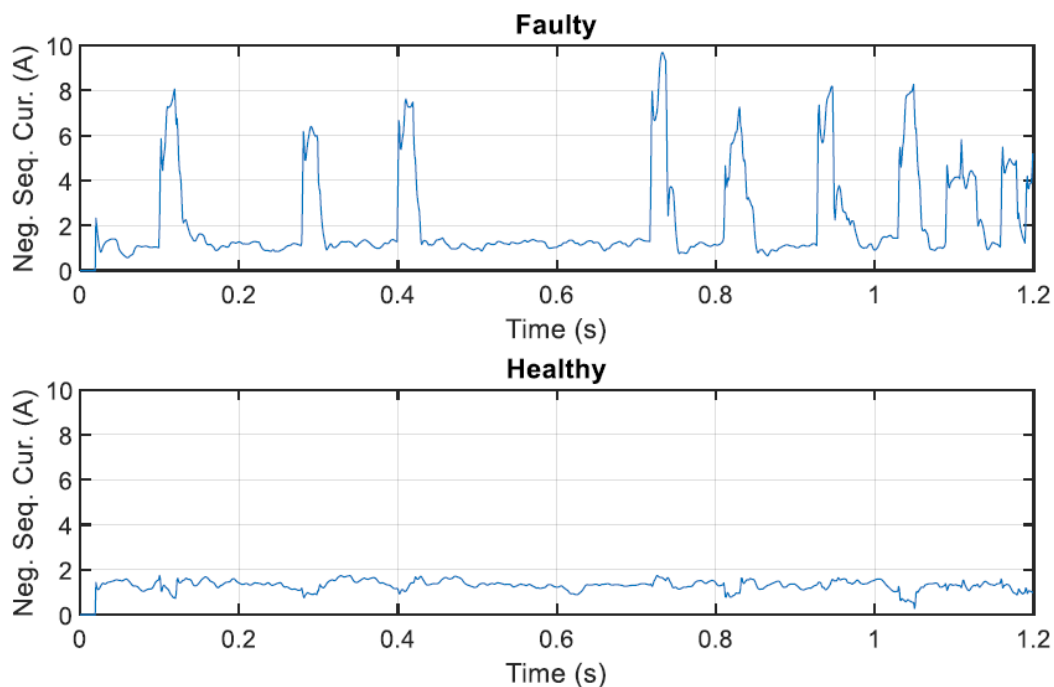


Figure 35. NSC (magnitudes) of the real-life recordings of the intermittent earth fault shown in Figure 32.

5.7 Discussion

The proposed method attempts to overcome the challenge caused by the intermittent characteristics of the intermittent earth fault. The proposed method has some differences with the original Method 2. An FPI device is supposed to detect the fault regardless of its type. It is not practical to first detect the type of the fault and then based on the type employ Method 2 or its modified version.

Therefore, when implementing Method 2, both algorithms need to run simultaneously since the type of the earth fault is unknown. Whichever algorithm detects the fault is prioritized over the other one.

The proposed method is based on the assumption that the NSC spikes are significant on the fault passage and insignificant off the fault passage. However, if the NSC spikes at points off the fault passage are large enough, then the method will fail and those points will be incorrectly determined to be located on the fault passage.

Intermittent earth fault detection and passage indication is a more challenging task than the detection and passage indication of permanent earth faults. The proposed method is not an ultimate solution and certainly, there is room for further improvement when applying this approach for either protection relays or fault passage indicators.

6 TECHNICAL REQUIREMENTS AND EXPERIMENTAL VERIFICATION

In this chapter, the following research questions raised earlier in Chapter 1 will be answered.

- *How can the proposed methods be implemented in practice and what are the key technical requirements and apparatus?*
- *What is the efficacy of the proposed methods in practice on real MV distribution networks?*

This chapter consists of two main parts. The first part is mainly based on Publication V. It deals with the key technical aspects of implementing the proposed methods in practice. In the second part, fault recordings obtained from field tests are presented and used to investigate the effectiveness of the proposed methods. One of the main objectives of this chapter is to compare the field tests results with the simulations results discussed in Chapter 4 and also the theory developed in Chapter 3. The field tests were carried out at the request of some Finnish DSOs. The actual tests were conducted by a company which specializes in performing test faults using dedicated equipment. The tests were performed in such a manner that they did not cause a power outage to the customers of the networks under testing.

6.1 Technical aspects

This section sheds light on some of the practical aspects of the realization of the proposed methods. The coverage includes apparatus recommended for carrying out current measurements, the structure of fault recordings, sampling rates, sensitivity, communication, etc. This chapter does not intend to present strict rules but some insights into how the proposed methods can be realized in practice. The guidelines and recommendations put forward in this section are the same ones used in performing the field tests and obtaining the data (fault recordings). The field test data and results will be discussed in depth in Section 6.2.

6.1.1 Measurements

The proposed FPI methods require only the measurement of phase currents and therefore no apparatus is needed for measuring any voltages. For measuring currents, there are different technologies available, such as:

- Iron-core current transformers

- Gapped-core current transformer.
- Linear couplers.
- Optical current sensor systems.
- Rogowski coils.

For measuring currents in the field tests Rogowski coil-based sensors were used. Rogowski coils were introduced in 1912. Due to their low-power output, their early applications were limited to magnetic field measurements. But later, with the development of low-burden microprocessor-based IEDs, they started to be used for current measurements. (IEEE Guide for Rogowski Coils, 2008) (IEEE Guide Rogowski, 2021). A Rogowski coil current sensor is an air-core coil that is wrapped around the conductor whose current is to be measured. The voltage induced across its terminals is a scaled time derivative of current enclosed by the coil. (IEEE Guide Rogowski, 2021). Rogowski coil-based current sensors offer many advantages over current transformers (CTs). As opposed to CTs, Rogowski coils do not saturate (linear output). In addition, since the secondary voltages of Rogowski coils are in the range of millivolt, they pose no hazard to personnel. From the environment viewpoint, oil-insulated CTs can leak oil and rupture whereas Rogowski coils do not have such disadvantages and therefore they are environmentally friendly. Moreover, their small size and light weight make them suitable for retrofit installations. They also offer a higher accuracy and cover a wider range of frequencies.

The output voltage signal induced in the coil is proportional to the time derivative of the current to be measured (Figure 36). Therefore, the induced voltage across the terminals needs to be integrated with a proper gain to be converted into current. The integration could be implemented through an embedded integration circuit or through software. In the field tests, the software integration was applied.

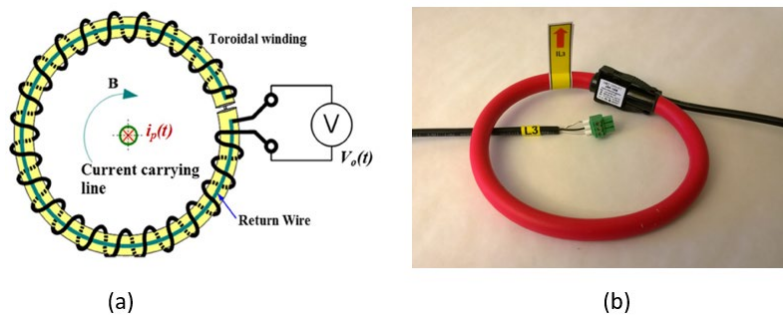


Figure 36. Rogowski-coil-based current sensor, showing a) operational principles, and b) actual sensor (Publication V).

Calculating NSC phasors using equation (3.4) requires phase angles of currents phasors. If one Rogowski coil in the sensor set is incorrectly installed in terms of polarity, it affects the calculated phase angle and consequently leads to incorrect phasor calculations. Therefore, it is essential that Rogowski coils for all phases are installed uniformly in a set of sensors. Correct installation of a Rogowski coil set is shown in Figure 37. The arrows marked on the sensors signify the polarity. However, it is not necessary to have different Rogowski coil sets installed uniformly i.e. the polarity of a set of current sensors at a given measuring point can be different than the polarity of the sensor set at another measuring point. In Section 6.2 where the field tests results are examined, this will be further demonstrated. In addition, when calculating the phasors, it is essential to ensure that the sequence of phase currents is *a-b-c*. Otherwise, for calculating NSC phasors, equation (3.4) must be modified accordingly.

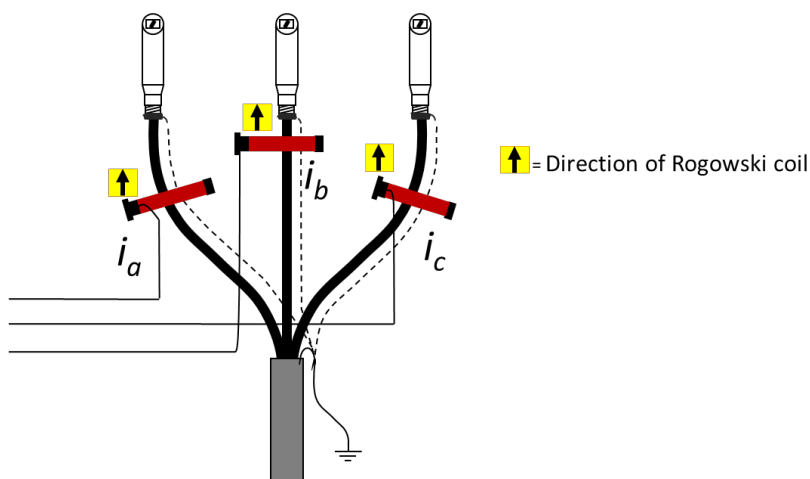


Figure 37. Correct installation of a Rogowski coil set at a given measuring point (Publication V, modified).

6.1.2 Data acquisition

The proposed methods determine the passage of the earth fault through a comparison between the sequence currents computed from phase currents measured at measuring points. In order to compute sequence currents and then perform the comparison analysis, the measured quantities need to be converted into sequence currents. Therefore, there is a need to collect all measurements for signal processing in one place i.e. the control center. As mentioned in Chapter 4, Section 4.4, an alternative is that the FPI unit installed at the measuring point computes the zero and negative sequence current phasors and sends only these two values to the control center. This approach provides a benefit i.e. the amount of data required to be transferred over the communication channel is reduced significantly. However, the downside would be that some additional computing resources would be required at the FPI unit.

In the following, the general operational principles regarding the structure of fault recordings, triggering logic, sampling rates, etc. are outlined.

6.1.3 Triggering and sensitivity

The FPI device constantly measures phase currents. However, recording (storing the data in the device memory) starts once the summation of phase currents (residual current) exceeds a pre-defined threshold. The system operator can adjust the threshold remotely at any time to achieve the desired sensitivity. Lowering the pre-defined value provides a higher sensitivity. The higher the earth fault resistance is, the lower the residual current will be and therefore, the higher sensitivity is required to detect it. Although higher sensitivity enables detection of high-resistance earth fault, there is a downside i.e. small disturbances that are not actual earth faults could trigger devices. This could result in a stream of disturbance recordings being sent to the control center for unnecessary detailed analysis.

6.1.4 Recording structure

The measurements are saved in the memory of the device once the device is triggered as a result of an abnormality in the network. The modem embedded in the device sends the recordings to the control center where they are further analyzed. Each recording that arrives at the control center consists of two parts:

1. No-fault period

2. During-fault period

As briefly discussed in Chapter 4, in an ideal network with perfect symmetry, no ZSC or NSC would exist in the network in a no-fault period. In practice, however, there could be cases where some zero or negative sequence currents exist even in the no-fault period. When an earth fault occurs, the NSC and ZSC levels increase. If Method 2 was based on the NSC during a fault condition, then there would be a need to know the NSC levels of the network at the measuring points in normal condition (in order to determine how much of the NSC during the fault condition is caused by the asymmetry of the network already existing in the pre-fault condition and how much of it is caused by the earth fault). However, the NSC level depends on asymmetry of load in the network and it can change as the load changes. Therefore, the NSC level at a given measuring point under normal condition is usually unknown and no assumption that will be always valid regarding the NSC level can be made. For this reason, to implement the proposed methods, each fault recording needs to contain measurements in normal pre-fault condition as well.

6.1.5 Sampling rate

There are different sampling rates used by feeder protection relays and FPI units. Some sampling rates that some relay and FPI manufacturers use include 1.6 kHz (ABB, 2021), and 3.2 kHz (Arcteq, 2021). These sampling rates are adequate for accurately detecting permanent earth faults. As described earlier, an intermittent earth fault causes short duration current spikes with a typical of typically 0.1 ms to 1 ms. In order to capture the spikes completely, higher sampling rates are needed. For instance, Ref. (a-eberle, 2020) uses a 10.24 kHz sampling rate and Ref. (Pettissalo, 2017) 25.6 kHz. For implementing the proposed methods, those commonly used sampling rates are sufficient. In theory, there is no upper limit on the sampling frequency. However, when it comes to practical implementation, there are hardware limitations and the hardware price increases as the sampling rate increases.

6.1.6 Communication

Every FPI device that has been triggered as a result of an abnormality in the network reports its recordings to an upper-level system. The recordings are eventually received at the control center where the signal processing and analysis are carried out to determine the passage of the earth fault. This is illustrated in Figure 38. The communication technologies that can be used for transferring the

data include the common wireless mobile networks (3G, 4G, or 5G). In principle, the fault recordings can be transmitted through any available communication system at secondary substations using some common telecommunication protocol such as IEC 60870-5-104, taking into account that it needs to be compatible with the systems at the control center.

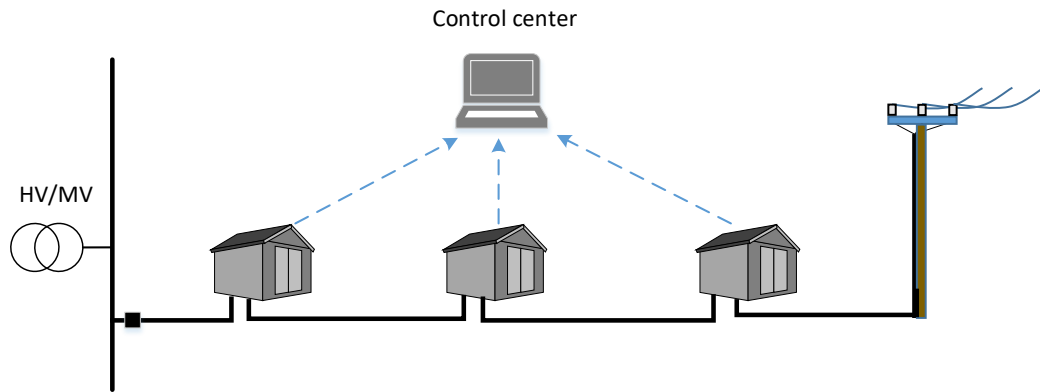


Figure 38. FPI devices installed at pad-mounted secondary substations (Publication V).

6.2 Field tests

In this section, a number of recordings obtained from two sets of field tests are used to examine the validity of the proposed methods. The field tests were performed on two MV distribution networks in rural areas in Finland. A series of tests were conducted on each of the networks. The tests included earth faults with various fault resistances. In the first network under study, the measurements were obtained from the faulty feeder from the points on the fault passage and the points off the fault passage. In the second network, there were measuring points on the adjacent healthy feeder as well. In addition, there was a measuring point located on a branch of the faulted feeder.

6.2.1 Network 1 specifications

The type of the network on which the first set of tests was carried out was compensated. The feeder under study was mixed i.e. it consisted of both cables and overhead lines. Six FPI devices were installed at six secondary substations as shown in Figure 39. The distance of each measuring point from the fault location is given in the table. The earth faults were applied at the segment between measuring Point 1 and measuring Point 2. The tests were conducted with various

earth fault resistances. In these tests, the measuring Point 1 was located near the beginning of the feeder and not at the primary substation. This was due to safety risks and also to avoid complication that could have been caused by installing anything new at the primary substation. For these tests, it was safer to install the current sensors at the secondary substations along the feeder.

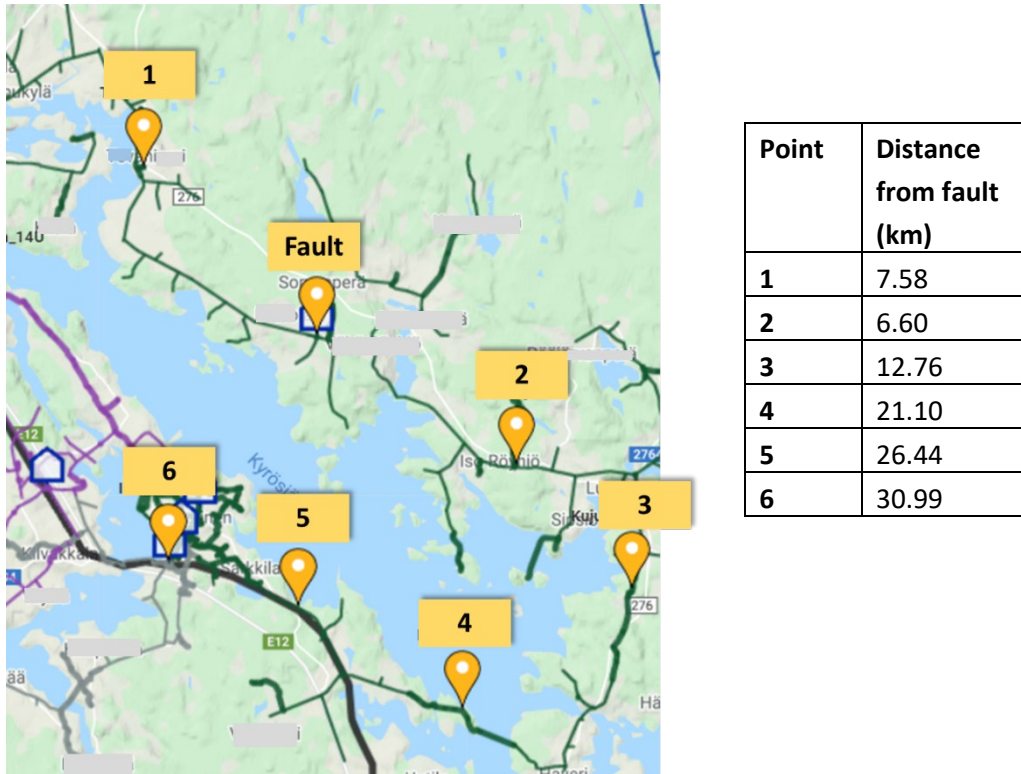


Figure 39. Earth fault field testing on an MV distribution feeder with seven secondary substations and six measurement points, courtesy of Safegrid Oy.

6.2.2 Scenario 1

The type of the network in this scenario is compensated and therefore, Method 1 is not applicable. The power supply is behind Point 1 which makes Point 1 the first measuring point on the faulted feeder located near the beginning of the feeder and Point 6 the last measuring point located near the end of the feeder. The faulted segment is the one between Point 1 and Point 2; therefore, Point 1 is considered to be located on the fault passage and other points off the fault passage. The phase-current measurements obtained by the FPI devices installed at points 1 to 5 are shown in Figure 40. The fault resistance $R_F = 0.2 \Omega$. No attempt has been made to synchronize the recordings either during the tests or after receiving the recordings. However, for all the recordings, the fault occurs at around $t = 0.1$ s. By making a

one-on-one comparison between phase currents of Point 1 and phase currents of Point 2, it can be seen that phase 'a', phase 'b' and phase 'c' at Point 1 correspond to phase 'b', phase 'c', and phase 'a' at Point 2, respectively. However, this mismatch is not a concern and does not affect the outputs of the proposed methods. The reason for this mismatch is that in practice, it is not easy to identify what conductor is phase 'a' and what conductor is phase 'b' and etc. In fact, naming the conductors as phases 'a', 'b' or 'c' does not matter as long as they are named so that the positive sequence is $a-b-c$. Even if the naming is done so that the sequence is $a-c-b$, it is not a concern as the sensors and conductors can be renamed in the signal processing stage. In addition, note that there are no measurements from Point 6. This is due to the fact that device 6 in this scenario was not triggered. The reason is that device 6 was installed near the end of the feeder where the length of the feeder after the device was short. Therefore, the line-to-ground capacitances of the line section behind this device were not noticeable. As a result, the ZSC measured at Point 6 during the earth fault occurrence was not large enough to trigger the device. The ZSC and NSC for each measuring point are plotted in Figure 41.

Table 8 presents the phasor amplitudes of zero and negative sequence currents computed using equations (3.3) and (3.4) for no-fault period and during-fault period (for the steady states). The notations used in the table are the same ones introduced in Chapter 3 and used in Chapter 4 (the list of notations can be found in Chapter 3, Section 3.2). The table also presents the outputs of Method 1 and Method 2 for each point. To calculate the sequence currents equations (3.3) and (3.4) are used. In this scenario, Method 1 yields correct results although Method 1 is not intended for compensated networks. Using Method 2, each point can be correctly identified and the faulted segment (the segment between Point 1 and Point 2) can be determined.

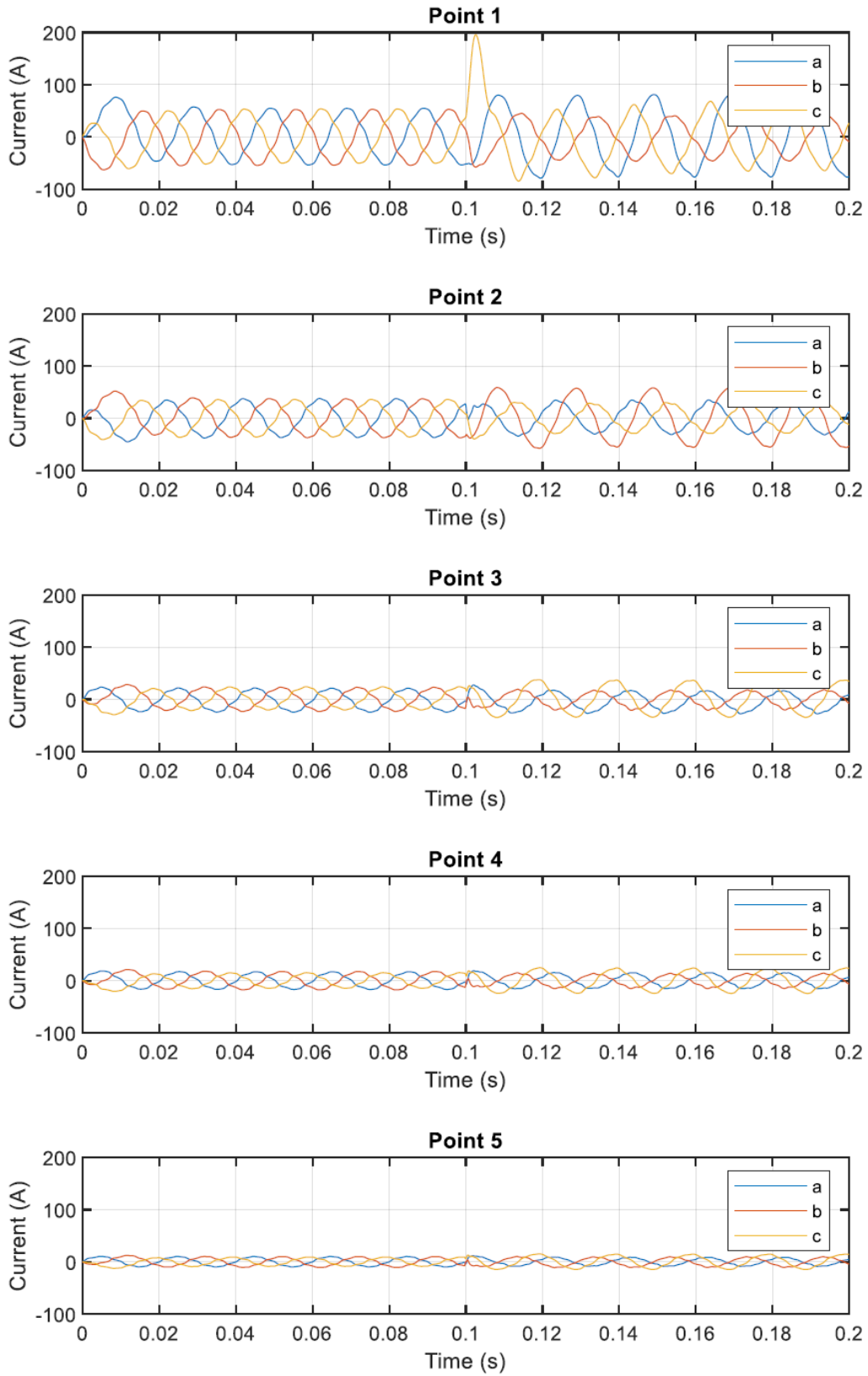


Figure 40. Current measurements at five points during earth fault testing, Scenario 1, courtesy of Safegrid Oy.

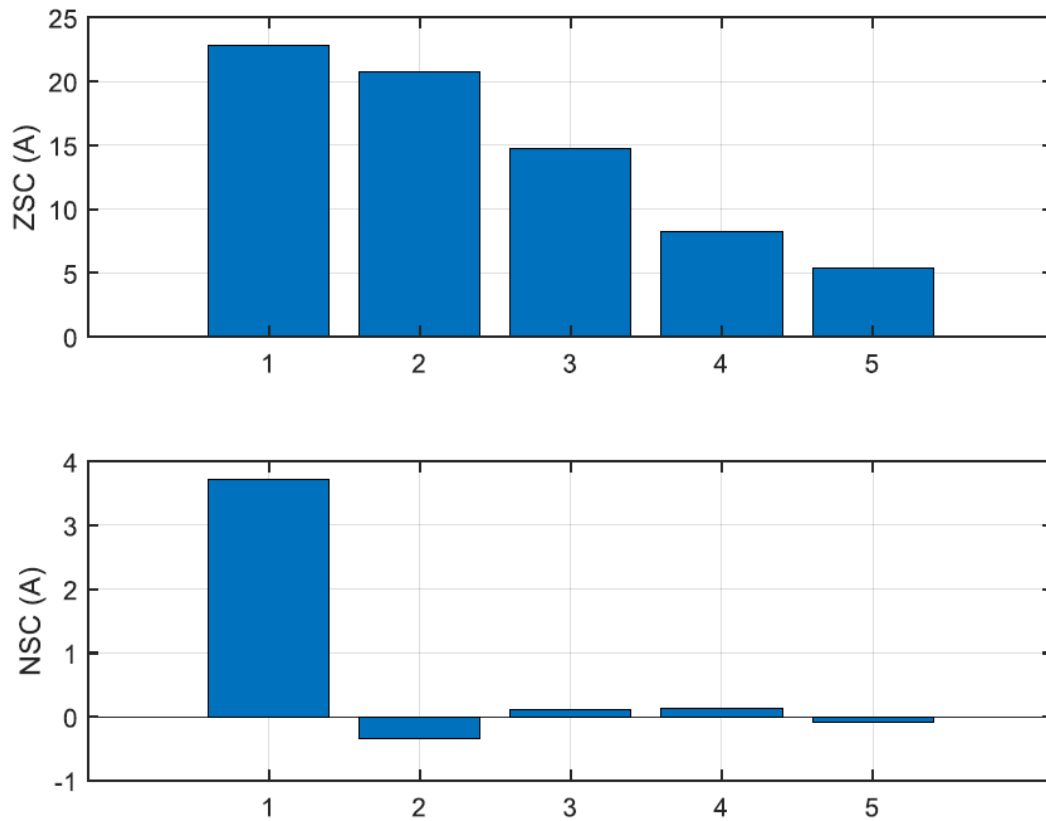


Figure 41. Amplitudes of zero and negative sequence current phasors of recordings shown in Figure 40.

Table 8. Sequence currents for pre- and during-fault periods.

| | $R_F = 0.2 \Omega$ | | | | | |
|-----------------------|--------------------|---------|---------|---------|---------|---------|
| | Point 1 | Point 2 | Point 3 | Point 4 | Point 5 | Point 6 |
| $ I_{pre}^{(0)} $ (A) | 0.89 | 0.20 | 0.14 | 0.44 | 0.38 | - |
| $ I_{dur}^{(0)} $ (A) | 23.68 | 20.91 | 14.84 | 8.71 | 5.75 | - |
| $\Delta I^{(0)}$ (A) | 22.79 | 20.71 | 14.70 | 8.27 | 5.36 | - |
| $\Delta I_N^{(0)}$ | 1.00 | 0.90 | 0.64 | 0.36 | 0.23 | - |
| Method 1 | On | Off | Off | Off | Off | Off |
| $ I_{pre}^{(2)} $ (A) | 0.82 | 0.97 | 0.71 | 1.13 | 1.18 | - |
| $ I_{dur}^{(2)} $ (A) | 4.54 | 0.62 | 0.83 | 1.27 | 1.10 | - |
| $\Delta I^{(2)}$ (A) | 3.71 | -0.35 | 0.12 | 0.14 | -0.08 | - |
| $\Delta I_N^{(2)}$ | 1.00 | -0.09 | 0.03 | 0.04 | -0.02 | - |
| Method 2 | On | Off | Off | Off | Off | Off |

The residual currents (summation of all three phase currents) at Point 1 and Point 2 are shown in Figure 42. The figure shows pre- and during-fault periods. In the transient period, the residual currents flow in opposite directions. However, in the steady state period, they almost flow in the same direction with a small phase-angle difference. This is in line with the findings of Chapter 4, Section 4.3.2.

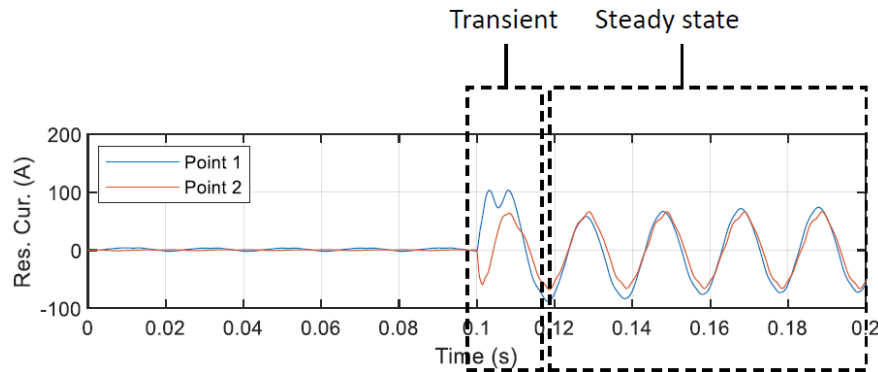


Figure 42. Residual currents at Point 1 (on fault passage) and Point 2 (off fault passage) for network of Figure 39 when operating in compensated mode.

6.2.3 Scenario 2

The fault location remains the same but power flow is reversed i.e. the power supply is now behind Point 6. This makes Point 6 the first measuring point on the faulted feeder located near the beginning of the feeder and Point 1 the last measuring point. Therefore, in this scenario, points 2 to 6 are considered to be located on the fault passage and Point 1 off the fault passage.

The phase-current measurements obtained by the FPI devices are shown in Figure 43. All devices were triggered and recorded their measurements. The ZSC and NSC for each measuring point are plotted in Figure 44. The ZSC level during the earth fault decreases as we move from Point 6 to Point 2. The NSC remains practically constant. This is in line with the findings of Chapter 3 and Chapter 4 regarding the behavior of sequence currents along the faulted feeder during an earth fault in a compensated distribution network.

Table 9 presents the phasor amplitudes of zero and negative sequence currents computed using equations (3.3) and (3.4) for the no-fault period and the during-fault period for four fault resistances. It also presents the outputs of Method 1 and Method 2 for each point. Method 1 leads to incorrect results as this method is not intended for compensated networks. However, using Method 2, each point can be correctly identified and the faulted segment can be determined.

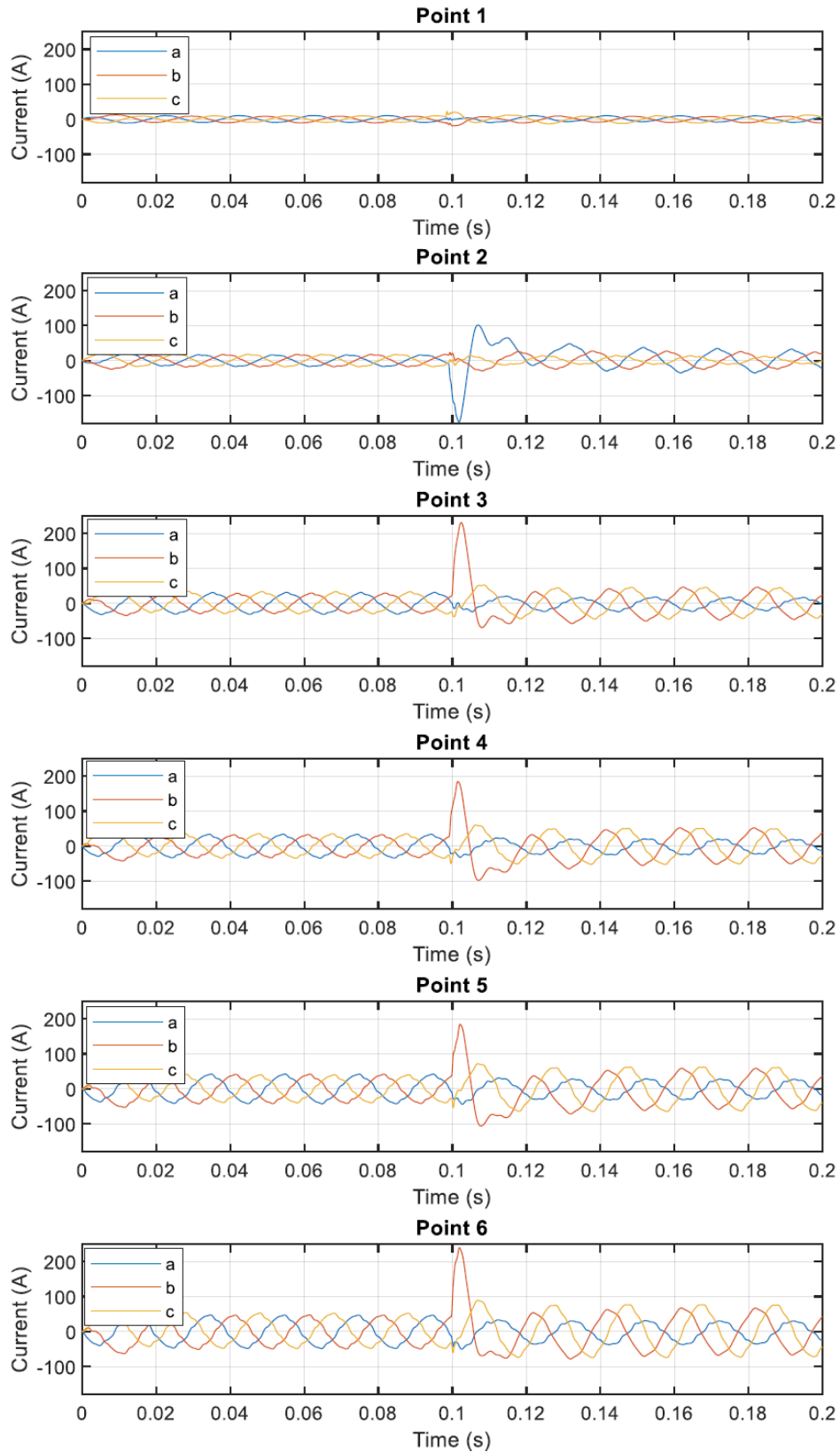


Figure 43. Current measurements at six points during earth fault testing, Scenario 2, courtesy of Safegrid Oy.

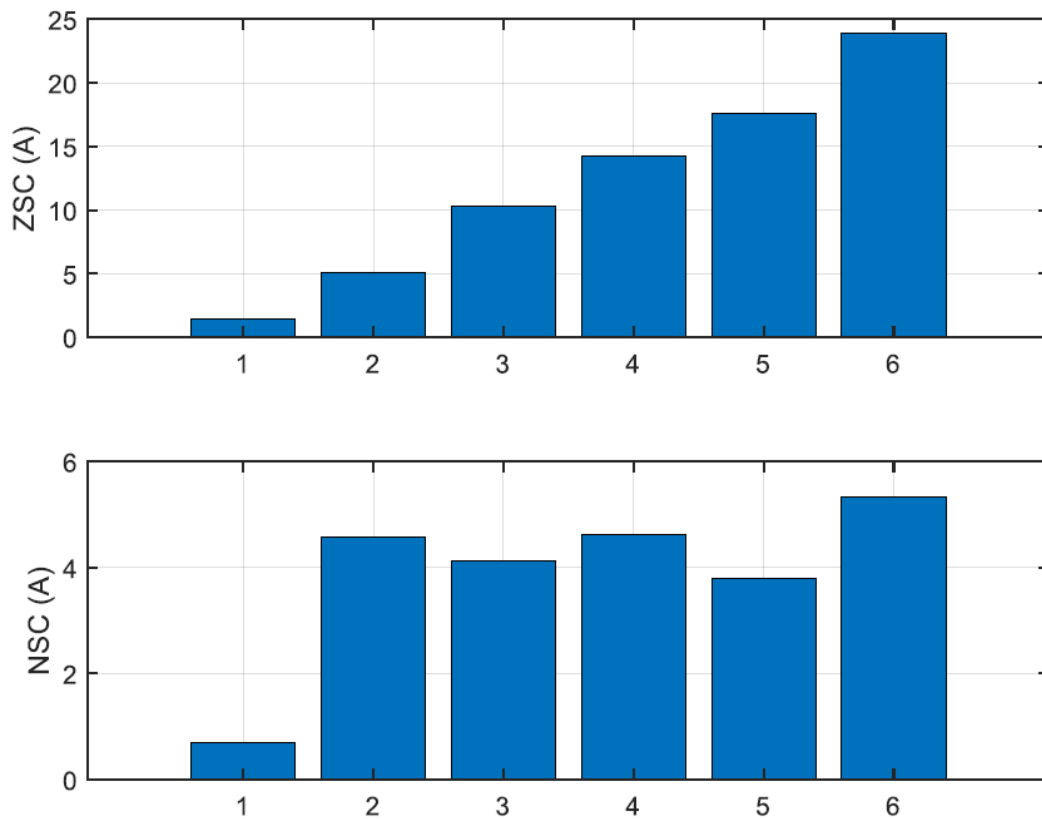


Figure 44. Increase in amplitudes of ZSC and NSC phasors as a result of an earth fault occurrence for recordings of Figure 39, when the network type is compensated.

Table 9. Sequence currents for pre- and during-fault periods for various fault resistances, when the network type is compensated.

| | $R_F = 0.2 \Omega$ | | | | | |
|-----------------------|--------------------|------|------|-------|-------|-------|
| | 1 | 2 | 3 | 4 | 5 | 6 |
| $ I_{pre}^{(0)} $ (A) | 0.04 | 0.26 | 0.53 | 0.56 | 0.37 | 0.81 |
| $ I_{dur}^{(0)} $ (A) | 0.95 | 4.39 | 7.64 | 10.55 | 12.57 | 16.59 |
| $\Delta I^{(0)}$ (A) | 0.91 | 4.13 | 7.11 | 9.99 | 12.2 | 15.78 |
| $\Delta I_N^{(0)}$ | 0.06 | 0.26 | 0.45 | 0.63 | 0.77 | 1.00 |
| Method 1 | Off | Off | Off | Off | Off | On |
| $ I_{pre}^{(2)} $ (A) | 0.22 | 0.28 | 0.40 | 0.15 | 0.57 | 0.41 |
| $ I_{dur}^{(2)} $ (A) | 0.50 | 3.05 | 3.08 | 3.13 | 3.23 | 3.89 |
| $\Delta I^{(2)}$ (A) | 0.28 | 2.77 | 2.68 | 2.99 | 2.66 | 3.48 |
| $\Delta I_N^{(2)}$ | 0.13 | 0.78 | 0.79 | 0.80 | 0.83 | 1.00 |
| Method 2 | Off | On | On | On | On | On |

| $R_F = 50 \Omega$ | | | | | | |
|-----------------------|------|------|------|-------|-------|-------|
| | 1 | 2 | 3 | 4 | 5 | 6 |
| $ I_{pre}^{(0)} $ (A) | 003 | 0.26 | 0.52 | 0.55 | 0.37 | 0.81 |
| $ I_{dur}^{(0)} $ (A) | 0.91 | 4.36 | 7.48 | 10.28 | 12.20 | 16.06 |
| $\Delta I^{(0)}$ (A) | 0.87 | 4.10 | 6.95 | 9.73 | 11.83 | 15.25 |
| $\Delta I_N^{(0)}$ | 0.06 | 0.27 | 0.46 | 0.64 | 0.78 | 1.00 |
| Method 1 | Off | Off | Off | Off | Off | On |
| $ I_{pre}^{(2)} $ (A) | 0.31 | 0.49 | 1.22 | 0.87 | 0.40 | 0.67 |
| $ I_{dur}^{(2)} $ (A) | 0.44 | 3.25 | 3.16 | 3.02 | 2.99 | 3.68 |
| $\Delta I^{(2)}$ (A) | 0.13 | 2.76 | 1.94 | 2.15 | 2.59 | 3.01 |
| $\Delta I_N^{(2)}$ | 0.12 | 0.88 | 0.86 | 0.82 | 0.81 | 1.00 |
| Method 2 | Off | On | On | On | On | On |
| $R_F = 250 \Omega$ | | | | | | |
| | 1 | 2 | 3 | 4 | 5 | 6 |
| $ I_{pre}^{(0)} $ (A) | 0.06 | 0.22 | 0.44 | 0.43 | 0.44 | 0.74 |
| $ I_{dur}^{(0)} $ (A) | 0.74 | 4.24 | 6.25 | 8.19 | 9.46 | 12.52 |
| $\Delta I^{(0)}$ (A) | 0.68 | 4,02 | 5.81 | 7.76 | 9.02 | 11.79 |
| $\Delta I_N^{(0)}$ | 0.06 | 0.34 | 0.49 | 0.66 | 0.77 | 1.00 |
| Method 1 | Off | Off | Off | Off | Off | On |
| $ I_{pre}^{(2)} $ (A) | 0.65 | 0.79 | 1.17 | 0.96 | 0.40 | 0.59 |
| $ I_{dur}^{(2)} $ (A) | 1.19 | 3.21 | 2.96 | 3.02 | 3.37 | 3.88 |
| $\Delta I^{(2)}$ (A) | 0.54 | 2.41 | 1.79 | 2.06 | 2.97 | 3.28 |
| $\Delta I_N^{(2)}$ | 0.31 | 0.83 | 0.76 | 0.78 | 0.87 | 1.00 |
| Method 2 | Off | On | On | On | On | On |
| $R_F = 500 \Omega$ | | | | | | |
| | 1 | 2 | 3 | 4 | 5 | 6 |
| $ I_{pre}^{(0)} $ (A) | 0.05 | 0.22 | 0.44 | 0.45 | 0.43 | 0.75 |
| $ I_{dur}^{(0)} $ (A) | 0.57 | 3.49 | 4.83 | 6.23 | 7.06 | 9.52 |
| $\Delta I^{(0)}$ (A) | 0.53 | 3.27 | 4.39 | 5.78 | 6.64 | 8.76 |
| $\Delta I_N^{(0)}$ | 0.06 | 0.37 | 0.50 | 0.66 | 0.76 | 1.00 |
| Method 1 | Off | Off | Off | Off | Off | On |

| | | | | | | |
|-----------------------|------|------|------|------|------|------|
| $ I_{pre}^{(2)} $ (A) | 0.33 | 0.77 | 0.91 | 0.67 | 0.35 | 0.46 |
| $ I_{dur}^{(2)} $ (A) | 0.77 | 2.71 | 2.46 | 2.66 | 2.83 | 3.31 |
| $\Delta I^{(2)}$ (A) | 0.45 | 1.95 | 1.55 | 1.99 | 2.48 | 2.85 |
| $\Delta I_N^{(2)}$ | 0.23 | 0.82 | 0.74 | 0.80 | 0.85 | 1.00 |
| Method 2 | Off | On | On | On | On | On |

6.2.4 Scenario 3

In this scenario, the fault location and power flow direction remain the same i.e. the power supply is behind Point 6. The compensation coil is disconnected and therefore, the network operates as a neutral-isolated network. As in Scenario 2, Point 6 is the first point located at the beginning of the faulted feeder and Point 1 is the last measuring point. Therefore, similar to Scenario 2, points 2 to 6 are considered to be located on the fault passage and Point 1 off the fault passage. As in this scenario the network type is neutral-isolated, both Method 1 and Method 2 are applicable. Earth fault recordings from the measuring points are shown in Figure 45. The increase in the ZSC i.e. $\Delta I^{(0)}$ and the increase in the NSC i.e. $\Delta I^{(2)}$ are shown in Figure 46. Table 10 presents the phasor amplitudes of zero and negative sequence currents computed using equations (3.3) and (3.4) for the no-fault period and the during-fault period. It can be seen from the table that one can determine the faulted segment using either of the proposed methods.

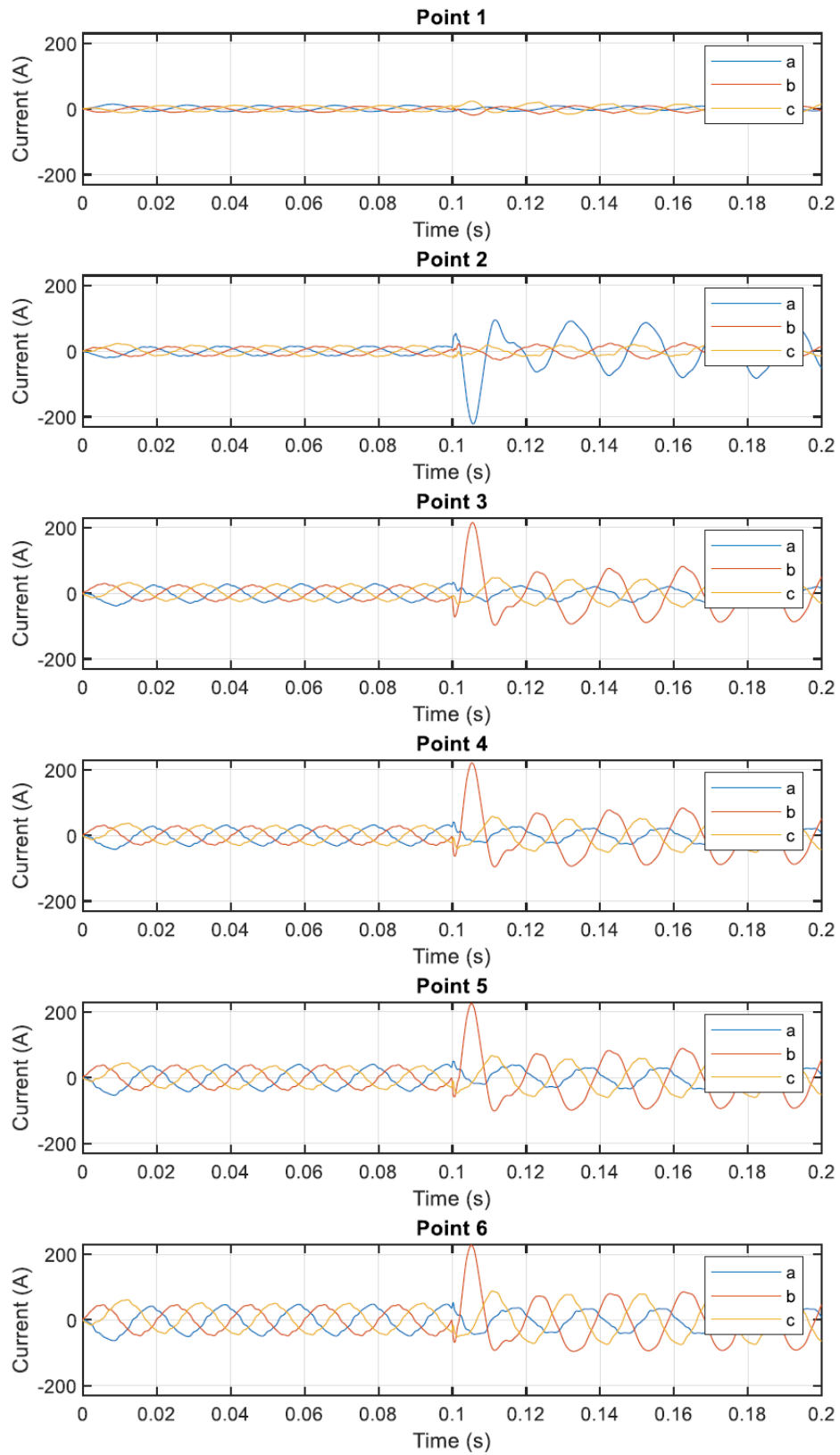


Figure 45. Current measurements at six points during earth fault testing, Scenario 3, courtesy of Safegrid Oy.

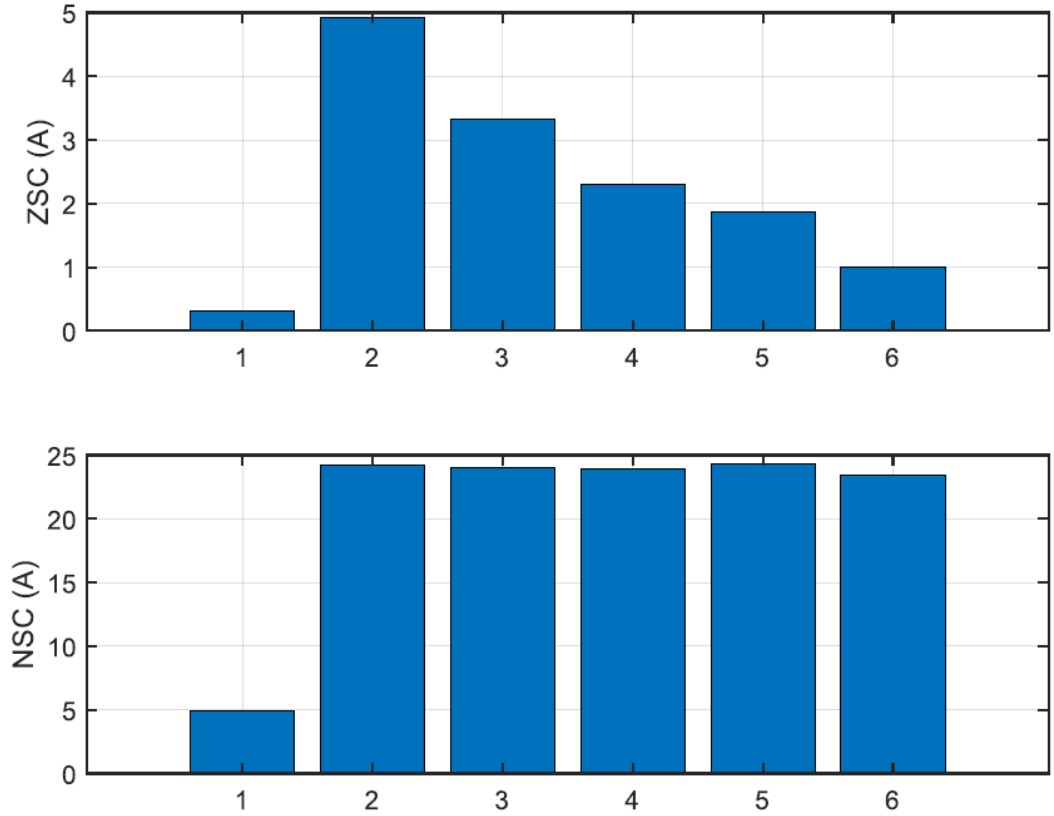


Figure 46. Increase in amplitudes of ZSC and NSC phasors as a result of an earth fault occurrence for recordings of Figure 39, when the network type is neutral-isolated.

Table 10. Sequence currents for pre- and during-fault periods, when the network type is neutral-isolated.

| $R_F = 0.2 \Omega$ | | | | | | |
|-----------------------|------|-------|-------|-------|-------|-------|
| | 1 | 2 | 3 | 4 | 5 | 6 |
| $ I_{pre}^{(0)} $ (A) | 0.09 | 0.35 | 0.61 | 0.68 | 0.66 | 1.13 |
| $ I_{dur}^{(0)} $ (A) | 1.52 | 22.27 | 15.43 | 10.95 | 8.93 | 5.57 |
| $\Delta I^{(0)}$ (A) | 1.43 | 21.92 | 14.81 | 10.26 | 8.27 | 4.44 |
| $\Delta I_N^{(0)}$ | 0.32 | 4.93 | 3.33 | 2.31 | 1.86 | 1.00 |
| Method 1 | Off | On | On | On | On | On |
| $ I_{pre}^{(2)} $ (A) | 0.25 | 1.18 | 1.05 | 0.6 | 1.64 | 0.62 |
| $ I_{dur}^{(2)} $ (A) | 4.88 | 24.23 | 24.01 | 23.9 | 24.31 | 23.44 |
| $\Delta I^{(2)}$ (A) | 4.63 | 23.05 | 22.96 | 23.31 | 22.68 | 22.82 |
| $\Delta I_N^{(2)}$ | 0.2 | 1.01 | 1.01 | 1.02 | 0.99 | 1.00 |
| Method 2 | Off | On | On | On | On | On |

6.2.5 Network 2

To further investigate the effectiveness of Method 2, another set of field tests was conducted on another compensated MV distribution network. In this section, one set of the recordings is analyzed. In addition to the fact that the network under study is not the same network as in Section 6.2.1, the main difference between the tests that will be discussed in this section and other tests discussed earlier in Section 6.2.1 is the location of the first measuring point. In Network 2, the first measuring point is located on the secondary side of the HV/MV transformer. The winding type of the secondary side of the transformer is delta and therefore, the residual current (and consequently the ZSC) is always around 0A. The objective is to investigate the impact of this type of measurement arrangement on the proposed methods.

A simplified schematic of the network under study is shown in Figure 47 (the real network consists of several feeders and branches). The distance of each measuring point to the fault location is presented in the table of the figure. The feeders are mixed i.e. they consist of underground cables in areas near the secondary substations and overhead lines in areas far away from the secondary substations. There are eight measuring points. Point 1 is located at the primary substation on the secondary side of the main transformer as shown in the figure. Measuring points 2 to 5 are spread along the faulty feeder (the feeder on which the earth fault tests were conducted). The earth fault occurs at the segment between Point 2 and Point 3. Therefore, points 1 and 2 are located on the fault passage and points 3 to 5 off it. Point 6 is located on a branch. This makes Point 6 an off-the-fault-passage point. Points 7 and Point 8 are located at the adjacent feeder which is unfaulty and hence, located off the fault path.

The computed sequence currents and the output of each method are presented in Table 11. Point 1 is chosen as the first device. Using Method 1 leads to incorrect fault passage indication, as expected, since it is not possible to get meaningful measurements of ZSC from Point 1. Using the original version of Method 2 leads to correct determinations except for Point 1. This is due to the fact that Method 2 takes into account $\Delta I^{(0)}$ as well. For Point 1, the condition regarding $\Delta I^{(0)}$ is not met ($\Delta I^{(0)}$ is insignificant). Therefore, in measurement arrangements where the first device is installed on the secondary side of the main transformer with delta type of winding, a small modification to Method 2 is needed. The modification is that for such measuring points, the condition regarding the $\Delta I^{(0)}$ does not need to be met.

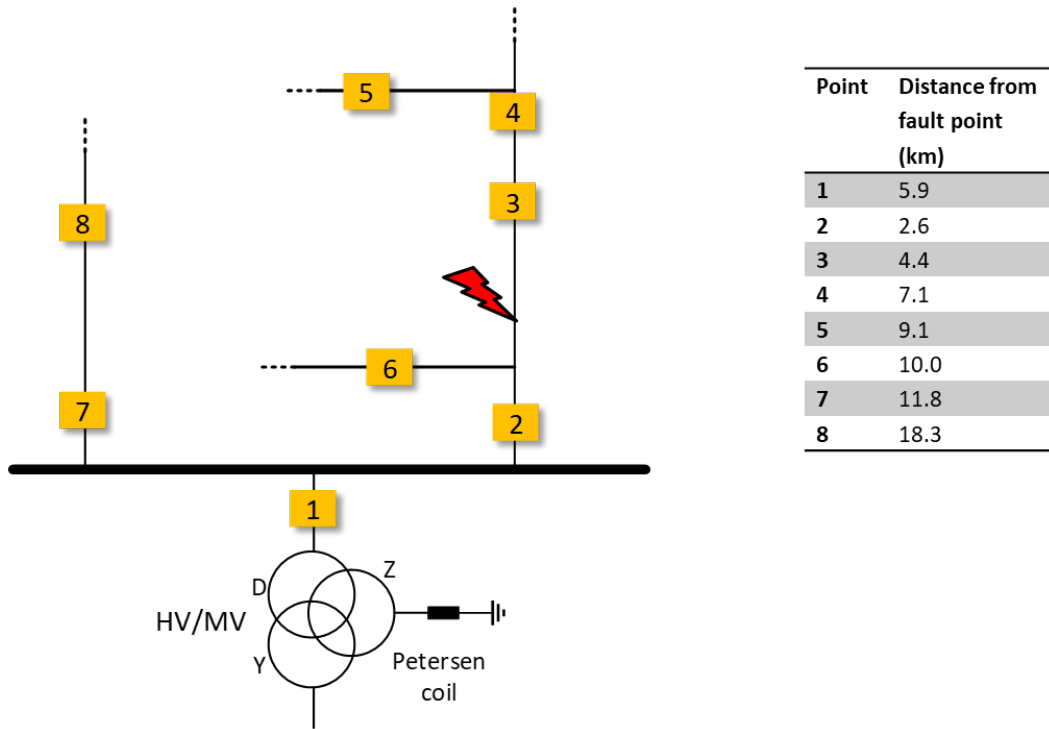


Figure 47. Earth fault field testing on a real compensated MV distribution network, with FPI units installed at eight measuring points, courtesy of Safegrid Oy.

Table 11. Sequence currents computed for pre and during-fault periods for the eight measuring points of the network of Figure 47.

| | 1 | 2 | 3 | 4 | 5 | 6 | 7 | 8 |
|-----------------------|------|--------|-------|------|------|-------|--------|--------|
| $ I_{pre}^{(0)} $ (A) | 0.39 | 0.58 | 0.40 | 0.13 | 0.01 | 0.17 | 0.34 | 0.31 |
| $ I_{dur}^{(0)} $ (A) | 0.45 | 11.50 | 0.35 | 0.18 | 0.33 | 5.65 | 10.68 | 10.30 |
| $\Delta I^{(0)}$ (A) | 0.06 | 10.92 | -0.05 | 0.06 | 0.32 | 5.48 | 10.34 | 10.00 |
| $\Delta I_N^{(0)}$ | 1.00 | 182.00 | -0.79 | 0.96 | 5.41 | 92.72 | 174.89 | 169.11 |
| M 1 | On | On | Off | Off | On | On | On | On |
| $ I_{pre}^{(2)} $ (A) | 0.70 | 1.21 | 0.56 | 0.35 | 0.07 | 0.25 | 0.06 | 0.06 |
| $ I_{dur}^{(2)} $ (A) | 2.47 | 2.19 | 0.54 | 0.54 | 0.72 | 0.27 | 0.16 | 0.15 |
| $\Delta I^{(2)}$ (A) | 1.77 | 0.97 | -0.02 | 0.19 | 0.64 | 0.02 | 0.10 | 0.09 |
| $\Delta I_N^{(2)}$ | 1.00 | 0.89 | 0.22 | 0.22 | 0.29 | 0.11 | 0.07 | 0.06 |
| M 2 | Off | On | Off | Off | Off | Off | Off | Off |

7 CONCLUSION

This doctoral dissertation dealt with earth fault passage indication in medium voltage distribution networks. The type of fault on which this work focused was the single-phase earth fault. The focus was placed on two types (from the viewpoint of neutral treatment) of networks in particular i.e. the neutral-isolated network and the compensated network. The reason was that earth fault detection, location, and path indication in these types of networks is more difficult compared to in other networks as the earth fault current in these networks is generally lower. This dissertation proposed two methods for earth FPI applications for these types of networks. In Method 1 and original Method 2, earth FPI is realized through collecting current measurements from various measuring points and transferring them to a central location where the data is processed and a comparison between the measurements of the first point and other points is conducted (in the modified version of Method 2, this comparison is not made). In brief, Method 1 is intended for isolated networks and utilizes the ZSC and Method 2 is meant for compensated networks and employs both the ZSC and NSC. In this dissertation, the performances of the proposed methods were verified through simulations and data from field tests.

In this chapter, main contributions and findings are highlighted and future research items are identified.

7.1 Main conclusions and findings

The neutral treatment of a network affects the amount of earth fault current which consequently affects the amount of fault current flowing through the points located on the fault passage. Isolated neutral networks and compensated networks are the two types of networks in which the earth fault current level is lower than in other networks which makes earth FPI a more difficult task. The theoretical analysis, simulation results, and field test results showed that in isolated networks, the ZSC provides sufficient information for FPI applications. In a realistic isolated network, the magnitude of the ZSC phasor increases from the beginning of the faulted feeder towards the fault point and then drops after that. However, this is not the case in a network with a long single feeder (with no background network) when the earth fault is so close to the beginning of the feeder. However, such a network is unrealistic (the details were discussed in Section 4.4).

In contrast, the ZSC is insufficient for earth FPI applications in compensated networks. The reason is that the compensation coil causes the behavior of the ZSC along the faulted feeder to change so that the magnitude of the ZSC phasor during

an earth fault condition decreases from the beginning of the faulted feeder towards the fault point. Therefore, it is not possible to determine which point is located on the earth fault path and which point is off using solely the ZSC. In contrary to the ZSC, the behaviors of the NSC in both types of networks are similar. According to the simulations and field tests results presented in this dissertation, the magnitude of the NSC remains almost the same from the beginning of the faulted feeder towards the fault point and drops after that.

However, asymmetry in the network, caused by e.g. imbalance load, etc, causes the NSC to increase. In other words, not every increase in the NSC is indicative of an earth fault. For this reason, both proposed methods employ the ZSC to primarily detect an earth fault condition. In addition, both methods require knowledge of which device is the first device in the feeder so that it can be used as a reference.

There is a specific type of earth fault phenomenon that is common in compensated networks with underground cables known as the intermittent earth fault. The applicability of the developed methods for this type of fault was also studied. Method 2 in its original form is incapable of reliably detecting this type of fault. Therefore, a modified version of it was devised to overcome the challenges posed by the unique characteristics of these types of faults.

In conclusion, according to the simulations and field tests results, utilizing sequence current quantities, in the manner proposed in this work, enable locating of continuous (permanent) and intermittent earth faults in non-effectively grounded MV distribution networks with radial feeders. The fault resistances could range from zero to several kilo-ohms. In practice, the methods are reliable as long as the current measurements are accurate enough.

7.2 Contributions

The research work reported in this dissertation contributes to the topic of earth fault path indication. In brief, the main contributions of this dissertation include:

1. A comprehensive review of existing state-of-the-art methods for locating earth faults in MV distribution networks (Publication I). For each method, the review covered their basic principles, evaluated their pros and cons, and provided a comparison of their key features.
2. Two novel methods for earth fault path indication in non-effectively grounded MV distribution networks (publications II, III, IV). The distinctive feature of the developed methods is that they do not require any

voltage measurement. The strength of both methods lies in the comparison made between the calculated symmetrical sequence components of the currents at each measuring point with that of the first device. For the comparison, accurate time synchronization between recordings collected and transferred to the central location is not required. The aspects of this contribution include:

Theory: The reasoning behind the proposed methods was discussed in depth utilizing a solid and established theoretical foundation.

Simulations (publications II, III, IV): The proposed methods were validated through a verified PSCAD model of a real distribution network. In addition, for both isolate networks and compensated networks, the proposed methods were compared with one of the conventional FPI methods i.e. the zero sequence admittance.

Field tests: A series of earth fault recordings obtained from field testing on two Finnish distribution networks with both isolated and compensated grounding arrangements further validated the effectiveness of the proposed methods. The evaluation of the methods effectiveness utilizing the field test data can be considered as one of the most significant results of this dissertation. The field test results were in line with the simulation results.

Suggestions and guidelines related to technical requirements and practical implementation (Publication V): The aspects covered include apparatus recommended for carrying out current measurements, the structure of fault recordings, sampling rates, sensitivity, and communication.

In addition, one of the objectives was to answer the questions raised at the beginning of the thesis in the Introduction (Chapter 1). Each chapter (except Chapter 5) intended to answer certain questions. To sum up, the refined answers to those research questions along with the questions are presented below.

1. What are the state-of-the-art methodologies that are proposed or already in use and what are the current trends? What are the pros and cons of the existing methods?

There are various earth fault location and earth fault passage indication methods. Pros and cons of each method were summarized in Table 1. The most accurate fault location methodology appears to be traveling-wave methodology although these

methods, when implemented in practice, might identify more than one fault location. Therefore, a possible ultimate solution could be a hybrid method i.e. a combination of an FPI-based method and traveling-wave methods so that the FPI-based method would identify the faulted segment and narrow down the fault location candidates to one.

2. How do symmetrical sequence currents behave when the electricity network is under an earth fault condition?

The behaviors of the zero and negative sequence currents on the faulted feeder during an earth fault condition were analyzed in Chapter 3 and summarized in Section 3.4. It was found that the zero sequence current either decreases or increases, depending on the network type, as we move towards the fault point from the beginning of the feeder. On the other hand, the negative sequence current remains almost the same.

3. How can symmetrical sequence currents be utilized to locate the faulted segment of the network? How do the developed methods perform on different types of networks?

The symmetrical sequence currents can be utilized, in the manner proposed in Chapter 4, to determine the on/off-the-fault-path status of a measuring point. Two methods have been developed and both employ the ZSC to primarily detect an earth fault condition. In an isolated distribution network, the ZSC provides sufficient information for earth FPI purposes. In compensated networks, the NSC is required in addition to the ZSC. By distributing FPI units throughout the distribution network, earth fault passage indication can be achieved and the faulted segment identified.

4. How can the proposed methods be implemented in practice and what are the technical requirements and apparatus? What is the efficacy of the proposed methods in practice on real distribution networks?

To implement the methods in practice, the FPI units are installed at the beginning of feeders and along them. It is not recommended to install an FPI unit at the primary substation on the secondary side of the main transformer with delta winding, as illustrated in Figure 47. The reason is that the ZSC is always zero there. Essentially, each FPI device consists of a current measurement unit, a memory for storing fault recordings before transmitting them to the control center, and a modem. In addition, to implement the methods, a control center where the signal processing and analysis are carried out is required.

7.3 Future research work

One of the main contributions of this dissertation is the two current-based FPI methods developed as a result of research and studying field test recordings. During the process of developing those methods, new ideas emerged and further questions were raised that could be the topic of future work. The following section outlines possible future research items.

7.3.1 Fault passage indication using direction of transient part of residual current

In Section 4.3, it was seen that the transient part of the residual current at the start of the earth fault can provide a clue regarding the on/off-fault-passage status of the measuring point in question. For a group of measuring points at which the current sensor sets installed uniformly in terms of polarity, the direction of the transient part of the residual current at all on-the-fault-passage points are the same. This raises the question of why not solely utilizing the transient part of the residual current to determine the on/off-fault-passage status of a measuring point. The reason is that implementing this idea in practice requires that all the current sensor sets are installed uniformly in terms of polarity. Fulfilling this requirement in practice has technical difficulty. Determining the polarity of a set of conductors (underground cables, overhead lines) for the DSO crew is not always possible. This will become even more complicated when the topology of the network changes. Nevertheless, utilizing the transient part of the residual current for FPI applications is certainly worth further study. The idea along with its requirements including the proper range of sampling rates, the need for accurate GPS timing, time synchronizations, etc., will be the topic of future work.

7.3.2 Universal method

In Chapter 5, Section 5.5, a slightly different version of Method 2 was developed. It was aimed at enabling the method to specifically be capable of detecting intermittent earth faults as the method in its original form was unable to guarantee reliable detection of these types of earth faults. The problem is that when an actual earth fault occurs, its type (permanent or intermittent) is unknown to FPI devices and therefore there will be a question of which algorithm must be used. In order to address the issue, Section 5.7 proposed that both algorithms run simultaneously and whichever algorithm detects a fault is prioritized over the other one. Despite the proposal, an ideal method that would work for both permanent and

intermittent earth faults is still missing. Developing such a universal method will be the topic of future work.

References

- ABB. (2021). *615 series, Technical Manual*.
<https://search.abb.com/library/Download.aspx?DocumentID=1MRS756887&LanguageCode=en&DocumentPartId=&Action=Launch>
- a-eberle. (2020). *Earth Fault Detection Relay*. a-eberle. https://www.a-eberle.de/wp-content/uploads/2020/08/TD_EOR-D_EN.pdf
- Akke, M. (2011). *Method and device for detecting an intermittent earth fault in a multiple feeder system* (European Union Patent No. EP2390980A1).
<https://patents.google.com/patent/EP2390980A1/en>
- Altonen, J., Mäkinen, O., Kauhaniemi, K., & Persson, K. (2003). *Intermittent earth faults—Need to improve the existing feeder earth fault protection schemes?* 6.
- Altonen, J., & Wahlroos, A. (2007). Advancements in fundamental frequency impedance based earth-fault location in unearthed distribution networks. *19th International Conference on Electricity Distribution (CIRED 2007)*, 4.
- Altonen, J., & Wahlroos, A. (2013). Novel algorithm for earth-fault location in compensated MV-networks. *22nd International Conference and Exhibition on Electricity Distribution (CIRED 2013)*, 1–4.
<https://doi.org/10.1049/cp.2013.0832>
- Altonen, J., & Wahlroos, A. (2016). Performance of modern fault passage indicator concept in compensated MV-networks. *CIRED Workshop 2016*, 1–4.
<https://doi.org/10.1049/cp.2016.0733>
- Altonen, J., Wahlroos, A., & Pirskanen, M. (2011). Advancement in earth-fault location in compensated MV-networks. *CIRED 21st International Conference on Electricity Distribution*, 4.
- Altonen, J., Wahlroos, A., Vähäkuopus, S., & Oy, E. (2017). *Application of multi-frequency admittance-based fault passage indication in practical compensated MV-network*. 5.
- Arcteq. (2021). *AQ-F213E Feeder Protection IED*. Arcteq.
<https://www.arcteq.fi/products/aq-f213e-feeder-protection-ied/?pdf=3932>
- Balouji, E., Bäckström, K., & Hovila, P. (2020). A Deep Learning Approach to Earth Fault Classification and Source Localization. *2020 IEEE PES Innovative Smart Grid Technologies Europe (ISGT-Europe)*, 635–639.
<https://doi.org/10.1109/ISGT-Europe47291.2020.9248944>
- Banjanin, M. S., & Savic, M. S. (2021). Experimental registration and numerical simulation of the transient overvoltages caused by single phase intermittent arc earth fault in 35 kV network with isolated neutral. *IEEE Transactions on Power Delivery*, 1–1. <https://doi.org/10.1109/TPWRD.2021.3098829>

Borghetti, A., Bosetti, M., Di Silvestro, M., Nucci, C. A., & Paolone, M. (2008). Continuous-Wavelet Transform for Fault Location in Distribution Power Networks: Definition of Mother Wavelets Inferred From Fault Originated Transients. *IEEE Transactions on Power Systems*, 23(2), 380–388. <https://doi.org/10.1109/TPWRS.2008.919249>

Borghetti, A., Bosetti, M., Nucci, C. A., Paolone, M., & Abur, A. (2010). Integrated Use of Time-Frequency Wavelet Decompositions for Fault Location in Distribution Networks: Theory and Experimental Validation. *IEEE Transactions on Power Delivery*, 25(4), 3139–3146. <https://doi.org/10.1109/TPWRD.2010.2046655>

Borghetti, A., Ishimoto, K., Napolitano, F., Nucci, C. A., & Tossani, F. (2021). Assessment of the Effects of the Electromagnetic Pulse on the Response of Overhead Distribution Lines to Direct Lightning Strikes. *IEEE Open Access Journal of Power and Energy*, 8, 522–531. <https://doi.org/10.1109/OAJPE.2021.3099596>

Brittain, J. E. (1998). Charles L.G. Fortescue and the method of symmetrical components [Scanning the Past]. *Proceedings of the IEEE*, 86(5), 1020–1021. <https://doi.org/10.1109/JPROC.1998.664289>

Buigues, G., Valverde, V., Zamora, I., Mazón, J., & Torres, E. (2012). Signal injection techniques for fault location in distribution networks. *Renewable Energy and Power Quality (ICREPQ'12)*, 412–417. <https://doi.org/10.24084/repqj10.330>

CEER Benchmarking Report 5.2 on the Continuity of Electricity Supply. (2015). Council of European Energy Regulators.

CEER Benchmarking Report 6.1 on the Continuity of Electricity and Gas Supply. (2018). Council of European Energy Regulators.

Chicco, G., & Mazza, A. (2019). 100 Years of Symmetrical Components. *Energies*, 12(3), Article 3. <https://doi.org/10.3390/en12030450>

Chollot, Y., Mcreant, J., Leblond, D., & Cumunel, P. (2017). New solution of fault directional detection for MV fault passage indicators. *CIREN - Open Access Proceedings Journal*, 2017(1), 1326–1329. <https://doi.org/10.1049/oap-cired.2017.0382>

Chunju, F., Li, K. K., Chan, W. L., Weiyong, Y., & Zhaoning, Z. (2007). Application of wavelet fuzzy neural network in locating single line to ground fault (SLG) in distribution lines. *International Journal of Electrical Power & Energy Systems*, 29(6), 497–503. <https://doi.org/10.1016/j.ijepes.2006.11.009>

Couto, M., Pascoal, J., Matos, J. D., & Antunes, J. (2017). Approach to reduce momentary average interruption frequency index – the quality of service indicator for momentary interruptions – the experience of the Portuguese DSO. *CIREN - Open Access Proceedings Journal*, 2017(1), 522–525. <https://doi.org/10.1049/oap-cired.2017.0465>

Cui, T., Dong, X., Bo, Z., & Juszczak, A. (2011). Hilbert-Transform-Based Transient/Intermittent Earth Fault Detection in Noneffectively Grounded Distribution Systems. *IEEE Transactions on Power Delivery*, 26(1), 143–151. <https://doi.org/10.1109/TPWRD.2010.2068578>

Das, B. (Ed.). (2016). *Power Distribution Automation*. Institution of Engineering and Technology. <https://doi.org/10.1049/PBPO075E>

Dong, X., CUI, T., Bo, Z., Klimek, A., & Juszczak, A. (2012). *Method and system for transient and intermittent earth fault detection and direction determination in a three-phase median voltage electric power distribution system* (European Union Patent No. EP2417467A1). <https://patents.google.com/patent/EP2417467A1/fi>

Drouere, B., & Mcreant, J. (2016). *DIRECTIONAL DETECTION OF EARTH FAULT IN AN ELECTRICAL DISTRIBUTION NETWORK* (Patent No. FR3026492A1). <https://patents.google.com/patent/FR3026492A1/en>

Druml, G., Klein, R.-W., & Seifert, O. (2009). New adaptive algorithm for detecting low- and high ohmic faults in meshed networks. *CIREN 2009 - 20th International Conference and Exhibition on Electricity Distribution - Part 1*, 1–5.

Druml, G., Raunig, C., Schegner, P., & Fickert, L. (2012). Earth fault localization with the help of the fast-pulse-detection-method using the new high-power-current-injection (HPCI). *2012 Electric Power Quality and Supply Reliability*, 1–5. <https://doi.org/10.1109/PQ.2012.6256231>

Druml, G., Raunig, C., Schegner, P., & Fickert, L. (2013). Fast selective earth fault localization using the new fast pulse detection method. *22nd International Conference and Exhibition on Electricity Distribution (CIREN 2013)*, 1–5. <https://doi.org/10.1049/cp.2013.1068>

Druml, G., Raunig, C., Schegner, P., & Fickert, L. (2014). Comparison of restriking cable-earthfaults in isolated and compensated networks. *2014 Electric Power Quality and Supply Reliability Conference (PQ)*, 75–80. <https://doi.org/10.1109/PQ.2014.6866788>

Druml, G., Seiert, O., & Marketz, M. (2011). *Directional detection of restriking earth faults in compensated networks*. 21st International Conference on Electricity Distribution (CIREN 2011), Frankfurt.

Druml, G., Skrbinjek, O., Hipp, W., Fickert, L., Schmidt, U., & Schegner, P. (2019, June). *First results concerning localisation of earthfaults in compensated 20-kV-networks based on travelling waves*. 25th International Conference on Electricity Distribution (CIREN 2019), Madrid. <https://www.cired-repository.org/handle/20.500.12455/160>

Elkalashy, N. I., Sabiha, N. A., & Lehtonen, M. (2015). Earth Fault Distance Estimation Using Active Traveling Waves in Energized-Compensated MV Networks. *IEEE Transactions on Power Delivery*, 30(2), 836–843. <https://doi.org/10.1109/TPWRD.2014.2365741>

Estebarsari, A., Pons, E., Bompard, E., Bahmanyar, A., & Jamali, S. (2016). An improved fault location method for distribution networks exploiting emerging LV smart meters. *2016 IEEE Workshop on Environmental, Energy, and Structural Monitoring Systems (EESMS)*, 1–6.

<https://doi.org/10.1109/EESMS.2016.7504815>

Fortescue, C. L. (1918). *Method of Symmetrical Co-Ordinates Applied to the Solution of Polyphase Networks* | *IEEE Journals & Magazine* | *IEEE Xplore*.
<https://ieeexplore.ieee.org/document/4765570>

Hand, M., & Donagh, N. M. (2010). ESB's adoption of smart neutral treatments on its 20 KV system. *CIREN Workshop*, 4.

Hänninen, S. (2001). *Single phase earth faults in high impedance grounded networks: Characteristics, indication and location*. VTT Technical Research Centre of Finland. <https://aaltodoc.aalto.fi:443/handle/123456789/2212>

IEEE Guide Transmission. (2016). IEEE Guide for Protective Relay Applications to Transmission Lines. *IEEE Std C37.113-2015 (Revision of IEEE Std C37.113-1999)*, 1–141. <https://doi.org/10.1109/IEEESTD.2016.7502047>

IEEE Guide Distribution Relays. (2021). IEEE Guide for Protective Relay Applications to Distribution Lines. *IEEE Std C37.230-2020 (Revision Of IEEE Std C37.230-2007)*, 1–106. <https://doi.org/10.1109/IEEESTD.2021.9382208>

IEEE Guide Fault Location. (2015). IEEE Guide for Determining Fault Location on AC Transmission and Distribution Lines. *IEEE Std C37.114-2014 (Revision of IEEE Std C37.114-2004)*, 1–76. <https://doi.org/10.1109/IEEESTD.2015.7024095>

IEEE Guide for Rogowski Coils. (2008). IEEE Guide for the Application of Rogowski Coils Used for Protective Relaying Purposes. *IEEE Std C37.235-2007*, 1–46. <https://doi.org/10.1109/IEEESTD.2008.4457884>

IEEE Guide FPI. (2017). IEEE Guide for the Application of Faulted Circuit Indicators on Distribution Circuits. *IEEE Std 1610-2016 (Revision of IEEE Std 1610-2007)*, 1–26. <https://doi.org/10.1109/IEEESTD.2017.7932241>

IEEE Guide Indices. (2012). IEEE Guide for Electric Power Distribution Reliability Indices. *IEEE Std 1366-2012 (Revision of IEEE Std 1366-2003)*, 1–43. <https://doi.org/10.1109/IEEESTD.2012.6209381>

IEEE Guide Interruption Events. (2014). IEEE Guide for Collecting, Categorizing, and Utilizing Information Related to Electric Power Distribution Interruption Events. *IEEE Std 1782-2014*, 1–98.
<https://doi.org/10.1109/IEEESTD.2014.6878409>

IEEE Guide Neutral Grounding. (2015). IEEE Guide for the Application of Neutral Grounding in Electrical Utility Systems—Part IV: Distribution. *IEEE Std C62.92.4-2014 (Revision of IEEE Std C62.92.4-1991)*, 1–44.
<https://doi.org/10.1109/IEEESTD.2015.7010855>

- IEEE Guide Reclosing. (2021). IEEE Draft Guide for Automatic Reclosing on AC Distribution and Transmission Lines. *IEEE PC37.104/D1.7, May 2021*, 1–76.
- IEEE Guide Rogowski. (2021). IEEE Draft Guide for the Application of Rogowski Coils Used for Protective Relaying Purposes. *IEEE PC37.235/D13, January 2021*, 1–48.
- IEEE Guide Smart Grid. (2019). IEEE Trial-Use Guide for Smart Distribution Applications. *IEEE Std 1854-2019*, 1–65.
<https://doi.org/10.1109/IEEESTD.2019.8820199>
- Iurinic, L. U., Herrera-Orozco, A. R., Ferraz, R. G., & Bretas, A. S. (2016). Distribution Systems High-Impedance Fault Location: A Parameter Estimation Approach. *IEEE Transactions on Power Delivery*, *31*(4), 1806–1814.
<https://doi.org/10.1109/TPWRD.2015.2507541>
- Jia, K., Ren, Z., Bi, T., & Yang, Q. (2015). Ground Fault Location Using the Low-Voltage-Side Recorded Data in Distribution Systems. *IEEE Transactions on Industry Applications*, *51*(6), 4994–5001.
<https://doi.org/10.1109/TIA.2015.2425358>
- Kulkarni, S., Santoso, S., & Short, T. A. (2014). Incipient Fault Location Algorithm for Underground Cables. *IEEE Transactions on Smart Grid*, *5*(3), 1165–1174.
<https://doi.org/10.1109/TSG.2014.2303483>
- Kumpulainen, L., Sauna-aho, S., Virtala, T., & Holmlund, J. (2008). A cost effective solution to intermittent transient earth-fault protection. *NORDAC 2008. Nordic Distribution and Asset Management Conference*, Bergen.
- Laaksonen, H., & Hovila, P. (2016). *Flexzone concept to enable resilient distribution grids—Possibilities in sundom smart grid*. 11 (4 .)-11 (4 .).
<https://doi.org/10.1049/cp.2016.0611>
- Lakervi, E., & Holmes, E. J. (1995). *Electricity Distribution Network Design*. IET.
- Lehtonen, M., Siirto, O., & Abdel-Fattah, M. F. (2014). Simple fault path indication techniques for earth faults. *2014 Electric Power Quality and Supply Reliability Conference (PQ)*, 371–378. <https://doi.org/10.1109/PQ.2014.6866844>
- Liang, R., Fu, G., Zhu, X., & Xue, X. (2015). Fault location based on single terminal travelling wave analysis in radial distribution network. *International Journal of Electrical Power & Energy Systems*, *66*, 160–165.
<https://doi.org/10.1016/j.ijepes.2014.10.026>
- Loukkalahti, M., Hyvärinen, M., Siirto, O., & Heine, P. (2017). Helen Electricity Network Ltd.'s process towards high level of supply reliability. *CIGRE - Open Access Proceedings Journal*, *2017*(1), 1172–1175. <https://doi.org/10.1049/oap-cired.2017.1037>
- Martins, L. S., Martins, J. F., Alegria, C. M., & Pires, V. F. (2003). A network distribution power system fault location based on neural eigenvalue algorithm.

2003 *IEEE Bologna Power Tech Conference Proceedings*, 2, 6 pp. Vol.2-.
<https://doi.org/10.1109/PTC.2003.1304592>

Matlab Help. (2022). *Implement three-phase transmission line section with lumped parameters—Simulink—MathWorks Nordic*.
<https://se.mathworks.com/help/physmod/sps/powersys/ref/threephasepisectionline.html>

Mora, J. J., Carrillo, G., & Perez, L. (2006). Fault Location in Power Distribution Systems using ANFIS Nets and Current Patterns. *2006 IEEE/PES Transmission Distribution Conference and Exposition: Latin America*, 1–6.
<https://doi.org/10.1109/TDCLA.2006.311428>

Mora-Florez, J., Barrera-Nunez, V., & Carrillo-Caicedo, G. (2007). Fault Location in Power Distribution Systems Using a Learning Algorithm for Multivariable Data Analysis. *IEEE Transactions on Power Delivery*, 22(3), 1715–1721.
<https://doi.org/10.1109/TPWRD.2006.883021>

Napolitano, F., Tossani, F., Borghetti, A., & Nucci, C. A. (2018). Lightning Performance Assessment of Power Distribution Lines by Means of Stratified Sampling Monte Carlo Method. *IEEE Transactions on Power Delivery*, 33(5), 2571–2577. <https://doi.org/10.1109/TPWRD.2018.2795743>

Paolone, M., Borghetti, A., & Nucci, C. A. (2011). An automatic system to locate phase-to-ground faults in medium voltage cable networks based on the wavelet analysis of high-frequency signals. *2011 IEEE Trondheim PowerTech*, 1–7.
<https://doi.org/10.1109/PTC.2011.6019280>

Pereira, R. A. F., da Silva, L. G. W., Kezunovic, M., & Mantovani, J. R. S. (2009). Improved Fault Location on Distribution Feeders Based on Matching During-Fault Voltage Sags. *IEEE Transactions on Power Delivery*, 24(2), 852–862.
<https://doi.org/10.1109/TPWRD.2009.2014480>

Pettissalo, S. (2017). *Method and Apparatus for Detecting Faults in a Three-Phase Electrical Distribution Network* (Patent No. WO/2017/203099).
<https://patentscope.wipo.int/search/en/detail.jsf?docId=WO2017203099>

Poethier, J.-Y., Lamberti, L., & Chollot, Y. (2019, June 3). *Improve your SAIDI with Advanced Fault Passage Indication*. 25th International Conference on Electricity Distribution, Madrid. <https://doi.org/10.34890/1024>

Pourahmadi-Nakhli, M., & Safavi, A. A. (2011). Path Characteristic Frequency-Based Fault Locating in Radial Distribution Systems Using Wavelets and Neural Networks. *IEEE Transactions on Power Delivery*, 26(2), 772–781.
<https://doi.org/10.1109/TPWRD.2010.2050218>

Rafinia, A., & Moshtagh, J. (2014). A new approach to fault location in three-phase underground distribution system using combination of wavelet analysis with ANN and FLS. *International Journal of Electrical Power & Energy Systems*, 55, 261–274. <https://doi.org/10.1016/j.ijepes.2013.09.011>

Raunig, C., Fickert, L., Obkircher, C., & Achleitner, G. (2010). Mobile earth fault localization by tracing current injection. *Proceedings of the 2010 Electric Power Quality and Supply Reliability Conference*, 243–246. <https://doi.org/10.1109/PQ.2010.5549991>

Rios Penaloza, J. D., Borghetti, A., Napolitano, F., Tossani, F., & Nucci, C. A. (2021). A New Transient-Based Earth Fault Protection System for Unearthed Meshed Distribution Networks. *IEEE Transactions on Power Delivery*, 36(5), 2585–2594. <https://doi.org/10.1109/TPWRD.2020.3022977>

Sadeh, J., Bakhshizadeh, E., & Kazemzadeh, R. (2013). A new fault location algorithm for radial distribution systems using modal analysis. *International Journal of Electrical Power & Energy Systems*, 45(1), 271–278. <https://doi.org/10.1016/j.ijepes.2012.08.053>

Siirto, O. (2016). *Distribution Automation and Self-Healing Urban Medium Voltage Networks*. Aalto University.

Siirto, O., Hyvärinen, M., Loukkalahti, M., Hämäläinen, A., & Lehtonen, M. (2015). Improving reliability in an urban network. *Electric Power Systems Research*, 120, 47–55. <https://doi.org/10.1016/j.epsr.2014.09.021>

Siirto, O., Vepsäläinen, J., Hämäläinen, A., & Loukkalahti, M. (2017). Improving reliability by focusing on the quality and condition of medium-voltage cables and cable accessories. *CIREN - Open Access Proceedings Journal*, 2017(1), 229–232. <https://doi.org/10.1049/oap-cired.2017.1104>

Sirviö, K., Kauhaniemi, K., Ali Memon, A., Laaksonen, H., & Kumpulainen, L. (2020). Functional Analysis of the Microgrid Concept Applied to Case Studies of the Sundom Smart Grid. *Energies*, 13(16), Article 16. <https://doi.org/10.3390/en13164223>

Stipetić, N., Filipović-Grčić, B., Uglešić, I., Xémard, A., & Andres, N. (2021). Earth-fault detection and localization in isolated industrial MV network – comparison of directional overcurrent protection and signal injection method. *Electric Power Systems Research*, 197, 107313. <https://doi.org/10.1016/j.epsr.2021.107313>

Tengg, C., Schmaranz, R., Schoass, K., Marketz, M., Druml, G., & Fickert, L. (2013). Evaluation of new earth fault localization methods by earth fault experiments. *22nd International Conference and Exhibition on Electricity Distribution (CIREN 2013)*, 1–4. <https://doi.org/10.1049/cp.2013.1179>

Topolanek, D., Lehtonen, M., Adzman, M. R., & Toman, P. (2015). Earth fault location based on evaluation of voltage sag at secondary side of medium voltage/low voltage transformers. *Transmission Distribution IET Generation*, 9(14), 2069–2077. <https://doi.org/10.1049/iet-gtd.2014.0460>

Topolanek, D., Lehtonen, M., Toman, P., Orsagova, J., & Drapela, J. (2020). An earth fault location method based on negative sequence voltage changes at low voltage side of distribution transformers. *International Journal of Electrical Power & Energy Systems*, 118, 105768. <https://doi.org/10.1016/j.ijepes.2019.105768>

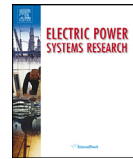
Trindade, F. C. L., Freitas, W., & Vieira, J. C. M. (2014). Fault Location in Distribution Systems Based on Smart Feeder Meters. *IEEE Transactions on Power Delivery*, 29(1), 251–260. <https://doi.org/10.1109/TPWRD.2013.2272057>

Virtala, T. (2016). *Method and protection device for eliminating earth faults of transient type in an electric distribution network* (World Intellectual Property Organization Patent No. WO2016066898A1). <https://patents.google.com/patent/WO2016066898A1/en>

Wahlroos, A., & Altonen, J. (2009). Performance of novel neutral admittance criterion in MV-feeder earth-fault protection. *CIGRE 2009 - 20th International Conference and Exhibition on Electricity Distribution - Part 1*, 1–4. <https://doi.org/10.1049/cp.2009.0716>

Wahlroos, A., & Altonen, J. (2014). Application of novel multi-frequency neutral admittance method into earth-fault protection in compensated MV-networks. *12th IET International Conference on Developments in Power System Protection (DPSP 2014)*, 1–6. <https://doi.org/10.1049/cp.2014.0032>

Wahlroos, A., Uggla, U., Altonen, J., & Wall, D. (2013). Application of novel cumulative phasor sum measurement for earth-fault protection in compensated MV-networks. *22nd International Conference and Exhibition on Electricity Distribution (CIGRE 2013)*, 0607–0607. <https://doi.org/10.1049/cp.2013.0833>



Review of methodologies for earth fault indication and location in compensated and unearthed MV distribution networks



Amir Farughian*, Lauri Kumpulainen, Kimmo Kauhaniemi

Department of Electrical Engineering and Energy Technology, University of Vaasa, P.O. Box 700, FI-65101 Vaasa, Finland

ARTICLE INFO

Article history:

Received 17 February 2017
Received in revised form 15 July 2017
Accepted 7 September 2017
Available online 20 September 2017

Keywords:

Earth fault location
Distribution networks
Impedance methods
Fault passage indicators
Injection
Smart metering
Travelling waves

ABSTRACT

Feeder automation is one of the key features of Smart Grids aiming at developing self-healing systems, able to locate the fault and automatically perform the isolation and supply restoration. Reliable fault indication and location is a prerequisite for this functionality. This paper reviews the state of the art technologies and techniques for determining single-phase earth fault location on MV distribution networks. Accurate information about the faulted line or cable section expedites system restoration following the fault occurrence. This paper presents a review of the principles of fault location and indication techniques and their application considerations. In order to gain further insight into the strengths and limitations of each method, a comparative analysis is carried out. Finally, the paper identifies further research and presents the selected promising approaches.

© 2017 Elsevier B.V. All rights reserved.

Contents

| | |
|--|-----|
| 1. Introduction | 374 |
| 1.1. Classification of fault location methods | 374 |
| 2. Centralized earth-fault location methods | 374 |
| 2.1. Impedance based methods | 374 |
| 2.1.1. Unearthed networks | 374 |
| 2.1.2. Compensated networks | 374 |
| 2.2. Travelling wave techniques | 375 |
| 2.3. Artificial intelligence based methods | 376 |
| 3. Decentralized methods | 376 |
| 3.1. Utilization of smart meters | 376 |
| 3.2. IEDs and fault passage indicators | 376 |
| 3.2.1. ENEL's FPI based system | 377 |
| 3.2.2. ABB's multi-frequency admittance based earth-fault location | 377 |
| 3.2.3. Negative sequence component based approach | 377 |
| 3.3. Signal injection based methods | 378 |
| 4. Discussion | 378 |
| 5. Conclusion and future work | 379 |
| Acknowledgements | 379 |
| References | 379 |

* Corresponding author.

E-mail addresses: amir.farughian@uva.fi, amir.farughian@gmail.com
(A. Farughian).

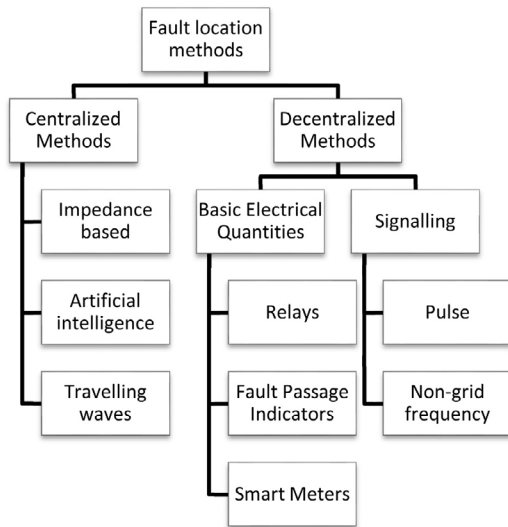


Fig. 1. Classification of earth-fault location methods.

1. Introduction

As the society is increasingly dependent on electricity, higher reliability of power supply is required. Fault distance estimation enables faster fault isolation and restoration of power supply. The ultimate goal is to develop a fully automatic, self-healing system. However, before the switching required by the FLIR (fault location, isolation and restoration) functionality can be automatic, fault indication should be very reliable, and safety issues must be examined. In any case, the information on the fault location must be delivered to the control room. In the control room, the SCADA (supervisory control and data acquisition) system or DMS (distribution management system) processes the information to illustrate the fault location to the operator or to generate an automatic FLIR switching sequence.

For short-circuit faults, there are established methods for fault location. However, there is not a universally accepted, reliable, cost-effective method for earth-fault location on the market for isolated neutral or compensated networks. In this paper, the state-of-the-art methods for determining earth fault location on MV distribution networks are discussed. The topic is very relevant since the most common type of fault is the single-phase-to-earth fault (in the Nordic countries about 50–90% of faults) [1]. The aim is to classify and compare different approaches and particularly to find the most promising approaches either for practical implementation or for further development.

1.1. Classification of fault location methods

A number of earth-fault location methods have been proposed. They can be categorized according to Fig. 1, where the main division is made between centralized and decentralized methods. In centralized methods, the measurements are carried out at the primary substation. In decentralized methods, measurements along the feeders together with suitable communication are utilized. In this paper, various methods are reviewed utilizing this classification.

Based on the above figure, fault location methods are outlined in Sections 2 and 3. In order to gain further insight into the strengths

and limitations of each method, a comparative analysis is carried out in Section 4. Finally, the paper identifies further research and presents the promising approaches in Section 5.

2. Centralized earth-fault location methods

2.1. Impedance based methods

These methods are based on measuring the apparent impedance seen looking into the line from either end when a fault occurs. As the line length from the measuring point to the fault location is proportional to the measured impedance, by knowing the line impedance per unit length, the fault distance is obtained.

Accurate location of earth faults in compensated and ungrounded networks is a more challenging task as the fault current in those types of networks is often small compared to load currents. In general, perhaps one of the main challenges in fault locating is the fault impedance as it is unknown. Attempts have been made to address the problem [2–5]. Ref. [6] tests a number of impedance methods under same conditions and draw comparisons between them.

In this section, the impedance-based fault locating methods based on fundamental frequency (grid-frequency) phasors are discussed as they have become an industry standard in modern microprocessor-based protective relays.

In practice, numerous methods have been put forward to locate faults on distribution networks using current and voltage phasors. These methods are designed based on the grounding principles of the network, namely:

- Solidly grounded
- Unearthed networks
- Compensated networks
- Resistance grounded

In this section, only unearthed and compensated networks are discussed because fault location is more challenging in those types of networks.

2.1.1. Unearthed networks

In traditional impedance-based fault location [7], the reactance of the line following a fault occurrence is computed and compared to the line reactance measured before the fault occurrence so that the fault distance is estimated. Sometimes, for simplicity, the fault resistance is assumed to be zero. However, that might result in a substantial error especially in overhead lines where the fault resistance is often not zero. Ref. [8] advances the traditional impedance-based method by making assumptions about the fault resistance and the distribution of load current along the feeder. The results show that the method is limited to low impedance faults up to 30Ω and it is not widely applied in practice.

Another algorithm is presented in Ref. [9]. The analysis relies on the symmetrical components theory. In this method, the whole load of the feeder is modelled as one equivalent load tap located at a certain distance from the substation (in per unit) where the voltage drop due to an earth fault is at a maximum. The soundness of this method is validated by field tests. The method works in faults with low fault resistances.

2.1.2. Compensated networks

The fault location algorithm presented in Ref. [8] determines the reactance from the substation to the fault location by measuring the changes in the zero sequence current and the faulty phase voltage caused by switching the shunt resistor in parallel with the suppression coil during the fault. Subsequently, by knowing the sequence reactance per kilometer of the line, the distance

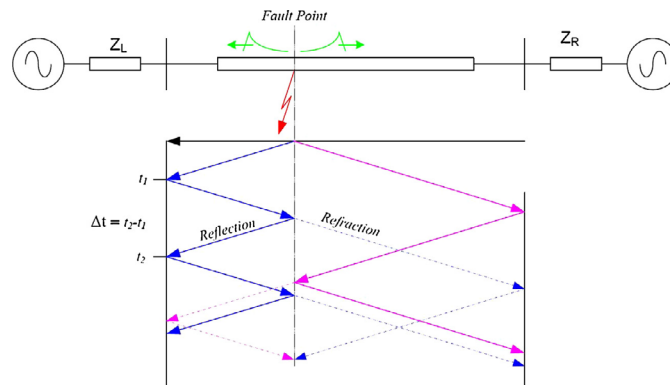


Fig. 2. Reflections and refractions of traveling waves caused by a fault on a power line [13].

to fault is calculated. Note that a change in the impedance of the zero sequence circuit brings about corresponding changes in the zero sequence voltage and current. As a rule of thumb, a change in the zero sequence voltage leads to an equal change in the voltage of the faulted phase.

Ref. [10] applies the concept presented in Ref. [9] to compensated networks. However, the equations required to estimate the reactance to fault are formed based on the concept introduced in Ref. [8] i.e. measuring changes in the zero sequence current and the faulted phase voltage by switching the shunt resistor in parallel with the compensation (Petersen) coil during fault condition. Moreover, the paper performs a sensitivity analysis to investigate the effects of uncertainties existing in practice such as the fault resistance and inaccuracy in primary measurements and line data. The findings of this research indicate that as the fault resistance increases, the requirements on the accuracy of measurements or line parameters become more demanding.

Six years later, in another attempt by the same authors, a novel algorithm was put forward for compensated MV networks which required a fewer number of settings [11]. The algorithm suggests setting up four equations, as opposed to previous algorithms with two equations, using the sequence equivalent circuit of the network. This can be achieved through switching the shunt resistor in parallel with the arc suppression coil during fault condition and by separating the equations into real and imaginary parts. Utilizing the concept presented in Ref. [10], the earth fault distance can be estimated. One advantage of the proposed method is that it enables fault location with no need of knowing the value of the shunt admittance. This value varies with the protected feeder configuration and in overhead lines with weather conditions. The proposed algorithm has been validated by field test results.

Although, Ref. [12] states the status of computational earth fault distance estimation in compensated networks very directly, its application is currently limited to short-circuit faults. In spite of extensive research work, commercial solutions are not yet available.

2.2. Travelling wave techniques

When a fault occurs on a power system, transient voltages and currents called travelling waves (impulses) are generated at the fault location and propagate away from that point in both directions towards the terminals of the line. Given that a current wave or a voltage wave travels at the speed of light, by measuring the wave and its reflection arrival times at either terminal of the line, the distance to the fault point can be determined.

The principle of the operation of this method is illustrated in Fig. 2. If the propagation velocity of the travelling wave in the line is known, the distance to fault d is calculated as follows:

$$d = v \times \frac{\Delta t}{2} \quad (1)$$

where,

v is the propagation velocity of the traveling wave in the line.

Δt is the time difference in the arrival of the first traveling wave and its reflection.

However, in distribution networks, due to the many reflections of injected impulses from line laterals and branches, it is a major challenge to identify the right reflections caused by the fault. Refs. [1,14] and [15] claim to have overcome this limitation by utilizing aerial mode 1 reflected pulse. This method can locate up to rather high fault resistances, however, it requires a complicated system and no field tests have been done to verify the method.

A different method is presented in Ref. [16] which is based on injecting a continuous series of high frequency pulses into the distribution network and recording the response with the aim of building up a picture of the system behavior under pre-fault conditions. Once a fault is detected, the same procedure will be performed. Because of the fault, this time the response will be different. Considering the pulse propagation speed through the line, the fault distance is calculated based on the time difference between the moments when the pulse is injected and when the two responses move apart from each other as shown in Fig. 3.

This method has not been used in practice and only a laboratory test has been carried out. Even the laboratory test is in question as the cross section of the test underground cable (1.5 mm^2) is much smaller than those used in practice. Moreover, the maximum fault resistance applied in the tests was as low as 150Ω .

Other attempts have been made to apply travelling-wave based methods to distribution networks [17–19]. However, when applying these methods in distribution networks, the main problem is that due to many branches, the reflections may come from different sources and not only from the fault point. This makes these methods problematic to be used in distribution networks. Research on how to apply travelling wave based fault location techniques in MV level continues. It is possible that a useful method will be developed at least for some limited application areas.

Ref. [20] proposes an approach using continuous wavelet transform (CWT). The method is based on the correlation between the frequencies of the transients captured at the measuring point and the paths in which they travel. The paper illustrates that each path corresponds to a certain frequency. For a path with no fault, the

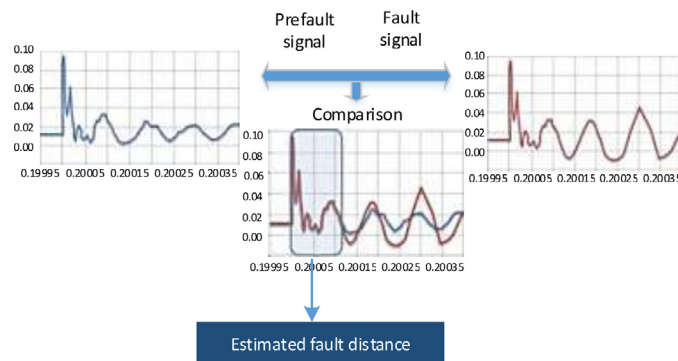


Fig. 3. Principles of fault location presented in Ref. [16].

corresponding frequency can be calculated by knowing the path length and the traveling wave speed. For a path containing a fault, the measured frequency and the calculated one will be different. Therefore, by analyzing the transients using CWT, the path containing the fault can be identified. The method has been advanced in Refs. [21] and [22] by means of integrating frequency domain data with time domain data obtained from CWT. However, this method has not been verified by field tests.

2.3. Artificial intelligence based methods

Methods based on artificial intelligence involve training an artificial intelligent system to detect the faulted area [23–28]. This may be of great advantage to certain networks where the complexity is high. In Ref. [23], fault locating is accomplished by training an adaptive neurofuzzy inference system (ANFIS). The inputs of the system are obtained from a current, measured at the substation, waveform analysis. In Ref. [25], a learning algorithm for multivariable data analysis (LAMDA) classification is developed for fault location.

In Refs. [26–28], the wavelet transform or a form of it is used to decompose transients, originated from a fault, into various frequency components. These components contain exclusive information of the fault location. This information is used to train an artificial intelligence system, a fuzzy neural system in Refs. [26] and [28] and an artificial neural network in Ref. [27] to locate faults.

However, it is difficult to find evidence on real-life implementations of AI based fault location. Moreover, the number of research papers on these methods seems to be declining. At present, AI based methods do not look much promising.

In general, methods using one measuring point might result in multi fault location candidates. Ref. [29] proposes an approach to address this problem by integrating different fault location methods.

3. Decentralized methods

With the increased installation of intelligent electronic devices (IEDs) and smart meters in distribution networks and the developments in communication, the decentralized fault location process has been facilitated in Refs. [30–34]. Fault indicators (fault circuit indicators FCIs, fault passage indicators FPIs) are capable of detecting a fault condition and sending a signal indicating the fault condition to the control room. The deduction of the fault location can be carried out locally by the distributed IEDs, or the upper level systems can deduce the faulted line section by utilizing the measurements from the devices along the feeder. As modern smart grid ready secondary substations are equipped with monitoring and

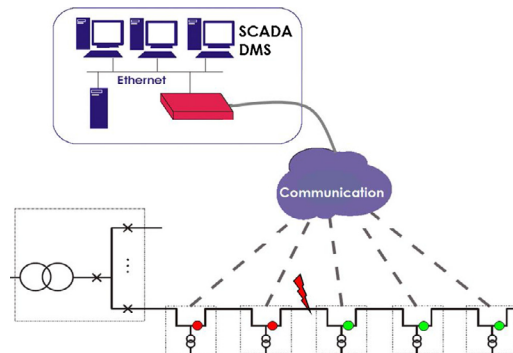


Fig. 4. Decentralized fault location based on fault indicators in secondary substations [35].

communication, secondary substations and switching stations are natural locations for devices enabling decentralized fault location. The principles of decentralized fault location are presented in Fig. 4.

Advanced metering infrastructure (AMI) is another decentralized way to enhance fault location. However, at least methods utilizing voltage dip data are only applicable to short circuits, not to earth faults in non-solidly grounded networks [36].

3.1. Utilization of smart meters

Fault location in Refs. [30], [33] and [34] is realized based on monitoring (through smart meters) the imbalances in phase voltages at different measuring points along the feeder.

Despite the availability of smart meters at LV side, the methods presented in these papers have not been verified by field tests. Moreover, the fault resistances used in the simulation studies are only up to $19\ \Omega$ which throws the effectiveness of the method for rural networks into doubt. In rural networks, the aim is to be able to locate faults with resistances up to several thousands of Ohms.

3.2. IEDs and fault passage indicators

The development of distribution networks towards Smart Grids also requires the addition of measurements and monitoring along MV feeders. Fault passage indicators (FPIs) are well-known technology applied especially in locating short-circuit faults. Secondary substations and switching stations are natural locations for FPIs.

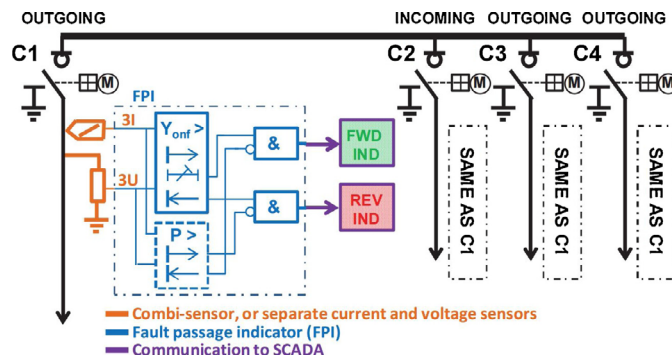


Fig. 5. Simplified diagram of the MFA concept implementation in secondary substation [12].

Reliable FPIs, equipped with communication to upper level information systems, enable e.g. SCADA or DMS to visualize the path of the fault current to the operator in the control room. Advancements in sensor technology, processing power of IEDs and communication provide new opportunities also to effective fault indication. IEC TC 38 has established a working group for standardizing FPIs [37].

3.2.1. ENEL's FPI based system

Ref. [37] describes many generations of FPIs, successfully implemented. The developed system includes a number of functionalities, e.g. directional detection of phase-to-earth fault and detection of re-striking faults. The method requires measurement of both current and voltage, and there are thousands of installed FPIs. In the fourth generation of FPIs, integrated sensors have been introduced. The IED utilizing these sensors, named RGDM (directional fault detection and measurement) will even be equipped with IEC 61850 based communication [37].

3.2.2. ABB's multi-frequency admittance based earth-fault location

Ref. [12] describes a novel concept for earth-fault indication in compensated MV networks, utilizing current and voltage measurements at secondary substations. The concept is called multi-frequency admittance (MFA) method. The aim of the concept is ambitious, including directional indication (forward and reverse), detection of faults with as high as 10 k Ω fault resistance, and the detection of intermittent earth faults. A simplified diagram of the indication concept is presented in Fig. 5 for a secondary substation with one incoming and two outgoing feeders. The method requires both residual signals (U_0 , I_0) measurements at secondary substations which are obtained based on phase currents (3I) and phase voltages (3U).

A forward indication is given if the fault current flow from the busbar towards the line and a reverse one is shown if the direction of the fault current is from the line to the busbar. In the MFA concept, the faulty line section can be determined by combining the directional fault indications in an upper level system, such as DMS. The MFA method has been successfully field tested in 60 individual primary earth faults varying e.g. the fault resistance between 0 to 6.2 k Ω . This indicates that the MFA concept can provide universal earth-fault indication, capable of also detecting intermittent faults [12].

3.2.3. Negative sequence component based approach

Fault indication and location is more challenging in isolated and compensated neutral networks due to the small fault currents in these types of networks. One solution to that is to utilize neutral

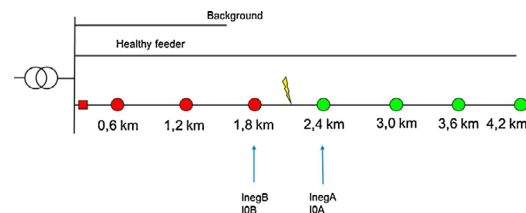


Fig. 6. Earth fault on an MV network between two secondary substations.

voltage measurement, in addition to current measurement. However, voltage measurement is usually cost prohibitive. Therefore, there is a need for a method which requires current measurements only.

Ref. [38] presents three methods solely based on current measurements. One noteworthy one is based on measuring the changes in symmetrical components of currents during fault situation. The paper claims that under fault condition, the negative sequence current is rather significant with small variations from the feeding substation up to the fault location whereas it is negligible after the fault point. That forms the basis for the method.

To understand the principles of the method, consider the network shown in Fig. 6. There is an earth fault between the third and fourth secondary substations. The following is the basic fault indication procedure:

Step 1: Fault condition is detected once the change in the zero sequence current exceeds a threshold.

$$\Delta I_0 > I_{0_set}$$

Step 2: Similarly, the change in the negative sequence current is computed/measured and compared to a preset threshold value.

$$\Delta I_{neg} > I_{neg_set}$$

If both conditions are met, it means the measuring point is within the fault path, otherwise it is behind the fault point.

Step 3: The faulted section is identified as the one between the last secondary substation in which $\Delta I_{neg} > I_{neg_set}$ and the first secondary substation with $\Delta I_{neg} < I_{neg_set}$.

However, the assessment of the method presented in this paper is only based on simulations that have been carried out. Also, it does not provide sufficient information about the negative sequence component behind the fault point.

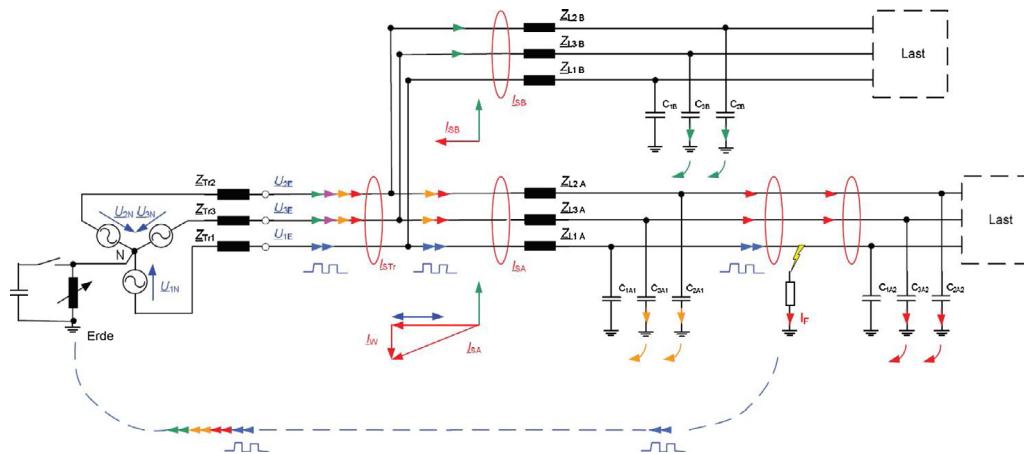


Fig. 7. Signal injection based method [39].

3.3. Signal injection based methods

Approaches based on pulse injection and on injection of non-grid-frequency current have been proposed. In addition to injection, signal detection and communication is required. These methods have received limited attention in general reviews and overviews. However, the principle of the pulse detection method, illustrated in Fig. 4, is very old and the method is widespread in compensated networks [39] (Fig. 7).

The idea is to inject a pulsating current into the neutral of the system following the fault occurrence. This results in a change in the current at the fault point. A current that its RMS value is a rectangular pulse is injected into the neutral of the network by switching a capacitor bank on and off in parallel with the compensation coil. The change in the current can be measured only in the faulted feeder and from the location of the switched capacitor bank up to the fault point. The identification of the faulted segment is achieved by the measurement of the zero-sequence current using relays distributed along the feeder. It is sufficient to measure only the RMS value of the zero-sequence current. For low-ohmic earth faults, the pulses can be detected by the devices between the primary substation and the fault point. However, this standard pulse method includes a number of additional requirements. One of the major drawbacks, in addition to its inability to detect faults other than low-ohmic faults, is that the fault must last for about 25 s [39].

To overcome the restrictions of the standard pulse method, a fast pulse method utilizing high power current injection with a non-grid-frequency, has been developed in Ref. [39]. One of the benefits of this system is that the results of the localization are available within a second. This method has been field tested [40] however the results show that it can be used only for fault resistances up to 10 k Ω .

Thanks to developments in active grounding systems for distribution networks [41] and [42], injection-based fault location techniques can now be applied and further researched with more ease. Ref. [43] reviews a number of research studies conducted on signal injection methodologies among which [44] is noteworthy. The algorithm presented in Ref. [44] is developed for resonant grounded (compensated) networks. A non-grid-frequency current with the amplitude of 1 A and frequency of 183 Hz is injected to the neutral through the suppression coil. Fault localization is achieved by magnetic field detection sensors tuned to the frequency of the

injected current and installed in the close vicinity of the faulted line. Another appealing algorithm based on signal injection is presented in Ref. [45] where two sinusoidal signals with different frequencies are injected to the faulted line to determine the fault distance and resistance.

4. Discussion

Over recent decades, a lot of effort has been put into the development of MV network fault location. An optimal method has to be simple and cost effective, applicable in various types of networks, accurate, sensitive, and verified at least by field tests.

Many of the attempts have been focused on the impedance method based on fundamental frequency. However, a breakthrough utilizing this approach is still missing. A few years ago, methods based on artificial intelligence attracted some attention, but the number of research papers on these methods seems to be declining, and it is difficult to find evidence of real-life implementations.

In theory, the most accurate fault location approach is the travelling-wave-based method. In practice, since in distribution networks there are branches, the reflection captured at the measuring point (beginning of the feeder) may come from different sources and not necessarily only from the fault point. This makes the practical application of this approach in distribution networks challenging.

Some signal injection based methods have been validated by field tests. Only current measurements are required which is an advantage. However, injection based methods require an injection device installed at the primary substation which causes more complexity and challenges. Moreover, these methods are not applicable to unearthed-neutral networks.

Today's fault passage indicators appear to be promising. Improvements in sensor technology and communication in secondary substations advance the development of these methods. Real life implementations can be found. One of the drawbacks of FPI based methods is that they are only capable of identifying the faulted section and not the accurate fault location. However, that is not a major concern as in many cases only knowing the faulted section is sufficient.

Among decentralized methods, a highly interesting method is the one based on monitoring the negative sequence current, not

Table 1
Summary of the main characteristics of the methods.

| Method | Impedance based | Travelling wave | Injection | IED/FPI |
|---|---|--|--|--|
| Main advantages | <ul style="list-style-type: none"> ● Simple implementation ● Cost effective | Theoretical accuracy | <ul style="list-style-type: none"> ● Verified in practice ● Only current measurements required along the feeders | <ul style="list-style-type: none"> ● Verified functionality ● High sensitivity ● Supported by smart grid development |
| Main drawbacks | <ul style="list-style-type: none"> ● No convincing verification in compensated networks ● Dependent on line parameters estimation | <ul style="list-style-type: none"> ● Branches ● Very limited experience in distribution networks | <ul style="list-style-type: none"> ● Requires a transmitter ● Requires IEDs along the feeders ● A number of practical limitations ● Accurate fault location must be found by other means | <ul style="list-style-type: none"> ● Requires IEDs along the feeders ● Accurate fault location must be found by other means ● At least most implementations require costly measurements |
| Applicable in compensated networks | No | Yes | Yes | Yes |
| Applicable in isolated neutral networks | Yes | Yes | No | Yes |
| Verified by field tests | Partly | Not in distribution networks | Yes | Yes |
| Highlighted requirements | <ul style="list-style-type: none"> ● Requires measurement accuracy ● Network data | <ul style="list-style-type: none"> ● High sampling rate ● Costly detection device | <ul style="list-style-type: none"> ● Injection device at the primary substation ● Current sensors ● Communication | <ul style="list-style-type: none"> ● IEDs along the feeder ● At least current sensors ● Communication |
| Outlook | After a number of unsatisfactory approaches, the prospect is unpromising | Worth further investigations | Applicable in compensated networks | Along with the development of smart grids, these types of methods will be increasingly common |

requiring voltage measurement. It has a definite advantage over the injection method, i.e. no injection device is required. However, field tests are needed for the verification of this method.

Under certain circumstances, a combination of decentralized and travelling wave based methods might overcome the drawbacks of the two methods. A decentralized method would indicate the faulty branch and line section between two indicators, and the travelling wave based method could provide the accurate distance. However, in case of a network with short lines, high sampling rates are required.

In order to facilitate comparison between the methods discussed in this paper, the main characteristics of the most important ones are summarized in the following table (Table 1).

5. Conclusion and future work

In this paper, the state of the art methods for fault location on distribution networks were discussed. The focus was on single-phase earth faults as they were the most common type of faults in distribution lines. The principles of the methods along with their application considerations were outlined and a comparison was made. Taking into account the development of Smart Grid and smart secondary substation technology, including communication and IEDs with high processing capacity, the most promising fault location techniques are decentralized, based on IEDs along the feeder.

Intermittent transient earth fault is a special type of fault which requires dedicated protection. Today's intermittent earth fault protection is a standard requirement for protection relays. Selective protection approaches are available but intermittent fault location still requires research and development.

Acknowledgements

The authors would like to acknowledge the financial support provided by the European Regional Development Fund (ERDF), the Finnish Funding Agency for Technology and Innovation – Tekes (grant No. 4332/31/2014), and the industrial partners to the Protect-DG project.

References


- [1] S. Hänninen, Single phase earth faults in high impedance grounded networks—characteristics, indication and location, VTT Publ. 453 (2001), 139 p.
- [2] L.U. Iurinic, A.R. Herrera-Orozco, R.G. Ferraz, A.S. Bretas, Distribution systems high impedance fault location: a parameter estimation approach, IEEE Trans. Power Deliv. PP (99) (2015) 1.
- [3] M.B. Djurić, Z.M. Radojević, V.V. Terzija, Digital signal processing algorithm for arcing faults detection and fault distance calculation on transmission lines, Int. J. Electr. Power Energy Syst. 19 (3) (1997) 165–170.
- [4] S. Kulkarni, S. Santoso, T. Short, Incipient fault location algorithm for underground cables, IEEE Trans. Smart Grid 5 (3) (2014) 1165–1174.
- [5] Z.M. Radojević, V.V. Terzija, M.B. Djurić, Numerical algorithm for overhead lines arcing faults detection and distance and directional protection, IEEE Trans. Power Deliv. 15 (1) (2000) 31–37.
- [6] J. Mora-Florez, J. Melendez, G. Carillo-Cacedo, Comparison of impedance based location methods for power distribution systems, Elsevier Electr. Power Syst. Res. 78 (4) (2008) 657–666.
- [7] D. Novosel, D. Hart, Y. Hu, J. Myllymäki, System for Locating Faults and Estimating Fault Resistance in Distribution Networks with Tapped Loads. US Patent 5839093, 17 November 1998.
- [8] S. Hänninen, M. Lehtonen, Earth Fault Distance Computation with Fundamental Frequency Signals based on Measurements in Substation Supply Bay, VTT Research Notes 2153, Espoo, 2002.
- [9] J. Altonen, A. Wahlroos, Advancements in fundamental frequency impedance based earth-fault location in unearthed distribution systems, in: CIREED 19th International Conference on Electricity Distribution, Vienna, Austria, 2007.

- [10] J. Altonen, A. Wahlroos, M. Pirskanen, Advancements in earth-fault location in compensated MV-networks, in: CIREN 21st International Conference on Electricity Distribution, Frankfurt, 2011.
- [11] J. Altonen, A. Wahlroos, Novel algorithm for earth-fault location in compensated MV-networks, in: CIREN 22nd International Conference on Electricity Distribution, Stockholm, Sweden, 2013.
- [12] J. Altonen, A. Wahlroos, Performance of modern fault passage indicator concept, in: CIREN Workshop, Helsinki, 14–15 June, 2016.
- [13] IEEE Guide for Determining Fault Location on AC Transmission and Distribution Lines, IEEE, New York, USA, 2014, pp. 1–72.
- [14] N.I. Elkalashy, N.A. Sabiha, M. Lehtonen, Earth fault distance estimation using active traveling waves in energized-compensated MV networks, *IEEE Trans. Power Deliv.* 30 (2) (2015) 836–843.
- [15] J. Sadeh, E. Bakhshizadeh, K. Rasoul, A new fault location algorithm for radial distribution systems using modal analysis, *Elsevier Electr. Power Energy Syst.* 45 (1) (2013) 271–278.
- [16] M. Abad, S. Borroy, D. López, N. El Halabi, M. Garcia, New fault location method for up-to-date and upcoming distribution networks, in: CIREN 23rd International Conference on Electricity Distribution, Lyon, France, 2015.
- [17] Rui Liang, Guoqing Fu, Xueyuan Zhu, Xue Xue, Fault location based on single terminal travelling wave analysis in radial distribution network, *Int. J. Electr. Power Energy Syst.* 66 (2015) 160–165.
- [18] J. Sadeha, E. Bakhshizadeh, R. Kazemzadeh, A new fault location algorithm for radial distribution systems using modal analysis, *Int. J. Electr. Power Energy Syst.* 45 (1) (2013) 271–278.
- [19] D.W.P. Thomas, R.J.O. Carvalho, E.T. Pereira, C. Christopoulos, Field trial of fault location on a distribution system using high frequency transients, in: *IEEE Russia Power Tech*, St. Petersburg, 2005.
- [20] A. Borghetti, S. Corsi, C. Nucci, M. Paolone, L. Peretto, R. Tinarelli, On the use of continuous-wavelet transform for fault location in distribution power systems, *Int. J. Electr. Power Energy Syst.* 28 (November (9)) (2006) 608–617.
- [21] A. Borghetti, M. Bosetti, M. Silvestro, C. Nucci, M. Paolone, Continuous-wavelet transform for fault location in distribution power networks: definition of mother wavelets inferred from fault originated transients, *IEEE Trans. Power Syst.* 23 (May (2)) (2008) 380–388.
- [22] A. Borghetti, M. Bosetti, C. Nucci, M. Paolone, A. Abur, Integrated use of time-frequency wavelet decompositions for fault location in distribution networks: theory and experimental validation, *IEEE Trans. Power Deliv.* 25 (October (4)) (2010) 3139–3146.
- [23] J.J. Mora, G. Carrillo, L. Perez, Fault location in power distribution systems using ANFIS nets and current patterns, in: *Transmission & Distribution Conference and Exposition IEEE/PES: Latin America*, Caracas, 2006.
- [24] L.S. Martins, J.F. Martins, C.M. Alegria, V.F. Pires, A network distribution power system fault location based on neural eigenvalue algorithm, in: *Power Tech Conference Proceedings*, IEEE Bologna, Bologna, 2003.
- [25] J. Mora-Florez, V. Barrera-Nnez, G. Carrillo-Cacedo, Fault location in power distribution systems using a learning algorithm for multivariable data analysis, *IEEE Trans. Power Deliv.* 22 (3) (2007) 1715–1721.
- [26] F. Chunju, K. Li, W. Chan, Y. Weiyong, Z. Zhaoning, Application of wavelet fuzzy neural network in locating single line to ground fault (SLG) in distribution lines, *Int. J. Electr. Power Energy Syst.* 29 (July (6)) (2007) 497–503.
- [27] M. Pourahmadi-Nakhli, A. Safavi, Path characteristic frequency-based fault locating in radial distribution systems using wavelets and neural networks, *IEEE Trans. Power Deliv.* 26 (April (2)) (2011) 772–781.
- [28] A. Rafinia, J. Moshtagh, A new approach to fault location in three-phase underground distribution system using combination of wavelet analysis with ANN and FLS, *Int. J. Electr. Power Energy Syst.* 55 (February) (2014) 261–274.
- [29] S. Lotffard, M. Kezunovic, M. Mousavi, A systematic approach for ranking distribution systems fault location algorithms and eliminating false estimates, *IEEE Trans. Power Deliv.* 28 (January (1)) (2013) 285–293.
- [30] R.A.F. Pereira, L.G.W. da Silva, M. Kezunovic, J.R.S. Mantovani, Improved fault location on distribution feeders based on matching during-fault voltage sags, *IEEE Trans. Power Deliv.* 24 (April (2)) (2009) 852–862.
- [31] A. Estebsari, E. Pons, E. Bompard, A. Bahmanyar, S. Jamali, An improved fault location method for distribution networks exploiting emerging LV smart meters, in: *IEEE Workshop on Environmental, Energy, and Structural Monitoring Systems (EESMS)*, Bari, Italy, 2016.
- [32] W. Luan, Low cost feeder monitoring solution in support of utility operations, in: *CIGRE Conference on Power Systems*, Vancouver, BC, Canada, 2010.
- [33] K. Jia, Z. Ren, T. Bi, Q. Yang, Ground fault location using the low-voltage-side recorded data in distribution systems, *IEEE Trans. Ind. Appl.* 51 (6) (2015) 4994–5001.
- [34] F.C.L. Trindade, W. Freitas, J.C.M. Vieira, Fault location in distribution systems based on smart feeder meters, *IEEE Trans. Power Deliv.* 29 (1) (2014) 251–260.
- [35] L. Kumpulainen, S. Pettissalo, S. Sauna-aho, A secondary substation monitoring based method for earth-fault indication in MV cable networks, in: *Seminar on Methods and Techniques for Earth Fault Detection, Indication and Location*, Aalto University, Espoo, Finland, February 15, 2011.
- [36] A. Bagheri, M. Bollen, Additional information from voltage dips, in: *17th International Conference on Harmonics and Quality of Power (ICHQP)*, Belo Horizonte, Minas Gerais State, Brazil, 2016.
- [37] R. Calone, A. Cerretti, A. Fatica, Evolution of the fault locator on MV distribution networks from simple stand alone device to a sophisticated strategic component of the smart grid control system, in: *Proceedings of CIREN 2011*, Frankfurt 6–9 June, 2011.
- [38] M. Lehtonen, O. Siirto, M.F. Abdel-Fattah, Simple fault path indication techniques for earth faults, in: *IEEE Electric Power Quality and Supply Reliability Conference (PQ)*, Rakvere, Estonia, 11–13 June, 2014.
- [39] G. Druml, C. Raunig, P. Schenger, L. Fickert, Fast selective earth fault localization using the new fast pulse detection method, in: *22nd International Conference on Electricity Distribution*, Stockholm, 10–13 June, 2013.
- [40] C. Tengg, K. Schoass, G. Druml, R. Schmaranz, M. Marketz, L. Fickert, Evaluation of new earth fault localization methods by earth fault experiments, in: *CIREN 22nd International Conference on Electricity Distribution*, Stockholm, 10–13 June, 2013.
- [41] K.M. Winter, The RCC ground fault neutralizer—a novel scheme for fast earth-fault protection, in: *18th International Conference and Exhibition on Electricity Distribution*, Turin, Italy, 2005.
- [42] F.J. Pazos, A. Amezua, *Electronic Active Earthing System for Use in High-Voltage Distribution Networks*, Spain Patent EP2128951A1, 2008.
- [43] G. Buigues, V. Valverde, I. Zamora, J. Mazon, E. Torres, Signal injection techniques for fault location in distribution networks, in: *International Conference on Renewable Energies and Power Quality (ICREPQ'12)*, Santiago de Compostella, Spain, 2012.
- [44] C. Raunig, L. Fickert, C. Obkircher, G. Achleitner, Mobile earth fault localization by tracing current injection, in: *Electric Power Quality and Supply Reliability Conference (PQ)*, Kuressaare, Estonia, 2010.
- [45] F. Han, X. Yu, M. Al-Dabbagh, Y. Wang, Locating phase-to-ground short-circuit faults on radial distribution lines, *IEEE Trans. Ind. Electron.* 24 (3) (2007) 1581–1590.



Article

Earth Fault Location Using Negative Sequence Currents

Amir Farughian *, Lauri Kumpulainen and Kimmo Kauhaniemi 

School of Technology and Innovations, University of Vaasa, 6500 Vaasa, Finland;
lauri.kumpulainen@uva.fi (L.K.); kimmo.kauhaniemi@uva.fi (K.K.)

* Correspondence: amir.farughian@uva.fi

Received: 27 August 2019; Accepted: 27 September 2019; Published: 30 September 2019



Abstract: In this paper, a new method for locating single-phase earth faults on non-effectively earthed medium voltage distribution networks is proposed. The method requires only current measurements and is based on the analysis of the negative sequence components of the currents measured at secondary substations along medium voltage (MV) distribution feeders. The theory behind the proposed method is discussed in depth. The proposed method is examined by simulations, which are carried out for different types of networks. The results validate the effectiveness of the method in locating single-phase earth faults. In addition, some aspects of practical implementation are discussed. A brief comparative analysis is conducted between the behaviors of negative and zero sequence currents along a faulty feeder. The results reveal a considerably higher stability level of the negative sequence current over that of the zero sequence current.

Keywords: sequence components; earth fault location; negative sequence current

1. Introduction

Feeder automation is one of the distinguishing features of smart grids. It aims at developing self-healing systems, able to locate faults and perform isolation and supply restoration automatically. Reliable fault location and indication is the key to this functionality. For short circuit faults, there are established methods for locating them, whereas, for locating earth faults, there is not a universally accepted, reliable and cost-effective method in the market for isolated neutral or compensated networks. However, a number of methods have been put forward to address this matter. A comprehensive review of the state-of-the-art methods for locating single-phase earth faults in medium voltage (MV) distribution networks is provided in Reference [1].

There are different types of fault location methods. Impedance-based methods [2–7] work based on calculating the apparent impedance seen when looking into the line from an end (measuring point) during the fault condition [8]. Since the line length between the measuring point and the fault location is proportional to the calculated impedance, by knowing the line impedance per unit length, the fault distance can be estimated. In Reference [2], the fault location and resistance are estimated using an iterative method. In Reference [3], a model developed for high-impedance faults consisting of two antiparallel diodes is proposed. A parameter estimation procedure is performed which uses the proposed model along with voltage and current signals to estimate the fault distance and other parameters. In Reference [4], the whole load of the feeder is modelled as one equivalent load tap located where the voltage drop due to the fault is at a maximum. Two assumptions are made i.e., once the load tap is assumed to be located before the fault point and once it is assumed to be after the fault. By solving the equations corresponding to those assumptions, the fault distance is estimated in unearthed networks. The method presented in Reference [5] scans the data obtained from power quality monitors and relays to estimate the fault distance in terms of the line impedance. The concept introduced in Reference [4] can be adapted for compensated distribution networks as presented in Reference [6]. In Reference [7], a method for fault

distance calculation for compensated networks is put forward which requires a fewer number of settings compared to the method presented in Reference [4]. Despite all the efforts, these impedance-based methods are subject to errors as the fault impedance is unknown. Moreover, to locate single-phase to ground faults, the phase to ground voltages must be available [4], which is cost prohibitive. Generally, these methods are more suitable in transmission lines.

Travelling-wave based methods [9–13] work based on the transient voltages and currents (impulses) which are generated at the fault location. These waves propagate away from the fault point in both directions towards the ends. As these types of waves travel at the speed of light, by measuring the wave and their reflection arrival times at either terminal of the line, the fault distance can be determined [8]. A concept to create travelling waves is proposed in Reference [9], which is based on earthing the neutral via a controlled thyristor that provides a short period of high fault current. The method in Reference [10] works based on frequency spectrum components of waves generated as a result of fault occurrence. Reference [11] is based on the wave velocity of zero and aerial mode components and their arriving timestamps. Some results from field tests are reported in Reference [12] indicating the limitations of applying travelling wave fault location on distribution networks. In Reference [13], the frequency information of travelling voltage waves is integrated with their time domain information using continuous wavelet transform to locate faults. However, the main problem when using travelling-wave based methods is that due to the large number of branches and laterals in distribution networks, the reflections captured at the beginning of the feeder, may come from different sources and not necessarily from the fault location only. This makes the use of traveling wave-based methods problematic in distribution networks.

Signal injection-based methods are another type of fault location method [14–16]. The idea is to inject a pulsating current into the neutral of the system following a fault occurrence. The injected signal is detectable only in the faulted feeder and from the injection point up to the fault point. Although, this method has been field tested, the results show that it can be used for fault resistances only up to 300 Ω (without voltage measurement). In addition, the use of this method is limited to only compensated networks where the injection device can be coupled with the Petersen coil.

In References [17–20], earth fault location using zero sequence components is proposed. Despite the simplicity this approach offers, it suffers from a shortcoming i.e., false indication in networks where the length of the faulty feeder is long and the fault occurs close to the beginning of the feeder. In addition, this method in the manner proposed in Reference [20], when applied to compensated networks, requires connection and disconnection of the resistor in parallel with the Petersen coil in the right time, which could cause complexity.

Despite all these efforts, earth fault location in isolated and compensated neutral distribution networks remains a problem for which there does not seem to be a widely adopted solution and thus it is worth studying. Fault indication and location is a more challenging task in isolated and compensated neutral networks because their fault currents are so low that the simple threshold detection will often lead to poor results. One solution is to utilize neutral voltage measurement, in addition to current measurement. However, this neutral voltage measurement is not usually preferred at the MV side due to additional costs [18]. Therefore, there is a need for an earth fault indication method which is based on current measurement only. On the other hand, recent developments in smart grids have enabled communication between different parts of the network. By taking advantage of this feature, better solutions can be achieved as measurements from different parts of the network can be utilized to locate the fault.

In this paper, a new method for identifying the faulted segment (the segment between two secondary substations on which fault has occurred) in case of a single-phase to ground fault is presented. It is purely based on current measurements and no voltage measurement is required, which can be considered as an advantage. The proposed method employs the negative sequence current components to locate the fault. First, In Section 2, the negative sequence current along a faulted feeder is analysed in depth to gain insights into its behaviour. Then, based on that analysis, the fault location procedure is established in Section 3. In Section 4, the effectiveness of the method is evaluated by means of simulation using various types of medium voltage distribution networks. Lastly, some aspects of implementing the proposed method are discussed in Section 5.

2. Theoretical Background of the Proposed Method

In this section, to gain some insight into the proposed fault location method, the negative sequence currents on different locations on a feeder following a fault occurrence are discussed. The focus is on the difference between the negative sequence currents before and after the fault point.

To have a better understanding of the fault current, an MV distribution network with one healthy feeder and one with a single-phase to ground fault on it is shown in Figure 1. Earth capacitances and the flow of currents following a fault occurrence are shown in the figure. Fault current, especially in isolated neutral networks, is determined by network capacitances and mostly by the undamaged parts of the network.

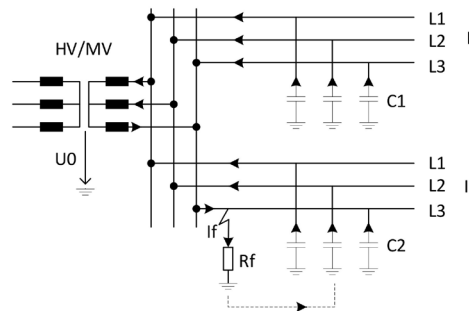
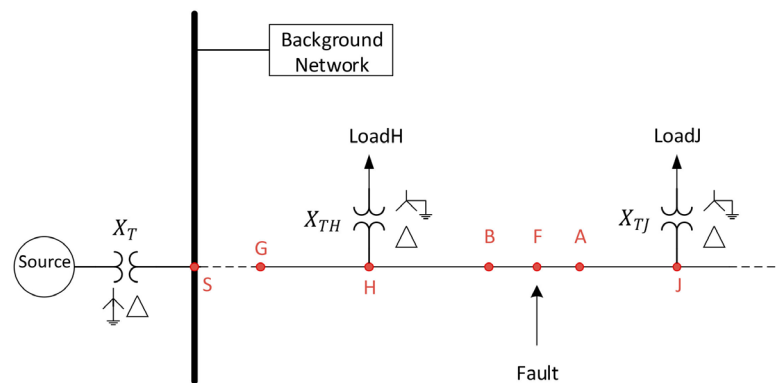


Figure 1. A single phase to ground fault in an isolated neutral system [21].

For studying the fault location problem with more details, the MV distribution network shown in Figure 2 is used. In this paper, the style of single line diagrams is derived from Reference [22]. A typical MV network consists of several feeders but from a theoretical viewpoint, only the faulty feeder needs to be studied with more details and others can be represented by a simple electrical equivalent circuit. This aspect is considered in the figure using the single block “Background network” representing all the healthy feeders. A single-phase to ground fault occurs on the feeder under study between two secondary substations H and J at point F with the fault resistance R_F . The dashed lines indicate that the feeder can be of any length and can have any number of secondary substations. In Figure 2a, two arbitrary secondary substations are shown which indicates that the following analysis is valid for any point on the feeder. The goal here is to analyse the negative sequence current at point B, which is before the fault point and the negative sequence current after the fault location at point A. Note that points B and A are not electrically the same location. This is shown, for clarification, in Figure 2b.



(a)

Figure 2. Cont.

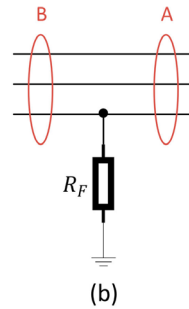


Figure 2. Single line diagram of a distribution network. (a) two arbitrary secondary substations are shown which indicates that the following analysis is valid for any point on the feeder. (b) B and A are not electrically the same location.

The sequence equivalent networks of the MV distribution system shown in Figure 2 can be obtained, as shown in Figures 3–5 (see also the notations list presented at the beginning of the paper). Note that line (to earth) capacitances only appear in the zero sequence network. In case of a single phase to ground fault, the sequence networks will be connected in series. The complete sequence network of the faulted network under study is shown in Figure 6. It can be simplified, as shown in Figure 7 where Z_G and Z_J are equivalent impedances of the parts marked on Figure 6. The currents \bar{I}_B and \bar{I}_A are the fundamental frequency components of the negative sequence currents at points B (before the fault) and A (after the fault) in Figure 2, respectively.

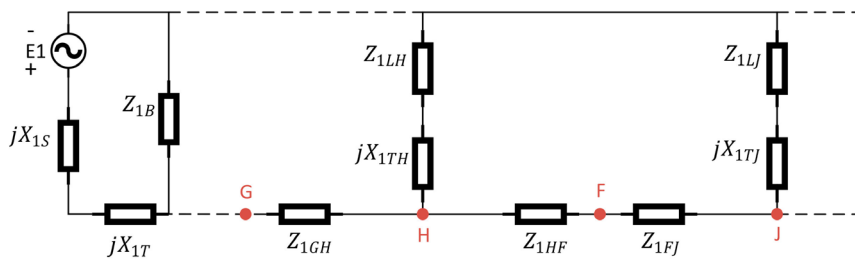


Figure 3. Positive sequence circuit.

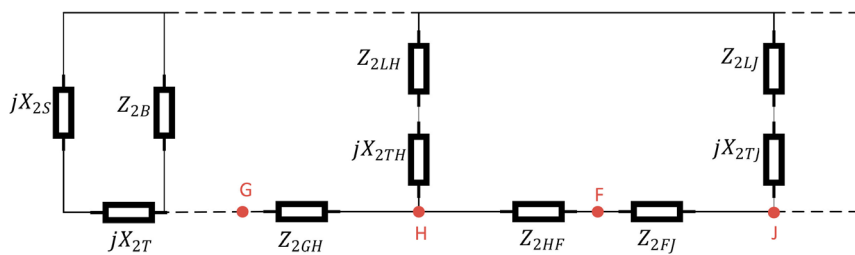


Figure 4. Negative sequence circuit.

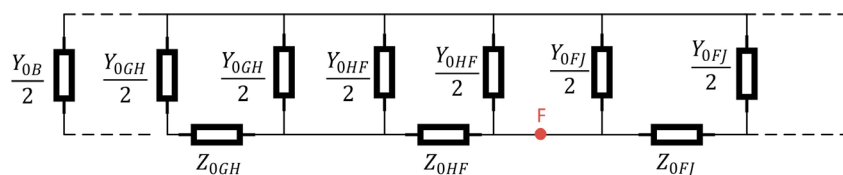


Figure 5. Zero sequence circuit.

The values of load impedances are normally rather large compared to the system impedances, so that they have a negligible effect on the faulted phase current. Therefore, it is common practice

in fault analysis to neglect load impedances for shunt faults [22]. However, in the following, both scenarios are discussed, i.e., one where the effect of load is neglected and another where its effect is considered.

2.1. With No Load

Consider Figure 6. Shunt branches consist of transformers' reactance in series with load impedances. With no load assumption, the values of all the load impedances in the shunt branches are infinite and hence no current flows through the shunt branches in the positive and negative sequence networks. As a result, the negative sequence current measured at any point from beginning of the feeder to the fault point is constant and it is zero after the fault point. Therefore:

$$I_B > I_A \quad (1)$$

where, I_B and I_A are the magnitudes of the phasors \bar{I}_B and \bar{I}_A , respectively.

2.2. With Load

In Figure 6, when taking load impedances into account, the negative sequence current measured along the feeder from S to F is not constant anymore as some currents will flow through the shunt branches as well. In addition, similarly, due to the flow of current through shunt branches after the fault point, the negative sequence current after the fault point is not zero anymore.

In practice, the series impedances in Figure 6 are negligible when compared to the shunt impedances, with the exception of Z_{2B} and X_{2s} . Indeed, Z_{2B} is comparatively low as it is the equivalent negative sequence impedance of several feeders i.e., the background network.

Now, consider Figure 7 which shows the simplified network where Z_G and Z_J are the total negative sequence impedances before and after the fault point, respectively. In Figure 7, the following is valid.

$$\bar{I}_B = \bar{I}_A + \bar{I}_F \quad (2)$$

$$\bar{I}_B = \frac{\bar{V}_f}{Z_G + Z_{2HF}} \quad (3)$$

$$\bar{I}_A = -\frac{\bar{V}_f}{Z_{2FJ} + Z_J} \quad (4)$$

As Z_G represents the part of the network which consists of negligible series impedances and the shunt branch Z_{2B} , it is a comparatively low impedance. In contrast, Z_J is a comparatively high impedance so that:

$$\text{abs}(Z_G + Z_{2HF}) < \text{abs}(Z_{2FJ} + Z_J) \quad (5)$$

Equations (3)–(5) yield:

$$I_B > I_A \quad (6)$$

Therefore, the negative sequence current before the fault point is higher than the negative sequence current after the fault point in both scenarios i.e., with and without considering the load.

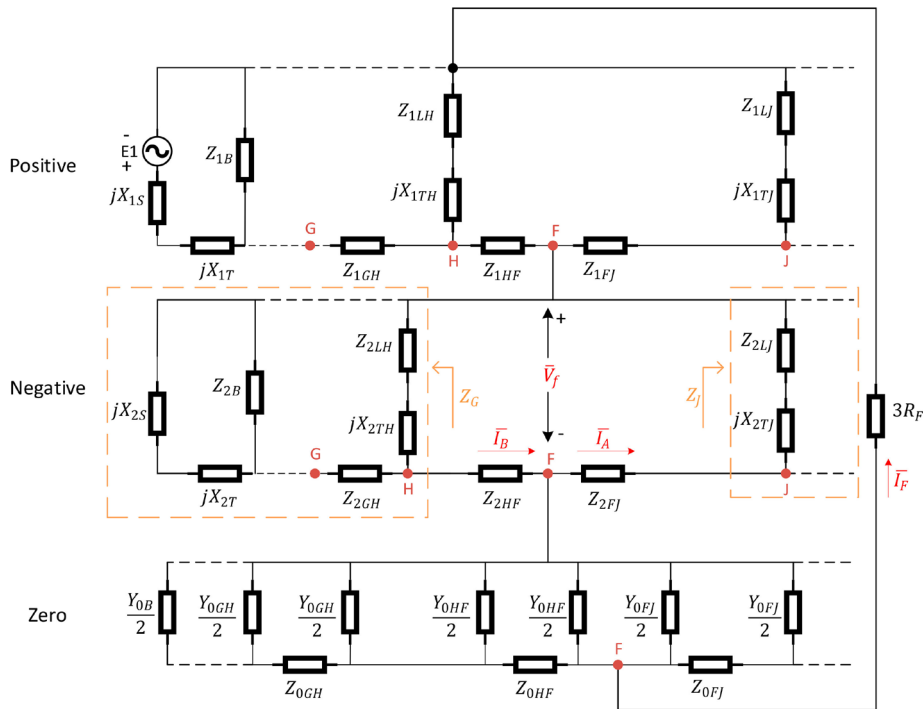


Figure 6. Sequence networks and interconnections for a phase-to-ground fault in the system of Figure 2.

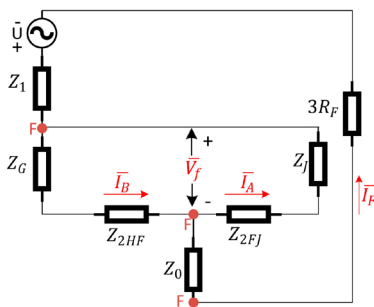


Figure 7. Simplified form of the network shown in Figure 6.

3. Outline of the Implementation of the Method

Considering the theory discussed in the previous section, when a single-phase-to-ground fault occurs, the negative sequence current exists and varies only a little in the section between the primary substation and the fault location whereas after the fault point, it is very low. This is simply illustrated in Figure 8.

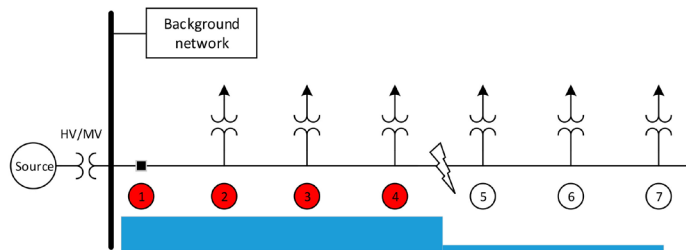


Figure 8. Negative sequence current magnitude along the feeder following a single-phase to ground fault occurrence.

Therefore, the proposed new fault location procedure is structured as follows:

1. The (change in the) negative sequence current at secondary substations (ideally at every substation) is obtained, following a fault occurrence.
2. These values are compared with a pre-set threshold at secondary substations.
3. Only from those secondary substations in which the threshold is exceeded, the fault detection information is sent to the control room.
4. The faulted segment is identified as the section between the last secondary substation that sends the fault detection information and the first secondary substation from which comes no signal.

For example, in Figure 8, the fault information is sent to the control room from those measuring points at which the magnitude of the negative sequence current has exceeded the threshold i.e., measuring points 1–4. The last three secondary substations (points 5–7) send no signal to the control room and therefore the faulted segment is identified as the one linking measuring points 4 and 5.

4. Simulation Results

To evaluate the validity of the proposed method, a set of simulations was carried out with PSCAD™/EMTDC™. The effectiveness of the proposed method was studied with different fault resistances in each of the following network types:

- Cabled urban compensated network;
- Cabled urban isolated neutral network;
- Rural compensated network;
- Rural isolated neutral network.

The network shown in Figure 9 is an urban compensated medium voltage distribution network with compensation degree 0.95. The voltage level in the medium voltage side is 20 kV which is fed from a 110-kV supply network using a 40 MVA transformer. The length of the feeder under study is 5.4 km consisting of AHXAMK underground cables. The feeder under study has five secondary substations equipped with current measurements. The current measurement points 2–6 are the secondary substations along the feeder, points 1 is at the beginning of the feeder and H refers to the measuring point at the beginning of an adjacent healthy feeder. A single-phase-to-earth fault, with the resistance of 30 Ω , occurs at 2.5 km from the beginning of the feeder.

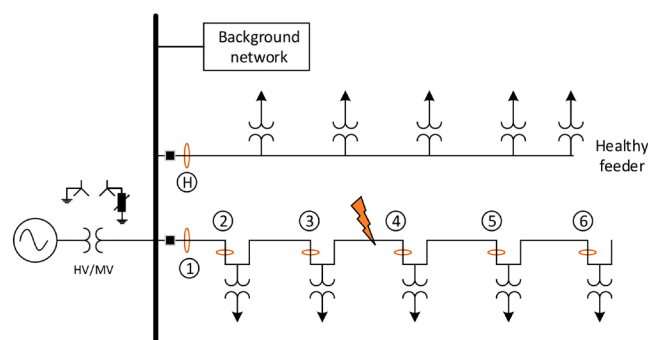


Figure 9. Cabled urban compensated network.

The magnitudes of the fundamental frequency phasors of the negative sequence currents with respect to time for faulty and healthy feeders are shown in Figure 10. The stabilized values obtained at $t = 0.2$ s are shown in a separate figure (Figure 11). Using the proposed method, one can readily determine the faulted section i.e., the one between secondary substations with measuring points 3 and 4. There is a considerable difference in the amplitude of the negative sequence currents before and

after the fault points so that the negative sequence current is practically negligible after the fault point. It is worth noticing that the negative sequence current of the healthy feeder behaves in a similar way as that of the points after the fault point.

In addition, the variations of the negative sequence currents along the feeder from the beginning of it up to the fault point are so insignificant that the first three graphs (corresponding to locations before the fault point) are almost matched. This highlights the strength of using the negative sequence current in locating faults.

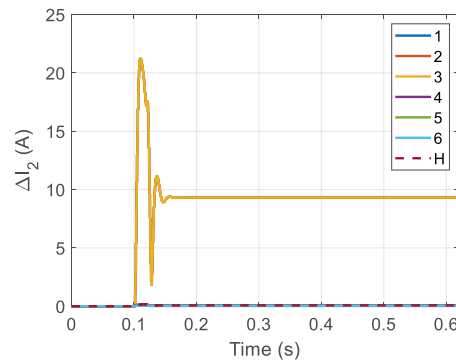


Figure 10. Negative sequence current magnitude.

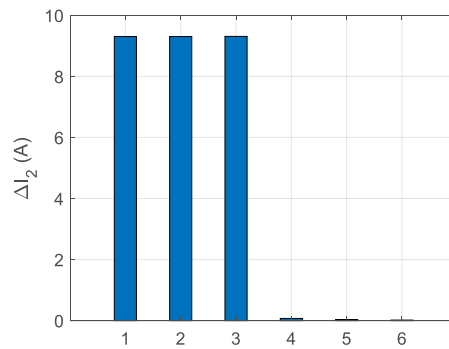


Figure 11. Negative sequence current magnitude.

To enable a comparison between negative and zero sequence currents, similar types of graphs are obtained for the zero sequence currents and shown in Figures 12 and 13. Contrary to the negative sequence current, the zero-sequence current varies considerably along the feeder and is not negligible after the fault point. This reveals the shortcoming of using the zero-sequence current over the negative sequence current.

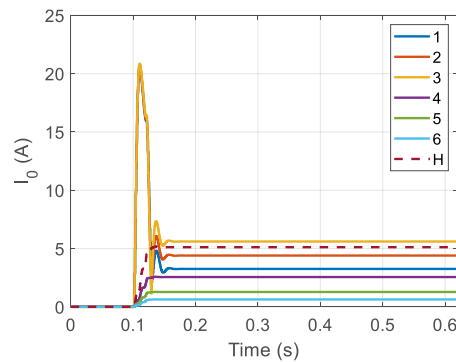


Figure 12. Zero sequence current magnitude.

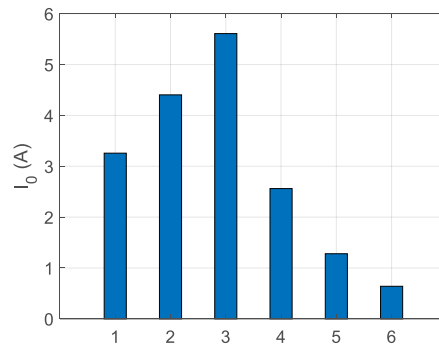


Figure 13. Zero sequence current magnitude.

To further investigate the validity and performance of the proposed method, five fault resistances are studied ranging from 0.01Ω up to $1 \text{ k}\Omega$. The changes in the negative sequence currents, caused by the fault, at the beginning of the healthy and faulty feeders and at each secondary substation of the faulty feeder are provided in Table 1. The choice of the threshold might vary from network to network. Developing a procedure to decide the proper threshold for a given network is not the focus of this paper. For simulations presented in this paper, the threshold is chosen to be 3 A for urban networks and 2 A for rural networks. For fault resistances between 0.01Ω and 1000Ω , it is clear from the table that for points 1 to 3, negative sequence currents exceed the threshold (3 A) whereas these values are below the threshold for points 4 to 6. Therefore, the faulted segment is the one between the second and third secondary substations i.e., between points 3 and 4.

Table 1. Negative sequence currents in urban compensated network.

| R_f (Ω) | ΔI_{n1} (A) | ΔI_{n2} (A) | ΔI_{n3} (A) | ΔI_{n4} (A) | ΔI_{n5} (A) | ΔI_{n6} (A) | ΔI_{nH} (A) |
|--------------------|---------------------|---------------------|---------------------|---------------------|---------------------|---------------------|---------------------|
| 0.01 | 9.57 | 9.57 | 9.57 | 2.6 | 0.04 | 0.02 | 0.08 |
| 1 | 9.48 | 9.48 | 9.49 | 2.6 | 0.04 | 0.02 | 0.08 |
| 10 | 9.41 | 9.41 | 9.41 | 2.59 | 0.04 | 0.02 | 0.08 |
| 100 | 8.81 | 8.81 | 8.82 | 2.42 | 0.03 | 0.02 | 0.07 |
| 1000 | 3.38 | 3.37 | 3.38 | 0.92 | 0.01 | 0.01 | 0.03 |

The same procedure can be applied to isolated networks, as shown in Figure 14. The changes in the negative sequence currents, following the fault occurrence, are provided in Table 2. Using the table and the same 3 A threshold, the faulted segment can be determined successfully for all the 5 fault resistances.

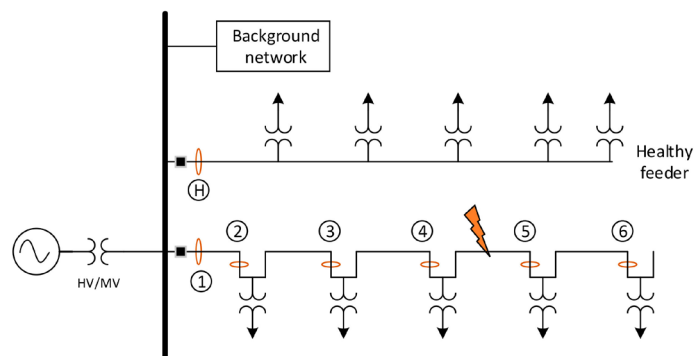


Figure 14. Urban isolated network.

Table 2. Negative sequence currents in urban isolated network.

| Rf (Ω) | ΔIn1 (A) | ΔIn2 (A) | ΔIn3 (A) | ΔIn4 (A) | ΔIn5 (A) | ΔIn6 (A) | ΔInH (A) |
|--------|----------|----------|----------|----------|----------|----------|----------|
| 0.01 | 58.91 | 58.9 | 58.94 | 56.54 | 0.26 | 0.13 | 0.48 |
| 1 | 58.89 | 58.88 | 58.92 | 56.51 | 0.26 | 0.13 | 0.48 |
| 10 | 58.06 | 58.06 | 58.09 | 55.72 | 0.25 | 0.13 | 0.48 |
| 100 | 31.73 | 31.73 | 31.75 | 30.45 | 0.14 | 0.07 | 0.26 |
| 1000 | 3.85 | 3.85 | 3.85 | 3.68 | 0.02 | 0.01 | 0.03 |

Now consider the rural compensated network shown in Figure 15. The first 5 km of the feeder under study consists of cables and the rest 45 km is overhead lines. The cable and overhead lines types modelled in the simulations are shown on the figure. A single-phase to ground occurs at 28 km from the beginning of the feeder. Similarly, using a threshold of 2 A and Table 3, the faulted segment is successfully identified, as the one between the second and third secondary substations (points 3 and 4).

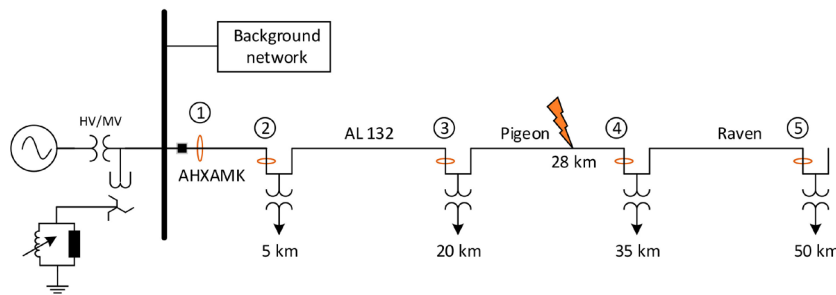


Figure 15. Rural compensated network.

Table 3. Negative sequence currents in rural compensated network.

| Rf (Ω) | ΔIn1 (A) | ΔIn2 (A) | ΔIn3 (A) | ΔIn4 (A) | ΔIn5 (A) |
|--------|----------|----------|----------|----------|----------|
| 0.01 | 5.25 | 5.25 | 5.26 | 0.59 | 0.29 |
| 1 | 5.25 | 5.24 | 5.26 | 0.59 | 0.29 |
| 10 | 5.21 | 5.21 | 5.22 | 0.59 | 0.29 |
| 100 | 4.94 | 4.94 | 4.95 | 0.56 | 0.27 |
| 1000 | 2.39 | 2.38 | 2.39 | 0.27 | 0.13 |

Lastly, in Figure 16, a rural isolated neutral network is shown. The change in the magnitude of the negative sequence currents for the points marked on the figure are shown in Table 4. In a similar fashion, the faulted segment is determined as the one between points 3 and 4 using the same 2 A threshold.

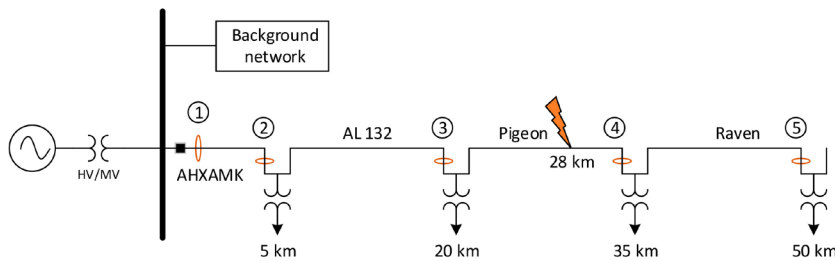


Figure 16. Rural isolated network.

Table 4. Negative sequence currents in rural isolated network.

| Rf (Ω) | ΔI_{n1} (A) | ΔI_{n2} (A) | ΔI_{n3} (A) | ΔI_{n4} (A) | ΔI_{n5} (A) |
|-----------------|---------------------|---------------------|---------------------|---------------------|---------------------|
| 0.01 | 15.21 | 15.19 | 15.23 | 1.72 | 0.85 |
| 1 | 15.21 | 15.19 | 15.23 | 1.72 | 0.85 |
| 10 | 15.16 | 15.13 | 15.18 | 1.72 | 0.84 |
| 100 | 13.4 | 13.37 | 13.41 | 1.52 | 0.74 |
| 1000 | 3 | 3 | 3.01 | 0.34 | 0.17 |

5. Discussion

In practice, current measurements at each secondary substation can be made using Rogowski coils, which are also suitable for retrofit installations. In the tables presented in Section 4, there are current values which are very low. It should be noted that the accuracy of the negative sequence current depends on the accuracy of CTs or current sensors (Rogowski coils) used and that decides the lowest possible value of the negative sequence current that can be reliably measured.

When a fault occurs on a distribution feeder, the information on the fault conditions must be delivered to the control room where SCADA system or DMS processes the information to visualize the fault location to the operator or to generate an automatic FLIR (fault location, isolation and restoration) switching sequence. The proposed method requires some level of communication between secondary substations and the primary substation. However, as communication will be widespread in future distribution networks, the proposed method is worth considering.

In an ideal symmetrical network, the negative zero sequence measured at any point is zero under normal condition. However, in practice, there is some level of negative sequence current even under no fault condition, for example due to asymmetry of loads. Therefore, it is important to note that the proposed method is based on the change in the negative sequence current and not the negative sequence current alone.

Compared to the current injection method presented in Reference [14], the proposed method in this paper has a clear advantage as there is no need for any extra injecting device. In addition, the pulse injection method works only with compensated neutral networks where the injection device can be connected in parallel with the Petersen coil. For isolated neutral networks where there is no possibility for connecting the injection device, the pulse injection method cannot be used.

In case of a single-phase-to-ground fault, unlike the zero sequence current, the negative sequence current remains almost constant with negligible variations along the feeder as shown in Section 4. Moreover, in compensated networks, the difference in the zero sequence current level for points before and after the fault could be too low for finding suitable and reliable criteria for locating the fault. Therefore, there is a need to increase this difference level somehow. Reference [20] suggests to connect and control an additional resistor in parallel with the Petersen coil. However, that action may lead to more complexity when it comes to practical implementation. In addition, there is a risk that in case of a long feeder, the line to ground capacitances of that part of the feeder, which is located after the fault point, provide a considerable amount of zero sequence current so that the zero-sequence based method fails to operate. This highlights the advantage of using the negative sequence current over the zero sequence current in locating faults in distribution networks.

In summary, the main advantages the negative sequence current based method offers are:

- No voltage measurement is required;
- Applicable to both isolated and compensated distribution networks;
- No need for any additional injection device or resistance.

6. Conclusions

Earth fault location on MV distribution networks using the negative sequence currents in the manner proposed in this paper appears to be promising. The proposed method is applicable to both

compensated and isolated neutral networks. When using this method, only current measurements are required and not voltage measurements, which is an advantage. The theoretical reasoning to justify the proposed method was discussed in detail and simulation results obtained from different types of practical MV distribution networks confirmed the validity and performance of the method. Some further studies are still needed to address the aspects relating to practical implementation and for example the effects of decentralized compensation.

Author Contributions: Conceptualization, L.K.; Formal analysis, A.F.; Funding acquisition, K.K.; Investigation, A.F.; Project administration, K.K.; Software, A.F.; Supervision, K.K.; Writing—original draft, A.F.; Writing—review & editing, L.K. and K.K.

Funding: This work was supported by the European Regional Development Fund (ERDF) (Business Finland grant No. 4332/31/2014 and Council of Tampere Region grant No. A73094).

Conflicts of Interest: The authors declare no conflict of interest.

List of Notations

| | |
|-----------|--|
| X_{0S} | Zero sequence source reactance |
| X_{1S} | Positive sequence source reactance |
| X_{2S} | Negative sequence source reactance |
| X_{0T} | Zero sequence reactance of the main transformer |
| X_{1T} | Positive sequence reactance of the main transformer |
| X_{2T} | Negative sequence reactance of the main transformer |
| Z_{0GH} | Zero sequence impedance of the feeder between nodes G and H |
| Z_{1GH} | Positive sequence impedance of the feeder between nodes G and H |
| Z_{2GH} | Negative sequence impedance of the feeder between nodes G and H |
| X_{0TH} | Zero sequence reactance of transformer H |
| X_{1TH} | Positive sequence reactance of transformer H |
| X_{2TH} | Negative sequence reactance of transformer H |
| Z_{0LH} | Zero sequence impedance of load H |
| Z_{1LH} | Positive sequence impedance of load H |
| Z_{2LH} | Negative sequence impedance of load H |
| Z_{0HF} | Zero sequence impedance of the feeder between node H and the fault location |
| Z_{1HF} | Positive sequence impedance of the feeder between node H and the fault location |
| Z_{2HF} | Negative sequence impedance of the feeder between node H and the fault location |
| R_F | Fault resistance |
| Z_{0FJ} | Zero sequence impedance of the feeder between the fault location and node J |
| Z_{1FJ} | Positive sequence impedance of the feeder between the fault location and node J |
| Z_{2FJ} | Negative sequence impedance of the feeder between the fault location and node J |
| X_{0TJ} | Zero sequence reactance of transformer J |
| X_{1TJ} | Positive sequence reactance of transformer J |
| X_{2TJ} | Negative sequence reactance of transformer J |
| Z_{0LJ} | Zero sequence impedance of load J |
| Z_{1LJ} | Positive sequence impedance of load J |
| Z_{2LJ} | Negative sequence impedance of load J |
| Y_{0B} | Equivalent zero sequence admittance representing the phase to earth capacitances of the background network |
| Z_{1B} | Equivalent positive sequence impedance of the background network |
| Z_{2B} | Equivalent negative sequence impedance of the background network |
| Y_{0GH} | Zero sequence admittance representing phase to earth capacitances between nodes G and H |
| Y_{0HF} | Zero sequence admittance representing phase to earth capacitances between nodes H and the fault location |
| Y_{0FJ} | Zero sequence admittance representing phase to earth capacitances between the fault location and node J |

References

1. Farughian, A.; Kumpulainen, L.; Kauhaniemi, K. Review of methodologies for earth fault indication and location in compensated and unearthed MV distribution networks. *Electr. Power Syst. Res.* **2018**, *154*, 373–380. [[CrossRef](#)]
2. Novosel, D.; Hart, D.; Hu, Y.; Myllymaki, J. System for locating faults and estimating fault resistance in distribution networks with tapped loads. U.S. Patent No. 5,839,093, 17 November 1998.
3. Iurinic, L.U.; Herrera-Orozco, A.R.; Ferraz, R.G.; Bretas, A.S. Distribution Systems High-Impedance Fault Location: A Parameter Estimation Approach. *IEEE Trans. Power Deliv.* **2016**, *31*, 1806–1814. [[CrossRef](#)]
4. Altonen, J.; Wahlroos, A. Advancements in fundamental frequency impedance based earth fault location in unearthed distribution systems. In Proceedings of the CIRED 19th International Conference on Electricity Distribution, Vienna, Austria, 21–24 May 2007.
5. Kulkarni, S.; Santoso, S.; Short, T.A. Incipient Fault Location Algorithm for Underground Cables. *IEEE Trans. Smart Grid* **2014**, *5*, 1165–1174. [[CrossRef](#)]
6. Altonen, J.; Wahlroos, A.; Pirskanen, M. Advancement in earth-fault location in compensated MV-networks. In Proceedings of the CIRED 21st International Conference on Electricity Distribution, Frankfurt, Germany, 6–9 June 2011; p. 4.
7. Altonen, J.; Wahlroos, A. Novel algorithm for earth-fault location in compensated MV-networks. In Proceedings of the 22nd International Conference and Exhibition on Electricity Distribution (CIRED 2013), Stockholm, Sweden, 10–13 June 2013; pp. 1–4.
8. *IEEE Guide for Determining Fault Location on AC Transmission and Distribution Lines*; IEEE Std C37.114-2014 (Revision of IEEE Std C37.114-2004); IEEE: New York, NY, USA, 2015; pp. 1–76.
9. Elkalashy, N.I.; Sabiha, N.A.; Lehtonen, M. Earth Fault Distance Estimation Using Active Traveling Waves in Energized-Compensated MV Networks. *IEEE Trans. Power Deliv.* **2015**, *30*, 836–843. [[CrossRef](#)]
10. Sadeh, J.; Bakhshizadeh, E.; Kazemzadeh, R. A new fault location algorithm for radial distribution systems using modal analysis. *Int. J. Electr. Power Energy Syst.* **2013**, *45*, 271–278. [[CrossRef](#)]
11. Liang, R.; Fu, G.; Zhu, X.; Xue, X. Fault location based on single terminal travelling wave analysis in radial distribution network. *Int. J. Electr. Power Energy Syst.* **2015**, *66*, 160–165. [[CrossRef](#)]
12. Thomas, D.W.P.; Carvalho, R.J.O.; Pereira, E.T.; Christopoulos, C. Field trial of fault location on a distribution system using high frequency transients. In Proceedings of the 2005 IEEE Russia Power Tech, St. Petersburg, Russia, 27–30 June 2005; pp. 1–7.
13. Borghetti, A.; Bosetti, M.; Nucci, C.A.; Paolone, M.; Abur, A. Integrated Use of Time-Frequency Wavelet Decompositions for Fault Location in Distribution Networks: Theory and Experimental Validation. *IEEE Trans. Power Deliv.* **2010**, *25*, 3139–3146. [[CrossRef](#)]
14. Druml, G.; Raunig, C.; Schegner, P.; Fickert, L. Fast selective earth fault localization using the new fast pulse detection method. In Proceedings of the 22nd International Conference and Exhibition on Electricity Distribution (CIRED 2013), Stockholm, Sweden, 10–13 June 2013; pp. 1–5.
15. Teng, C.; Schmaranz, R.; Schoass, K.; Marketz, M.; Druml, G.; Fickert, L. Evaluation of new earth fault localization methods by earth fault experiments. In Proceedings of the 22nd International Conference and Exhibition on Electricity Distribution (CIRED 2013), Stockholm, Sweden, 10–13 June 2013; pp. 1–4.
16. Raunig, C.; Fickert, L.; Obkircher, C.; Achleitner, G. Mobile earth fault localization by tracing current injection. In Proceedings of the 2010 Electric Power Quality and Supply Reliability Conference, Kuressaare, Estonia, 16–18 June 2010; pp. 243–246.
17. Kumpulainen, L.; Pettisalo, S.; Sauna-aho, S. *A Secondary Substation Monitoring Based Method for Earth-Fault Indication in MV Cable Networks*; Aalto University: Espoo, Finland, 2011.
18. Lehtonen, M.; Siirto, O.; Abdel-Fattah, M.F. Simple fault path indication techniques for earth faults. In Proceedings of the 2014 Electric Power Quality and Supply Reliability Conference (PQ), Rakvere, Estonia, 11–13 June 2014; pp. 371–378.
19. Horák, M.; Vinklár, P.; Kordas, J.; Grossmann, J. Earth fault location in compensated MV network using a handheld measuring device. *J. Eng.* **2018**, *2018*, 1281–1285. [[CrossRef](#)]
20. Wang, P.; Chen, B.; Zhou, H.; Cuihua, T.; Sun, B. Fault Location in Resonant Grounded Network by Adaptive Control of Neutral-to-Earth Complex Impedance. *IEEE Trans. Power Deliv.* **2018**, *33*, 689–698. [[CrossRef](#)]

21. Lakervi, E.; Partanen, J. *Sähköjälketechniikka*; Otatieto: Helsinki, Finland, 2004; ISBN 978-951-672-359-7.
22. Blackburn, L.J. *Symmetrical Components for Power Systems Engineering*; Electrical and Computer Engineering; CRC Press: Boca Raton, FL, USA, 1993; ISBN 978-0-8247-8767-7.



© 2019 by the authors. Licensee MDPI, Basel, Switzerland. This article is an open access article distributed under the terms and conditions of the Creative Commons Attribution (CC BY) license (<http://creativecommons.org/licenses/by/4.0/>).



Article

Non-Directional Earth Fault Passage Indication in Isolated Neutral Distribution Networks

Amir Farughian *^{ORCID}, Lauri Kumpulainen^{ORCID} and Kimmo Kauhaniemi^{ORCID}

School of Technology and Innovations, University of Vaasa, 65200 Vaasa, Finland;

lauri.kumpulainen@uva.fi (L.K.); kimmo.kauhaniemi@uva.fi (K.K.)

* Correspondence: amir.farughian@uva.fi

Received: 14 August 2020; Accepted: 10 September 2020; Published: 11 September 2020



Abstract: In this paper, two new methods for locating single-phase to ground faults in isolated neutral distribution networks are proposed. The methods are based on the analysis of symmetrical sequence currents. They are solely based on currents, not requiring voltage measurement. The first method employs only the zero sequence current and the second one utilizes the negative sequence current in combination with the zero sequence current. It is revealed why using only zero sequence current with a simple threshold is insufficient and may lead to false results. Using the proposed methods, earth faults with high resistances can be located in isolated neutral distribution networks with overhead lines or cables.

Keywords: fault passage indication; fault location; symmetrical sequence currents

1. Introduction

Fault location has become an essential supplementary function for utilities as the importance of supply continuity and reliability is constantly increasing in modern distribution networks. With accurate and reliable fault location, faults can be isolated with a minimum number of switching operations. As a result, the duration of outages can be minimized. In general, faulty feeder identification and fault location in distribution networks could be performed at three levels:

- (1) Feeder identification: Only the faulty feeder is identified. This is usually an integral part of the feeder relay protection.
- (2) Fault Passage Indication (FPI): The faulted segment, e.g., lines or cables linking two secondary substations on the feeder, is identified. The purpose of FPI is to indicate whether the fault current has passed through the measurement point at which the FPI device is installed. By installing multiple FPI devices at various points (typically secondary substations) in the network, the faulted segment can be identified and visualized for the operator at the control center.
- (3) Distance estimation: The accurate fault location i.e., its distance from the beginning of the faulted feeder is estimated.

In [1], a method is proposed for identifying the faulted feeder in distribution networks. The method is applicable to isolated and compensated distribution networks. In this method, faulty feeder identification is realized by estimating the fault resistance using the approach proposed in the paper. To estimate the fault resistance, it is assumed that the phase-to-earth susceptance of each feeder prior to the occurrence of a fault is known to the system operator. However, due to the complexity of distribution networks, this assumption is not always valid in practice. In addition, the method appears to be suitable only for faulted feeder identification and is unable to locate the fault point on the faulty feeder. In [2], the faulted feeder identification is realized using the zero sequence admittance which requires measuring the zero sequence voltage U_0 and zero sequence current I_0 . The faulted feeder is

identified once the criteria that the method sets out for the zero sequence admittance or its components are met.

In [3], an impedance-based method is presented that falls into the third category i.e., the fault distance from the beginning of the faulted feeder is estimated. The method is developed by analyzing the equivalent sequence model of the distribution network using symmetrical components. In this method also, the assumption is that the capacitance of each feeder under no fault condition is known to the network operator. The effectiveness of the method, however, appears to be limited to fault resistances up to 500 ohms. In addition, a small inaccuracy in the estimated capacitance values of the feeders can result in a large error in the estimated fault distance.

In [4,5], the concept of cumulative phasor summation along with its application in earth fault protection, i.e., faulted feeder identification, is introduced. The same concept can also be applied for fault passage indication. In this concept the admittance at each measurement point is calculated using the cumulative phasors of zero sequence voltage and current. Thus, in addition to current measurement, the voltage measurement is required. The sign of the real part of the calculated admittance indicates whether the measuring point in question is on the fault passage or off the fault passage. In the field tests presented in [4,5], all the measuring points were located only at the primary substation and therefore the method was demonstrated only to identify the faulted feeder.

In [6], the same method is extended to various measurement points in a compensated network in order to enable FPI (level 2). If this method is intended to be used as FPI, three individual phase-to-phase voltage measurements are required at each measurement point in order to calculate the zero sequence voltage, which means extra costs.

In [7], a method is proposed for identifying the faulted feeder in isolated distribution networks. The proposed method attempts to achieve directional faulted feeder identification but without voltage measurement. The zero sequence voltage, which is usually used in directional methods as the reference, is replaced with phase currents in the manner proposed in the paper. However, the method appears to be unable to operate as FPI.

The methods presented in [8,9] are signal processing type of methods and fall into the first category. The initial transient features of the residual currents caused by the earth fault are analyzed using the wavelet transform to determine the faulted feeder. Both voltage and current measurements are required in these methods.

This paper presents two new methods, which fall into the second category, i.e., FPI. They are solely based on current measurements and no voltage input is required. The first method is based on the analysis of the zero sequence current along the faulted feeder and the second one is the improved version of the method introduced in [10]. It combines the zero and negative sequence currents to remedy the shortcomings of the original method. In Section 2, the behavior of zero and negative sequence currents during a fault condition are analyzed in depth in order to gain some insight into sequence currents during a fault. Based on the analysis, two FPI algorithms are formulated. The effectiveness of the proposed methods is investigated through simulations in Section 3. Some practical aspects regarding the implementation of the methods in practice are discussed in Section 4. Conclusions are drawn in Section 5.

2. Proposed Methods

2.1. Theory

An isolated neutral medium voltage (MV) distribution network is shown in Figure 1. It consists of a healthy feeder, the faulted feeder, and an equivalent circuit representing the rest of the healthy feeders which is shown as “Background network” in the figure. The dashed lines on the faulted feeder signify that it could consist of more than only the two secondary substations shown in the figure. Two secondary substations located at points E and G are shown. The choice of these substations is

arbitrary which means the following analysis is valid for any point on the feeder between any two consecutive secondary substations.

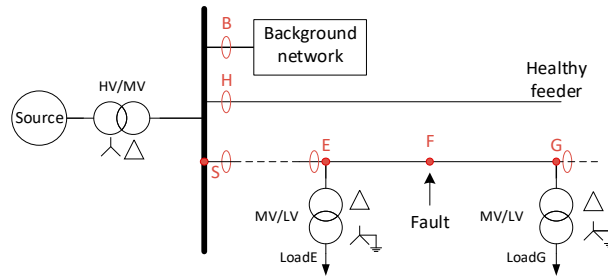


Figure 1. Distribution network with isolated neutral under earth fault condition.

The symmetrical sequence equivalent circuit of this network is shown in Figure 2. In the following, the analysis of the positive sequence current is neglected as this current is not used in the proposed methods. The reason is that in practice, the value and changes of the positive sequence current are dictated mainly by changes in the load. For this reason, only the negative and zero sequence circuits are shown in detail and the positive sequence circuit is simplified as a voltage source \bar{E}_1 in series with an impedance \bar{Z}_{1E} . In addition, the proposed methods and the following analysis are based on steady state currents during the fault and do not consider the transient phenomena. The list of notations is given in the Abbreviations Section.

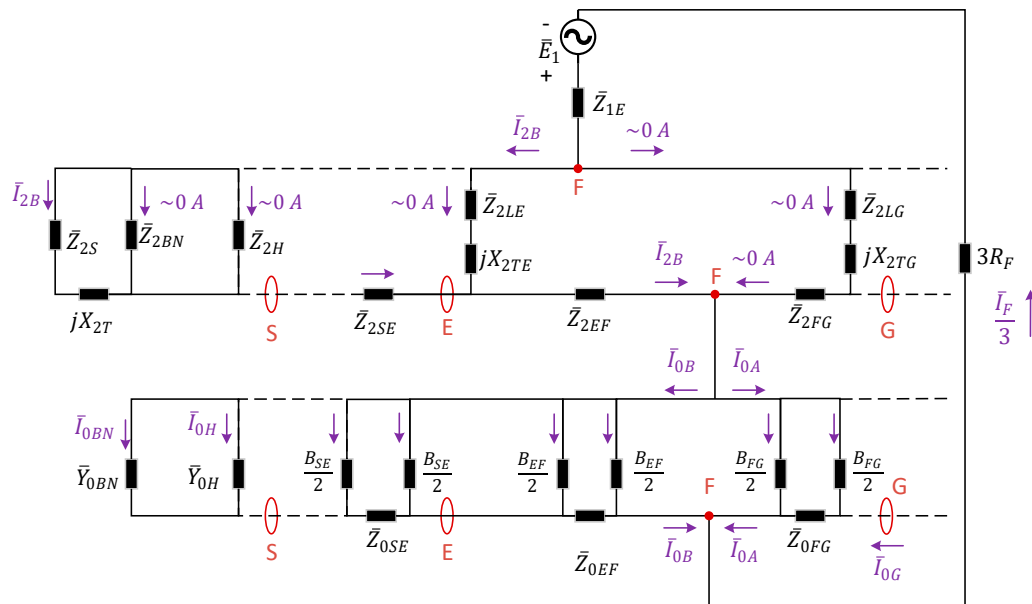


Figure 2. Symmetrical sequence equivalent circuit of the network shown in Figure 1.

The negative sequence circuit consists of series impedances representing the line negative sequence impedances and shunt branches representing the negative sequence impedances of the background network, the healthy feeder, and the loads. In practice, load impedances are typically much larger than the system impedances in such a way that their effect on the faulted phase current is insignificant. For this reason, it is common practice in fault studies to neglect load impedances for shunt faults [11]. When the values of the load impedances are assumed to be infinite, then the currents flowing through

them in the negative sequence circuit are zero. Therefore, the negative sequence current at points after the fault location is negligible. Similarly, the negative sequence currents flowing through the impedances of the background network and the healthy feeder are negligible in the negative sequence circuit. Almost all the negative sequence current flows through the system branch (\bar{Z}_{2S} in series with \bar{Z}_{2T}). As a result, the negative sequence current remains to a great extent constant from the beginning of the faulted feeder up to the fault point (from S to F). In addition, as can be seen from the figure, the negative sequence current at any point on the faulted feeder between S and F equals one third of the fault current.

$$\bar{I}_{2B} = \frac{\bar{I}_F}{3} \quad (1)$$

This feature is used in [12] to determine the fault current in order to estimate the fault distance (level 3). In contrast, the shunt reactances in the zero sequence circuit are not negligible as they represent the line to earth capacitances of the feeders. The zero sequence current increases from S to F so that just before the fault point, it reaches its maximum, since at that point it is the summation of all the currents flowing through all the shunt branches from S to F.

$$\bar{I}_{0BN} + \bar{I}_{0H} + \dots = \bar{I}_{0B} \quad (2)$$

In summary, the negative sequence current at the beginning of the faulty feeder is almost constant for points before the fault locations and one third of the fault current. This current is negligible for points located after the fault point. The zero sequence increases as we move towards the fault point and reaches its maximum just before the fault point. The zero and negative sequence currents (in magnitudes) on the faulted feeder are graphically shown in Figure 3.

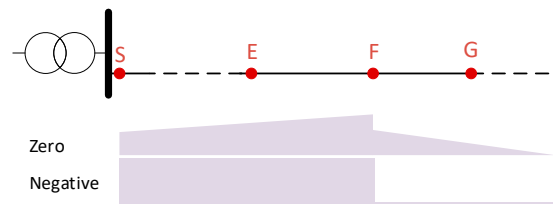


Figure 3. Behavior of zero and negative sequence currents on the faulted feeder in an isolated neutral network.

2.2. Method I

The first proposed fault location procedure is structured as follows:

- (1) The faulted feeder is indicated first by the operation of the feeder protection relay.
- (2) The zero sequence current for each measurement point (ideally at every secondary substation) on the faulted feeder is calculated and sent to a control center where all calculated zero sequence currents are collected.
- (3) For each measuring point, these values are scaled so that they are divided by the one from the beginning of the feeder. If the scaled value is greater than 1, it is concluded that the measuring point in question is on the fault passage. Otherwise, it is off the fault passage.
- (4) The faulty segment is determined as the segment linking the last secondary substation on the fault passage and the first secondary substation off the fault passage.

2.3. Method II

This method employs the concept introduced in [10]. It is based on the (change in the) negative sequence current in addition to monitoring the zero sequence current. In this method, the fault location procedure is performed locally.

- (1) The procedure at each measuring point is triggered once the magnitude of the zero sequence current exceeds a pre-set threshold.
- (2) The magnitude of the negative sequence current is calculated (ideally at every secondary substation).
- (3) If the calculated value exceeds a low pre-set threshold, a fault indication signal is issued to the control room.
- (4) The faulty segment is determined as the segment linking the last measurement point from which the fault indication signal is received and the first measurement point that sends no signal.

3. Simulation Results

The simulations were carried out with PSCADTM (Winnipeg, MB, Canada) by using a verified model of a Finnish distribution network. The simplified schematic diagram of the network is shown in Figure 4. It is a rural distribution network consisting of multiple feeders. The feeders are mixed i.e., they start from the primary substation as cables and end as overhead lines. Three different scenarios are simulated so that the earth fault occurs in one of the three different locations along the feeder J07. The measurements are taken from various points on the network including the beginning of feeders J07 and J06 at the primary substation and the four secondary substations along the studied feeder (J17, J27, J37, and J47). Fault resistances considered in this study range from 0.01 Ω to 3 k Ω .

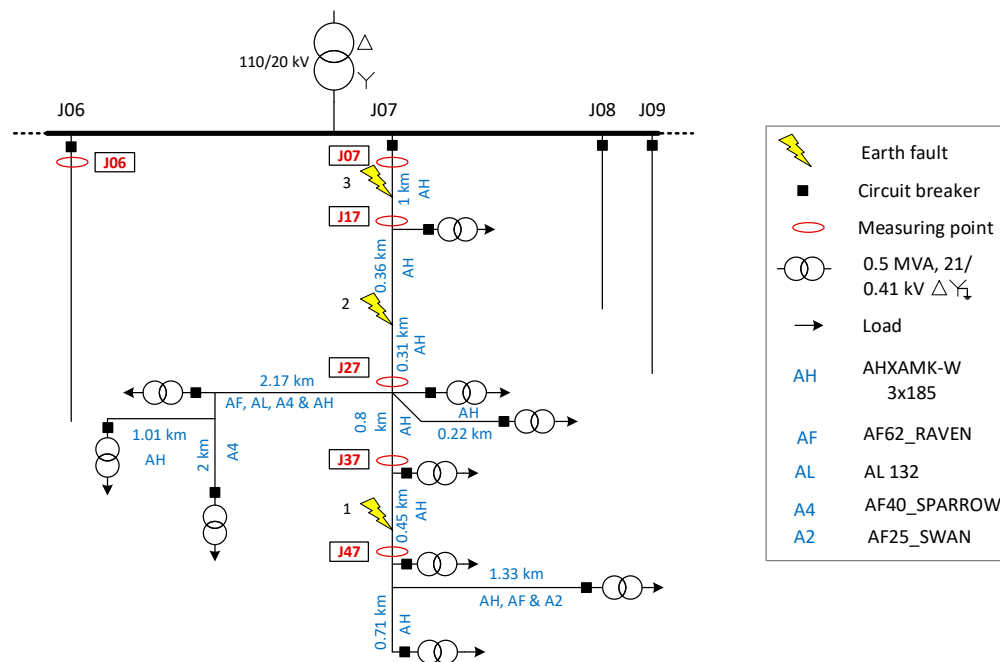


Figure 4. Medium voltage network with isolated neutral under three fault location scenarios with various measuring points along the feeder.

First, consider Fault 1 which occurs at $t = 2$ s on phase “a” at the section between measurement points J37 and J47 with the resistance of 1 k Ω . The phase voltages measured at the primary substation and currents measured at J07 and J06 are shown in Figure 5.

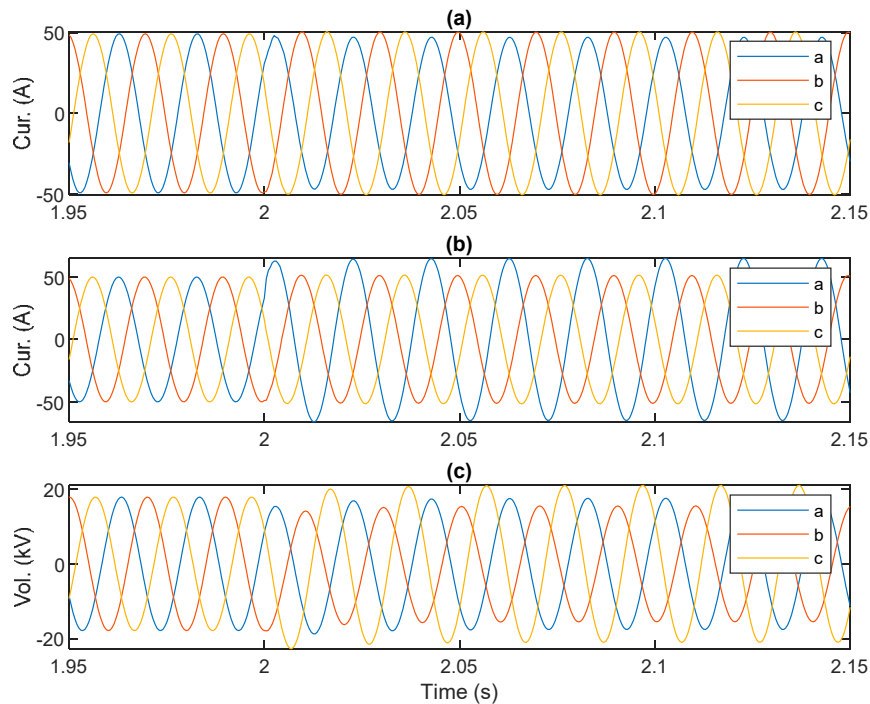


Figure 5. Simulated values during Fault 1, (a) phase currents at healthy feeder J06; (b) phase currents at faulted feeder J07; (c) phase to ground voltages at the primary substation.

Let us denote the phasors of phase currents by \bar{I}_a , \bar{I}_b , and \bar{I}_c . The corresponding sequence components can be obtained using the definition of symmetrical components [1] as follows:

$$\bar{I}_2^{(a)} = 1/3 (\bar{I}_a + a^2 \bar{I}_b + a \bar{I}_c) \quad (3)$$

$$\bar{I}_0^{(a)} = 1/3 (\bar{I}_a + \bar{I}_b + \bar{I}_c) \quad (4)$$

where, $\bar{I}_2^{(a)}$ and $\bar{I}_0^{(a)}$ are the phasors of the negative and zero sequence currents of phase “a”, respectively and the operator $a = 1 \angle 120^\circ$. Note that, by definition, the phasors of sequence currents calculated for all three phases are equal in magnitudes while there is only a 120-degree phase shift between them. As the proposed algorithms are based on magnitudes, the calculations can be made for any phase.

The calculated magnitudes of sequence currents using Equations (3) and (4) are shown in Figure 6 for J06 and J07. For simulations presented in this paper, the threshold is set to be 0.5 A. In Figure 6, the zero sequence current has exceeded the threshold both in healthy and faulted feeders, whereas the negative sequence current is negligible on the healthy feeder J06 and has exceeded the threshold only on the faulty feeder J07. This highlights the fact that the zero sequence current could be significant even on healthy feeders and therefore insufficient for fault passage indication purposes if used alone. In other words, exceeding a pre-set threshold by zero sequence currents is not necessarily indicative of being on the fault passage.

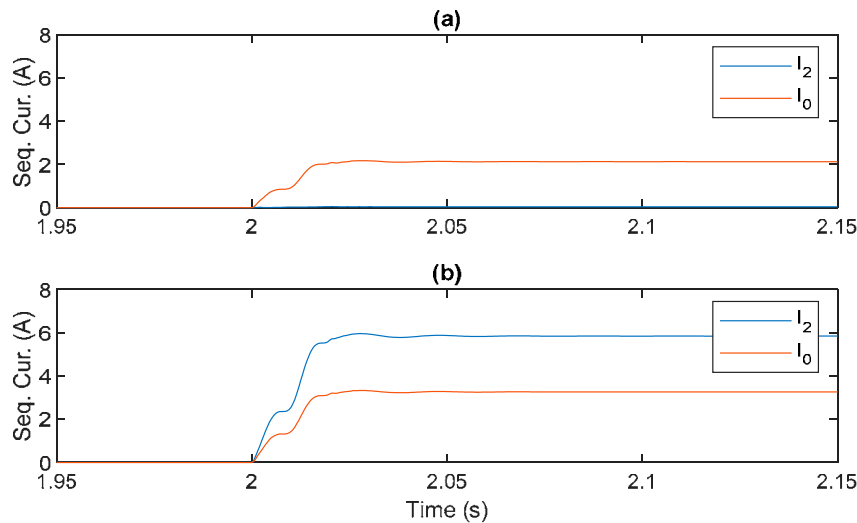


Figure 6. Zero and negative sequence currents at (a) healthy feeder J06; (b) faulted feeder J07.

In Table 1, the sequence currents as well as the scaled zero sequence currents are presented for various fault resistances. The presented values are taken at $t = 2.06$ s, i.e., three cycles after the fault occurrence, as at this point the calculated sequence currents seem to reach the steady state.

Table 1. Sequence currents at various point during earth fault 1.

| Points | On/off | $R_F = 0.01 \Omega$ | | | $R_F = 100 \Omega$ | | | $R_F = 3000 \Omega$ | | |
|--------|--------|---------------------|--------------|-----------|--------------------|--------------|-----------|---------------------|--------------|-----------|
| | | I_0 (A) | I_0/I_{0S} | I_2 (A) | I_0 (A) | I_0/I_{0S} | I_2 (A) | I_0 (A) | I_0/I_{0S} | I_2 (A) |
| J07 | on | 18.0 | 1.0 | 32.2 | 15.8 | 1.0 | 28.3 | 1.1 | 1.0 | 2.0 |
| J17 | on | 19.9 | 1.1 | 32.2 | 17.5 | 1.1 | 28.3 | 1.2 | 1.1 | 2.0 |
| J27 | on | 21.5 | 1.2 | 32.2 | 18.9 | 1.2 | 28.2 | 1.3 | 1.2 | 2.0 |
| J37 | on | 27.1 | 1.5 | 32.2 | 23.7 | 1.5 | 28.2 | 1.7 | 1.5 | 2.0 |
| J47 | off | 4.5 | 0.2 | 0.1 | 3.9 | 0.2 | 0.1 | 0.3 | 0.2 | 0.0 |

For all the points off the fault passage, the zero sequence current is below 5 A. Similarly, for all the points located on the fault passage, the zero sequence current is higher than 1 A. Therefore, one might think by setting a threshold for the zero sequence current, FPI can be realized. However, such an approach may lead to false results. For instance, the zero sequence current at J47 (which is located off the fault passage) with the fault resistance of 0.01Ω is higher than the zero sequence current at J37 (which is on the fault passage) when the fault resistance is $3 \text{ k}\Omega$ (green cells in Table 1). Therefore, setting the threshold of 5 A leads to false results. A similar argument can be made for the threshold of 1 A. It should be noted that no threshold can be found with which FPI can be realized. Therefore, the simple threshold method is insufficient to locate faults. However, using either one of the proposed algorithms, the points located on and off the fault passage are identified correctly. In Method I, the scaled zero sequence currents have values above 1 in all points on the fault passage. In Method II, a suitable threshold for negative sequence current can be easily selected in the cases shown.

To investigate the impact of the fault location, consider Faults 2 and 3. The sequence currents as well as scaled zero sequence currents are presented for various fault resistances in the following tables (Tables 2 and 3). Again, using either one of the proposed algorithms, the points on and off the fault passage can be identified successfully.

Table 2. Sequence currents at various point during earth fault 2.

| Points | On/off | $R_F = 0.01 \Omega$ | | | $R_F = 100 \Omega$ | | | $R_F = 3000 \Omega$ | | |
|--------|--------|---------------------|--------------|-----------|--------------------|--------------|-----------|---------------------|--------------|-----------|
| | | I_0 (A) | I_0/I_{0S} | I_2 (A) | I_0 (A) | I_0/I_{0S} | I_2 (A) | I_0 (A) | I_0/I_{0S} | I_2 (A) |
| J07 | on | 18.0 | 1.0 | 32.2 | 15.8 | 1.0 | 28.3 | 1.1 | 1.0 | 2.0 |
| J17 | on | 19.9 | 1.1 | 32.2 | 17.5 | 1.1 | 28.3 | 1.2 | 1.1 | 2.0 |
| J27 | off | 10.7 | 0.6 | 0.2 | 9.4 | 0.6 | 0.2 | 0.7 | 0.6 | 0.0 |
| J37 | off | 5.1 | 0.3 | 0.1 | 4.5 | 0.3 | 0.1 | 0.3 | 0.3 | 0.0 |
| J47 | off | 4.5 | 0.2 | 0.1 | 3.9 | 0.2 | 0.1 | 0.3 | 0.2 | 0.0 |

Table 3. Sequence currents at various point during earth fault 3.

| Points | On/off | $R_F = 0.01 \Omega$ | | | $R_F = 100 \Omega$ | | | $R_F = 3000 \Omega$ | | |
|--------|--------|---------------------|--------------|-----------|--------------------|--------------|-----------|---------------------|--------------|-----------|
| | | I_0 (A) | I_0/I_{0S} | I_2 (A) | I_0 (A) | I_0/I_{0S} | I_2 (A) | I_0 (A) | I_0/I_{0S} | I_2 (A) |
| J07 | on | 18.0 | 1.0 | 32.2 | 15.8 | 1.0 | 28.3 | 1.1 | 1.0 | 2.0 |
| J17 | off | 12.3 | 0.7 | 0.3 | 10.8 | 0.7 | 0.2 | 0.8 | 0.7 | 0.0 |
| J27 | off | 10.7 | 0.6 | 0.2 | 9.4 | 0.6 | 0.2 | 0.7 | 0.6 | 0.0 |
| J37 | off | 5.1 | 0.3 | 0.1 | 4.5 | 0.3 | 0.1 | 0.3 | 0.3 | 0.0 |
| J47 | off | 4.5 | 0.2 | 0.1 | 3.9 | 0.2 | 0.1 | 0.3 | 0.2 | 0.0 |

4. Discussion

As the proposed methods are based on FPIs, they are able to locate the fault between consecutive FPIs. The accuracy of the fault location thus depends on the density of the FPIs.

4.1. Limitations of the Proposed Methods

The first proposed method was developed only for isolated neutral networks. It is not applicable to compensated distribution networks as in these networks, unlike in isolated neutral networks, the zero sequence current decreases from the beginning of the feeder towards the fault point. This decrease is due to the compensation/Petersen coil. Therefore, the idea of scaling the zero sequence current at each measuring point would be pointless as for every point on the faulted feeder, the scaled zero sequence current would be less than 1 regardless of whether the point in question was off the fault passage or on it.

The other limitation that concerns both of the methods is sensitivity. For the network studied in this paper, the fault resistance of 3 k Ω caused the sequence currents for points located at the fault passage to be as low as 1 A which is still within the acceptable range. However, higher fault resistances would cause lower sequence currents that could be problematic to measure reliably in a real network.

4.2. Effect of Unbalanced Load

For simulations presented in this paper, the network under study was symmetrical. In practice, however, distribution networks are not perfectly symmetrical e.g., due to unbalanced load and therefore there is usually some level of negative sequence current detectable even when there has been no earth fault occurrence. Therefore, in the second proposed method, instead of using the negative sequence current, the “change” in the negative sequence current must be used.

Another concern regarding the second proposed method is that the rise in the negative sequence current could be caused by a sudden unbalanced change in the load and not necessarily by an earth fault. This is a situation where the zero sequence current, which acts as a trigger for both methods, comes into play. The zero sequence current is not affected by unbalanced load due to the type of winding of the secondary transformers on the medium voltage side i.e., delta winding. In other words, an unbalanced change in the load on the low voltage side does not cause zero sequence currents on the medium voltage side. Therefore, the performance of the second method is not affected.

5. Conclusions

Two methods were presented to identify the faulted segment following an earth fault occurrence in isolated neutral distribution networks. The proposed methods fall into the category of FPIs and require no voltage input, which helps to reduce costs when implementing the methods in practice. The first method was solely based on zero sequence currents and the second method combined the zero sequence current with the negative sequence current. The theory behind each proposed method was presented using symmetrical sequence component analysis. The methods were validated using simulations carried out on a verified network model with PSCADTM software. The FPI-based methods presented are non-directional as only the magnitudes of zero and negative sequence currents are required and not their phase angles. For the isolated neutral network studied in this paper, earth faults up to 3 k Ω can be located using either of the proposed methods.

Author Contributions: Conceptualization, L.K.; Formal analysis, A.F.; Funding acquisition, L.K. and K.K.; Investigation, A.F.; Project administration, L.K. and K.K.; Software, A.F.; Supervision, K.K.; Writing—original draft, A.F.; Writing—review and editing, L.K. and K.K. All authors have read and agreed to the published version of the manuscript.

Funding: This work was partly carried out in VINPOWER project which was supported by the European Regional Development Fund (ERDF), Project No. A73094.

Conflicts of Interest: The authors declare no conflict of interest.

Abbreviations

| | |
|-----------------|---|
| \bar{Z}_{1E} | Equivalent impedance of the positive sequence circuit of the network |
| \bar{Z}_{2S} | Negative sequence source impedance |
| X_{2T} | Negative sequence reactance of the main transformer |
| \bar{Z}_{2BN} | Equivalent negative sequence impedance of the background network |
| \bar{Z}_{2H} | Equivalent negative sequence impedance of the healthy feeder |
| \bar{Z}_{2SE} | Negative sequence impedance of the faulted feeder between S and E |
| \bar{Z}_{2LE} | Negative sequence impedance of load E |
| X_{2TE} | Negative sequence reactance of transformer E |
| \bar{Z}_{2EF} | Negative sequence impedance of the feeder between E and the fault location |
| \bar{Z}_{2FG} | Negative sequence impedance of the feeder between the fault location and G |
| \bar{Z}_{2LG} | Negative sequence impedance of load G |
| X_{2TG} | Negative sequence reactance of transformer G |
| \bar{Y}_{0BN} | Zero sequence admittance of phase to earth capacitances of the background network |
| \bar{Y}_{0H} | Zero sequence admittance of phase to earth capacitances of the healthy feeder |
| \bar{Z}_{0SE} | Zero sequence series impedance between S and E |
| B_{SE} | Zero sequence susceptance of phase to earth capacitances between nodes S and E |
| \bar{Z}_{0EF} | Zero sequence series impedance between E and F |
| B_{EF} | Zero sequence susceptance of phase to earth capacitances between nodes E and F |
| \bar{Z}_{0FG} | Zero sequence series impedance between F and G |
| B_{FG} | Zero sequence susceptance of phase to earth capacitances between F and G |

References

1. Nikander, A.; Järventausta, P. Identification of High-Impedance Earth Faults in Neutral Isolated or Compensated MV Networks. *IEEE Trans. Power Deliv.* **2017**, *32*, 1187–1195. [[CrossRef](#)]
2. Lorenc, J.; Marszalkiewicz, K.; Andruszkiewicz, J. Admittance criteria for earth fault detection in substation automation systems in Polish distribution power networks. In Proceedings of the 14th International Conference and Exhibition on Electricity Distribution. Part 1. Contributions, (IEE Conf. Publ. No. 438), Birmingham, UK, 2–5 June 1997; Volume 4, pp. 19/1–19/5.
3. Altonen, J.; Wahlroos, A. Advancements in fundamental frequency impedance based earth fault location in unearthened distribution systems. In Proceedings of the CIRED 19th International Conference on Electricity Distribution, Vienna, Austria, 21–24 May 2007.

4. Wahlroos, A.; Uggla, U.; Altonen, J.; Wall, D. Application of novel cumulative phasor sum measurement for earth-fault protection in compensated MV-networks. In Proceedings of the 22nd International Conference and Exhibition on Electricity Distribution (CIRED 2013), Stockholm, Sweden, 10–13 June 2013; p. 607.
5. Wahlroos, A.; Altonen, J. Application of novel multi-frequency neutral admittance method into earth-fault protection in compensated MV-networks. In Proceedings of the 12th IET International Conference on Developments in Power System Protection (DPSP 2014), Copenhagen, Denmark, 31 March–3 April 2014; pp. 1–6.
6. Altonen, J.; Wahlroos, A.; Vähäkuopus, S.; Oy, E. Application of multi-frequency admittance-based fault passage indication in practical compensated MV-network. *CIRED* **2017**, *2017*, 947–951. [[CrossRef](#)]
7. Stojanović, Z.N.; Djurić, M.B. An algorithm for directional earth-fault relay with no voltage inputs. *Electr. Power Syst. Res.* **2013**, *96*, 144–149. [[CrossRef](#)]
8. Elkalashy, N.I.; Tarhuni, N.G.; Lehtonen, M. Simplified probabilistic selectivity technique for earth fault detection in unearthed MV networks. *IET Transm. Distrib. Gener.* **2009**, *3*, 145–153. [[CrossRef](#)]
9. Elkalashy, N.I.; Lehtonen, M.; Darwish, H.A.; Taalab, A.-M.I.; Izzularab, M.A. Operation evaluation of DWT-based earth fault detection in unearthed MV networks. In Proceedings of the 12th International Middle-East Power System Conference, Aswan, Egypt, 12–15 March 2008; pp. 208–212.
10. Farughian, A.; Kumpulainen, L.; Kauhaniemi, K. Earth Fault Location Using Negative Sequence Currents. *Energies* **2019**, *12*, 3759. [[CrossRef](#)]
11. Blackburn, L.J. *Symmetrical Components for Power Systems Engineering*; CRC Press: Boca Raton, FL, USA, 1993; ISBN 978-0-8247-8767-7.
12. Wahlroos, A.; Altonen, J.; Pitkänen, R.; Kauppinen, S. Improving personal safety in MV-networks through novel earth-fault current based feeder protection. In Proceedings of the 25th International Conference on Electricity Distribution (CIRED 2019), Madrid, Spain, 3–6 June 2019; p. 5.



© 2020 by the authors. Licensee MDPI, Basel, Switzerland. This article is an open access article distributed under the terms and conditions of the Creative Commons Attribution (CC BY) license (<http://creativecommons.org/licenses/by/4.0/>).

Received March 2, 2021, accepted March 13, 2021, date of publication March 19, 2021, date of current version March 29, 2021.

Digital Object Identifier 10.1109/ACCESS.2021.3067497

Intermittent Earth Fault Passage Indication in Compensated Distribution Networks

AMIR FARUGHIAN¹, LAURI KUMPULAINEN¹, (Senior Member, IEEE),
KIMMO KAUHANIEMI¹, AND PETRI HOVILA², (Member, IEEE)

¹School of Technology and Innovations, University of Vaasa, 65101 Vaasa, Finland

²ABB Oy, 65320 Vaasa, Finland

Corresponding author: Amir Farughian (amir.farughian@uva.fi)

This work was supported by the VINPOWER Project through the European Regional Development Fund (ERDF) under Project A73094.

ABSTRACT An intermittent or restriking earth fault is a special type of earth fault that is common mostly in compensated cable networks. A great deal of effort has gone into protection against this type of fault. However, locating this fault has not received much attention. Therefore, there is a need to have a reliable method for locating this fault to repair the damaged cable. In this paper, the principles of a new method developed for locating transient intermittent earth faults on distribution networks are presented. The proposed method employs negative and zero sequence currents, and no voltage measurement is required, which means the proposed method has the potential to reduce cost when implemented in practice. It is intended mainly for typical intermittent earth faults in cable distribution networks where the typical fault resistance is in the range of a few ohms. Real data obtained from practical field tests is used to explain the phenomenon. A series of disturbance recordings obtained from field tests validate the proposed method.

INDEX TERMS Fault passage indication, intermittent earth fault, symmetrical sequence currents.

I. INTRODUCTION

Uninterruptable power supply is essential in today's networks. Distribution system operators (DSOs) always try to improve their System Average Interruption Duration Index (SAIDI) using various solutions. Overhead lines are prone to faults and disruptions, especially because of storms, lightning, etc. As a result, in many countries, DSOs have started to replace overhead lines massively with underground cables in urban and rural areas [1]–[3]. Despite the benefits this transition from overhead lines to cables provides, it brings about a new challenge to fault management systems, i.e., a special type of earth fault called an intermittent or restriking earth fault. These types of faults occur mainly in compensated cable networks. An intermittent or restriking earth fault is a special type of earth fault. It can be characterized as a series of cable insulation breakdowns in which a sudden electric discharge to the ground occurs. This type of fault is repetitive, and it ignites and self-extinguishes in irregular time intervals, which causes short current spikes. Because of these irregular current waveforms, conventional directional protection relays may fail to operate correctly.

The associate editor coordinating the review of this manuscript and approving it for publication was Amedeo Andreotti¹.

The cause of intermittent earth faults on cables is the deterioration of the cable insulation layer. Many reasons can cause insulation deteriorations. For instance, it could be from the penetration of impurities and moisture because of chemical reactions caused by insulation material aging or impurities originating from the cable manufacturing process, etc. [4].

Intermittent earth faults will eventually develop into permanent faults, where the fault current flows continuously if they are left to ignite for long enough. Most earth faults on cabled and compensated medium voltage (MV) distribution networks are intermittent ones [1], [5]. Almost all earth faults in compensated cable networks start as intermittent faults and then instantly or gradually evolve into short circuits or cross country faults [1]. Therefore, they are perhaps the most important type of fault to locate. In general, fault location and detection can be classified into three categories:

1) Feeder identification: Only the faulted feeder is determined; this function is normally an integral part of feeder protection implemented into modern protection relays.

2) Fault Passage Indication (FPI): The faulted segment, i.e., the faulted cable segment connecting two consecutive secondary substations, is pinpointed. The function of FPI is to issue an indication signal when a fault current passes the location at which the FPI device is mounted. If enough FPI

devices are used in the network, any faulted segment can be identified.

3) Distance estimation: The exact fault location, i.e., the fault distance from the primary substation, is estimated.

For permanent (continuous) single-phase to ground faults, several fault location methods are proposed or already in use that fall into the second or third categories defined above. These methods include injection-based methods [6], [7], traveling wave-based methods [8], [9], impedance-based methods [10], [11]. A comprehensive review of permanent earth fault location methods in distribution networks is presented in [12]. However, when it comes to intermittent fault location, it appears that the majority of the efforts are focused only on faulted feeder identification, which is necessary to have properly functioning feeder protection. Therefore, there is a need for a cost-effective method that gives more accurate information on the fault location than only identifying the faulted feeder.

In this paper, the principles of a new FPI method to identify the faulted segment in compensated distribution networks are presented. The proposed method utilizes the concept introduced in [13], which is targeted for locating permanent earth faults but adapts it for intermittent earth faults.

In Section II, we discuss the intermittent earth fault phenomenon, its characteristics, and why it is problematic for conventional relays using disturbance recordings obtained from field tests. The state-of-the-art methods proposed in the literature to remedy the shortcomings of conventional relays are reviewed. The principles of operation of the proposed new method are presented in Section III. The effectiveness of the method is validated through the simulations in Section IV, and recordings obtained from field tests in Section V. Some implementation aspects of the method are discussed in Section VI. Conclusions are drawn in Section VII.

II. PROBLEM FORMULATION

Compensated networks with underground cables are prone to intermittent earth faults. Intermittent earth faults are usually caused by damage to the insulation of a cable. The damaged spot on the cable has a reduced insulation level so that when the faulted phase voltage rises, a sudden discharge of current occurs through that damaged spot. This is due to the discharge current of faulty phase capacitances and the charge current of the capacitances of healthy phases. These sudden charge and discharge currents cause spikes in phase currents in faulted and healthy feeders. If the faulted phase is not in direct contact with the ground, the fault is likely to self-extinguish in compensated networks as the fault current is low in these types of networks. However, as the damaged spot has a lower insulation level, discharges occur again every time the voltage of the faulty phase reaches a high enough value. This pattern repeats again and again and the result is what is known as an intermittent earth fault [14].

Fig. 1 shows the data from a disturbance recording obtained from a field test on a compensated distribution network in the event of an intermittent fault. For the purpose

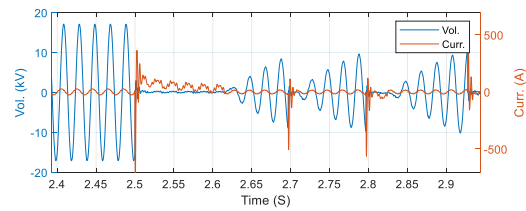


FIGURE 1. The faulty phase current and voltage were obtained from the field test recording, courtesy of Emtele Oy.

of comparison, the faulted phase voltage and current are shown in the same figure. The measurements are made at the beginning of the faulted feeder with 10 kHz sampling rates. The fault is initiated when the phase voltage exceeds a certain value at the point where the insulation level is reduced. The fault extinguishes itself in one of the first zero crossings of the transient fault current. After the fault has been extinguished, the faulty phase's phase-to-earth voltage starts to recover, but not immediately.

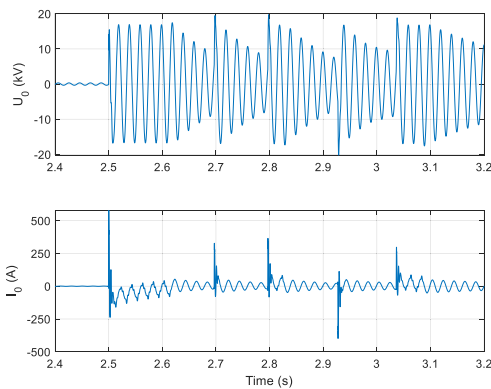
The behavior of the zero-sequence current I_0 measured at the beginning of the faulty feeder, along with the zero-sequence voltage U_0 (the residual voltage measured across the Petersen coil), is shown in Fig. 2. Similarly, the zero-sequence current extinguishes rapidly, whereas the zero-sequence voltage attenuates slowly, as can be seen from the figure.

Conventional earth fault protection is fundamentally aimed at detecting permanent faults [15]. The essential difference between permanent earth faults and intermittent earth faults is in the waveforms of residual voltages and currents. Permanent faults have almost a fundamental frequency in measured quantities, and the residual current and residual voltage waveforms are sinusoidal. In the case of an intermittent earth fault, the problem is that because of irregular waveforms of the residual current, conventional directional earth fault protection relays (DE/F) often fail to detect this type of earth fault. Because of the more stabilized waveform of U_0 , residual overvoltage relays (RO/V relays) are more likely to detect the fault condition. As a result, intermittent earth faults could cause non-selective tripping of the substation's back-up protection. This situation eventually leads to an outage with substantial costs to a wide area.

Several methods have been put forward to overcome the problem of conventional relays [16]–[22]. The patented method presented in [16] requires the Petersen coil voltage (neutral to ground voltage) and zero sequence current of each feeder. The first-order derivative of the measured voltage is calculated. This derivative is correlated to each of the feeder zero sequence currents. The feeder with the highest correlation is determined to be the faulted feeder. It is, however, unclear how this method differentiates intermittent types of faults from regular earth faults. It appears that the intermittent characteristics of phase currents are not specifically considered in this method. In [17] and [18], another patented method for identifying the direction of intermittent earth faults

TABLE 1. State-of-the-art methods for protection against intermittent faults.

| Method | Requirements | Principles | Advantages | Disadvantages |
|-----------|---|---|---|---|
| Ref. [16] | Neutral voltage measurement and zero-sequence current | Correlation between $\frac{dU_0}{dt}$ and I_0 | ZSC sufficient as opposed to three phase currents | Oscillatory characteristics of intermittent faults not well addressed, and voltage measurement required |
| Ref. [17] | Voltage measurement and zero sequence current | Instantaneous powers P and Q and counting current spikes | ZSC sufficient as opposed to three phase currents | Voltage measurement at every measurement point required for FPI applications |
| Ref. [19] | Two phase currents and zero-sequence current | Comparison of phase current magnitudes and directions | No need for voltage measurement | The assumption on the ratio of NSC to ZSC not always valid |
| Ref. [20] | Zero-sequence voltages and currents | $\frac{\Delta I_0}{\Delta U_0}$ | ZSC sufficient as opposed to three phase currents | Voltage measurement at every measurement point required for FPI applications |
| Ref. [21] | Zero-sequence voltages and currents | $\frac{\sum I_0}{\sum U_0}$ | Oscillatory characteristics of intermittent faults well addressed | Voltage measurement at every measurement point required for FPI applications |
| Ref. [24] | The voltage on the LV side with time synchronization | Correlation between voltages on LV side and currents on MV side | Utilizing voltage measurements normally available in the LV side of the network | Difficulty with practical implementation as accurate time synchronization required |

FIGURE 2. The field test recording of U_0 and I_0 was obtained from a faulted feeder in the case of an intermittent fault, courtesy of Emtele Oy.

is presented. It is based on measuring the residual current and voltage and then calculating the instantaneous active and reactive powers using Hilbert's transform. The method also keeps a count of current spikes to identify the event type, i.e., intermittent faults or transient events and noises. Another patented method is presented in [19]. The method requires two-phase currents and the ZSC (zero-sequence current). It is partly based on the assumption that the ratio of the magnitude of the NSC (negative sequence current) to the magnitude of the ZSC is high on the faulty feeder and low on healthy feeders. However, this assumption is not always valid. On the faulted feeder, both zero and negative sequence currents could be high in such a way that their ratio is not necessarily high. In [20], a method is proposed based on calculating the zero sequence admittance for each feeder using a centralized residual voltage (measured across the Petersen coil) and zero sequence currents. The direction of the fault on a specific feeder is determined based on the sign of the real part of the calculated zero-sequence admittance

so that a negative admittance means reverse (faulty) and a positive value indicates forward (healthy). In [21], a concept of cumulative phasor summing introduced in [22] is used to improve the zero sequence admittance method and remedy the shortcoming of the method presented in [20]. Ref. [23] reports on the results of experimenting with this method as FPI on a compensated distribution network.

The presented methods ([16]–[22]) deal with faulted feeder identification (in the event of intermittent earth faults) and not FPI. On the other hand, these methods (except for [19]) require voltage measurement. Therefore, even if these methods are used as FPIs, voltage measurement will be required at every point where the FPI device is installed, leading to extra cost. The method proposed in [24] attempts to avoid these costs by using the voltage measurements ordinarily available on the low-voltage side of distribution transformers. The drawback is the difficulties with practical implementation as the measurements need to be accurately time-synchronized. Therefore, what is missing is a reliable FPI method, which offers the potential to reduce the cost of implementation by eliminating the need for voltage measurement. The main characteristics of the reviewed methods are summarized in Table 1 to facilitate comparison.

III. PROPOSED METHOD

The proposed method combines the ZSC with the NSC to locate the intermittent earth fault. The trigger of the process at each measurement point is the rise in the magnitude of ZSC. The proposed method falls into the category of fault passage indication, i.e., the fault indication is performed locally. Therefore, there is no need for synchronization of the measurements from various locations.

In [13], a method based on the steady-state value of the negative sequence current at the fundamental frequency is proposed for locating permanent earth faults. It is based on a theoretical analysis of symmetrical sequence components, which shows that the negative sequence current at healthy

feeders is insignificant. In contrast, it is significant on the faulty feeder from the beginning of the feeder up to the fault point. After the fault point, it is again negligible. In addition, the paper argues that sequence currents of measurement points located on the healthy feeder and points after the fault location behave similarly. They are both considered to be located off the fault passage.

The measured currents in a compensated network during an earth fault contain the following components [25]:

- fundamental frequency components of the fault and load currents as well as their harmonics
- charging and discharging transient components
- decaying DC-transient component originating from the Petersen coil circuit
- interline compensating transient component

Transients caused by charging the line to ground capacitances of the healthy feeders and discharging the line to ground capacitances of the faulty feeder occur simultaneously but with different durations. For a compensated network with full compensation, the fault location's fundamental frequency fault current is completely compensated [26]. The frequency of the transients is typically in the range of 100 to 800 Hz, and their amplitudes could be much larger than the fundamental frequency component, although decaying rapidly [25]. An intermittent earth fault can be described as a series of self-extinguishing faults. The time interval between two consecutive fault re-occurrences is typically in the range of few tens of milliseconds. Intermittent earth faults have typically broad frequency content [23]. This broad frequency content, or in other words harmonics, originates from the oscillatory nature of these types of faults.

The method presented in [13] is largely based on utilizing the negative sequence current's fundamental frequency, primarily developed for permanent faults. If it is used in its original form for intermittent earth fault location purposes, there will be a risk that the FPI device installed on the fault passage misses the fault. The method presented in [13] and, in general, methods based on fundamental frequency quantities may fail to operate correctly when the measured quantities have significant transient characteristics or harmonics. Earth faults of the intermittent type normally have significant transient characteristics and harmonics and therefore problematic for fundamental frequency-based methods. Therefore, there is a need for a method that overcomes the challenges caused by transients and harmonics of intermittent earth faults. The newly proposed method utilizes a wider range of frequencies to address the oscillatory characteristics of intermittent faults. It employs harmonics of NSC in addition to its fundamental frequency. This way, the harmonic content in the measured currents work in favor of the FPI functionality.

A. THEORY

By definition [27], the phasor of the NSC of phase "a" $\bar{I}_2^{(a)}$ is obtained using the following equation:

$$\bar{I}_2^{(a)} = \frac{1}{3}(\bar{I}_a + a^2\bar{I}_b + a\bar{I}_c) \quad (1)$$

where, \bar{I}_a , \bar{I}_b and \bar{I}_c are the phasors of the phase currents of phases a, b, and c, respectively, and the operator $a = 1 \angle 120^\circ$. By definition, the phasors of the negative sequence currents calculated for each phase are equal in magnitudes. Only they are 120-degree phase shifted. The following relations are valid between the phasors and their magnitudes.

$$\begin{aligned} \bar{I}_2^{(b)} &= a\bar{I}_2^{(a)} \\ \bar{I}_2^{(c)} &= a^2\bar{I}_2^{(a)} \\ I_2^{(a)} &= I_2^{(b)} = I_2^{(c)} \end{aligned} \quad (2)$$

where $\bar{I}_2^{(b)}$ and $\bar{I}_2^{(c)}$ are the NSC phasors of phases b and c, respectively and $I_2^{(a)}$, $I_2^{(b)}$ and $I_2^{(c)}$ are the magnitudes of the phasors. As the proposed method is based on the magnitude of the phasor of the NSC and not the phasor itself, there is no need to know the faulted phase when implementing the method. The idea of phasor summation is introduced to adapt (1) for intermittent earth faults, i.e., harmonic components of the NSC are added to the fundamental frequency expressed in the following equation. This adaptation is based on the discussion presented earlier.

$$I_{2i} = \left| \sum_{n=1}^m \bar{I}_{2i}^n \right| \quad (3)$$

where \bar{I}_{2i}^n is the phasor of the NSC at the n^{th} harmonic at measurement point i .

The calculation process is triggered at each measurement point once a rise (greater than a pre-defined value) in the ZSC is detected. The ZSC phasor for any phase is obtained as follows:

$$\bar{I}_0 = \frac{1}{3}(\bar{I}_a + \bar{I}_b + \bar{I}_c) \quad (4)$$

$$I_0 = |\bar{I}_0| \quad (5)$$

B. FAULT LOCATION PROCEDURE

Installing more FPI devices provides more visibility to the network. Every secondary substation must be equipped with an FPI device to achieve full visibility to every segment connecting two consecutive secondary substations. The faulted segment can be pinpointed as follows.

- 1- The procedure at measurement points is triggered once the magnitude of the ZSC is above a certain value.
- 2- The phase currents at measurement points (ideally at all of the secondary substations) are measured, and the magnitudes of the negative sequence currents using (3) are calculated.
- 3- The magnitude of the NSC over a certain period is calculated. If the calculated value rises above a pre-determined value, a fault indication signal is issued to the system operator.
- 4- The faulted section is determined as the one between the last measurement point from which the fault indication signal is received and the first measurement point from which no signal is received.

As the magnitude of the NSC is negligible on healthy feeders, choosing a threshold is relatively straightforward. For the simulated and field tests results presented in this paper, the threshold for the zero and negative sequence currents is chosen to be 5.5 A. This choice has been made based on studying the values obtained from field tests measurements. The parameter m in (3) is chosen to be 3.

The proposed method is based on monitoring the NSC and especially the peak magnitude of it. The maximum value of NSC is detected. Every time the fault condition is met, i.e., NSC exceeds the thresholds, a peak occurrence is detected. The number of peaks over a certain period is counted, and the fault indication signal is issued based on that. The choice of the certain period is concerned with the method's sensitivity. The user can set it according to the desired sensitivity. The reason for counting peaks and issuing the fault signal based on multiple peaks and not only one is to avoid having fault indication signals when other types of events are temporarily causing spikes in the phase currents. Similarly, setting the number of peaks is a sensitivity issue. It is up to the network operator to set the desired number of peaks when utilizing the method.

The threshold for I_2 , i.e., 5.5 A, has been obtained experimentally through studying a series of simulations and the field tests results. Like overcurrent and earth-fault protection settings, no universal value for the threshold can be given. The reason is that the NSC depends on the network's symmetry, length of the feeders, the line types, the transformers impedances, etc. However, as the NSC of healthy feeders and points off the fault passage is significantly lower than the NSC of the faulted feeder and points off the fault passage, it is possible to set a proper threshold with which points on and off the fault passage can be differentiated. The development of tools for finding practical threshold settings is beyond the scope of this paper.

IV. SIMULATION RESULTS

The effectiveness of the proposed method is investigated using simulations carried out in the PSCAD/EMTDC environment. The network shown in Fig. 3 is a compensated cable MV distribution network consisting of multiple feeders with a faulted feeder and a healthy feeder shown in the figure. A 110 kV high voltage network supplies a 20 kV medium-voltage network through a 40 MVA transformer. The feeder under study is 5.4 km long, consisting of AHXAMK-W underground cables, and has five secondary substations. Three faults at three locations are examined. The first intermittent earth fault occurs at 3 km from the HV/MV transformer on phase "a". The intermittent fault is simulated so that whenever the voltage exceeds a certain level, the cable's insulation level at the fault spot breaks down and the fault current starts to flow. The fault current flow stops as soon as it reaches a zero crossing. The insulation breakdown is modeled by a specific logic controlling the regular fault block in PSCAD. Some degraded insulation level is given to start. This insulation level is then compared with the instantaneous

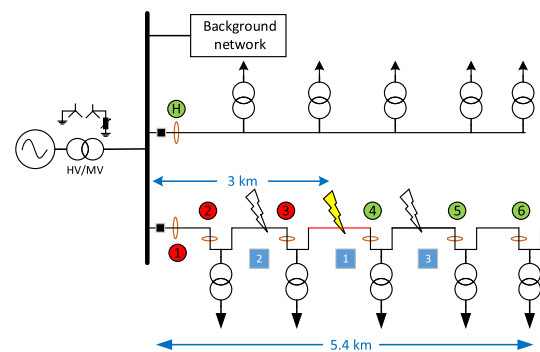


FIGURE 3. Intermittent earth fault on a compensated MV distribution network consisting of multiple underground cable feeders under three fault condition scenarios.

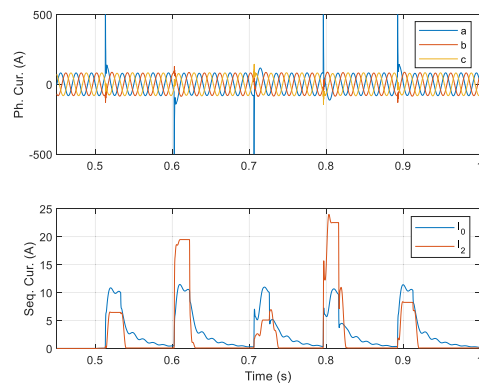


FIGURE 4. Phase currents and corresponding sequence currents under an intermittent earth fault condition, before fault point (Point 3), on fault passage.

phase to ground voltage measured at the fault location. If the voltage is above the insulation level, the fault block is turned on, resulting in a phase-to-ground fault. The fault current, which starts with large transients, is monitored and as soon as there is the first zero crossing of the current, the fault block is turned off, stopping the fault current. The description of the simulation parameters is given in Appendix.

Phase currents and sequence currents (magnitudes) using (3) and (5) are shown in Fig. 4 and Fig. 5 for points 3 and 4, respectively. For Point 3, which is located behind the fault point, both sequence currents exceeded the thresholds, and hence the proposed method correctly identifies this point to be on the fault passage.

On the contrary, for Point 4, which is located after the fault point, only the zero-sequence current is significant (around 4 A). Therefore, the proposed method correctly identifies this point to be off the fault passage.

The calculated zero and negative sequence currents (magnitudes) at various measurement points for faults 1, 2 and 3 are presented in Table 2. The measurements are taken from five points on the faulted feeder and the adjacent healthy

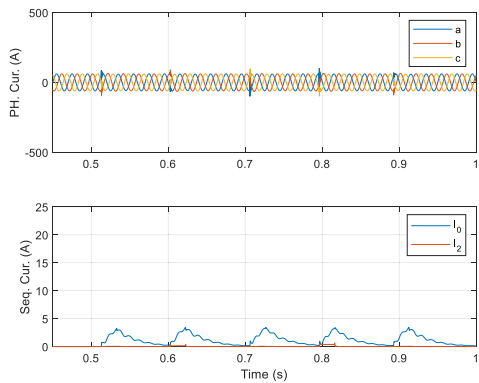


FIGURE 5. Phase currents and corresponding sequence currents under an intermittent earth fault condition, after fault point (Point 4), off fault passage.

TABLE 2. Sequence currents at various measurement points for three faults at three locations.

| Points | Fault | On/off | I_0 (A) | I_2 (A) |
|--------|-------|--------|-----------|-----------|
| 1 | 1 | on | 8.4 | 24.3 |
| 2 | 1 | on | 10.4 | 24.2 |
| 3 | 1 | on | 10.7 | 24.1 |
| 4 | 1 | off | 3.4 | 0.6 |
| 5 | 1 | off | 1.7 | 0.4 |
| H | 1 | off | 7.1 | 0.7 |
| 1 | 2 | on | 8.7 | 17.5 |
| 2 | 2 | on | 10.5 | 17.4 |
| 3 | 2 | off | 5.3 | 0.7 |
| 4 | 2 | off | 3.6 | 0.4 |
| 5 | 2 | off | 1.8 | 0.3 |
| H | 2 | off | 7.2 | 0.7 |
| 1 | 3 | on | 8.1 | 24.4 |
| 2 | 3 | on | 10.5 | 24.4 |
| 3 | 3 | on | 10.9 | 24.3 |
| 4 | 3 | on | 11.4 | 24.2 |
| 5 | 3 | off | 1.7 | 0.4 |
| H | 3 | off | 7.2 | 0.7 |

feeder’s beginning. The values presented in the table are the maximum values of the calculated zero and negative sequence currents in the period between $t = 0.45\text{ s}$ and $t = 0.9\text{ s}$. Each measuring point is identified correctly to be on or off the fault passage using the proposed method. Subsequently, the faulted segments can be identified successfully.

To highlight the advantage that utilizing harmonics provides, the new proposed method is contrasted with the method presented in [13], by way of example. Consider Fault 2 when the fault resistance increases to 150 ohms. The phase currents and corresponding negative sequence currents for Point 2, which is located on the fault passage, are plotted in Fig. 6. The method presented in [13] is largely based on using the fundamental frequency of the NSC. In the figure, the NSC

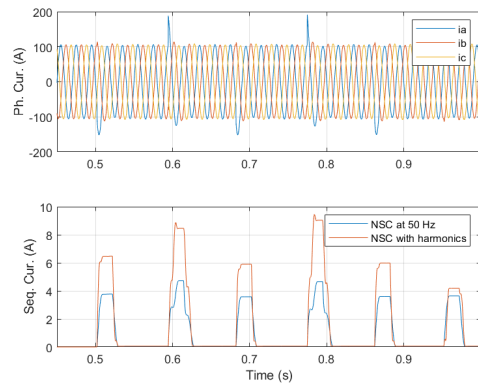


FIGURE 6. The proposed method utilizes harmonics and fundamental frequency components versus the method presented in [13].

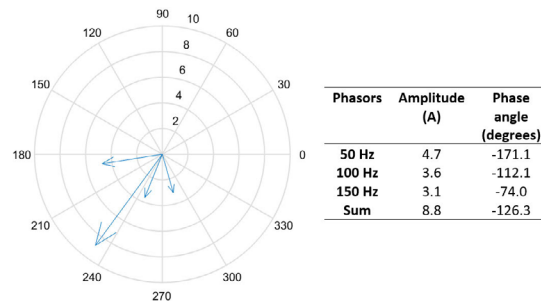


FIGURE 7. Phasors of NSC at the fundamental frequency and its harmonics.

is calculated once only based on the fundamental frequency component excluding harmonics (method [13]) and once including harmonics (the newly proposed method).

The NSC at 50 Hz is below the pre-set threshold and therefore, the method [13] incorrectly identifies Point 2 to be located off the fault passage. The phasor diagrams of the fundamental frequency, second and third harmonics along with their summation for the second spike which occurs at $t = 0.6\text{ s}$ are illustrated in Fig. 7.

V. FIELD TEST VERIFICATION

The proposed method has been examined using a series of disturbance recordings obtained from field tests carried out by DSOs in cooperation with network automation system providers in Finland. In this section, the results of two sets of recordings obtained from field tests are presented. The simplified diagram of the network on which the tests were performed is shown in Fig. 8.

The network consisted of several feeders and a 110/20kV primary substation. The feeders consisted of cables and overhead lines, so that they left the primary substation as cables and ended as overhead lines. The measurements were taken from the beginning of each feeder (M06 and M07), as well as one secondary substation on feeder A06 (M16) and two

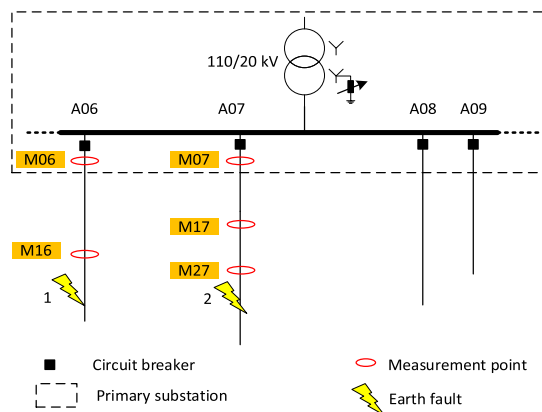


FIGURE 8. The compensated network used in field tests for fault studies.



FIGURE 9. Earth fault field tests (photo credit: Jukka Rinta-Luoma).

secondary substations on feeder A06 (M16 and M26). Intermittent earth faults were implemented on feeders A06 and A07 using special techniques and dedicated test equipment (Fig. 9). Two fault location scenarios are studied.

A. SCENARIO I

The intermittent earth fault (Fault 1 in Fig. 8) occurs on feeder A06, which means measurement points M06 and M16 are located on the fault passage and M07, M17 and M27 off the fault passage. The fault occurs at $t = 0.76s$ on phase “a” and the network under study is under-compensated with the compensation degree of 95%. The phase-to-ground voltages, along with the zero-sequence voltage measured at the primary substation, are illustrated in Fig. 10.

Phase currents and their corresponding negative and zero sequence currents (magnitudes) calculated using (3) and (5) are presented in Fig. 11 and Fig. 12 for measurement points M06 and M16, respectively. Both measurement points are correctly identified to be located on the fault passage using the proposed method. Both sequence currents exceed the pre-set threshold of 5.5 A.

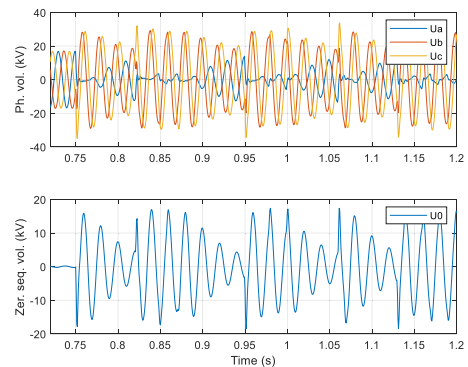


FIGURE 10. The phase-to-ground and zero-sequence voltages under intermittent fault condition, courtesy of ABB.

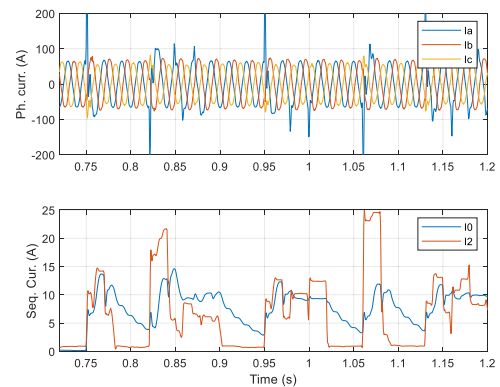


FIGURE 11. Phase currents and their corresponding zero and negative sequence currents (magnitudes) were measured at M06.

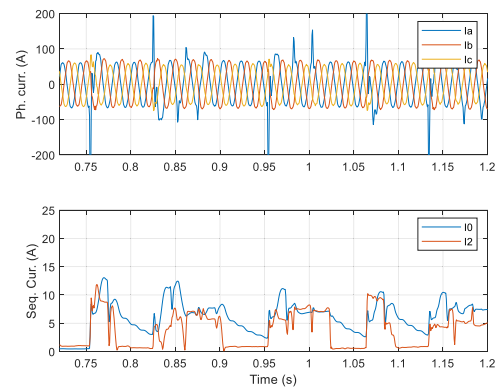


FIGURE 12. Phase currents and their corresponding zero and negative sequence currents (magnitudes) measured at M16.

Similarly, phase currents and their corresponding negative and zero sequence currents (magnitudes) calculated using equations (3) and (5) are presented in Fig. 13, Fig. 14 and Fig. 15 for measurement points M07, M17 and M27, respectively.

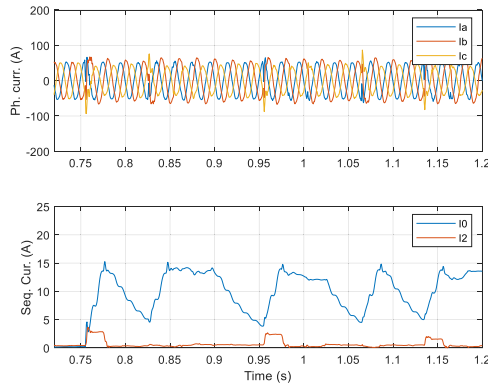


FIGURE 13. Phase currents and their corresponding zero and negative sequence currents (magnitudes) measured at M07.

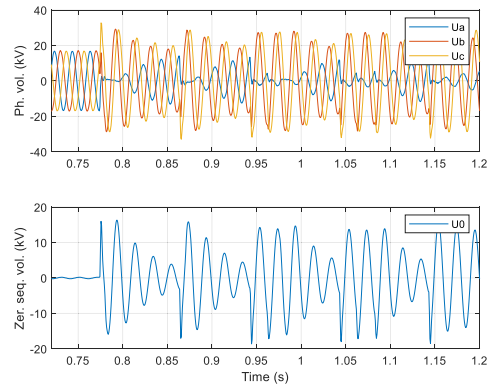


FIGURE 16. The phase-to-ground and zero-sequence voltages under intermittent fault condition, courtesy of ABB.

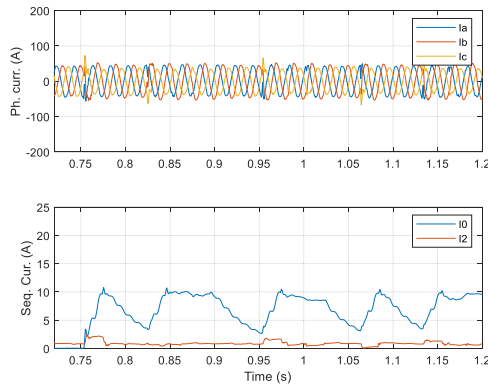


FIGURE 14. Phase currents and their corresponding zero and negative sequence currents (magnitudes) were measured at M17.

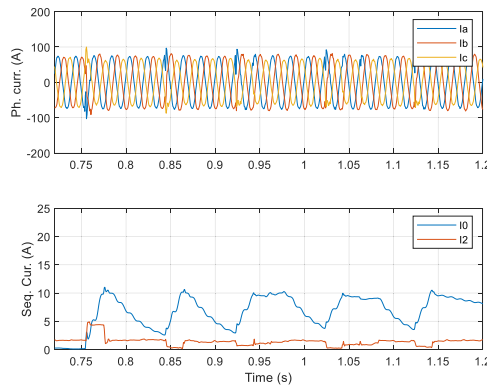


FIGURE 17. Phase currents and their corresponding zero and negative sequence currents (magnitudes) were measured at M06.

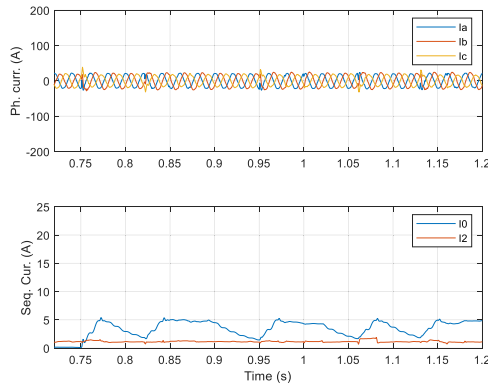


FIGURE 15. Phase currents and their corresponding zero and negative sequence currents (magnitudes) were measured at M27.

For these measurement points, which are located on the healthy feeder, although the ZSC magnitude is significant, the NSC magnitude is negligible. According to the proposed method, this indicates that the measurement points in question are located off the fault passage.

B. SCENARIO II

To further investigate the effectiveness of the proposed method in the case of different fault locations, Fault 2 is studied, which occurs on A07. Phase-to-ground voltages along with the zero-sequence voltages measured at the primary substation are illustrated in Fig. 16. Phase currents and their corresponding sequence currents for all measurement points are presented in Fig. 17 to Fig. 21. All the points on and off the fault passage can be identified successfully using the proposed method.

It should be noted that in both scenarios and in all measurement points, which are either on or off the fault passage, the zero sequence currents exceed the pre-set threshold. This result reveals the fact that the simple zero-sequence threshold method is insufficient for FPI applications.

All the measurement points can be successfully identified using the proposed method, as summarized in Table 3. In the table, the maximum values are presented.

As the results show, it is sufficient for the data used in this study to consider the second and third harmonics. If higher harmonics are considered, i.e., $m > 3$, then the threshold for I_2 must be determined accordingly. For comparison purposes,

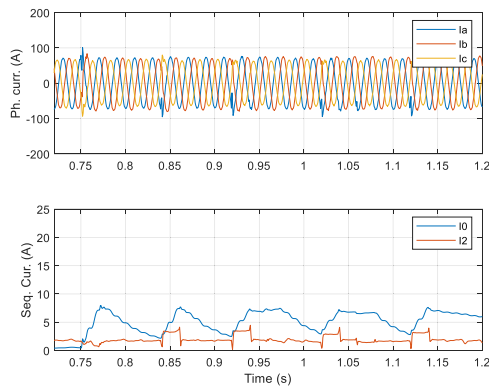


FIGURE 18. Phase currents and their corresponding zero and negative sequence currents (magnitudes) measured at M16.

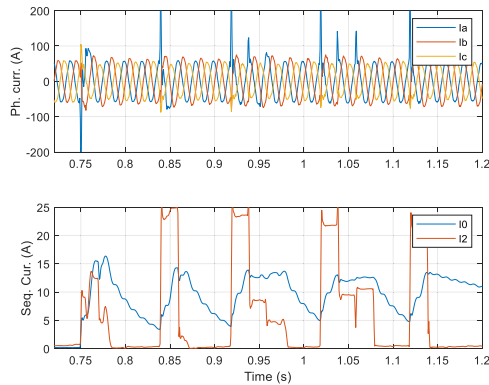


FIGURE 19. Phase currents and their corresponding zero and negative sequence currents (magnitudes) measured at M07.

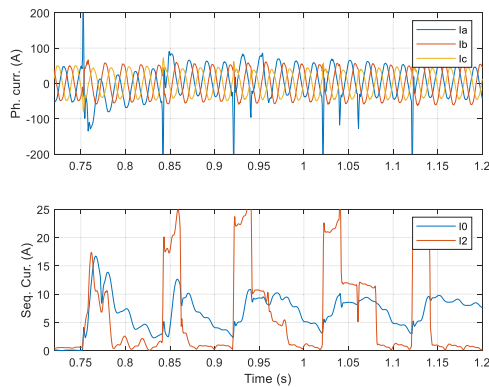


FIGURE 20. Phase currents and their corresponding zero and negative sequence currents (magnitudes) were measured at M17.

negative sequence currents are calculated for $m = 7$ and shown in Table 4. Using the same threshold of 5.5 A for I_2 leads to a false fault indication as I_2 at M16 for Fault 2 is 10 A. Therefore, a new threshold for I_2 must be set. The choice for setting a proper threshold is narrower now. In this particular

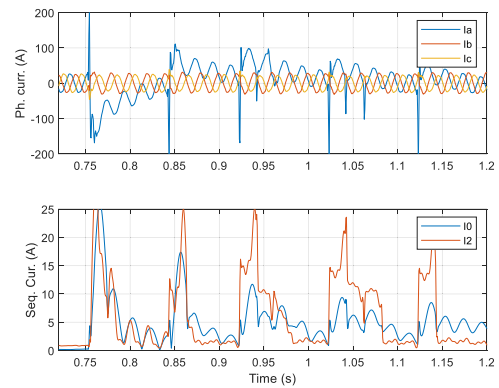


FIGURE 21. Phase currents and their corresponding zero and negative sequence currents (magnitudes) were measured at M27.

TABLE 3. Maximum values of sequence currents.

| Measuring point | Fault | I_0 (A) | I_2 (A) | On/off fault passage |
|-----------------|-------|-----------|-----------|----------------------|
| M06 | 1 | 14.6 | 25.4 | on |
| M16 | 1 | 13.1 | 19.8 | on |
| M07 | 1 | 16.2 | 3.6 | off |
| M17 | 1 | 11.5 | 2.4 | off |
| M27 | 1 | 5.7 | 1.9 | off |
| M06 | 2 | 11.9 | 5.0 | off |
| M16 | 2 | 8.6 | 5.0 | off |
| M07 | 2 | 16.4 | 27.2 | on |
| M17 | 2 | 16.7 | 28.9 | on |
| M27 | 2 | 25.9 | 33.2 | on |

TABLE 4. Maximum values of sequence currents for $m = 7$.

| Measuring point | Fault | I_0 (A) | I_2 (A) | On/off fault passage |
|-----------------|-------|-----------|-----------|----------------------|
| M06 | 1 | 14.6 | 55.1 | on |
| M16 | 1 | 13.1 | 13.6 | on |
| M07 | 1 | 16.2 | 3.2 | off |
| M17 | 1 | 11.5 | 3.2 | off |
| M27 | 1 | 5.7 | 3.5 | off |
| M06 | 2 | 11.9 | 5.1 | off |
| M16 | 2 | 8.6 | 10.0 | off |
| M07 | 2 | 16.4 | 57.9 | on |
| M17 | 2 | 16.7 | 55.9 | on |
| M27 | 2 | 25.9 | 47.9 | on |

case, 11 A would be a proper threshold with which points on and off the fault passage can be differentiated. The more harmonics considered in the method, the higher the value of the threshold for I_2 will have to be as NSC increases for points located off the fault passage. The relationship between the number of harmonics considered in the method and the predetermined threshold for I_2 depends on the distribution network's characteristics.

VI. DISCUSSION

In practice, phase currents can be measured using Rogowski coils which have the advantage of being suitable for retrofit installations. The measured phase currents or the computed

sequence currents, following a fault occurrence, are sent from the measuring points (secondary substations) to the control room. The SCADA system or DMS (Distribution Management System) analyzes the data to visualize the fault location on a map to the operator or perform an automatic FLIR (fault location, isolation and restoration) switching sequence.

As seen earlier, the magnitude of the ZSC alone cannot determine the fault passage as it could be high in both faulty and healthy feeders. However, in this method, it is used as an auxiliary indication i.e. the fault location procedure is triggered when the zero-sequence current exceeds a threshold. In an ideal symmetrical network, no negative or zero sequence currents exist in the network under normal condition. However, in some cases in practice, some level of NSC could exist even when there is no actual earth fault, for example, due to asymmetry of loads. This result would lead to a false indication of an earth fault if the NSC was used alone. However, that is not a concern in the proposed method for the following reason. Typically, the connection type of MV/LV transformers is D/Y. This means that the unbalanced loads on the LV side do not cause zero sequence currents on the MV side (because the primary side is a delta connection). Therefore, the problem of false indication is avoided if the ZSC is used in combination with the NSC in the manner proposed in this paper.

Intermittent earth faults are most often of low resistances, in the range of a few ohms. This range of resistance causes a high negative sequence current, as seen in sections IV and V. The proposed method could also be used for permanent earth faults provided the resulting NSC is high enough. However, the proposed method is not intended for earth faults with high resistances. The reason is that the NSC is so tiny that it is unusable in practice.

VII. CONCLUSION AND FUTURE WORK

The principles of a new FPI method for identifying the faulted segment in compensated MV distribution networks in case of intermittent earth faults were presented. The proposed method was based on only current measurement with no voltage measurement required, which would be a significant advantage from a cost point of view. The proposed method utilized the magnitude of the summation of negative sequence currents calculated for the fundamental frequency and multiple harmonics. In addition, the zero-sequence current was used as an auxiliary tool to determine the fault passage. It was shown that the zero-sequence current alone would not be enough as it could be significant in both faulty and healthy feeders. The operation principles were presented, and it was pointed out that if enough FPI devices are installed in the network, any faulted segment can be identified. The method's effectiveness was investigated using simulations and a series of field tests that provided strong preliminary validation of the method.

Investigating the performance of the method in networks with decentralized compensation units and the impact of the fault initial phase angle with respect to the phase angle of

voltage will be the subject of future studies. Moreover, wider tests with measurement points located both at the beginning and various points along the feeders, especially after the fault point, are needed. In addition, developing a method for setting the proper threshold for I_2 for any given distribution network needs further investigation. Finding an accurate relationship between the number of harmonics that has to be considered in the method and the predetermined threshold for I_2 is an open question that is one of the subjects of future work. Eventually, the implementation of the method with all the apparatus (current sensors, etc.) will be in future work.

APPENDIX

TABLE 5. Simulation Parameters.

| Peterson coil | |
|--|--|
| Compensation degree | 0.95 under-compensated (1 = fully-compensated) |
| Resistance of the parallel resistor | 2309 Ω |
| Inductance of the Peterson coil | 0.248511 H |
| Line parameters | |
| Positive sequence resistance | 0.15 [ohms/km] |
| Positive sequence inductive reactance | 0.110 [ohms/km] |
| Positive sequence capacitive reactance | 0.01061033 [Mohms*km] |
| Zero-sequence resistance | 0.954 [ohms/km] |
| Zero-sequence inductive reactance | 0.44 [ohms/km] |
| Zero-sequence capacitive reactance | 0.01082532 [Mohms*km] |
| Main transformer parameters | |
| 3 phase transformer MVA | 40 MVR |
| Base operation frequency | 50 Hz |
| Winding 1 voltage line to line (RMS) | 110 kV |
| Winding 2 voltage line to line (RMS) | 20 kV |
| Winding #1 type | Y |
| Winding #2 type | Y |
| Positive sequence leakage reactance | 0.1 [pu] |
| Eddy current losses | 0.0006 [p.u.] |
| Copper losses | 0.0037 [p.u.] |
| Intermittent earth fault resistance | more than 10 Ω |

ACKNOWLEDGMENT

The authors would like to thank ABB and Emtele Oy for providing the field test recordings.

REFERENCES

- [1] M. Loukkalahti, M. Hyvärinen, O. Siirto, and P. Heine, "Helen electricity network Ltd.'s process towards high level of supply reliability," *CIRED-Open Access Proc. J.*, vol. 2017, no. 1, pp. 1172–1175, Oct. 2017, doi: 10.1049/oap-cired.2017.1037.
- [2] O. Siirto, J. Vepsäläinen, A. Hämäläinen, and M. Loukkalahti, "Improving reliability by focusing on the quality and condition of medium-voltage cables and cable accessories," *CIRED-Open Access Proc. J.*, vol. 2017, no. 1, pp. 229–232, Oct. 2017, doi: 10.1049/oap-cired.2017.1104.
- [3] O. Siirto, M. Hyvärinen, M. Loukkalahti, A. Hämäläinen, and M. Lehtonen, "Improving reliability in an urban network," *Electr. Power Syst. Res.*, vol. 120, pp. 47–55, Mar. 2015, doi: 10.1016/j.epr.2014.09.021.
- [4] J. Altonen, O. Mäkinen, K. Kauhaniemi, and K. Persson, "Intermittent earth faults-need to improve the existing feeder earth fault protection schemes," in *Proc. CIREC*, Barcelona, Spain, May 2003, p. 6.

- [5] M. Loukkahti, B. J. O. Sousua, M. Celko, and K. Majer, "Digitalization in power distribution systems: The Kalasatama smart grid project," presented at the CIGRE, 2018.
- [6] G. Druml, O. Skrbinek, U. Schmidt, K. Frowein, and P. Schegner, "New method for identification and localisation of an earthfault in compensated networks," presented at the 25th Int. Conf. Electr. Distrib. (CIRED), Madrid, Spain, Jun. 2019. Accessed: Jan. 23, 2020. [Online]. Available: <https://www.cired-repository.org/handle/20.500.12455/149>.
- [7] G. Druml, P. Schegner, L. Fickert, and C. Raunig, "Fast selective earth fault localization using the new fast pulse detection method," in *Proc. 22nd Int. Conf. Exhib. Electr. Distrib. (CIRED)*, 2013, pp. 1–5, doi: 10.1049/cp.2013.1068.
- [8] G. Druml, O. Skrbinek, W. Hipp, L. Fickert, U. Schmidt, and P. Schegner, "First results concerning localisation of earthfaults in compensated 20-kV-networks based on travelling waves," presented at the 25th Int. Conf. Electr. Distrib. (CIRED), Madrid, Spain, Jun. 2019. Accessed: Jan. 23, 2020. [Online]. Available: <https://www.cired-repository.org/handle/20.500.12455/160>.
- [9] N. I. Elkalashy, N. A. Sabiha, and M. Lehtonen, "Earth fault distance estimation using active traveling waves in energized-compensated MV networks," *IEEE Trans. Power Del.*, vol. 30, no. 2, pp. 836–843, Apr. 2015, doi: 10.1109/TPWRD.2014.2365741.
- [10] J. Altonen and A. Wahlroos, "Novel algorithm for Earth-fault location in compensated MV-networks," in *Proc. 22nd Int. Conf. Exhib. Electr. Distrib. (CIRED)*, 2013, pp. 1–4, doi: 10.1049/cp.2013.0832.
- [11] *IEEE Guide for Determining Fault Location on AC Transmission and Distribution Lines*, IEEE Std C37.114-2014 (Revision IEEE Std C37.114-2004), Jan. 2015, pp. 1–76, doi: 10.1109/IEEESTD.2015.7024095.
- [12] A. Farughian, L. Kumpulainen, and K. Kauhaniemi, "Review of methodologies for Earth fault indication and location in compensated and unearthened MV distribution networks," *Electr. Power Syst. Res.*, vol. 154, pp. 373–380, Jan. 2018, doi: 10.1016/j.epr.2017.09.006.
- [13] A. Farughian, L. Kumpulainen, and K. Kauhaniemi, "Earth fault location using negative sequence currents," *Energies*, vol. 12, no. 19, p. 3759, Sep. 2019, doi: 10.3390/en12193759.
- [14] L. Kumpulainen, S. Sauna-aho, T. Virtala, and J. Holmlund, "A cost effective solution to intermittent transient earth-fault protection," presented at the Nordic Distrib. Asset Manage. Conf., Bergen, Norway, 2008.
- [15] G. Druml, O. Seiert, and M. Marketz, "Directional detection of restriking earth faults in compensated networks," presented at the 21st Int. Conf. Electr. Distrib. (CIRED), Frankfurt, Germany, 2011.
- [16] M. Akke, "Method and device for detecting an intermittent earth fault in a multiple feeder system," U.S. Patent EP2 390 980 A1, Nov. 30, 2011.
- [17] X. Dong, T. Cui, Z. Bo, A. Klimek, and A. Juszczak, "Method and system for transient and intermittent earth fault detection and direction determination in a three-phase median voltage electric power distribution system," U.S. Patent EP2 417 467 A1, Feb. 15, 2012.
- [18] T. Cui, X. Dong, Z. Bo, and A. Juszczak, "Hilbert-transform-based transient/intermittent earth fault detection in noneffectively grounded distribution systems," *IEEE Trans. Power Del.*, vol. 26, no. 1, pp. 143–151, Jan. 2011, doi: 10.1109/TPWRD.2010.2068578.
- [19] S. Pettisalo, "Method and apparatus for detecting faults in a three-phase electrical distribution network," U.S. Patent WO2 017 203 099, Nov. 30, 2017.
- [20] T. Virtala, "Method and protection device for eliminating earth faults of transient type in an electric distribution network," U.S. Patent WO2 016 066 898 A1, May 6, 2016.
- [21] A. Wahlroos and J. Altonen, "Application of novel multi-frequency neutral admittance method into Earth-fault protection in compensated MV-networks," in *Proc. 12th IET Int. Conf. Develop. Power Syst. Protection (DPSP)*, 2014, pp. 1–6, doi: 10.1049/cp.2014.0032.
- [22] A. Wahlroos, U. Uggla, J. Altonen, and D. Wall, "Application of novel cumulative phasor sum measurement for Earth-fault protection in compensated MV-networks," in *Proc. 22nd Int. Conf. Exhib. Electr. Distrib. (CIRED)*, Stockholm, Sweden, 2013, p. 0607, doi: 10.1049/cp.2013.0833.
- [23] J. Altonen, A. Wahlroos, S. Vähäkuopus, and E. Oy, "Application of multi-frequency admittance-based fault passage indication in practical compensated MV-network," in *Proc. 24th Int. Conf. Electricity Distrib. (CIRED)*, Glasgow, U.K., Jun. 2017, p. 5.
- [24] D. Topolanek, M. Lehtonen, P. Toman, J. Orsagova, and J. Drapela, "An Earth fault location method based on negative sequence voltage changes at low voltage side of distribution transformers," *Int. J. Electr. Power Energy Syst.*, vol. 118, Jun. 2020, Art. no. 105768, doi: 10.1016/j.jepes.2019.105768.
- [25] S. Hänninen, *Single Phase Earth Faults in High Impedance Grounded Networks: Characteristics, Indication and Location*. Espoo, Finland: VTT Technical Research Centre Finland, 2001.
- [26] G. Druml, S. Automation, O. Skrbinek, U. Schmidt, P. Schegner, and L. Fickert, "Why does the Earth-fault detection method based on third harmonic work in large meshed 110 kV networks," in *Proc. 24th Int. Conf. Electricity Distrib. (CIRED)*, Glasgow, U.K., 2017, p. 5, doi: 10.1049/oap-cired.2017.0564.
- [27] J. J. Grainger and W. D. Stevenson, *Power System Analysis*. New York, NY, USA: McGraw-Hill, 2003.



AMIR FARUGHIAN received the B.Sc. degree in electrical engineering from the Shiraz University of Technology, Iran, in 2010, and the M.Sc. degree in smart grids from the Tampere University of Technology, Finland, in 2015. He is currently pursuing the Ph.D. degree with the University of Vaasa, Finland.

He was involved in several research projects as a Project Researcher from 2015 to 2019. His research interest includes earth fault location in medium voltage distribution networks.

Mr. Farughian is a member of the FRESI Smart Grid Laboratory, which is a member of the DERlab, an international network of leading research laboratories focusing on distributed energy resources.



LAURI KUMPUAINEN (Senior Member, IEEE) was born in Padasjoki, Finland, in 1962. He received the M.Sc. and Lic.Tech. degrees in electrical engineering from the Tampere University of Technology, in 1987 and 2000, respectively, and the D.Sc. (Tech.) degree from the University of Vaasa, in 2016.

His career includes positions at the Electric Utility Company, Polytechnic University, the Research Institute, and Protective Relay Company. Since 2013, he has been with the University of Vaasa. He has been a Professor of smart and flexible power systems, since 2018. He is the author of dozens of scientific publications. His research interests include future energy systems, cross-sector integration, renewable energy, and power system protection.

Dr. Kumpulainen was the first recipient of the award for meritorious energy-related research from the Ostrobothnia Chamber of Commerce.



KIMMO KAUHANIEMI received the M.S. and Ph.D. degrees in electrical engineering from the Tampere University of Technology, Finland, in 1987 and 1993, respectively. He has been employed with ABB Corporate Research and VTT Technical Research Centre of Finland. He is currently with the University of Vaasa, where he is a Professor of electrical engineering and leads the Smart Electric Systems Research Group. His special research interests include the power system transient simulation, protection of power systems, grid integration of distributed generation, and microgrids.



PETRI HOVILA (Member, IEEE) received the B.Sc. degree in electrical, electronics and communications engineering from the Central Ostrobothnia University of Applied Sciences, Finland, in 1999. Has been working for energy industry over 20 years. He has held several engineering, project-manager, and line-manager positions in ABB, Finland, where he is currently working as a Senior Principal Engineer. He is also responsible for the research program and IPRs for the distribution solutions business.

...

Technical requirements for practical implementation of fault passage indication

Amir Farughian
School of Technology and Innovations
University of Vaasa
Vaasa, Finland
amir.farughian@uva.fi

Lauri Kumpulainen
School of Technology and Innovations
University of Vaasa
Vaasa, Finland
lauri.kumpulainen@uva.fi

Kimmo Kauhaniemi
School of Technology and Innovations
University of Vaasa
Vaasa, Finland
kimmo.kauhaniemi@uva.fi

Seppo Pettissalo
Vaspec Oy
Vaasa, Finland
seppo.pettissalo@vaspec.fi

Ville Sallinen
Emtele Oy
Tampere, Finland
ville.sallinen@emtele.com

Abstract—One of the distinctive features of smart grids is feeder automation. Fault location is an important part of this feature and has become an essential function for distribution system operators. Reliable fault location expedites the restoration of power following an outage caused by a permanent fault. The most common type of faults in distribution networks is the single phase to ground fault. To locate earth faults in non-effectively earthed medium-voltage distribution networks, a number of methods have been put forward among which methods that are based on fault passage indication appear to be promising. This paper discusses the technical apparatus required for implementing two FPI-based methods in practice.

Keywords—application considerations, earth fault location, symmetrical sequence components, technical apparatus

I. INTRODUCTION

Fault location has become an essential function for distribution system operators. Some permanent faults could lead to power outage. A reliable fault location method can help system operators to locate the actual fault in the network as soon as possible. The most common type of faults in distribution networks is the earth fault. Generally, faulty feeder identification and fault location in distribution networks could be performed at three levels:

1. Faulty feeder identification: Only the faulted feeder is determined. This is usually an integral part of the feeder relay protection.
2. Fault Passage Indication (FPI): The faulted section, e.g., lines or cables connecting two consecutive secondary substations on a radial feeder, is identified.
3. Distance estimation: The fault distance from the measurement point (usually the beginning of the faulted feeder) is estimated.

A number of methods have been proposed to locate earth faults in distribution networks [1].

- Impedance based methods [2] [3] [4]
- Injection methods [5]
- Voltage sag measured at the low voltage side of transformers at secondary substations [6]
- Traveling wave based methods [7]

- Signal processing [8] [9]
- Fault passage indicators (FPIs) [10] [11] [12] [13]

A comprehensive review on the state-of-the-art earth fault location methods along with their limitations is presented in [14]. One of the findings of Ref. [14] is that FPI-based methods appear to be a promising approach for locating earth faults in distribution networks. The purpose of FPI-based methods is to find, on the faulty feeder, the faulted section i.e. the faulted segment linking two consecutive secondary substations. FPI aims at indicating if any fault current has passed through the measurement point at which the FPI device is installed. By installing multiple FPI devices at various locations (typically secondary substations) throughout the network, the faulted section identification can be achieved and visualized for the system operator. In general, the more FPI devices installed throughout the network, the more accurate fault location can be achieved. Two FPI-based methods have been presented by the authors in [12] and [13] which utilize current measurements and no voltage measurement is required. They have shown promising preliminary results in successfully identifying the points located on or off the fault passage. The methods employ symmetrical components of the currents to determine whether the FPI device is located on the fault passage or off the fault passage. In this paper, technical aspects and apparatus regarding the implementation of these methods in practice are discussed.

In Section II, the operational principles of the methods are presented shortly. Simulation results are used to help outlining the methods. In Section III, implementing the methods in practice is discussed in depth. Some field tests results are presented in Section IV. Conclusions are drawn in Section V.

II. METHOD OVERVIEW

A. Principles of operation

The method presented in [12] employs zero and negative sequence currents computed from measured phase currents. The negative sequence current (NSC) phasor for phase “a”, by definition, is obtained as follows.

$$\bar{I}_2^{(a)} = \frac{1}{3} (\bar{I}_a + \alpha^2 \bar{I}_b + \alpha \bar{I}_c) \quad (1)$$

Where, \bar{I}_a , \bar{I}_b and \bar{I}_c denote the phasors of phase currents of phases a, b and c, respectively and the operator α is

$1 \angle 120^\circ$. The phasor of the zero sequence current is calculated using the following equation.

$$\bar{I}_0 = \frac{1}{3} (\bar{I}_a + \bar{I}_b + \bar{I}_c) \quad (2)$$

The method presented in [12] is based on a finding that on the fault passage, both zero and negative sequence currents are significant whereas on points off the fault passage, only the zero sequence current (ZSC) is significant and the negative sequence current is negligible. Using this finding, the faulted segment can be identified.

The method presented in [13], requires only ZSC to locate the faulted segment. However, this method is applicable only to isolated networks. This method is based on the finding that ZSC on the faulty feeder increases from the beginning of the feeder up to the fault point.

B. Fault location procedure in practice

FPI devices that are installed along distribution feeders constantly measure phase currents and record the measurement data within a moving window of one second. Once the summation of phase currents or alternatively the zero sequence current measured by a device exceeds a pre-set threshold, that device gets triggered and saves the recorded measurement window so that the first half of the window contains measurements in no fault condition (pre-trigger period) and the second half contains during the fault condition data (post-trigger period). The device then sends the recording through 3G, 4G or 5G to a control center where the raw data is processed. In the control center, the phasors of the sequence currents are computed using equations (1) and (2) for both pre and post-fault periods. The fault passage indication then can be realized using method 1 and method 2.

1) Method 1

Based on the comparison of the computed negative sequence currents between pre and post-fault periods, it is determined whether the device in question is located on the fault passage or off the fault passage. The control center carries out this analysis for every device whose recording has arrived to the control center. The devices with no recordings in the control center are determined to be located off the fault passage. The devices' locations are known to the control center. The faulted segment is determined to be the segment between the last device on the fault passage and the first device off the fault passage. Finally, the faulted segment is visualized on the map for the operator.

2) Method 2

The control center collects all the recordings that have arrived at around the same time. The amplitude of the phasor of ZSC of each recording is divided by the amplitude of the phasor of the ZSC of the first device (the device that is installed at the beginning of the feeder). If the result of this division is greater than one, then that device is determined to be located on the fault passage. Otherwise, the device is off the fault passage. Similarly, if a device has no recording in the group of recordings, that device is determined to be located off the fault passage. The faulted segment is determined to be the segment between the last FPI device on the fault passage and the first device off the fault passage. Finally, the faulted segment is visualized on the map for the system operator.

When there is an earth fault on the feeder, the ZSC at devices that are located after the fault point could be so tiny that it does not exceed the pre-set threshold and, as a result, the device will not get triggered. This is however, not a concern when it comes to fault passage indication as missing a recording from a device is an indication that the device in question is located after the fault point i.e. off the fault passage. The concept of fault passage indication is illustrated in Fig. 1.

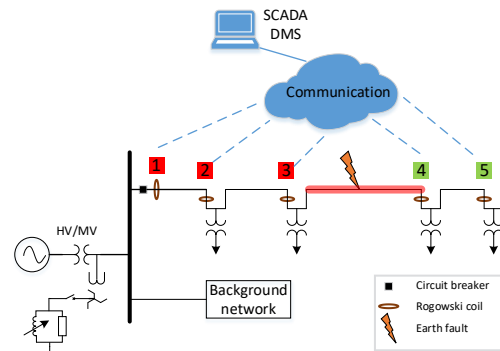


Fig. 1 Fault passage indication on a radial distribution feeder.

C. Simulation results

The operational principles of the methods can be better understood by way of example. The simulations are carried out using a verified model based on a real medium voltage distribution network in Finland. Fig. 2 shows the simplified diagram of the medium-voltage distribution network modeled in PSCADTM/EMTDCTM. A 110 kV high-voltage network supplies the 20 kV medium-voltage network through a 40 MVA transformer. The network type from the viewpoint of neutral point treatment can alter between isolated and compensated. The medium-voltage network consists of several feeders from which a single one is depicted in the figure and the rest are shown as a single block "Background network". The feeder under study consists of a mixture of underground cables and overhead lines. It has four secondary substations equipped with current measurements. Naturally, there is also a measurement point at the beginning of the feeder (at the primary substation). An earth fault occurs at one of the feeders on phase "a" between measurement points 3 and 4. The fault resistance is 0.01 Ω .

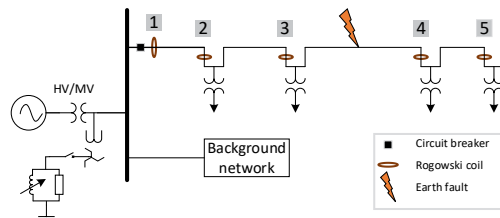


Fig. 2 Earth fault on a medium-voltage distribution network with four secondary substations equipped with Rogowski-coil-based current sensors.

Sequence currents at their steady state during the fault period can be calculated using equations (1) and (2). The calculated zero and negative sequence currents at the measurement points marked on Fig. 2 are shown in Fig. 3.

1) Compensated network

When the network is in its compensated mode i.e. the Petersen coil is connected to the neutral of the network, the NSC remains almost the same value of 3 A from measurement point 1 to measurement point 3. It is negligible at points 4 and 5. Therefore, one can identify the faulted segment using the NSC. The ZSC decreases from the beginning of the feeder towards the end.

2) Isolated network

When the network is in its isolated mode, it means the neutral point is disconnected from the Petersen coil. This results in higher fault current and consequently higher levels of zero and negative sequence currents. NSC remains almost at the same value of 32 A from measurement point 1 to measurement point 3 and is negligible after the fault point. The ZSC current increases slightly from point 1 towards point 3. After that, it drops. Therefore, one can determine the faulted segment using the ZSC alone.

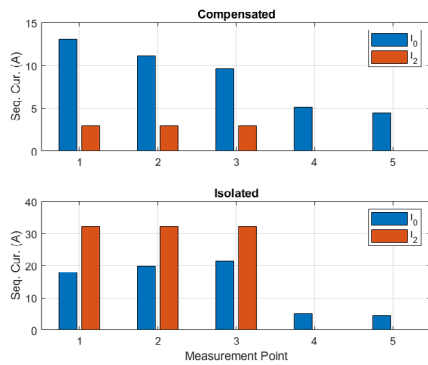


Fig. 3 Sequence currents during an earth fault obtained from the five measurement points shown in Fig. 2.

The calculated zero and negative sequence currents at various points on the faulted feeder are presented in Table 1 and Table 2 for two fault resistances of 0.01 Ω and 100 Ω . The values presented in the tables are calculated during the fault period. Under no fault condition, in a symmetrical network like the simulated model in question, negative and zero sequence currents are 0 A at any point along the distribution feeder. For this reason, the values presented in the tables are only from the during the fault period. Table 1 presents the sequence currents when the network is in its compensated mode.

Table 1. Zero and negative sequence currents at five measurement points (MP) for the network of Fig. 2 in its compensated mode.

| MP | $R = 0.01 \Omega$ | | $R = 100 \Omega$ | | FPI |
|----|-------------------|-----------|------------------|-----------|-----|
| | I_0 (A) | I_2 (A) | I_0 (A) | I_2 (A) | |
| 1 | 13.0 | 3.0 | 12.3 | 2.7 | On |
| 2 | 11.1 | 3.0 | 10.6 | 2.7 | On |
| 3 | 9.6 | 3.0 | 9.1 | 2.7 | On |
| 4 | 5.1 | 0 | 4.9 | 0 | Off |
| 5 | 4.4 | 0 | 4.3 | 0 | Off |

In Table 2, zero sequence currents for each measurement point are given. In addition, these values are scaled so that they are divided by the one from measurement point 1 (I_{0s}). According to method 2, if the scaled value is greater than or equal to 1, the measurement point in question is on the fault passage. Otherwise, it is off the fault passage.

Table 2. Zero sequence currents and their normalized values for the network of Fig. 2 in its isolated mode.

| MP | $R = 0.01 \Omega$ | | $R = 100 \Omega$ | | FPI |
|----|-------------------|----------------|------------------|----------------|-----|
| | I_0 (A) | I_0 / I_{0s} | I_0 (A) | I_0 / I_{0s} | |
| 1 | 18.0 | 1 | 15.8 | 1 | On |
| 2 | 19.9 | 1.1 | 17.5 | 1.1 | On |
| 3 | 21.5 | 1.2 | 18.9 | 1.2 | On |
| 4 | 5.1 | 0.3 | 4.5 | 0.3 | Off |
| 5 | 4.5 | 0.2 | 3.9 | 0.2 | Off |

III. PRACTICAL ASPECTS

A. Measurements

The proposed FPI methods require no voltage measurement. For measuring the phase currents required for implementing the FPI method, Rogowski-coil-based sensors are recommended (Fig. 4). They have the advantage of being suitable for retrofit installations. In addition, unlike CTs, they do not saturate. A Rogowski coil current sensor is an air-core coil that wraps around the cable or overhead line. The voltage signal induced in the coil is proportional to the derivative of the current flowing through the coil. Therefore, using an integration circuit or alternatively integrating on the software side, the voltage signal can be converted into a current signal. Since there is no iron core in the coil, no saturation takes place. As a result, current sensors are more accurate compared to conventional CTs. In addition, the coil's output is linear when subjected to large currents. This makes Rogowski-coil-based sensors suitable for measuring large fault currents in transmission and distribution networks. One other advantage that this type of sensor offers is that thanks to its low voltage output, it causes no hazard to personnel and equipment. In the practical implementation described below, the smallest measurable current level is 0.1 A. The Rogowski coils used in the implementation of the discussed methods have the accuracy of 0,5 %. The angle accuracy is about one degree.

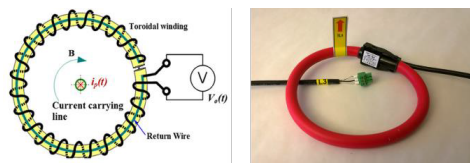


Fig. 4 Rogowski-coil-based current sensor [15].

To calculate the phasor of the NSC using equation (1), the phase angle of each phase current phasor is required. If one Rogowski is incorrectly installed in terms of polarity, it affects the phasor calculations. Therefore, it is essential that Rogowski coils for all phases are installed uniformly. Correct installation of Rogowski coils are shown in Fig. 5. The arrow marked on the sensor signifies the polarity.

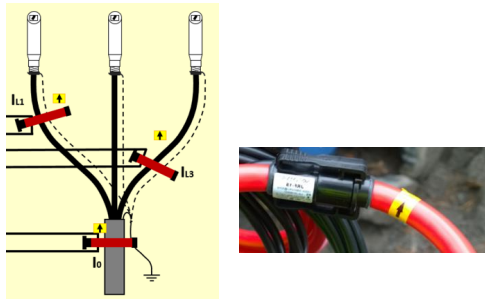


Fig. 5 Rogowski coil installation on a measurement point, arrows show polarity.

B. Communication

In Fig. 6, the block diagram of an FPI unit connected to a remote secondary substation is illustrated. Some technical specifications of an FPI device are presented in Appendix. The recorded measurement along with the time stamp of the disturbance are sent to a control center. A modem embedded in the FPI device sends the recorded data to the control center. This is illustrated in Fig. 7.

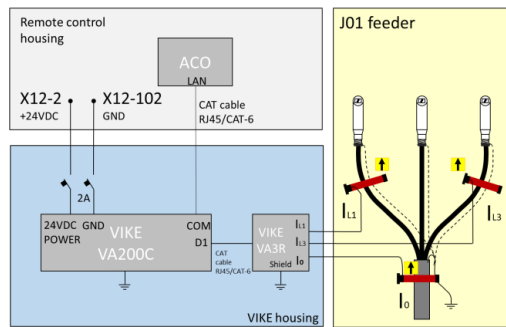


Fig. 6 Single FPI unit and its connection to a remote secondary substation.

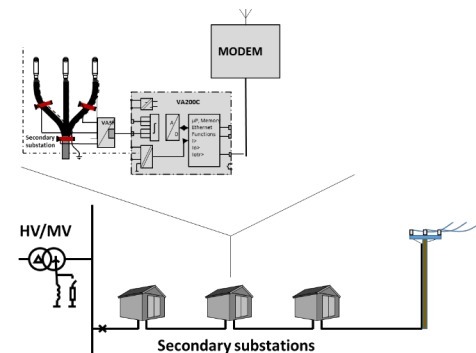


Fig. 7 Intelligent fault indicator at a secondary substation.

3G, 4G or 5G communication technology can be used for transferring the data. An alternative for sending the data to the control center is through the available automation systems at secondary substations using telecommunication protocol IEC 60870-5-104.

C. Data acquisition

1) Sampling rates

In the real world implementation, FPI devices constantly measure phase currents using two sampling rates of 1.6 and 25.6 kHz. The sampling rate of 1.6 kHz is used for detecting permanent earth faults and the sampling rate of 25.6 kHz is used to detect intermittent earth faults. An intermittent earth fault is a special type of fault, which is common mostly in compensated cable networks. It causes short current spikes whose durations are typically only 0.1 to 1 ms. If only the sampling rate of 1.6 kHz is used to measure currents, these spikes might be missed. Therefore, another set of measurements is carried out using the sampling rate of 25.6 kHz.

The length of the recording windows for both sets of measurements is the same in terms of samples, i.e. the number of samples for each phase current for each sampling rate is 1600. This means that the recording window of measurements obtained by sampling rate of 1.6 kHz is 1 s and the recording window of measurements obtained by sampling rate of 25.6 kHz is 0.0625 s.

2) Recording structure

An FPI device is triggered once the summation of phase currents (or alternatively the ZSC) that the device measures exceeds a pre-set threshold. The two sets of recordings that are obtained with two sampling rates are saved in the memory of the device. The modem embedded in the device sends the recording to the control center where the recordings are further analyzed. Each recording that arrives to the control center consists of two parts:

- pre-fault period
- during fault period

In an ideal network with no asymmetry, no ZSC or NSC exists in the network under normal condition. In practice, however, there could be cases where some level of NSC exists even when there is no actual earth fault. This could be, for example, due to unbalanced loads. In practice, one advantage that recording and analyzing the measurements in the pre-fault period provides is that there is no need to know the negative sequence current level of the network in no fault condition.

D. Sensitivity and network types

As mentioned before, the FPI device triggering mechanism is based on detecting an increase in the ZSC (or alternatively the summation of phase currents). The system operators can set the threshold of this increase remotely. In fact, the system operator can update the firmware of the device anytime remotely to achieve the desired sensitivity. For higher sensitivity, the system operator can configure the pre-set threshold to a lower value. The downside of the high sensitivity would be that many disturbances that are not actual earth faults could trigger devices. This leads to many recordings being unnecessarily sent to the control center for further processing.

In terms of the neutral point treatment, the discussed FPI methods are applicable to non-effectively grounded networks i.e.

- isolated neutral network
- centrally compensated network
- centrally and decentrally compensated network

The compensated network seems to be the most challenging type of network when it comes to earth fault location, as the fault current in this type of network could be very low. This is due to the fact that the Petersen coil (compensation coil) compensates the capacitive component of the fault current.

IV. FIELD TESTS

To examine the validity of the discussed methods, a series of disturbance recordings was performed on an MV distribution network in Finland (Fig. 8). The tests were carried out by DSOs in cooperation with network automation system providers in Finland. Current and voltage measurement devices were installed at the beginning of two feeders. The earth faults were applied to one of the feeders while the other feeder remained healthy. A set of raw recordings obtained from these two feeders during an earth fault test is presented in this section. Phase voltages measured at the primary substation are shown in Fig. 9. The faulted phase is "c", as can be seen in Fig. 9. The phase currents of faulty and healthy feeders are shown in Fig. 10. For better readability, the figures have different scales.



Fig. 8 Field testing, courtesy of Maviko Oy.

The corresponding negative and zero sequence currents for the faulty and healthy feeders calculated using equations (1) and (2) are shown in Fig. 11. ZSC is significant in both feeders whereas NSC is negligible on the healthy feeder.

A. No fault period

For the healthy feeder, the no fault period is the period prior to $t = 2.5$ s and for the faulty feeder, the no fault period is the period prior to $t = 2.08$ s. The zero sequence currents for faulty and healthy feeders are 0.65 and 0.35, respectively. The negative sequence currents are 0.10 and 0.45 A, respectively.

B. During fault period

For the faulty and healthy feeders, the during fault periods are the period after $t = 2.08$ s and $t = 2.50$ s, respectively. The zero sequence currents for faulty and healthy feeders at their steady states are and zero sequence currents are 25.80 A and 15.10 A, respectively. The negative sequence currents at their steady states 5.60 A and 0.40 A.

Therefore, by comparing the sequence currents calculated for the two periods (before and during fault period), it can be readily determined if the measurement point in question is on or off the fault passage.

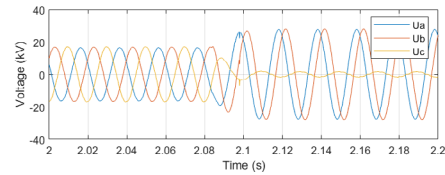


Fig. 9 Phase to ground voltages measured at the primary substation, faulted phase c, courtesy of Emtele Oy.

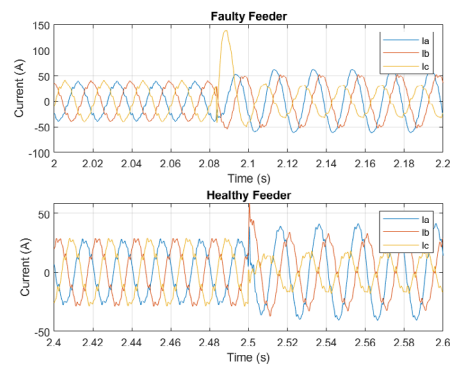


Fig. 10 Phase currents measured at (the beginning of) faulty and healthy feeders, pre- and during fault periods, courtesy of Emtele Oy.

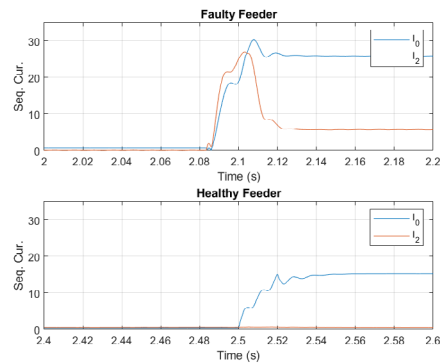


Fig. 11 Sequence current calculated for the phase currents shown in Fig. 10.

V. CONCLUSION

The technical apparatus required for implementing two FPI-based methods in practice was discussed in depth. It appears the presented methods can be successfully implemented in practice. However, the methods are applicable to high-impedance earth faults as long as the resulting fault current causes large enough sequence currents that are measurable. The FPI-based methods required no voltage measurement. In addition, the

operational principles of the methods were outlined with the help of simulations. Technical aspects such as fault location procedure, measurement, sensitivity of the method, the required communication, network types, etc. were covered in the discussion. Installing more FPI devices throughout a distribution network including measurement points behind the fault point is the subject of the future work.

VI. APPENDIX

| | |
|------------------------------------|---|
| Operating voltage | 8... 36 VDC |
| Current measurement | 2x3 / Rogowski coils |
| Digital outputs | 2 |
| Communication | Ethernet |
| Protocol | IEC 60870-5-104 |
| Software can be updated remotely | |
| Phase current measurement | 0...2500 A |
| Residual current measurement | 0...250 A |
| Serial buses | 1 for the expansion unit |
| A / D converter | 16 bit |
| Sampling frequency | 25.6 kHz / channel |
| Fault recorder | For transients and RMS values of currents |
| Phase voltage measurement (option) | capacitive or resistive |
| Housing | DIN rail mounted |

REFERENCES

- [1] "IEEE Guide for Determining Fault Location on AC Transmission and Distribution Lines," *IEEE Std C37.114-2014 (Revision of IEEE Std C37.114-2004)*, pp. 1–76, Jan. 2015, doi: 10.1109/IEEESTD.2015.7024095.
- [2] "Comparison of Impedance Based Location Methods for Power Distribution Systems," *Elsevier, Electric Power Systems Research*, vol. 78, no. 4, pp. 657–666, 2008.
- [3] A. Nikander and P. Järventausta, "Identification of High-Impedance Earth Faults in Neutral Isolated or Compensated MV Networks," *IEEE Transactions on Power Delivery*, vol. 32, no. 3, pp. 1187–1195, Jun. 2017, doi: 10.1109/TPWRD.2014.2346831.
- [4] J. Altonen and A. Wahlroos, "Advancements in fundamental frequency impedance based earth fault location in unearthed distribution systems," presented at the CIREC 19th International Conference on Electricity Distribution, Vienna, May 2007, [Online]. Available: <https://pdfs.semanticscholar.org/37cc/a4bb8b1037b6ba840014b869f6b491bdcb7.pdf>.
- [5] G. Druml, C. Raunig, P. Schegner, and L. Fickert, "Fast selective earth fault localization using the new fast pulse detection method," in *22nd International Conference and Exhibition on Electricity Distribution (CIREC 2013)*, Jun. 2013, pp. 1–5, doi: 10.1049/cp.2013.1068.
- [6] D. Topolanek, M. Lehtonen, M. R. Adzman, and P. Toman, "Earth fault location based on evaluation of voltage sag at secondary side of medium voltage/low voltage transformers," *IET Generation, Transmission & Distribution*, vol. 9, no. 14, pp. 2069–2077, 2015, doi: 10.1049/iet-gtd.2014.0460.
- [7] G. Druml, O. Skrbinjek, W. Hipp, L. Fickert, U. Schmidt, and P. Schegner, "First results concerning localisation of earthfaults in compensated 20-kV-networks based on travelling waves," presented at the 25th International Conference on Electricity Distribution (CIREC 2019), Madrid, Jun. 2019, Accessed: Jan. 23, 2020. [Online]. Available: <https://www.cired-repository.org/handle/20.500.12455/160>.
- [8] N. I. Elkalashy, M. Lehtonen, H. A. Darwish, A.-M. I. Taalab, and M. A. Izzularab, "Operation evaluation of DWT-based earth fault detection in unearthed MV networks," in *2008 12th International Middle-East Power System Conference*, Mar. 2008, pp. 208–212, doi: 10.1109/MEPCON.2008.4562385.
- [9] N. I. Elkalashy, N. G. Tarhuni, and M. Lehtonen, "Simplified probabilistic selectivity technique for earth fault detection in unearthed MV networks," *Transmission Distribution IET Generation*, vol. 3, no. 2, pp. 145–153, Feb. 2009, doi: 10.1049/iet-gtd:20070523.
- [10] J. Altonen and A. Wahlroos, "Performance of modern fault passage indicator concept in compensated MV-networks," in *CIREC Workshop 2016*, Jun. 2016, pp. 1–4, doi: 10.1049/cp.2016.0733.
- [11] J. Altonen, A. Wahlroos, S. Vähäkuopus, and E. Oy, "Application of multi-frequency admittance-based fault passage indication in practical compensated MV-network," Glasgow, Jun. 2017, p. 5.
- [12] Farughian, Kumpulainen, and Kauhaniemi, "Earth Fault Location Using Negative Sequence Currents," *Energies*, vol. 12, no. 19, p. 3759, Sep. 2019, doi: 10.3390/en12193759.
- [13] A. Farughian, L. Kumpulainen, and K. Kauhaniemi, "Non-Directional Earth Fault Passage Indication in Isolated Neutral Distribution Networks," *Energies*, vol. 13, no. 18, p. 4732, Jan. 2020, doi: 10.3390/en13184732.
- [14] A. Farughian, L. Kumpulainen, and K. Kauhaniemi, "Review of methodologies for earth fault indication and location in compensated and unearthed MV distribution networks," *Electric Power Systems Research*, vol. 154, pp. 373–380, Jan. 2018, doi: 10.1016/j.epsr.2017.09.006.
- [15] L. Kumpulainen, G. A. Hussain, M. Lehtonen, and J. A. Kay, "Preemptive Arc Fault Detection Techniques in Switchgear and Controlgear," *IEEE Transactions on Industry Applications*, vol. 49, no. 4, pp. 1911–1919, Jul. 2013, doi: 10.1109/TIA.2013.2258314.